Updating the Simulation Model Using Dynamic Clusters Extracted From 4D Seismic Data

Valeriy Rukavishnikov

Submitted for the Degree of Doctor of Philosophy

Institute of Petroleum Engineering

Heriot-Watt University, Edinburgh, Scotland, UK

April, 2015

Abstract

The thesis shows the development and testing of a new method for updating simulation model using dynamic clusters extracted from time-lapse seismic data. The clusters represent reservoir volumes that share a similar 4D seismic response over time. Similarities over time between cumulative production and injection histories and the seismic signatures indicate hydrodynamic connections between wells and corresponding clusters. Once that connection is established, the spatial relationships of clusters determined for individual time segments define fluid pathways and help us to understand the track of the well connections and reservoir connectivity in general. The method allow direct usage of 4D date into simulation model and especially effective for locating baffles and barriers in the reservoir. Additional method advantage is 3D simulation grid based results, so it can be easily used for history matching process. The technique is applied to the two compartmentalized North Sea fields with encouraging results: one is structurally controlled, second is turbidite reservoir with complex geological settings. Overall, method demonstrates solid consistency with geology, can be used for quantitative transmissibility and connectivity update in simulation and even in geological models with sufficient history matching time reduction.

To my parents

Acknowledgements

My special thanks to Professor Colin MacBeth for giving me this unique opportunity to join Heriot-Watt University and Edinburgh Time-Lapse Project. This thesis could never have been accomplished without his endless understanding and support.

Grateful acknowledgements to the Phase IV and V sponsors of ETLP: BP, BG Group, CGG, Chevron, ConocoPhillips, ENI, ExxonMobil, Hess, Maersk, Nexen, Norsar, Shell, Statoil, Ikon Science, Landmark, Petoro, Petrobras, RSI, Suncor, Taqa, TGS, and Total for their funding, support of the project and providing the datasets.

I wish to thank my friends, who have been near me at this great time in Edinburgh: Dr. Hamed for his constant support and calmness during endless explanations about Sim-2-Seis software, Dr. Alejandro for jokes and permanent good mood, Dr. Reza for nice easy discussions, Dr. Yi for valuable 4D talks and sharing experience, Dr. Yesser for perfect example of persistence, Dr. Sean for cheering me up, Sergey, and Dr. Oleg and his wife Anna. I am a really lucky man to meet you all. Special thanks to Constanze for feeling like home.

The time I have spent working on this project, indeed gave much more than research experience and professional skills; it gave live experience and understanding of my own thoughts and plans. I wish to say thanks the city, which I really fell in love with, Edinburgh, for its atmosphere and spirit.

I also wish to thank my Mom and Dad for everything.

ACADEMIC REGISTRY
Research Thesis Submission

Name:	VALERIY RUKAVISHNIKOV		
School/PGI:	INSTITUTE OF PETROLEUM ENGINEERING		
Version: *(i.e. First, Resubmission, Final)*	FINAL	Degree Sought (Award **and** Subject area)	PhD, PETROLEUM ENGINEERING

Declaration

In accordance with the appropriate regulations I hereby submit my thesis and I declare that:

1) the thesis embodies the results of my own work and has been composed by myself
2) where appropriate, I have made acknowledgement of the work of others and have made reference to work carried out in collaboration with other persons
3) the thesis is the correct version of the thesis for submission and is the same version as any electronic versions submitted*.
4) my thesis for the award referred to, deposited in the Heriot-Watt University Library, should be made available for loan or photocopying and be available via the Institutional Repository, subject to such conditions as the Librarian may require
5) I understand that as a student of the University I am required to abide by the Regulations of the University and to conform to its discipline.

* *Please note that it is the responsibility of the candidate to ensure that the correct version of the thesis is submitted.*

Signature of Candidate:		Date:	

Submission

Submitted By *(name in capitals):*	
Signature of Individual Submitting:	
Date Submitted:	

For Completion in the Student Service Centre (SSC)

Received in the SSC by *(name in capitals):*			
Method of Submission *(Handed in to SSC; posted through internal/external mail):*			
E-thesis Submitted ***(mandatory for final theses)***			
Signature:		Date:	

Table of Contents

List of Figures

Chapter One

Introduction

"The result of work is proportional to the consciousness in it"

Gurjiev.

This chapter provides an introduction to the importance of 4D seismic data as a valuable tool in reservoir simulation and reservoir management. It is well known that a wide range of reservoir parameters- both static and dynamic can be extracted from time-lapse data. Application of 4D data in simulation model updating is a widely used method for matching models; however, direct import of time-lapse attributes into simulation models is not so well developed. This thesis will discuss existing methods for incorporating 4D data into simulation and introduce a new, direct and easy to implement technique.

When interpreting 3D seismic data (i.e. baseline) we are dealing only with static reservoir data which reflect the geological settings of the field, such as structure, facies distribution, net-to-gross and, in some cases, porosity and saturation. However, by moving to the time-lapse seismic domain, it is possible to reveal dynamic reservoir data.

The following are benefits of obtaining dynamic reservoir parameters by utilising 4D:

- Improved understanding of aquifer influx and strength, as 4D integrated with well tests and production data can produce rather good results
- Flood optimisation and control
- Identification of sub seismic barriers and baffles
- Access unswept oil
- Drilling infill wells, better placement of producers and injectors
- Early recognition of waterfronts

All these options are possible due to the nature of time-lapse seismic. As an example, Figure 1.1 shows P-wave velocity changes induced from a range of production mechanisms. Further detailed fundamentals of 3D/4D interpretation can be found in Jack (1998).

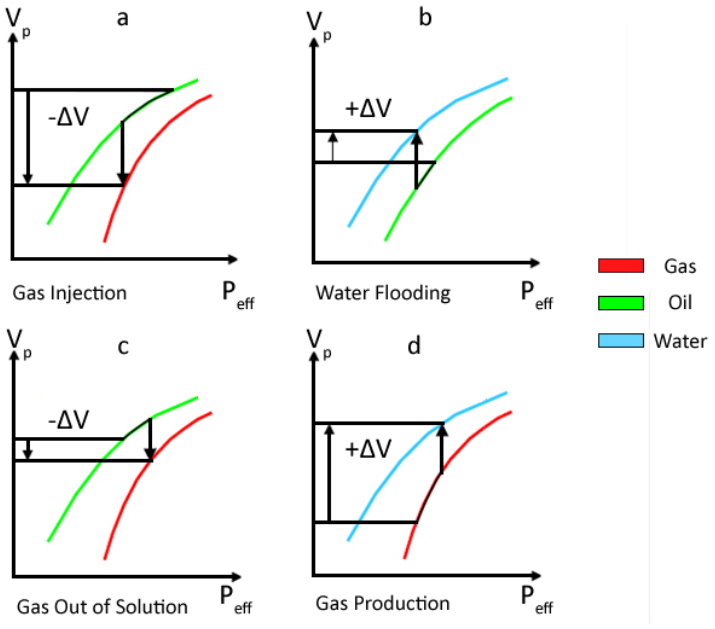

Figure 1.1 Generalised plots of P-wave velocity change for different production scenarios (after Marsh, 2004)

This figure represents simplified theory, but in practice the time-lapse signal is more complicated, as usually more than one reservoir property changes simultaneously, for example, it is not only an increase in water saturation that occurs. For instance, increased gas saturation during the gas injection operation increases the overall compressibility of the rock, reducing the seismic wave velocity. On the other hand, the injected gas volume may cause pressure increase within an area near wellbore, which reduces the effective stress– which will also reduce the velocity as shown in Figure 1.1 a. In this case, 4D signals related to increased gas saturation may be masked by 4D response driven by pressure build-up as both effects are associated with the same polarity. On the other hand, interpretation of the 4D signal as result of pressure and saturation change with contradictory effects on seismic velocity is quite challenging situation. This situation is associated with a variety of production scenarios, such as water injection and gas coming out of solution due to reservoir pressure below bubble point (see Figure 1.1 c and 1.1b). For instance, seismic velocity is reduced by increased pressure, but increased by increased water saturation within an area near injectors, which result in the weakening of 4D response associated with either production effect.

The more complicated and realistic situation presented in Figure 1.2.

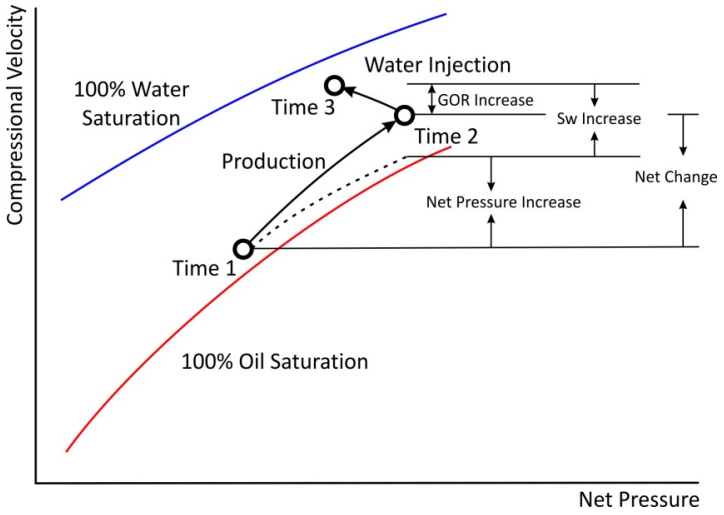

Figure 1.2 Combined effects of oil production and water injection on the P-wave velocity. As the field is produces, pressure drops, thus increasing the overburden pressure, and, consequently, water saturation. Then, as the pressure maintenance operation starts, water is injected, formation pressure increases, and thus overburden pressure decreases and water saturation increases. After Wang (1997) and Oldenzeil (2007)

According to Calvert (Calvert 2005), if we survey a producing oil or gas field before and during the production, we can estimate the changes that have occurred in the reservoir. As

hydrocarbons are replaced by water and as pressure changes (as a result of production), the seismic velocity and density of the reservoir change, so based on 4D surveys, we can measure effects of changes and identify where the changes are occurring in the reservoir (Figure 1.3).

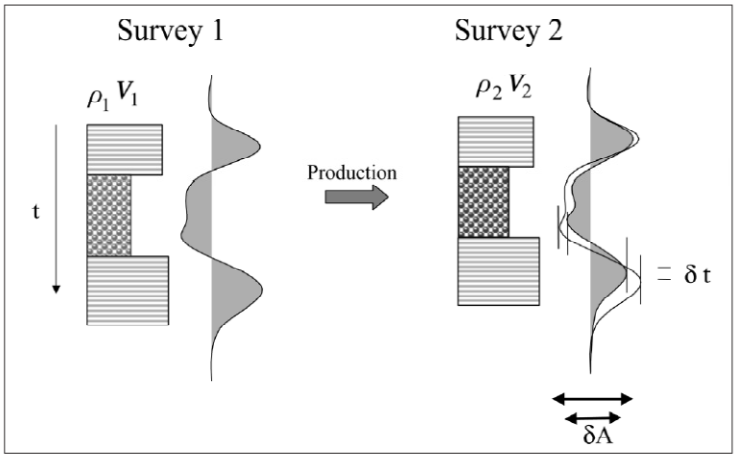

Figure 1.3 The simple physical principle of the 4D seismic. The Vp, Vs and density of a reservoir change as a result of production, thereby giving response changes that appear on seismic lines as amplitude and timing changes (Calvert 2005).

1.1 Interpretation and implementation

If we talk about reservoir 'dynamics' we should understand which reservoir properties can change with time, as all these changes will have an impact on the seismic signal. According to Jack (1998), these parameters can be divided into two groups, primary:

- Pore fluid-related (saturation, fluid type, viscosity)
- Pore pressure
- Temperature

and secondary:

- Compaction
- Porosity etc.

1.2 Inconsistencies between the 4D seismic and engineering domains

4D seismic is non-unique, due to number of factors, such as seismic noise, repeatability issues and etc., as well its' results strongly depends on seismic interpreter. Hence, it needs to be validated. A similar situation arises with the simulation model, which has related uncertainties which will be discussed later. Thus, these two domains can be used for cross validation of the results and uncertainty reduction in both domains. Due to the qualitative nature of 4D seismic interpretation, it relies on both the simulation model and production data at the same time. Seismic interpretation is based on a comparison of seismic changes with changes in saturation and pressure in the simulation model. This model depends mostly on the production data, with appropriate consideration for the 3D seismic, geology and 4D data, if this is available. Usually the results of the simulation model and the time-lapse seismic interpretation are comparable results, and usually their visual patterns, at least, show similarity.

However, this is valid only if the 4D has excellent quality (examples will be presented in following part). However, what if it is poor with large uncertainties? In this case, the simulation model will be irreplaceable for understanding of the time-lapse signal, yet this understanding may still be incomplete. In this case the integration of the time-lapse seismic with reservoir engineering problem arises. Usually there is a huge amount of data in the different domains, and the integration needs to be carried out quickly to increase the benefit, and finally any matching process or process of integration will be non-unique.

To compare the observed seismic with the simulation model, it is necessary to create a synthetic seismic from simulation model. The synthetic one is calculated using the Sim2Seis (detailed description will be provided in section 3.2.3) in-house software developed in Edinburgh Time Lapse Project (ETLP), which converts the simulated changes in the simulation model (pressure and saturation) to the 4D response . Differences between the observed and synthetic may lead to uncertainty in 4D interpretation. Hence, there is a risk in simply modifying the simulation model to create a similar response in the seismic without understanding the real meaning of the unexpected signal. So, how to integrate time-lapse data and reservoir engineering data?

1.3 Integration of time-lapse data into simulation

Integration of time-lapse data with reservoir engineering is associated with following challenges: disparate data, a huge amount of engineering data, especially production data, issues of parameterisation non-uniqueness and the need for a sufficiently rapid procedure to integrate these different domains. Time-lapse data are usually utilised in simulation model only in the form of 2D maps (areal data, not volumetric) - although this approach does not allow full integration of seismic data into the simulation process. It nevertheless gives solid guidelines for reservoir engineer for history matching, in the case of proper seismic interpretation. However, these guidelines are mostly qualitative; and do not give certain values of properties.

Sometimes 4D results may be mistakenly interpreted, for example, the fluid front could be misinterpreted as a barrier at the early production stage, and only later, after next monitoring of the water front will it be interpreted correctly. The same situation exists with reservoir pressure changes. So, through integration of all the available 4D surveys it is possible to reduce interpretation-related uncertainties. The quantitative approach supposes the presence of distinct reservoir regions which can be changed in simulation model and values of properties which also need to be changed.

1.3.1 Selected examples

This part presents existing successful examples of incorporation of 4D seismic into simulation and geological models.

The first example- is the well-known Marlim Field located in the Brazilian offshore area. A detailed description of this field is given by Olivera (2008). This paper describes how 4D-seismic results were incorporated into the geological model. The field is a turbidite reservoir with the reservoir facies comprising amalgamated graded beds of poorly consolidated, unstratified, medium- to fine-grained sandstones.

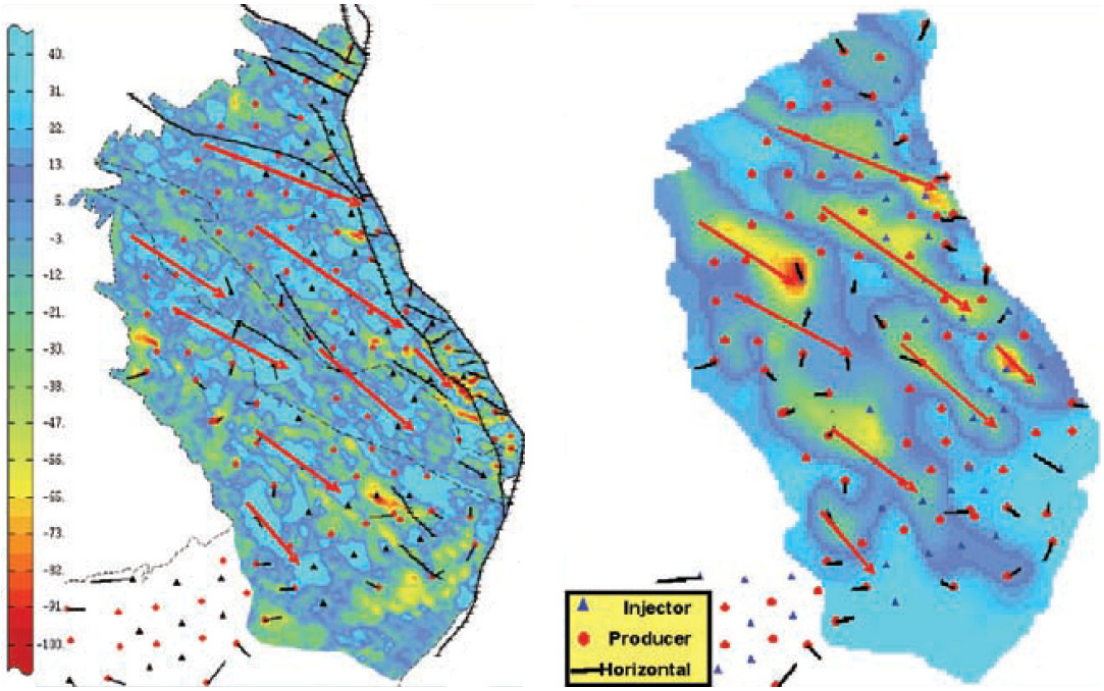

Figure 1.4 Left: reservoir amplitude difference map (Monitor 2005 - baseline 1997). Light blue: oil replacement by water. Right: absolute horizantal permeability map derived from 4D seismic and drill stem test (DST). (Olivera 2008)

Figure 1.4 represents the map of amplitude difference between baseline and monitor surveys, which reflects anisotropy in water displacement, and the permeability map based on this anisotropy. Latter map was finally used for history matching.

Figure 1.5 demonstrates differences as a result of utilising different approaches in history matching (this will be discussed in the next Chapter). B is the map derived after 1 year of fitting the data into the model and the matching process (Olivera 2008): however, the result still does not look geological. D illustrates improvements in the permeability map after integrating 4D seismic results into the history matching process, which takes about 3 months.

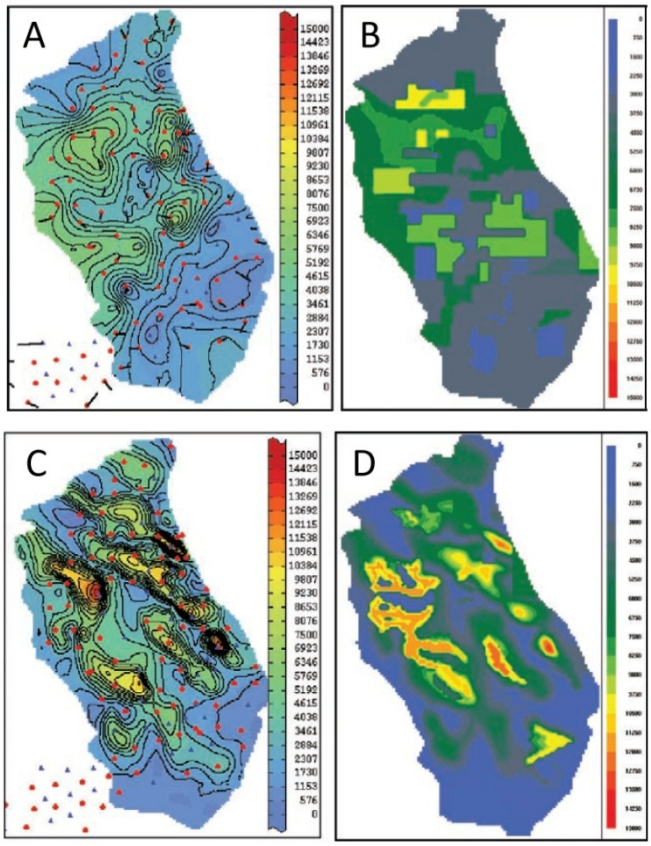

Figure 1.5 A: original horizontal permeability from DST. B: the same map changed after history matching but before 4D seismic interpretation. C: horizontal permeability map from 4D seismic. D: the same map after 4D seismic results were integrated into simulation model and after history matching (Olivera 2008).

Hence, this example clearly demonstrates the possibility of successful integration of two different domains- seismic and reservoir engineering. It shows that 4D interpretation can be used in matching, with rather good results.

Another example of 4D application is presented by Lumley et al. (2001): Meren Field, Nigeria: a 4D seismic case study. Unfortunately, here, the time-lapse interpretation results were not been used for the simulation model update, but sufficient improvements were obtained based on 4D.

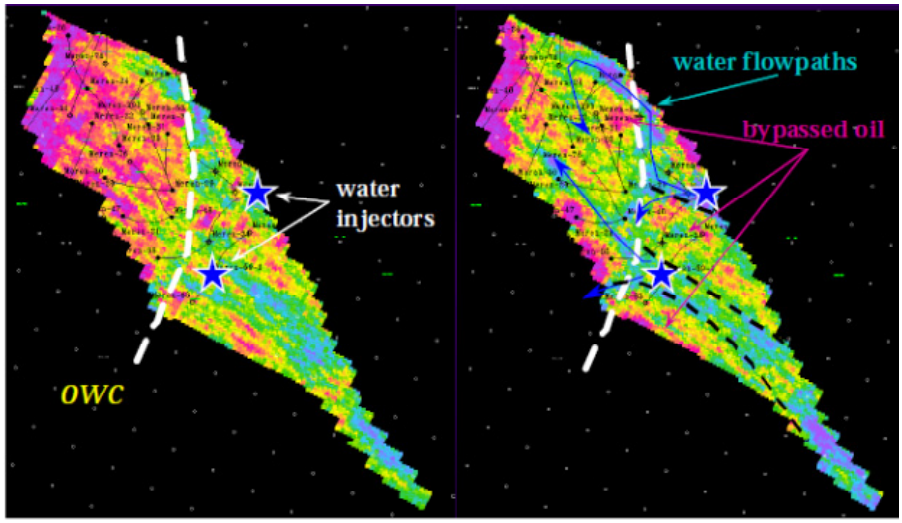

Figure 1.6 Meren E-05 reservoir: extracted horizon amplitude maps from 1987 survey (left) and 1996 survey (right). The blue stars show the positions of the two water injectors. The oil-water contact from well data (dashed white line) correlates with the 1987 seismic, but not the 1996. The 4D data suggest there are areas of bypassed oil, isolated from the injectors by sealing faults (dashed black lines). Additionally, the seismic images show highly heterogeneous water flow along channels and across a leaking fault into an adjacent production block (Lumley, et al. 2001)

As a result of this research potential bypassed oil zones were derived, due to stratigraphic channels, which control the fluid paths. This fact is approved by injected water from two injectors which appears to be channel-like in flow (Lumley, et al. 2001). Thus, these features can be included in the geological model, because the stratigraphic channel sufficiently affects the geological setting. They will then be presented in the simulation model, and their properties can be changed in order for proper matching.

The application of time-lapse on the Snorre field (Figure 1.7) allowed the disclosure of fluid pathways in the reservoir with integration of production data- injected radioactive tracers. Again very nice example of integration of different data sources in the reservoir management.

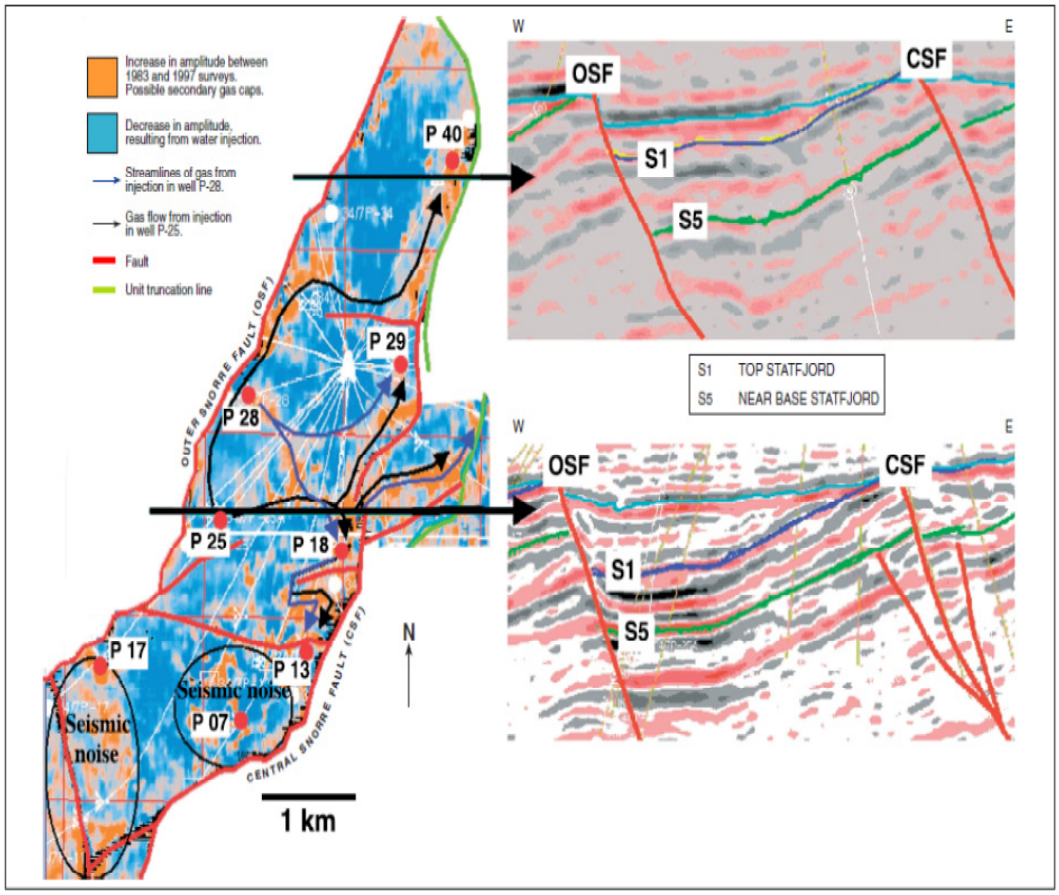

Figure 1.7 Fluid flow patterns in the Central Fault Block based on production performance and injected radioactive traces, superimposed on a seismic amplitude map (difference 1983-1997) for Statfjord units S1-S2, together with two W-E 3D seismic sections that illustrate structural settings in the northern and central Snorre Field (Sverdrup, Helgesen and Vold 2003). OSF- Outer Snorre Fault, CSF- Central Snorre Fault.

1.4 History matching

Reservoir engineering has to deal with something which is impossible to see or touch- the reservoir. The ultimate goal of simulation is to correctly understand the current state of the field and predict reservoir performance in order to optimise the project through facility maintenance, well-placement optimisation and identification of new well drilling opportunities. Mike Carlson in his 'Practical Reservoir Simulation' wrote- in this regard, a reservoir simulation is superb (Carlson 2003). It allows one to test quantitatively how different processes affect production results and to evaluate complex geometries which cannot be solved easily, if at all, by analytical equations.

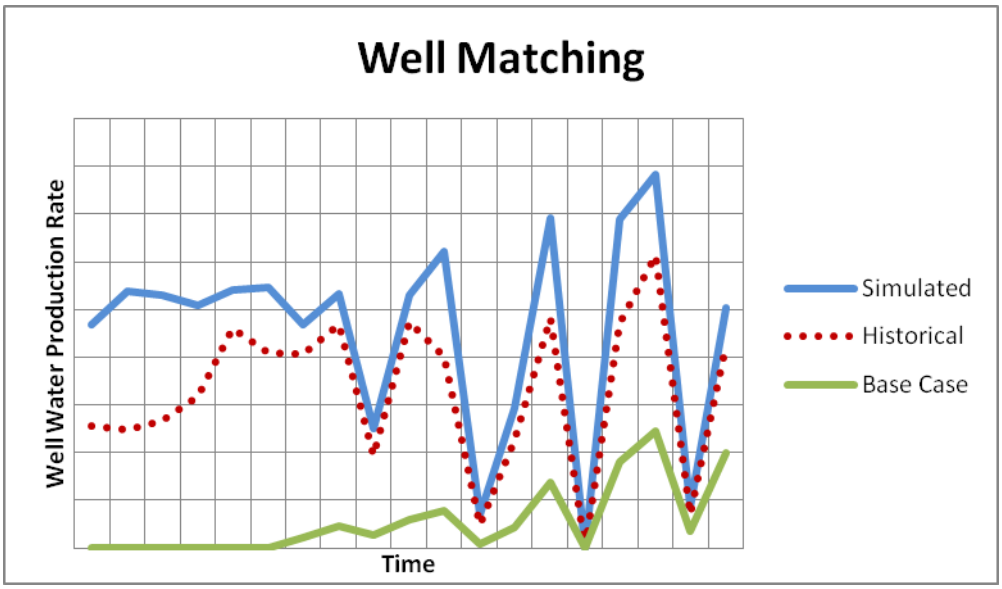

Figure 1.8 Well matching. The ultimate aim of history matching is to make the simulated curve (blue) similar to the historical data (red dotted curve) by alteration of the model parameters. The results of these changes are usually reflected in a decrease in the misfit of changes from the base case (green) to the blue curve.

The model, which can be used for prediction, should be validated against observed data at the wells. Therefore, the simulation model will be consistent with observed data with following misfit:

$$F = \frac{1}{2}\sum_{i=1}^{n_{obs}} w_i (d_i^{obs} - d_i^{sim})^2 \tag{1.1}$$

Where n_{obs} is the number of measurements of the production data, d_i is the i-th measurement of production data and w_i are weighting factors, which depends on certainty of data (Johansen 2008). For example, with transmissibility (see detailed discussion in chapter 4) as the unknown parameter the history matching problem can be stated as following:

$$T' = \underset{T}{Argmin}[F(T)] \tag{1.2}$$

In addition, history matching workflows are characterised by an enormous diversity of problem statements, because every reservoir may be unique (Schulze-Reigert R. 2007).

Source of Static and Dynamic Reservoir Data				
Reservoir Structural Data	Structure	Thickness	Fluid Contacts	Reservoir Geometry
	Geophysical data	Well logging data	Well logging data	3D Seismic data
	Well top data	3D seismic data	Well testing and pressure data	Facies analysis
	Well log data	Geology and geostatistics	Seismic data	Well correlation
Reservoir Geological Data	Facies	Grain Size Distribution	PTS Distribution	Pore Compressibility
	Geophysical data	Thin section analysis	Thin Section Analysis	Special core analysis
	Core data	NMR	Special core analysis	Correlation
	Well log data	X-Ray, SEM and CAT Scan	Well log data	Field data
Reservoir Rock Properties	Fluid Composition	Fluid PVT Properties	Fluid Viscosity	Fluid IFT Data
	Core Data	Core data	Core data	Core data
		Well log data	Well test data	Well log data
		Well test data	Log-derived permeability	Well test data
Reservoir Fluid Properties	Fluid Composition	Fluid PVT Properties	Fluid Viscosity	Fluid IFT Data
	PVT Samples	PVT Experiments	Lab Experiments	Lab Experiments
	Production testing	Correlation	Correlation	Correlation
		Equation of State		
Rock-Fluid Properties	Fluid Saturation	Wettability	Capillary Pressure	Relative Permeability
	Core data	SCAL	SCAL	SCAL
	OH and CH log		Well log data	Well test data
	Well test data			

Figure 1.9 Required simulation data and their sources (Schulze-Reigert R. 2007). Green highlight defines the main data that can be extracted from 4D analysis.

Traditional (integrated or multidisciplinary) combines introduced types of data. As mentioned before, all reservoir data can be divided into static and dynamic data. Usually static data provides information about the reservoir framework and solid properties (poro-perm and saturation) in well locations. Dynamic data provide data about fluid movements in the reservoir. Most of the dynamic data are volumetric source data.

Production data can be and usually are very important sources of information about the reservoir, reflecting information that cannot be obtained using any other source of data, so dynamic data should be used to update geological and simulation models. Generally speaking, "history matching" is the process of incorporation of this information into the simulation model. Matching is a necessary stage of studies, as prediction is not valid without it. However, it is a very time consuming and challenging task: the main goal is to in integrate information from production (or dynamic) data into the modeling process and to obtain uncertainty of the predictions based on this model.

It should be noted that the correct understanding of dynamic data is much broader than production data. Usually production data is data obtained from the wells, such rates and pressure. In addition to such production data, dynamic data, can include time-lapse seismic data as well. History is a phase of reservoir study that will take up the largest portion of study time (Carlson, 2008). Apart from the production data, there are some other types of data usually available and need to be integrated into simulation model- design of wells (or facilities), including initial reservoir fluid distribution, a fluid model and near wellbore perfomance. However, the engineer needs to be aware of uncertainties related to his or her project.

1.4.1 Conventional history matching (without 4D seismic)

Firstly I will consider history matching without time-lapse data, because it is not possible to utilise 4D seismic in history matching from first data of production, as time-lapse data are usually available only after 1-2 years of production and are sometimes inapplicable. In this part I will consider different approaches in history matching, depending on data availability.

1.4.2 "Classical" history matching approach

There are number of publications which have presented guidance for history matching: for example Crichlow (1977) suggests varying (within any reasonable range) the following parameters: rock data (porosity, permeability, thickness, saturation); fluid data (compressibilities, PVT, viscosity) and relative permeability data, and also individual well completion data (skin, bottomhole flowing pressure). Mattax and Dalton (1990) put forward a systematic approach by adding prioritisation to the guidelines, as well as suggesting changes should be avoided. The most classical and systematic workflow to history matching is presented by Carlson in his Practical Reservoir Simulation (see Figure 1.10).

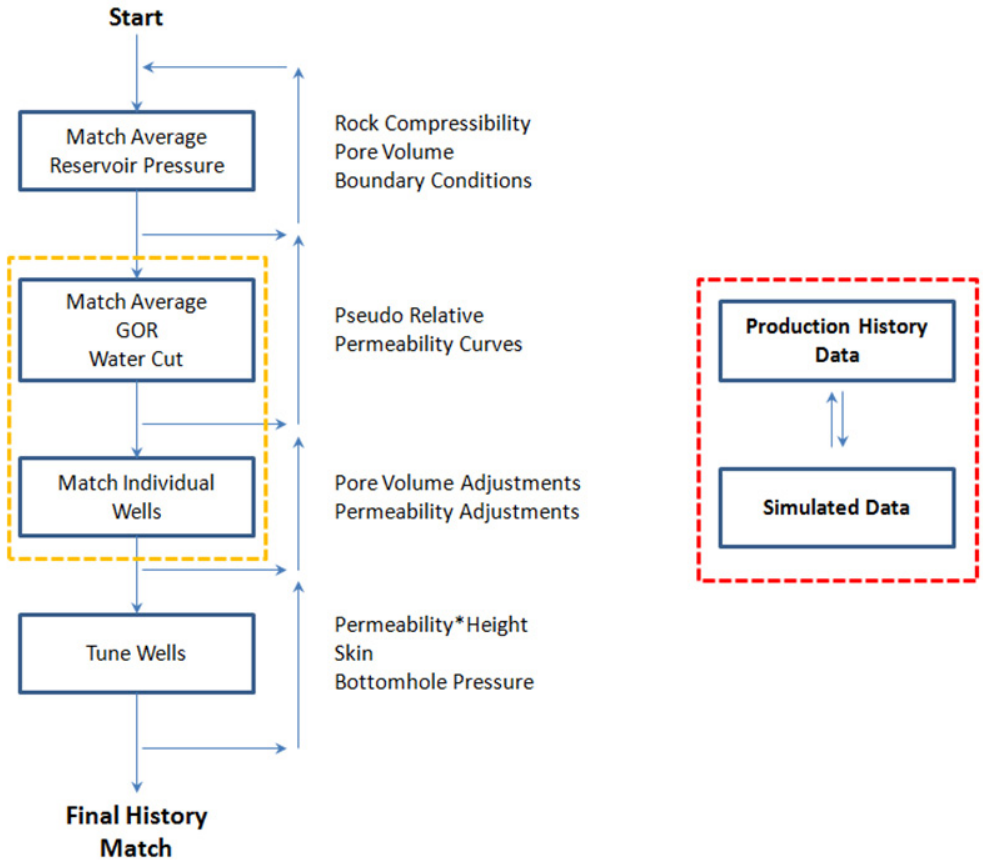

Figure 1.10 Systematic approach to history matching (Carlson 2003). In red frame- data need to be compared.

The initial parameter for matching is average reservoir pressure, which can usually be tuned by varying rock compressibility, pore volume or boundary conditions; the latter two are some approximation (derivative) of the connectivity function of reservoir. It is then recommended

to match the average gas-oil ratio and water cut, for which the most applicable method is to change the relative permeability curves for different fluids. Finally, it is necessary to match the individual wells and tune them. A convergence criterion is the similarity of the simulated and observed production data (in the red frame in Figure 1.10).Hence, although there are numerous parameters that can be changed for the aims of history matching, the main issue for matching is the integration between the geology and the reservoir model (Carlson, 2008).

Indeed, the geological input is most important in the matching and simulation process, as nearly all history matching issues can be solved just by mathematics, but if one did this without any attention to geology, the model would fail in prediction. So, the more geology data we add to history matching the better the result that can be expected. Due to the nature of existing reservoir uncertainties and nature of the history matching process, there is no one model which will satisfy the stated problem, none of the final models will provide a unique answer. The problem of non-uniqueness of history matching results will be discussed in the following chapters.

1.4.3 Using sophisticated numerical methods

The main idea behind using numerical methods is to save the valuable time of the reservoir engineer. There are number of numerical techniques for history matching presented in commercial software products and used in research groups (not commercialised). There are also a number of geostatistically based methods; the main advantage of these is that the resulting reservoir model is easily constrained to statistical properties and other types of information regarding the geology (Johansen, 2008).

According to Schulze-Reigert and Ghedan, the following optimization techniques are utilized in history matching:

- Evolutionary Algorithms (Soleng, 1999, Romero 2000, Schulze-Reigert, 2001, Williams, 2004).
- Gradient techniques (Anterion, 1989, Bissell, 1994, Lepine, 1998, Roggero, 1998, Hu, 2000).
- Response surface modeling and optimization on the response surface (Eide, 1994, Little, 2006, Cullick, 2006).

- Hybrid schemes which couple different optimization techniques (Gomez, 1999, Landa, 2003, Castellini, 2006).
- Ensemble Kalman Filter techniques (Naevdal, 2003, Evensen, 2007).

Most of these methods are concerned with issues such as non-uniqueness and the risk of trapping in local minima, requiring many iterations. Adjoint methods are gradient-driven methods in which the speed has been greatly increased by implementing derivatives calculated internally in the simulator (Valstar 2001). More global optimization techniques such as genetic algorithms and simulated annealing have the advantage that the risk of trapping in local minima is smaller; however, even more iterations are required to obtain a reasonable history match (Zhang, et al. 2005).

The common weakness of all statistical methods is geological data integration. Even if the software packages obtain the acceptable level of matching, control by the reservoir engineer is still needed. According to Carlson, most of the statistical techniques used for matching have not been successful. As discussed by Fisher and Jolley (2007), history matches do not 'prove' a model's validity – they can be achieved in models that bear little resemblance to the 'true' geology, and do not necessarily predict true flow and depletion behavior.

1.4.4 Using 4D

In this part I will look how reservoir engineers can use 4D results to improve and update simulation models.

As discussed above, time-lapse seismic is valuable tool for reservoir monitoring and an additional source of dynamic information for simulation and field development optimisation. What are reservoir models? They are represented by number of properties, such as porosity, permeability, saturations (water, oil and gas) and pressures. What will change in the models and history matching, if we have time-lapse data? A common workflow for matching using 4D data is presented in Figure 1.11. The key difference is the presence of a petroelastic model (PEM). This comes from seismic surveys that measure the changes in amplitudes and velocity of acoustic waves: other words- dynamic data from 4D is the combined signature of the well's activity and geology. Geology by itself is static, so by adding time-lapse data into the matching process we build the interrelation of the simulation model and the geology.

However, to understand and measure the mismatch of the reservoir model and the observed 4D, it is necessary to use common domain for them. A widely used method is to generate synthetic seismic data from a simulation model using PEM. PEM is a source of additional uncertainties, and to reduce these and make the PEM model applicable, it should be calibrated to measured elastic properties.

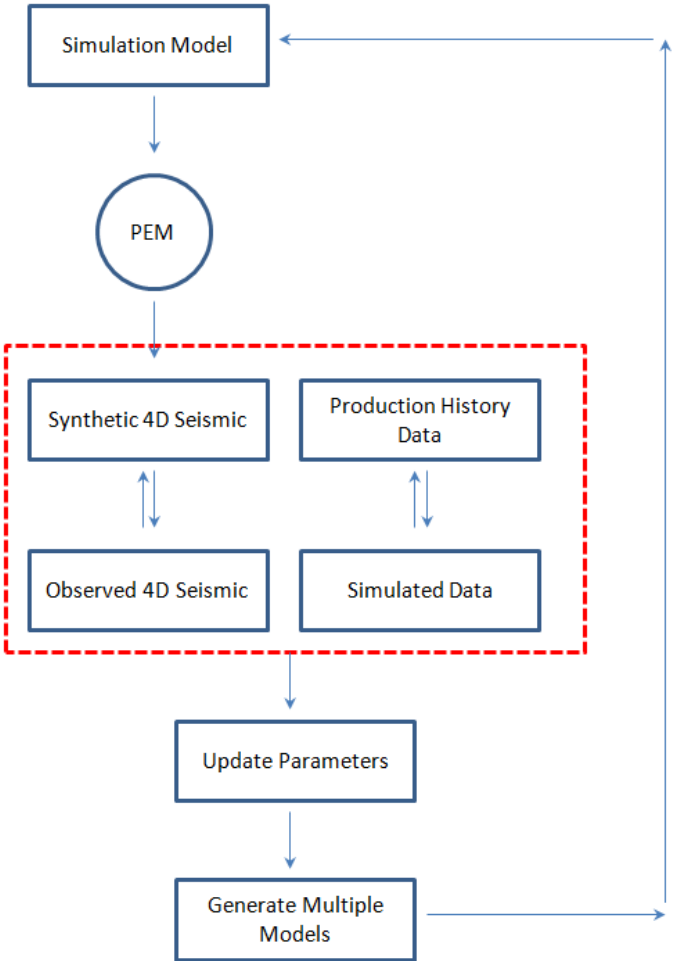

Figure 1.11 Typical History Matching Workflow Using Time-Lapse Data. After the application of PEM on the simulation model, we generate synthetic time-lapse seismic and compare it with observed data, same time compare history production data and simulated production data. Based on these- we can make a decision as to which property (usually permeability) and needs to be changed, and where, to match the observed data.

Jack (1998) recommends the following points regarding simulator and seismic: use qualitative information from time-lapse seismic to test different scenarios and where there is disagreement between observed and predicted seismic, update the reservoir model. In addition, simulation studies, properly tuned for production data, can provide valuable predictions about areas with pressure or saturation changes which can be utilised in feasibility

studies. Calvert (2005), after analysing a number of field cases wrote- "it appears that we can expect 4D monitoring at least to provide forecasts that successfully predict details a short time into the future and fewer details farther ahead, as is true for weather forecasts". There are number of studies of successful uses of 4D in history matching. Examples of these are the matching of the Draugen field (Guderian, et al. 2003), Gullfaks field (Talukdar and Instefjord 2008) and the Girassol field (Jourdan, Lefeuvre and Dubucq 2006).

1.4.5 Seismic History Matching (SHM) and other methods

Utilising dynamic data sources such as 4D seismic in the history matching process is a rather new area of research, but a number of methods and techniques exist. One should be aware this additional data source in matching has its own related uncertainties and the final matching will be still non-unique, but more constrained. One of the established methods was presented by Vasco et al. (1999), Vasco et al. (2000), and Vasco and Datta-Gupta (2001). This technique is based on streamline principles: streamlines do not cross each other, so a 3D problem can be partitioned into a series of 1D problems, which are easy to solve. Another well-known technique was presented by Stephen and MacBeth (2005, 2006 and 2007), who explain it thus: "A time to depth conversion is used to generate maps of observed seismic which can then be compared to predicted seismic along with production data. Models are then updated until set of best models is obtained. The result of this process generates a Posterior Probability Density function, which can then be resampled."

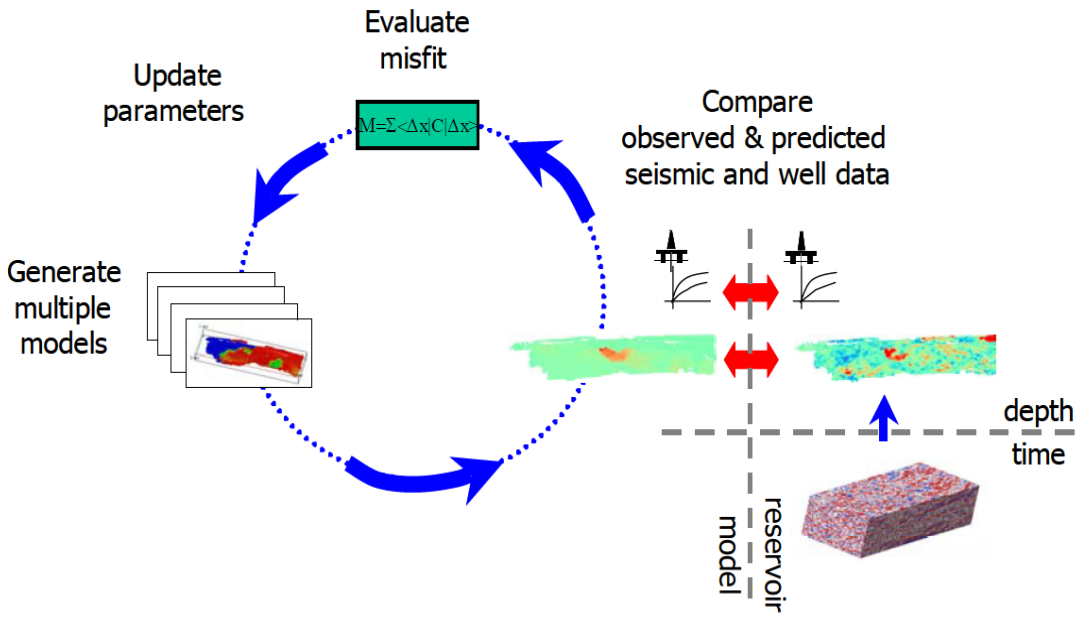

Figure 1.12 Schematic of the iterative automatic history matching process. (Stephen and MacBeth 2006)

Another interesting method, 4D seismic history matching using flood front information, was presented by Jin et al. (2011).

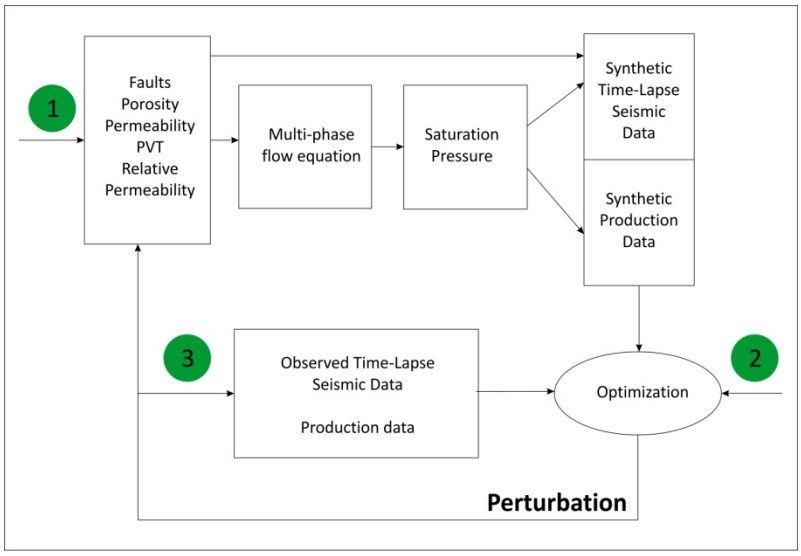

Figure 1.13 General workflow of method by Jin.(Jin, et al. 2011)

The main idea of this technique is to perturb the uncertain parameters, identified by simultaneously comparing the synthetic production and 4D seismic data with the measurements. Key steps in this method are:

- Identify sensitive uncertainty parameters.
- Choose appropriate optimisation method based on the applicability and efficiency.
- Use scaled 4D seismic s input. Different inputs can be used: amplitude difference, impedance difference and differences in reservoir properties.

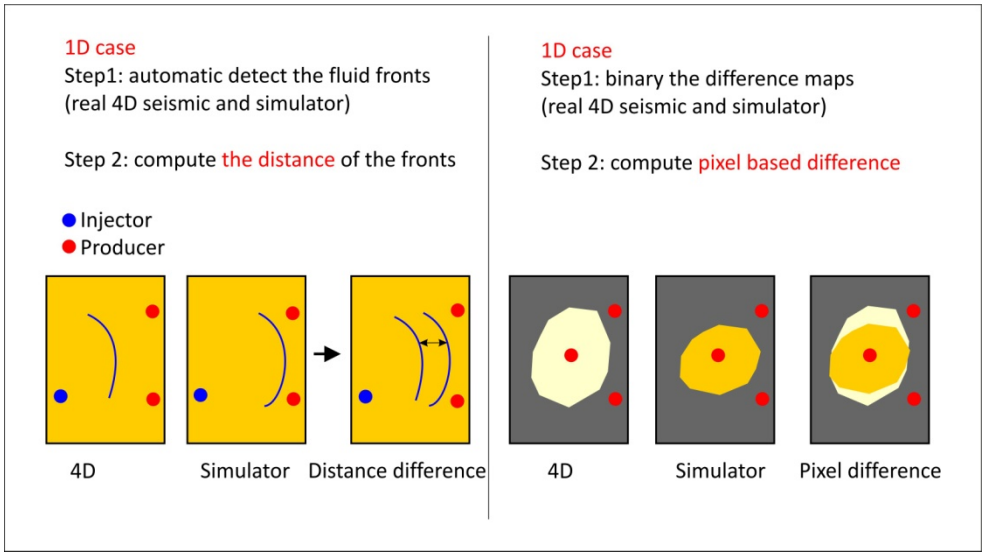

Figure 1.14 Fluid front analysis for history matching. (Jin, et al. 2011)

As this process is iterative, optimisation is the key factor in the workflow.

The scale difference between the actual 4D seismic difference and the changes in simulated reservoir properties is handled by comparing the front difference or areal region change of fluid flow, as shown in Figure 1.14. This is very useful to link directly the 4D seismic data with the key reservoir property changes used in the integrated workflow. Thus, through valid assumptions and simplification, the two disciplines, geoscience and reservoir engineering, can be integrated with minimum efforts (Jin, et al. 2011). All the methods described are proved with real field case studies. Indeed, the main criterion for successful implementation is proper integration of geological data.

The Gradual Deformation Method (GDM) was presented by Hu (2000) as a method to represent and constrain models (history matching models) to all available static information. For the detailed description of the method reader may refer the paper by Hu. Here I will briefly discuss the technique. Roggero et al. (2012) observed that, in most cases, simulations performed with different model realisations do not really reflect the observed dynamic behaviour of the field; therefore, engineers need to modify these realisations to perform the appropriate match with dynamic data (production history, 4D seismic etc.). GDM allows the

realisations to be adjusted and sufficiently improve matching while preserving the overall geological structure (Hu 2000). In other words, this method directly changes the geostatistical model during the matching process, while keeping the average properties unchanged, such as the variogram and facies proportions. The main idea behind the method is to control the stochastic simulation process from a continuous parameter, usually called the deformation parameter, instead of a random value (seed). Whatever the value of the deformation parameter, it corresponds to a new realisation of the reservoir model. The method is valid not only for Gaussian models, but for non-Gaussian stochastic simulations as well (Roggero, et al. 2012).

The new model realisation is formed from set of old models as a simple linear combination:

$$M_{new} = \sum_{i=1}^{N_r} \alpha_i M_i \tag{1.3}$$

However, sometimes changing realisations is not enough for appropriate matching of 4D seismic data. This can happen due to the facies proportion or variogram, which are the constants in GDM.

The Facies Proportion Calibration Method (FPMC) method allows the geological model realisations to be modified by the matching process while keeping the average geostatistical properties unchanged, for example facies proportions and variograms. The idea is that in adjusting of a given facies group with respect to the average proportion of a larger facies selection, this can be done either globally or locally. According to Roggero et al. (2012), the main steps of the process are as follows:

- Determine reservoir parts/zones/areas in which facies proportions have to be fixed/constrained.
- Define the facies to be changed by the transformation. This usually called "selection".
- Within the selection, select a facies sub-group to define a second entity called "association".
- Define a global parameter as a proportion ratio between facies in the association and in the selection.
- The algorithm can now calculate new average proportions for the selected facies.

It should be understood that changing petrophysical properties is sometimes not enough for proper history matching, because petrophysical trends have a sufficient impact on the reservoir dynamic behaviour, even more than just values of properties. These properties usually have a quite significant uncertainty. There are examples of this method of implementation: one of the successful ones is the Girassol case (Roggero et al. 2007). Actually, the Facies Proportion Calibration Method is complementary with the Gradual Deformation Method and the main advantage, according to Roggero, is the possibility to drive the average spatial trends, whereas gradual deformations affect the local distribution of heterogeneities with fixed facies proportions.

1.4.6 Non-uniqueness of history matching

Here I will look briefly into the main history matching problem- non-uniqueness. It is related to any matching process, independently of techniques utilised. There can be millions of reservoir-model parameters, yet often there are only a few wells with flow rates and pressure declines that are essentially controlled by tank size, fluid mobility and a skin or input resistance to the well (Calvert 2005). On the basis of these data, it is possible to build a number of model that satisfy the data. To minimise the effect of non-uniqueness it is necessary to use more data from different sources, for example adding time-lapse data into the objective function will generally cause a reduction in non-uniqueness, and correspondingly, a better match. What is the reason behind these improvements? First of all seismic data (3D or 4D) accounts for spatial reservoir properties, not only in well positions; moreover time-lapse seismic accounts for dynamic changes in the reservoir. According to Calvert: “It also appears that the model might be determined best over the interval passed by the fluid front” (see Figure 1.15). This statement is equally applicable for any matching technique.

The simulation model can be determined using 4D seismic data with the appropriate level of uncertainty just over the intervals passed by the fluid front (Calvert 2005). So 4D is able to produce nice simulation model for the time interval covered by these surveys, and short-term predictions (depending on conditions) will be good, but long-term prediction can be unreliable; however, this is the common feature for any model used for prediction. The good illustration of this is in the following diagram.

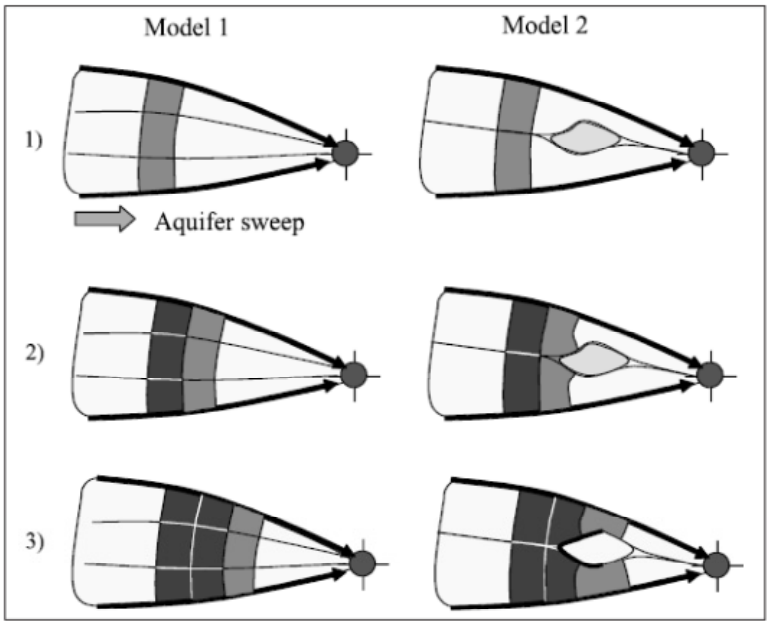

Figure 1.15 We cannot distinguish between model 1 and 2, until survey 2 or 3. We have good control only of the swept area, unless we have other information. (Calvert 2005)

Thus, to reduce the level of non-uniqueness of history matching, we need to integrate all the available reservoir data.

1.4.7 Summary

The choice of matching method depends on the available data and reservoir engineers' experience. Available reservoir data depends both on economics and existing uncertainties (including geological settings), so it is not right to compare history matching methods without 4D with techniques which include 4D data- they are on different levels of complexity and results. Nevertheless, still some key features can be listed. According to MacBeth and Stephen:

Conventional history matching:

1. Lacks spatial resolution. Situations then 3D seismic are used is rather rare. So there is a lack of understanding of the dynamic response of interwell areas.

2. Mostly manual. It can be automated, but needs control to be exercised over its results. Usually 'semi-automated' schemes are utilised.
3. Highly non-unique. The degree of non-uniqueness depends only on the amount of available data and level of its integration.

History matching using time-lapse data.

1. Time-lapse- spatial and temporal. Here the problem of special resolution is solved: the interwell area can be described with confidence at the time of the monitor surveys.
2. 'Semi-automated' or 'automated (for example, Seismic History Matching). It can also be performed manually.
3. Quantified or 'semi-quantified'.
4. Uncertainty analysis.

The main point of any history matching process is appropriate prediction of field behaviour, it is possible to reach this only with proper integration of geological settings into the models.

1.5 Motivation and challenge of thesis

During geomodelling (see Figure 1.16) and simulation modelling two types of data are presented:

Static data- such as core data, wireline log data, geological data (sedimentology and statigraphy), PVT data. Part of this data can be derived (by interpretation) from 3D seismic data (structural model, deposition environment, even poro-perm data) and this approach is well established. In addition, 3D seismic analysis often provides direct determination (validation) of geobodies and immediately utilises them in the process of geomodelling (Chapin, 2000).

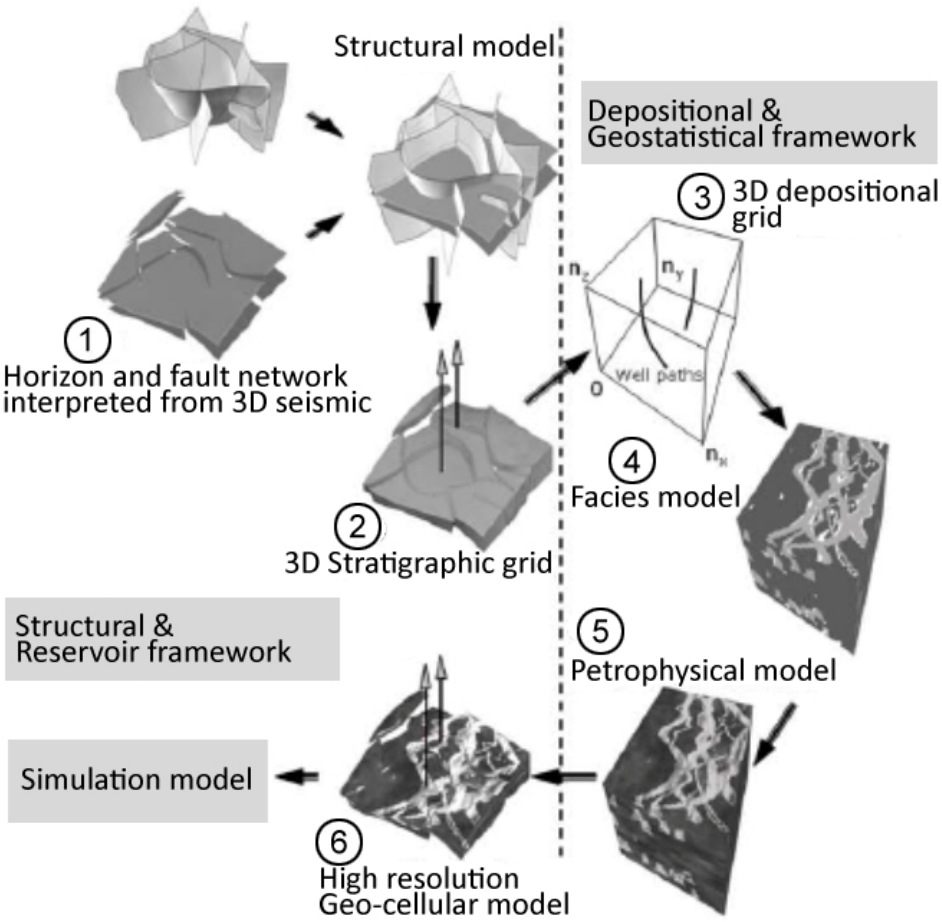

Figure 1.16. Step-by-step workflow for building geomodel (Caers 2005)

Dynamic data- unfortunately, this data is not abundant, and there are very few sources of it, including production data with production logging and 4D seismic data. Moreover, the main challenge is using this 4D data in the same domain in the simulation model.

The ultimate goal of this work is the development of a technique for using direct time-lapse data in a simulation model, especially for history matching purposes. In addition, this technique should be easy and fast to implement. It is clear, with rapid growth in the number of 4D surveys that the volume of reservoir data available is growing as well. Moreover, this information reflects changes in the reservoir, so it is essentially dynamic data, although, as was mentioned before, it is possible to clarify geological settings using 4D, as well. Inevitably, questions arise about the qualitative implementation of these data in already available domains, for example in a simulation model. It needs to be noted, that a simulation model is just a model; it is not an exact representation of subsurface but has numerous related uncertainties. The only data we can be sure about is well data, although with some degree of

related uncertainty. It is possible to calibrate 3D seismic for VSP in wells, but how we should calibrate 4D data? We need to answer the question of how to tie well data (dynamic-production data, pressures and etc.) with dynamic information based on time-lapse surveys. It is clear that material balance theory has a direct application to discussing these problems and should be applied during the analysis. We also need to question why well data need to be connected with seismic data. Wells (production or injection) are continually inducing changes in the reservoir, mostly, but not only, in pressure and saturation) (see Figure 1.17) but seismic only catches produced changes in the reservoir. According to Schulze-Reigert, reservoir data are either point-sourced or volume-sourced, point-source data are volumetrically insignificant, while volume-source data are volumetrically significant (Schulze-Reigert R. 2007). Even well is a point in field scale, changes which are caused by well activity are volumetrically significant and, indeed, if we use 4D seismic these changes are volume-source data. Therefore, the challenge of this work is to understand the dynamic relations of well-seismic data and find the geological background for this, and then to integrate these results into the simulation model in fast manner.

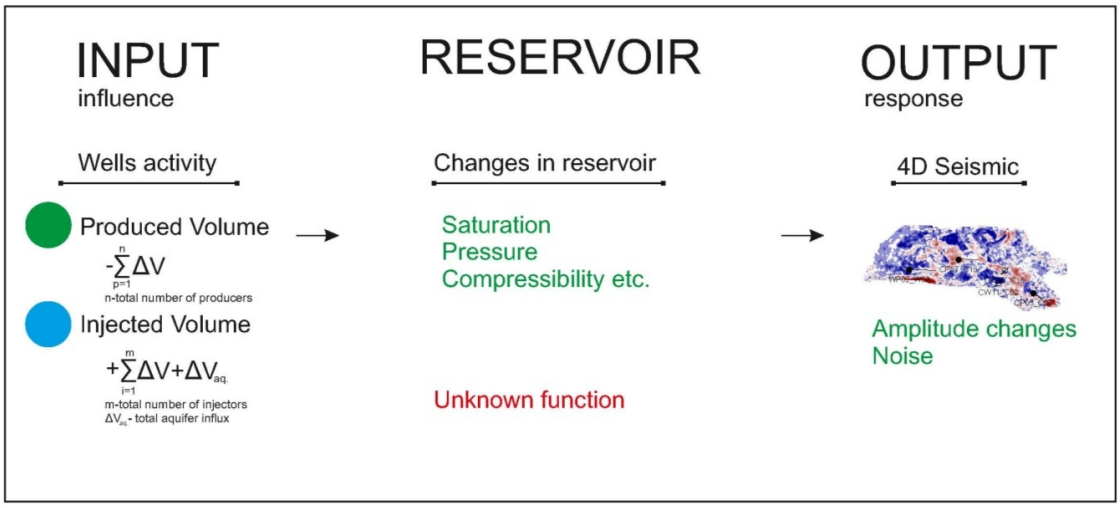

Figure 1.17. Relation of well activity and time-lapse seismic response. Visualisation of causality in seismic data due to well activity

1.6 Thesis outline

In this chapter I have covered existing history matching techniques with all corresponding advantages and disadvantages. There is an appropriate place for these methods in modern

industry, whether they are they easy to implement or not. The main data sources (static and dynamic) for matching with associated uncertainties were then analysed, to consider which aspects affect matching. Finally, the addition of 4D seismic data into history matching process, with all the limitations and uncertainties was discussed.

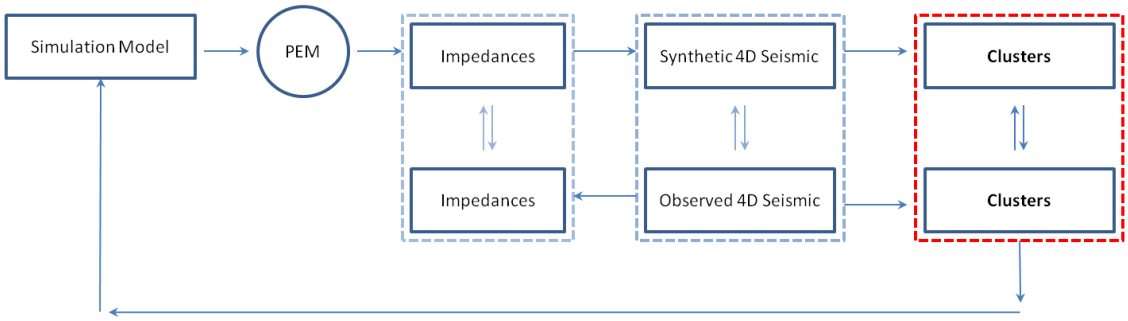

Figure 1.18 History matching workflow using the cluster technique.

The thesis is divided into 7 chapters. A short description of each one is presented here.

Chapter 2 presents the concept of connectivity. Assessing reservoir connectivity heterogeneity is crucial for reservoir management and understanding reservoir performance. Two domains exist, static connectivity and dynamic. Related data sources and their applicability and value are presented. The differences in these domains is highlighted and the ways in which connectivity can be used in history matching explained. The place for time-lapse data is proposed. In addition, Chapter 2 describes a new methodology for map based transmissibility model updating, using 4D seismic data and attribute analysis. Synthetic examples are presented and reasons for the method not being 100% successful are explained

Chapter 3 explains the nature of the clustering method, its existing industry application and describes how this concept can be transformed for time-lapse data interpretation. Necessary criteria are discussed and the method of correlation of different domain data is explained. The chapter also presents the method which will be used in the subsequent chapters.

Chapter 4 demonstrates the application of the proposed method to a turbidite reservoir in the UKCS field in the North Sea. A high level of reservoir heterogeneity, reflected in poor connectivity within the reservoir, impacts on production and field management. Here 4D and the cluster method are applied to locate dynamic geobodies within the reservoir and derive connectivity among these geobodies. In addition, existing techniques, which can be utilised

for connectivity estimation are compared. This chapter provides the description of the simulation model and field reservoir conditions.

Chapter 5 presents the application of the proposed method to a compartmentalised reservoir in the Norwegian Sea field in the North Sea. Structural compartmentalisation is rather high, as the reservoir is divided into major segments with a number of relatively small faults within the segments; hence, fault transmissibility impacts on production and field management. Here existing methods and the cluster method are applied to locate reservoir compartments within the reservoir and derive connectivity among these faults, for some cases. This chapter provides a description of the simulation model, field reservoir conditions and production history together with a management decisions review.

Chapter 6 shows all the uncertainty related to the proposed method. In order to reduce the uncertainty effect on the connectivity assessment it was considered better to integrate few methods of estimation, which are exist in the framework of the ETLP (Edinburgh Time Lapse Project). In addition, a technique for estimation of fault transmissibility is presented as a part of ETLP toolbox. This methodology is briefly described, compared and new modifications of the techniques presented.

Chapter 7 presents conclusions and recommendations for further research.

1.7 Thesis contribution

Most of the alterations, such as transmissibility or pore volume multipliers, inserted into the simulation model to represent the behavior of fluid flow are based on a geological understanding of the reservoir. Unfortunately, due to the sparse nature of well data, which is only hard data and less uncertain, the processes of geological model building and simulation model history matching are uncertain. Here, by direct application of 4D seismic data into the history matching process, I tried to reduce the mentioned uncertainties and add value to 4D in dynamic modelling. To do this, I introduce a new workflow and relatively new term "cluster" in 4D analysis. Time-lapse, here, is a valuable tool to qualify fluid flow pathways, compartments (geobodies, faults, baffles) and to quantify transmissibility between/within the mentioned features. To achieve this, 4D data are calibrated to well data. Then all the analysed data (4D and production data) in two domains (seismic and engineering) are aligned

to one reference (for which special types of data representation are done; all the data is divided into differences between particular time points (which are moments of 4D surveys). Special techniques have been introduced to link wells with seismic data and to interpret 4D in dynamic geobody manner (clusters). The results of this interpretation can be directly included into the simulation model for faster history matching. Application of this technique to the UKCS field and Norwegian Sea field produces encouraging results and indicate that it can be used as a tool for history matching. The results were assessed against reservoir geological settings, and they are in agreement with each other, hence the technique provides enhanced matching due to the reliable and incorporation of more precise geological features into the simulation model from 4D with a solid geological background.

Also, further development of the method is discussed in terms of volumetric calculations. This allows obtaining an additional estimation of pore volume, to assess the accuracy of the sweep process modeling and improve matching.

Chapter Two

Investigations of 4D Reservoir Connectivity.

This chapter presents the concept of connectivity. Assessing reservoir connectivity heterogeneity is crucial for reservoir management and understanding reservoir performance. Two domains are described- static connectivity and dynamic. Related data sources, their applicability and their value are presented and the differences in the domains are highlighted. The way in which connectivity can be used in history matching is explained and the place for time-lapse is proposed.

2.1 Existing definitions

As was discussed before, one of the main history matching tools is changing transmissibility. Hence, it is necessary to understand that this is transmissibility in the geological sense. The mathematical understanding is presented later in this chapter.

What is connectivity? Reservoir connectivity is the opposite of reservoir compartmentalisation. Reservoir compartmentalisation, the segregation of petroleum accumulations into a number of individual fluid/pressure compartments, occurs when flow is prevented across 'sealed' boundaries in the reservoir (Jolley, Fisher and Ainsworth2010). Assessing the heterogeneity of reservoir connectivity is crucial for reservoir management and understanding reservoir performance. In fact, connectivity is probably the main issue in reservoir management. With low porosity and permeability reservoirs there are more or less typical production options: even if we are not completely sure about their values, we only need a range. In addition, we have a number of options to estimate, even measure, permeability, such as core, wireline logs and test data. But what we should do about the reservoir if we do not know its connectivity and how to measure it? First of all we need to develop a geological concept of the reservoir being examined, based on core data and 3D seismic data, if these are available. At this stage it is possible to estimate, with different levels of uncertainty, reservoir static connectivity. Uncertainty here is not only at the connectivity level, but also in the geological settings. But what will occur then we start to produce oil or gas from this reservoir? Reservoir performance is a function of connectivity. It directly affects fluid flow. This study will investigate barriers and baffles which act in different ways, and thus we need to separate two different types of connectivity- static and dynamic. Snedden (2007) defines static connectivity as the native state of the field, prior to production start-up). In other words, it is the geologic time scale of fluid connectivity, and it is important for estimation of the hydrocarbons in place. Dynamic connectivity describes movement of fluids once production has begun. This production scale fluid connectivity needs to be estimated for development optimisation and ultimate recovery calculations. If a fluid is able to flow from one point to another, then these points are connected, from a reservoir engineering point of view. Both of these types of connectivity can be described as directional or non-directional, but direction is more applicable for dynamic connectivity, because in most of the cases there is a direction of fluid flow- from the injection well towards production.

2.1.1 Static connectivity.

There are number of different definitions of static connectivity. Larue and Hovadik (2006) define connectivity as the proportion of connected reservoir volume (above the permeability or transmissibility threshold) and connected to the wells (Larue, 2006). McLennan and Deutsch (2005) used the following definition for static connectivity: it is the fraction of total connected pore volume and it is assumed that it directly reflects the well drainage volume, and is thus an indicator of reservoir flow capacity. Although these definitions differ slightly, the main idea is the same: 'Static' refers to a time independent value; it is predefined and cannot be subsequently changed.

2.1.2 Dynamic Connectivity.

Term 'dynamic' suggests time dependence, and finally depends on well activity. Sometimes the term "heterogeneity" is used to describe dynamic connectivity. Heterogeneity is the opposite term for connectivity and tends to be defined more in the dynamic domain, rather than the static. Lake and Jensen (1989) propose the following definition: dispersity of the displacement front of the flooding process). In producing reservoirs, reservoir connectivity is a function of both reservoir architecture (static component) and well placement (dynamic component) (Larue and Hovadik 2006, 2007). Probably the most important characteristics for field development is reservoir to well connectivity, which is defined as the volume fraction of reservoir flow units connected to one or more completed well interval (Larue and Hovadik 2006, 2007). During the primary depletion phase of producing reservoirs, R2WC (reservoir-to-well connectivity) refers to the reservoir volume connected to the production wells, or to the reservoir volume connected to producing wells and to an aquifer. During the secondary phase, when the reservoir produces using pore voidage replacement, a more useful characterisation is to refer to the volume fraction of the reservoir connected to both injecting and producing wells. Dynamic connectivity is a product (function) of static connectivity (reservoir architecture), so it is dependent on geological settings of the field and cannot be separated from geological study.

2.1.3 Existing techniques

The Resistivity Index (RI) (Hird and Dubrule 1995) is used to estimate the hydrocarbon recovery and is determined by computing the least resistant paths between two locations in the reservoir. Dynamic Connectivity, replaced by reservoir tortuosity- can be quantified in numerical characterisations of reservoir by computing the geometrical path lengths that are fully contained within the connected flow units (Hovadik and Larue, 2007)

The following connectivity estimation methods are used:

1. The connectivity factor (improve upscaling, RF involved) RF- recovery factor.

$$CF = \frac{RF_{finescale\ 3D\ model}}{RF_{coarsescale\ 3D\ model}} \tag{2.1}$$

   There fine scale model differs from coarse scale model by cell size, so this will affect fluid flow movement and in recovery factor.

2. The Hydraulic Interwell Connectivity Index (HICI)

$$HICI = \frac{2}{\left[\frac{1}{k_1 h_1} + \frac{1}{k_2 h_2}\right] k_{max} h_{max}} \tag{2.2}$$

   There k- permeability and h- reservoir height, indexes means wells.

3. FRPE (Fast Reservoir Performance Estimators)
   a. Well flow capacity (predicted recovery from static properties)

$$FCI = \frac{k_1 h_1}{k_2 h_2} \tag{2.3}$$

      There k- permeability and h- reservoir height.

   b. Connected cell bodies (CCB) (modelled porosity and NTG involved)

$$PORO_{eff} = PORO * S_g * NTG \tag{2.4}$$

      There $PORO_{eff}$- effective porosity, PORO-porosity, S_g- gas saturation, NTG-net-to-gross.

   c. Resistivity Index (RI) (based on modelled permeability). Connectivity, in this case, is the least resistant path between two locations in the reservoir, for example, from a general grid block to a producer.

$$I_{Re}(i,j,k) = Min\left[\sum_{producer}^{i,j,k} \frac{\Delta L}{\overline{Ka} * Kr_g * A}\right] \tag{2.5}$$

$$DrainHCPV = \sum_{i,j,k}(V_{pHC})_{i,j,k} \quad (2.6)$$

There DrainHCPV- drained pore volume of hydrocarbons, L-length of the pathway, K_a-averaged permeability, K_{rg}- gas permeability.

All these mentioned techniques need appropriate data to be analysed. Let us consider these different sources of data.

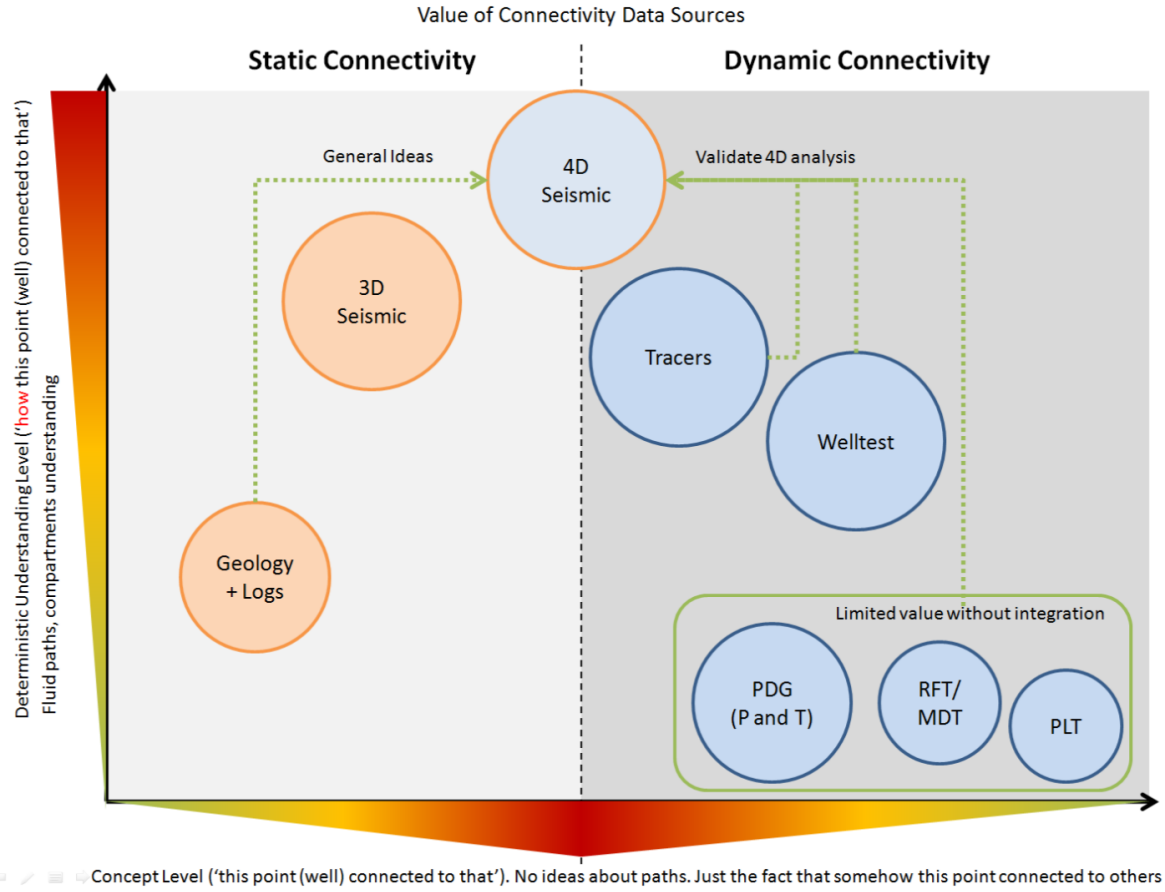

Figure 2.1 The comparative value of connectivity data sources. Sources are ranged on the basis of the concept of connectivity- one reservoir point (can be well) connected to another, without any data on how they are connected at the level of a deterministic understanding of how one point is connected to the other. So, using welltest data, we cannot predict or definitely recognise the connectivity path, whereas 3D seismic can provide such information. PLT-production logging tool, RFT/MDT- repeat formation tester/modular tester, PDG-permanent downhole gauge.

Figure 2.1 represents different data sources for understanding connectivity. On the X-axis-concept level: "this point (or well) is connected to that", we do not have the paths of these connections. The middle of the axis represents data with the maximum value regarding connectivity, whereas the data on the flanks has minimum value. The Y-axis represents

whether the data provides an exact understanding of how the reservoir's points are connected to each other. The maximum value is at the top of axis. All these data sources have their own limitations and associated uncertainties. For example, wireline logs have a limited resolution, usually about 20 cm and geological settings can be unpredictable. As with any other petroleum-related study, the key is integration. Geological concepts are based on our understanding of geological history, together with core data and wireline log data and need to be integrated with 3D seismic. Thus, at that stage we have an understanding of reservoir static connectivity but only a general idea how reservoir will perform, i.e. dynamic connectivity. The other sources, such as well-test data and data from PDG reveal near wellbore connectivity and well-to-well connectivity, tracers provide more complex information about dynamic connectivity. A tracer study provides additional benefits, in that a bigger area can be characterised. Thus, a combination of dynamic and static methods can give a rather good understanding of the subsurface. However, this can still be improved by additional surveys.

I expect, the only source that can be utilised for analysing static and dynamic connectivity simultaneously is 4D seismic. Time-lapse seismic is unique in that it is possible to present 4D seismic as set of baseline surveys, which obviously reflect pure geology, together with static connectivity and monitor surveys which reflect changes in the reservoir, so that it represents a dynamic connectivity. 4D seismic includes determination of both types of connectivity simultaneously in one domain; moreover, it reflects how these connectivity types are related to each other. The only issue here is extraction of these data from a sequence of time-lapse data.

Connectivity is one of the main aspects to be considered during history matching. For highly compartmentalised reservoirs, simulation is not realistic unless both major flow units and communication between them have been quantified (Stewart et al. 1988). Connectivity defines these flow units and these communications. The concept of transmissibility, which will be discussed later, is strongly associated with connectivity. Actually, transmissibility is a derivative of connectivity and a convenient tool to control and update it in simulation and geological models. Conventional history matching (see Conventional history matching (without 4D seismic) 1.4.1) usually implies changes primarily (sometimes only) in the simulation model; connectivity tuning is in NTG parameter.

Time-lapse data, should be considered, in this case, as a tool for updating connectivity in simulation models (including baffles and barriers); in this way 4D can be extremely valuable in matching. If we consider the connectivity update problem, there are two different ways of doing this. I have already discussed history matching procedures and connectivity issues; here I will be concentrating only on connectivity issues and the related time-lapse data. There are at least two ways are to perform history matching then we get new data of any kind regarding connectivity. The first is 'Small' Loop (see Figure 2.2), which is more or less standard in the industry. Here we utilise the 'classic' history-matching workflow, and only the simulation model is updated. In terms of examining connectivity, there are two main updating results. Firstly, we are able to assess dynamic connectivity at the conceptual level of identifying the presence of barriers and baffles (usually without a definite location) and secondly it provides the ability to update local properties (permeability, transmissibility and etc.). The main limitation here is local changes of properties. It is also possible to update connectivity in the geological model based only on production data (i.e. well data), but this is a rather rare procedure, mostly due to the lack of data.

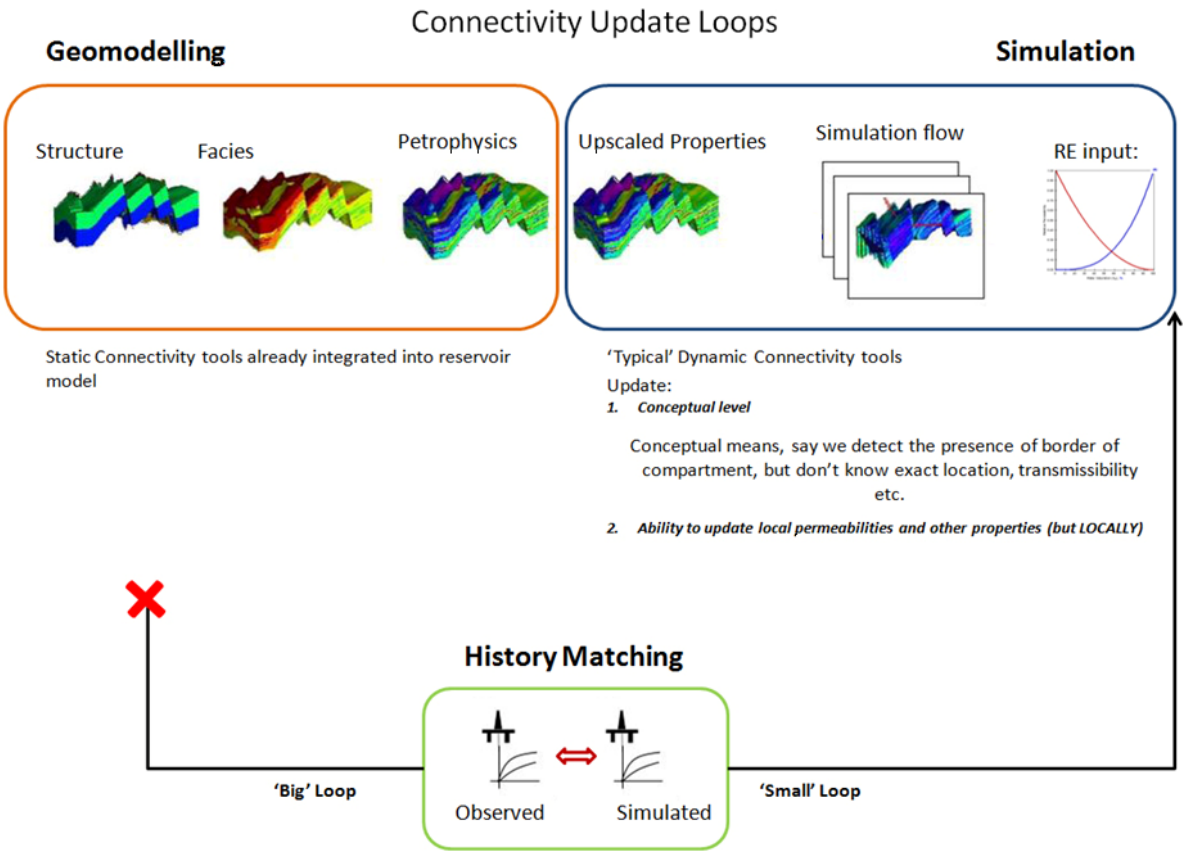

Figure 2.2 Connectivity update loops. 'Small' loop accounts only for the simulation model in which the model updates taking into account only dynamic data, in order to match the model, without any regard for the geology (in most cases). Geological changes can be quite hard to extract from observed production data only.

What if time-lapse survey data is added to the history matching process? This brings about obvious improvements in dynamic connectivity updates, in addition to those already listed, involving identifying fluid flow pathways and detection of barriers and baffles with immediate updates of their transmissibilities, even qualitative. Monitoring the movement of fluid from the injection well towards the producers has been a very successful application, proven during various secondary recovery operations (McInally et al. 2003, Parr and March 2000). In addition, 4D seismic can be utilised as an indication of the connectivity pathways within the reservoir ((Olivera 2008, Huang and Ling 2006 and Andersen et al. 2011). Sufficient benefit of using 4D is the ability to update the trends and distribution of geological properties, based on history matching, with better accuracy. This is referred to in this thesis as the 'Big Loop' (see Figure 2.3). The first application of this procedure is to help to validate the conceptual geological understanding of the reservoir and to refine the property trends, where necessary; however, in respect to the geology, all the updates are usually at the

qualitative level. The updated geological data (i.e. static connectivity) will be then included in the simulation model.

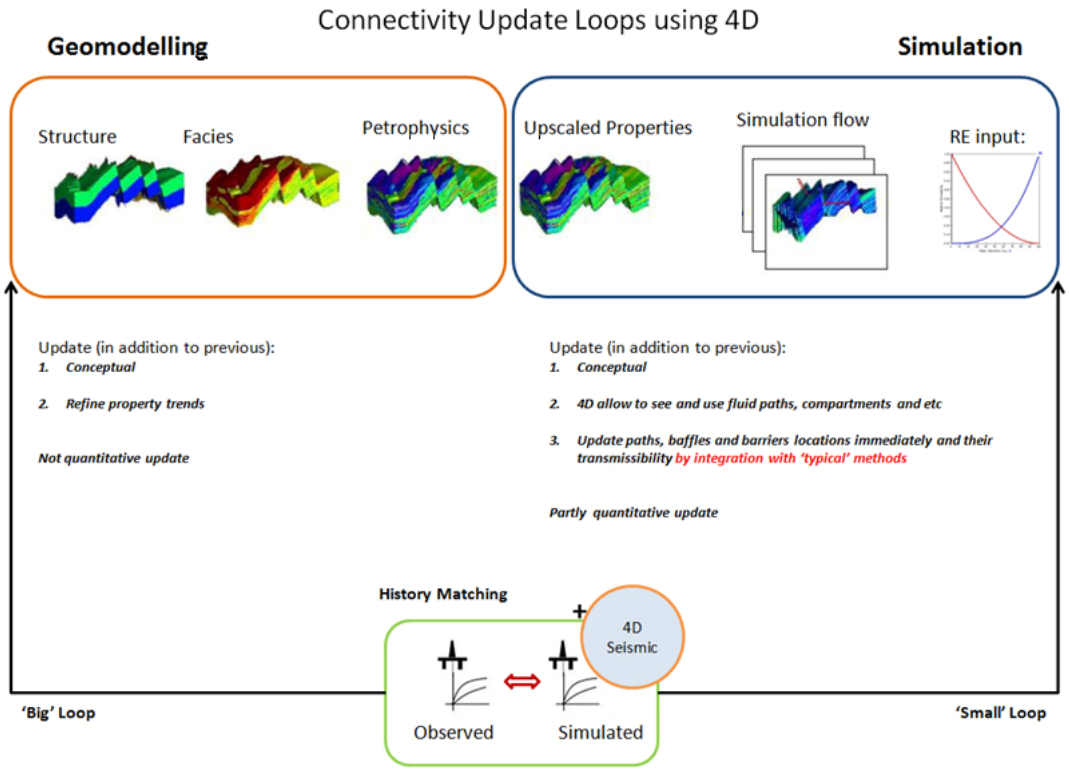

Figure 2.3 Connectivity update loops using 4D. The 'Big' loop of updating with 4D seismic data allows us to improve and update geological understanding of the reservoir and then add all the changes to the simulation model.

In terms of dynamic connectivity 4D gives huge opportunities (see Figure 2.3) - 'Small' loop, in addition to the previously mentioned- updating of compartments, barrier locations and transmissibility between different geobodies. This updating is partly quantitative. For example, permeability, which, conditionally, can be defined as a function of connectivity, is a crucial for simulation model updates and optimisation procedures (Villegas, MacBeth and Paydayesh 2009). 4D seismic can be valuable as well: it is possible to extract 2D permeability from time-lapse data. Usually can be performed by either of two methods: either the directly transformed into the simulation model using special methods (Al-Maskeri and MacBeth 2006, and Vasco 2004), or 4D used as a constraint in objective function during iterative history matching (Villegas 2006). Moreover, a quantification of fault sealing capacity, defined as fault transmissibility multipliers (Manzocchi, et al. 1999), is also possible using 4D seismic data. Fault transmissibility is the key and only parameter in the simulation

model that controls the seal behaviour of a fault (Benguigui and MacBeth 2009). The key is the integration of 3D- and 4D-seismic for estimation of connectivity. An example of such integration is hydraulic sand connectivity, which is defined as two (or more) connectivity estimations from 3D (i.e. NTG) merged with 4D seismic. This indicates reservoir regions in which flow sweep has occurred. This product reflects the presence of a channel and also filters the 4D-related noise, as described by Shams et al. (2007) (see Figure 2.4).

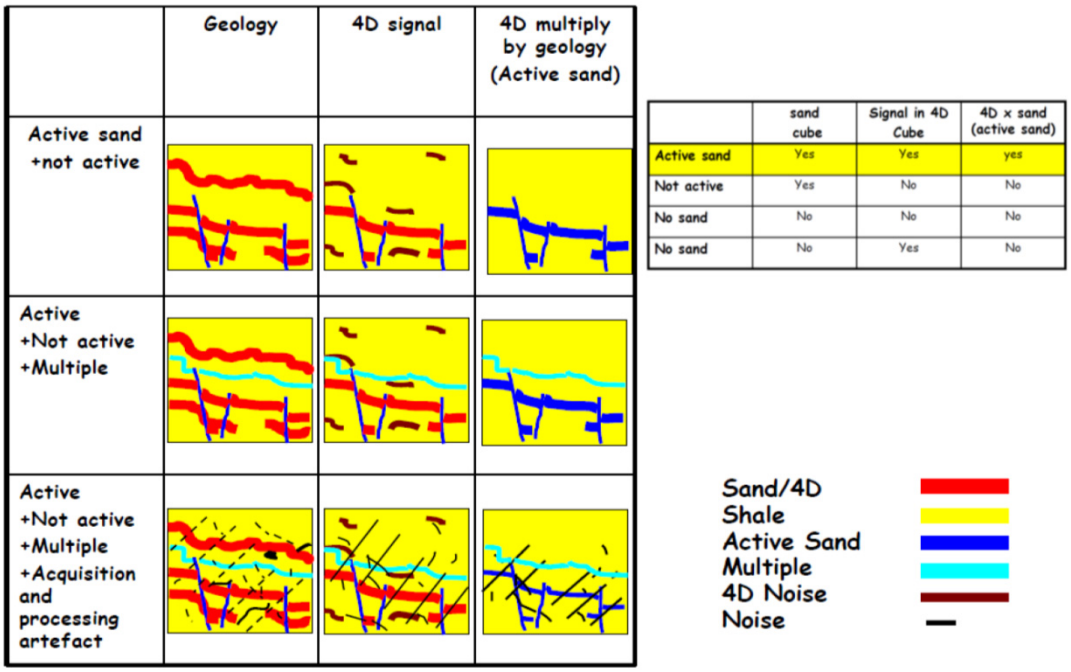

Figure 2.4 The hydraulic sand connectivity. Sand channels are highlighted in 4D seismic as the result of production activity. Assuming that the 4D-seismic response is the response of an active channel, the 3D seismic has to show a consistently recognised channel-sand body as well. However, the 4D signal may still be noisy and show a signature that can be interpreted as a sand responding to production. The 3D-seismic high-NTG helps to filter 4D-seismic-related artefacts, when it is multiplied by the 4D-seismic signal. (Shams, MacBeth and Barens 2007).

2.2 Transmissibility

Transmissibility (transmissivity of fluid flow in porous media) is a measure of how much fluid can be transmitted horizontally or vertically through porous media (the reservoir). According to Darcy's Law, fluid flow in a porous medium (e.g. a rock mass) is proportional to the transmissibility of the medium, and inversely proportional to the viscosity of the fluid,

under an applied pressure gradient (Darcy, 1856). Mathematically, transmissibility between two points in the medium is defined as the product of the harmonic average medium permeability and the area through which the flow occurs, divided by the distance between the two points. This definition is used in reservoir simulation models for calculation of fluxes between pairs of grid-blocks. Based on the calculation scheme in Eclipse software (Schlumberger Trademark), which was used for this work, transmissibility is defined as follows:

$$TRANX_i = \frac{CDARCY \cdot TMULTX_i \cdot A \cdot DIPC}{B} \quad , \tag{2.7}$$

where

TRANXi – transmissibility between cell I and j, its neighbor in the positive X-direction .

CDARCY - Darcy's constant, equal to 0.001127 in field units.

TMULTXi – transmissibility multiplier for cell i.

DIPC- Dip correction. Details of dip correction are in the Appendix.

This is the traditional block-centred form, based upon distances between the cell centres only. The expression for Y-transmissibility is the same. Calculations for Z-transmissibility are in the Appendix. A visual representation of transmissibility between two cells can be seen in Figure 2.5, plane A.

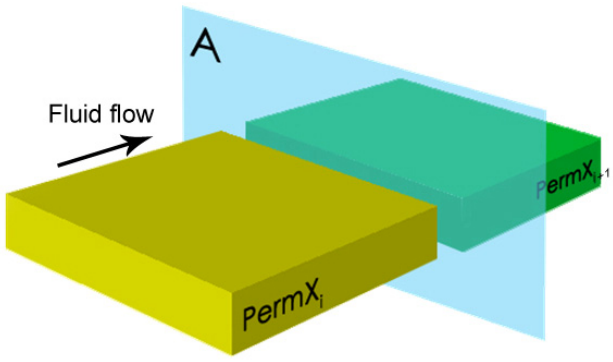

Figure 2.5. Plane A reflects transmissibility between two cells X_i and X_{i+1}. The same planes exist below and above each cell. Transmissibility value can be changed in this plane, affecting fluid flow from one cell to the other.

Thus, the flow in general will be controlled by the transmissibility distribution over the reservoir model. It is important to note that additional uncertainties in transmissibility will result from the presence of uncertainty in the definition of the grid geometry, permeability and NTG. This fundamental definition is the basis for this project and will be reflected in the following chapters.

2.3 Updating Transmissibility Using 4D Seismic Attributes.

In the initial stage of the project I pursued the following aim: to identify the value of the seismic in reducing uncertainty in the initial model for history matching and decrease the time needed for history matching. Generally speaking, I attempted to introduce a new method in the already exited workflow of the Edinburgh Time Lapse Project, and improve the existing technique of permeability estimation from time-lapse seismic data, which was developed by Paydayesh (2010).

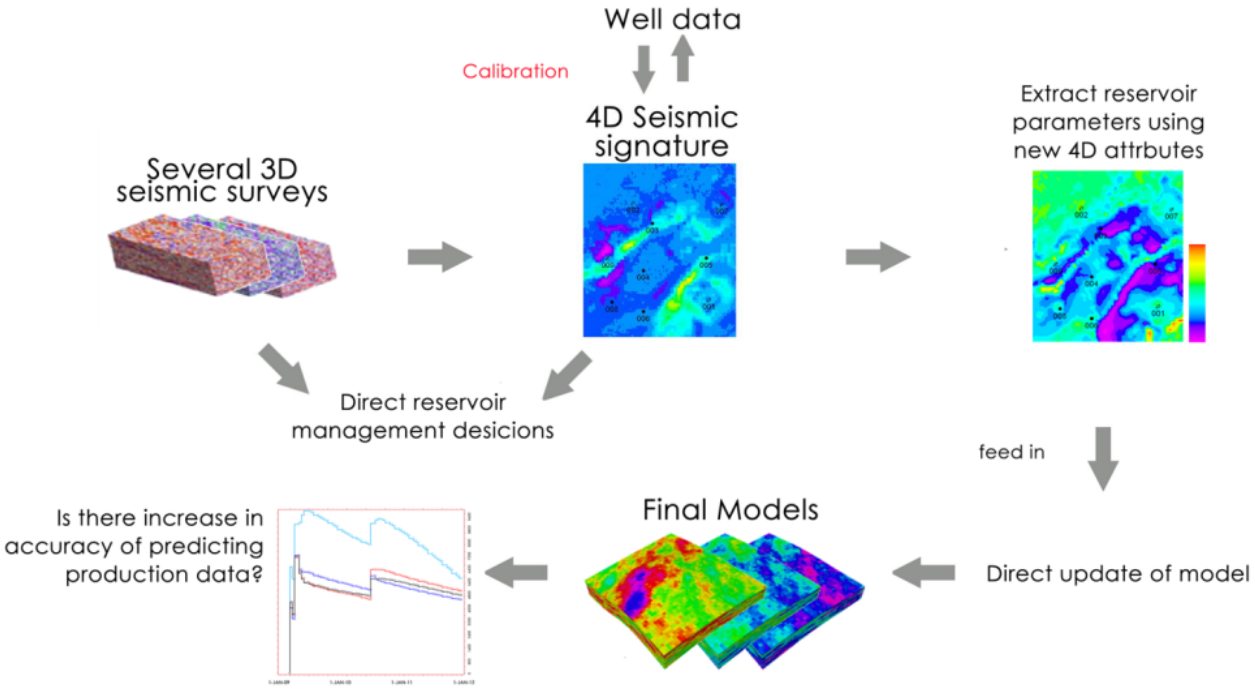

Figure 2.6 General Workflow for transmissibility update. The main feature is extraction of reservoir parameters (permeability or transmissibility, in this case) using new 4D attributes, and then using them in the history matching process.

In his work, a seismic connectivity attribute (SCA) approach is presented. The idea behind the method is the direct correlation of total reservoir connectivity calculated from Darcy-derived connectivities with the corresponding captured connectivity image in the seismic domain (Paydayesh 2010). This method has some assumptions, of which a significant one is linearity between total reservoir connectivity and SCA. I have taken this method as a base, using its results (or modified/improved versions) in simulation model history matching. To do this, the following workflow was produced (see Figure 2.7).

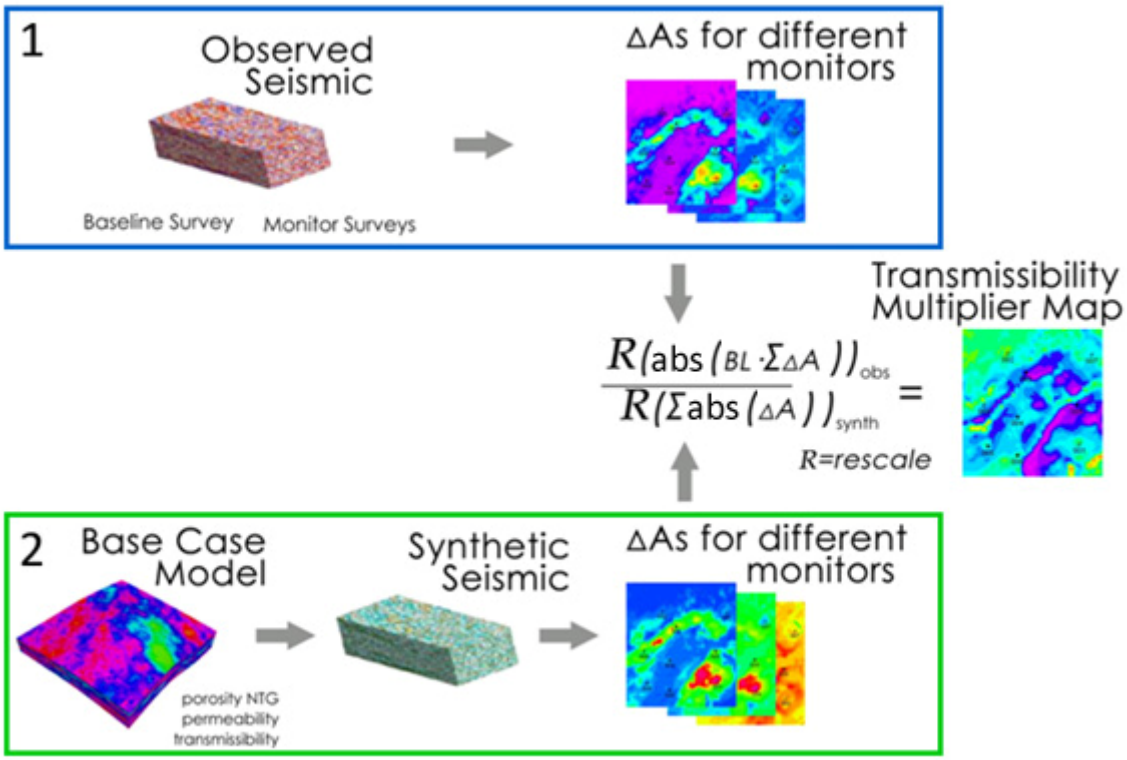

Figure 2.7 Specified workflow for transmissibility multiplier map calculation. The equation presented here is derived to calculate the transmissibility multiplier map, which should be used for history matching by multiplying the simulation model transmissibility grid. This is an attempt to introduce 'real/observed' transmissibility into the model.

Here, $R \cdot abs(BL \cdot \sum \Delta A)$ is a simplified SCA, there BL is root mean square (RMS) of seismic amplitude of baseline survey, ΔA is changes of RMS of amplitude between monitor surveys.

This workflow can be split into three stages: the first one is treated with observed ("true") data, the second with predicted data, while the last stage merges mentioned above and gives the results. The starting point for this workflow is the observed seismic data: the baseline

survey and monitor surveys (in this case there are 3 monitors). The next step is the creation of delta seismic attribute maps between surveys. It should be noted that I assume that delta A reflects only changes in transmissibility (which are related to permeability only, not NTG). This assumption comes from the SCA technique. Rearranging the transmissibility equation we get:

$$TRANX_i = \frac{CDARCY \cdot TMULTX_i \cdot \frac{DX_j \cdot DX_i \cdot DZ_i \cdot NTG_i + DX_i \cdot DX_j \cdot DZ_j \cdot NTG_j}{DX_i + DX_j}}{\frac{\left(\frac{DX_i}{PERMX_i} + \frac{DX_j}{PERMX_j}\right)}{2}} \quad (2.8)$$

There $TRANX_i$- transmissibility between cell *i* and *j*, CDARCY- Darcy's constant= 0.008527 (for the metric units), $TMULTX_i$- transmissibility multiplier for cell *i*, $DX_{i,j}$,- cell dimensions, NTG- net-to-gross ratio, $PERMX_i$ - permeability of the cell

So assuming NTG=1, because net-to-gross is already characterized by BL parameter.

$$TRANX_i = \frac{CDARCY \cdot TMULTX_i \cdot \frac{DX_j \cdot DX_i \cdot DZ_i + DX_i \cdot DX_j \cdot DZ_j}{DX_i + DX_j}}{\frac{\left(\frac{DX_i}{PERMX_i} + \frac{DX_j}{PERMX_j}\right)}{2}} \quad (2.9)$$

The second stage is the Base Case model. This involves the creation of a Base Case Model then generation of synthetic seismic. The method for this and related uncertainties were covered in the previous Chapter. The last stage is to produce maps of the delta seismic attribute and starts from this equation:

$$\frac{R \cdot abs(BL \cdot \sum_{i=1}^{n} \Delta A)_{observed}}{R \cdot abs(\sum_{i=1}^{n} \Delta A)_{synthetic}} = Transmissibility\ Multiplier\ Map; \quad (2.10)$$

where R= rescale from 0 to 1.

There is very important part in the numerator, BL, which is an attribute value for the baseline survey (which should reflect the geology and NTG as well). Hence, as it refers to the geological situation, it can be treated as initial transmissibility. The result of this is transmissibility map.

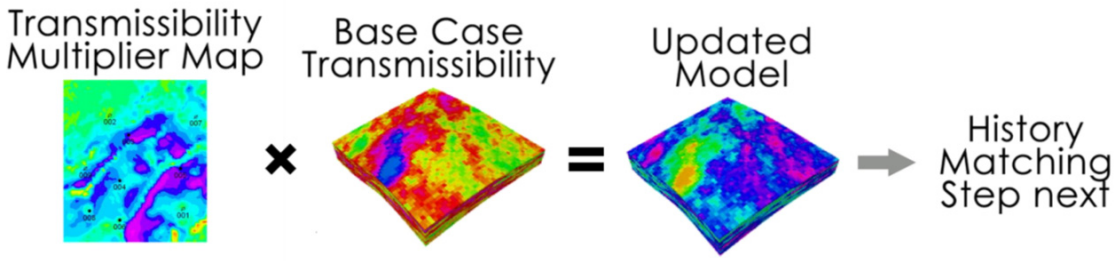

Figure 2.8 Method for simulation model update. Simple procedure for application of the derived transmissibility multiplier map.

After transmissibility extraction it is possible to update Base Case model (transmissibility grid values). The final step is history matching.

2.3.1 The model

A synthetic model was constructed for testing the method. The size of model is 49 on 56 on 20 cells. Vertical resolution is 2 metres and the horizontal resolution is 100m. There are 5 producers and 4 injectors. Based on the transmissibility map, we can assume fluid flow paths (wells 008-009, 005-001, 003-004).

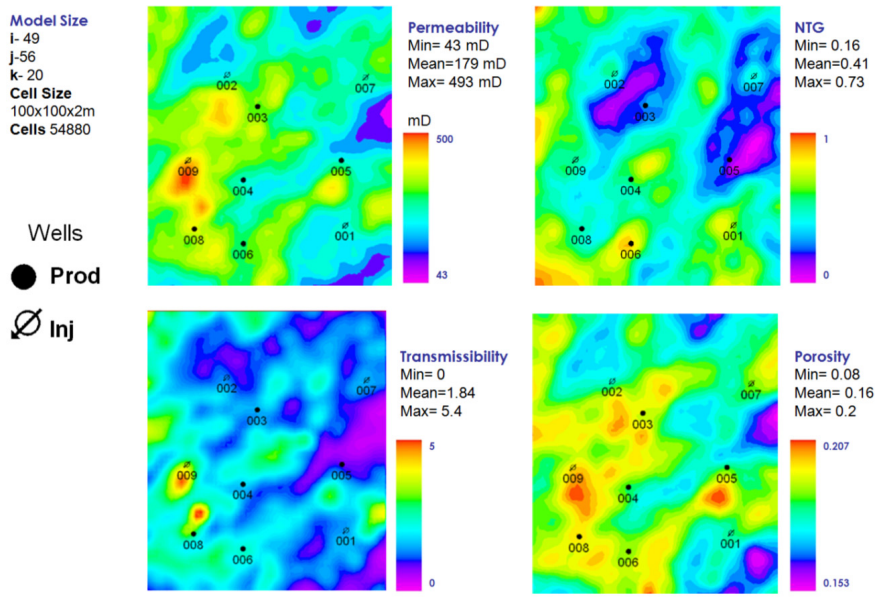

Figure 2.9 "True" Model Review. Four different reservoir properties are presented. A distinct north-east trend can be seen. Based on permeability and porosity values, the reservoir is quite good. 5 producers and 4 injectors exist in the model.

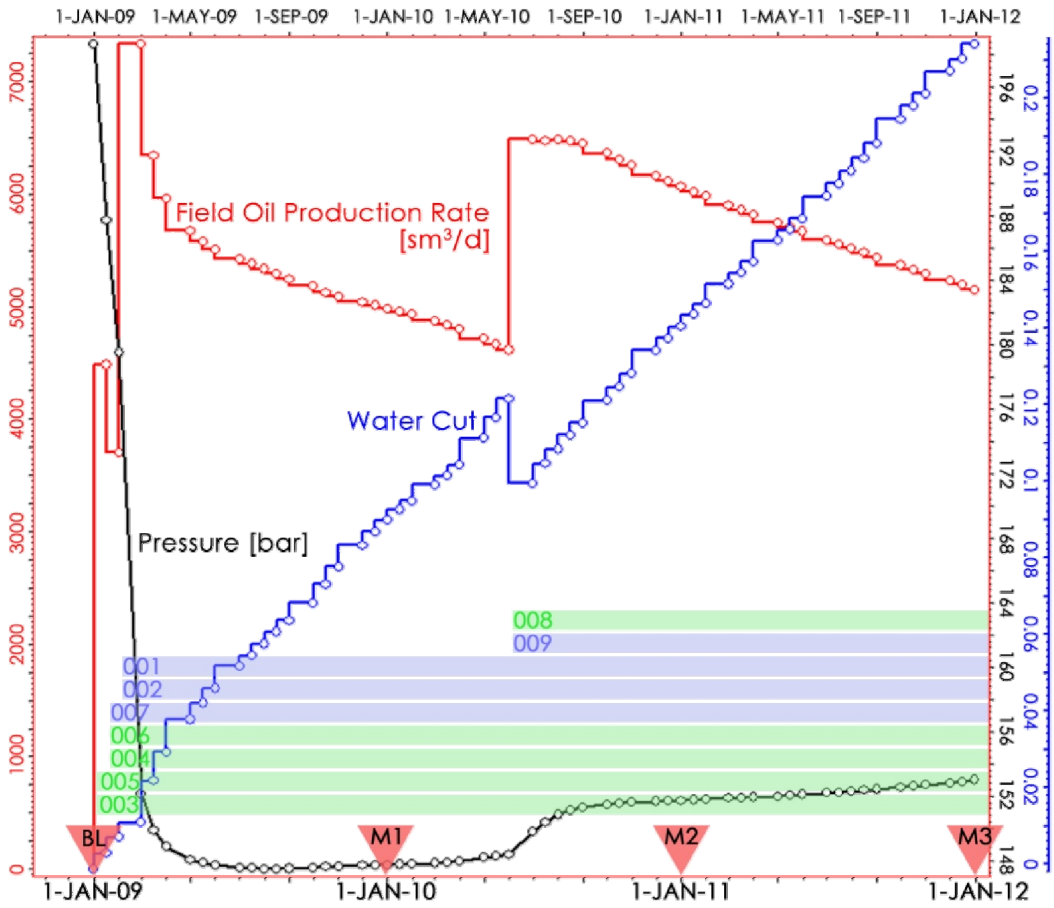

Figure 2.10 Synthetic History Data used for modeling the "true" case and matching of base case. Three history years are presented. Black curve: average reservoir pressure changes; blue curve: water cut changes: red line: field oil production rate. Horizontal blue (for injection wells) and green (for production wells) represents mean time of well online. Red triangles: time of seismic surveys.

Then it was calculated in reservoir simulation software Eclipse, as a result of which the production data were obtained. There are 3 curves; field oil production rate, pressure and water cut for five production wells and injection rate for four injectors (001, 002, 007 and 009). And it was assumed like observed history data for further simulations. The control parameter for wells is Bottom Hole Pressure: 110 bars for producers and 210 bars for injectors. Looking in the pressure curve, it is possible to conclude that pressure is dramatically decreasing, but looking at the absolute values, it can be seen that the change is not sufficient bars, so it is possible to assume that pressure does not affect the seismic of this reservoir. This occurs due to the relatively high oil production rate. The coloured lines show well activity: green is for production wells and blue is for injectors (see Figure 2.10).

Then increase in oil production in June 2010 is tied to the 2 new wells, one is a producer and second is injector. Red triangles show the time of the seismic surveys, baseline and monitors, correspondingly. The period between them is 1 year. After simulation, the synthetic seismic is generated, which will be treated as observed for further models.

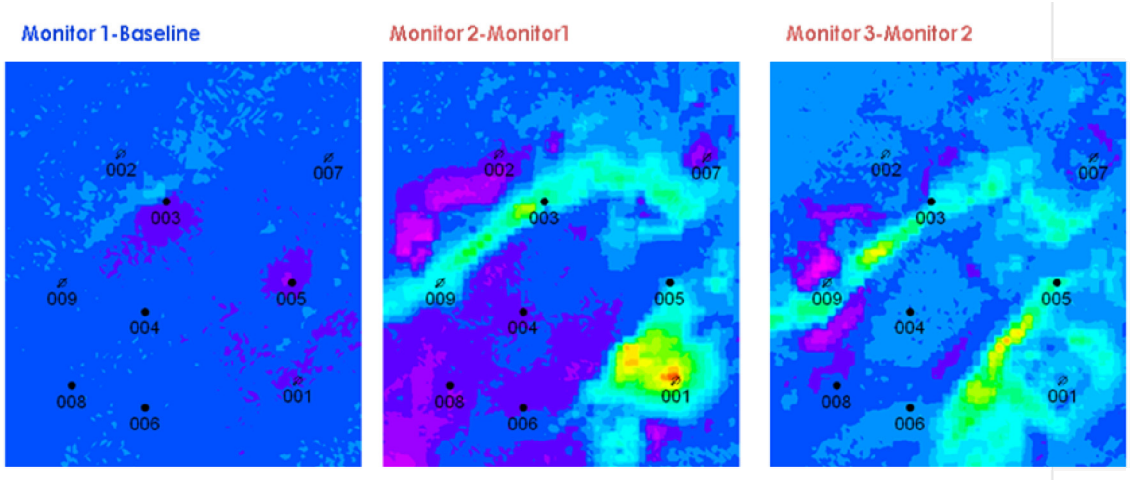

Figure 2.11 Changes in the RMS amplitude attribute in the reservoir window (Top-Base) between surveys

Difference maps of the Amplitude Root Mean Square (RMS) attribute between surveys were then generated (see Figure 2.11). RMS was defined in a certain window from Top to Base reservoir. They are used for analysing changes in the reservoir over time. Regions of maximum change can be seen, and it is possible to expect that these regions reflect maximum changes in saturation, as they correlate to the fluid flow paths shown on the transmissibility map in Figure 2.9. However, the difference between Baseline and Monitor 1 is not sufficient, compared to others maps. The explanation for this can be seen in Figure 2.12: there are significant changes in both saturation and pressure parameters, so that they compensate each other.

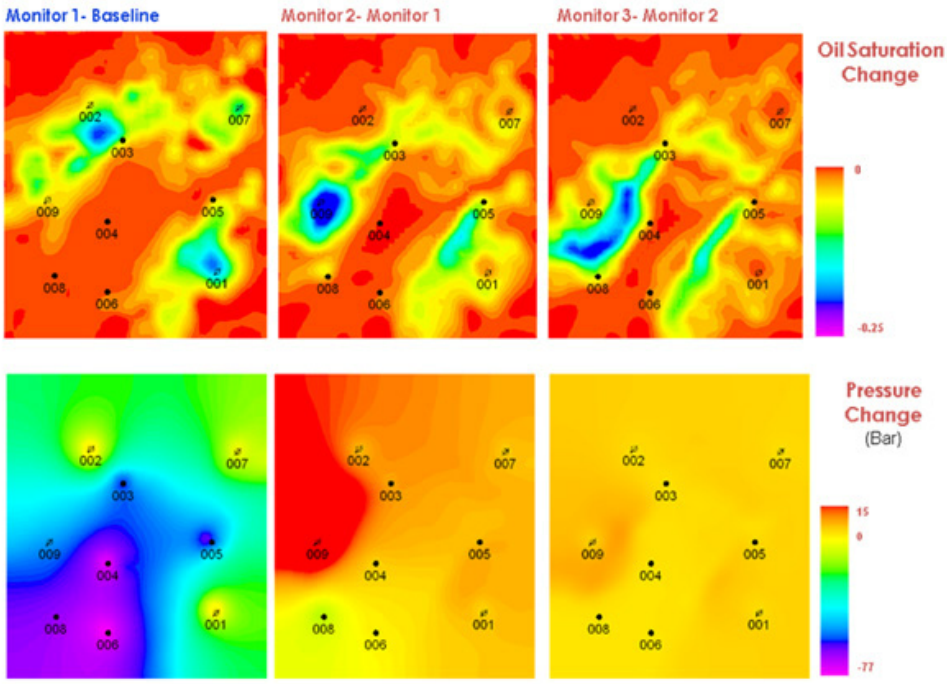

Figure 2.12 Changes in saturation and reservoir pressure within different time steps. It is clear that saturation is the dominant case. Water fronts are clearly seen.

Now let us compare the attribute maps with the maps of the oil saturation changes (upper row) and pressure change maps. There is a rather significant uncertainty in the separation of the saturation and pressure signals in the seismic. In the ideal case these need to be separated for proper analysis. However, if one type of signal (pressure or saturation) is if dominant, it can be used without signal separation. It can be concluded, that this is a saturation dominant case, because the saturation changes have a better correlation with the seismic signature changes than pressure, except for the time between the Baseline survey and Monitor 1, where it is pressure dominant; after this point the pressure pattern changes only very slightly. Thus, I have created a reference model, data from which is treated like an observed ("True" model), and it is possible to perturb it (Base Case Model) for further testing.

2.3.2 Application to a synthetic case

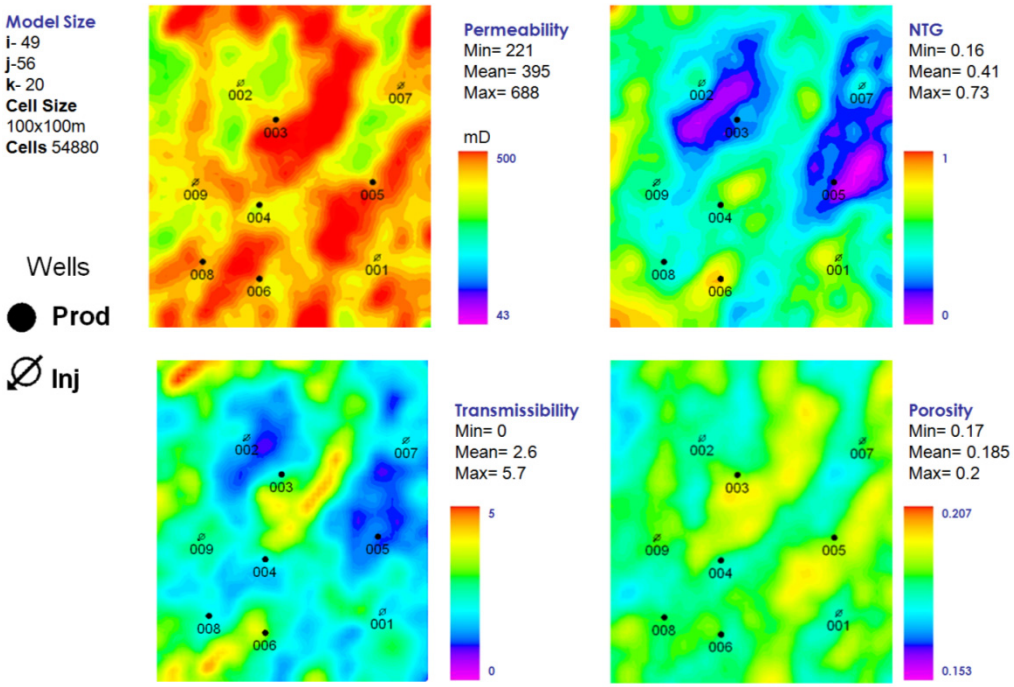

Figure 2.13 Base Case Model Review. Four different reservoir properties are presented. A distinct north-east trend can be seen. Based on permeability and porosity values the reservoir is very good. 5 producers and 4 injectors exist in the model. Reservoir properties are overestimated compare to the "True" Model.

Different variograms were used in the generation of porosity and permeability properties for this model. NTG is the same for both models, the "True" (observed) and Base Case. After building the geomodel, simulation was carried out in Eclipse software with the same control parameters for the wells as those in the "True" Model.

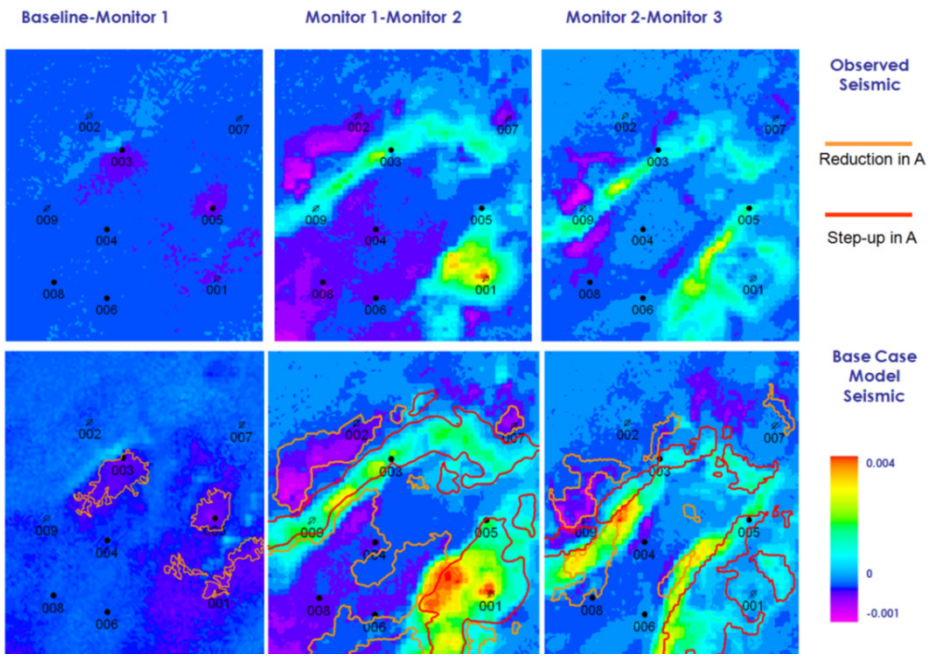

Figure 2.14. Seismic results comparison of dA (changes in amplitudes). Upper part: observed seismic; lower panels: base case seismic overlapped with seismic signatures from the observed seismic.

After creation of the synthetic seismic and RMS attributes, it is possible to compare the observed seismic data with the base case model seismic. The upper row is for the observed seismic and lower row is for the synthetic seismic of the Base Case Model. It is easy to see rather significant differences in delta A. In the ideal case, the base case model seismic should be equal to the observed one, after matching. Orange lines are for regions where delta A is decreased in the observed seismic; red is where delta A is increased. These regions were placed over the base case model seismic. The differences reflect fluid flow paths, which are controlled by the transmissibility pattern. This means the geology, which reflects fluid pathways, that was put into the base case model is different from that in the "true" case. Now we can try to minimise this difference by history matching.

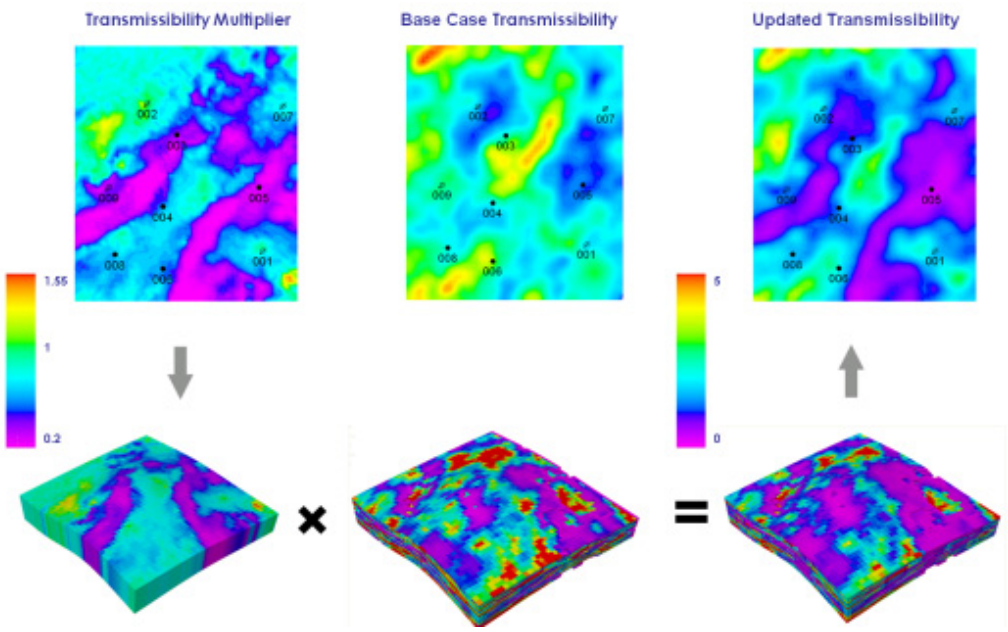

Figure 2.15 Showing how transmissibility was updated, using the base case model grid and derived multipliers map. The updated transmissibility grid was used for history matching process.

After calculation of the Transmissibility Multipliers Map, it was converted into 3D, which means that each layer in the model has the same values of transmissibility multipliers. The product of this grid and the Base Case Transmissibility grid is the Updated Transmissibility, which will be used in the history matching procedure.

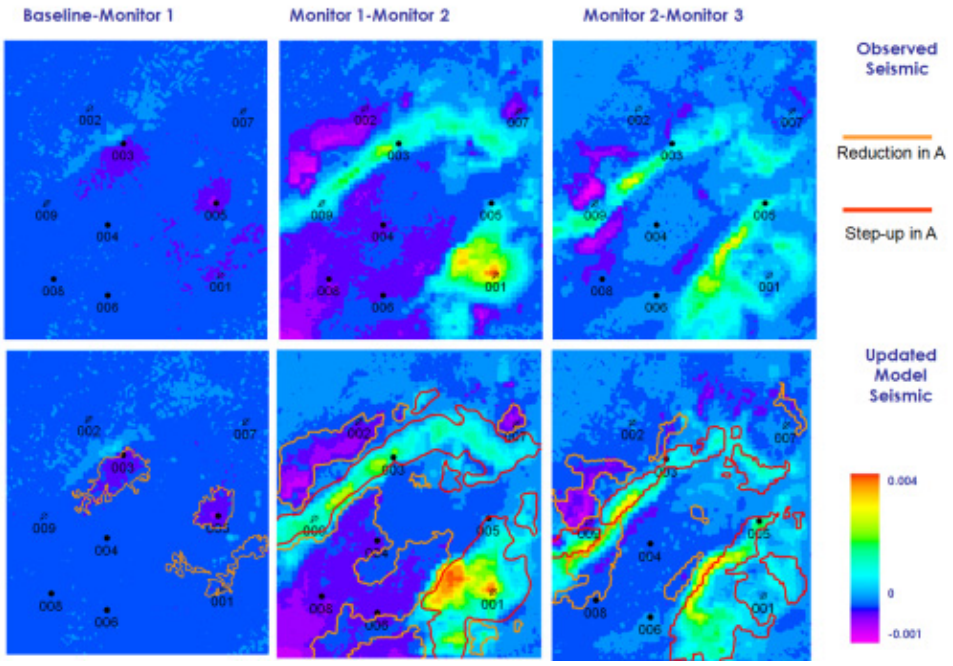

Figure 2.16. Seismic Comparison of dA (amplitude differences). Upper row:"observed seismic", lower row: synthetic seismic of updated simulation model overlapped with seismic signatures from the observed seismic.

Based on Figure 2.16, we can conclude that although the seismic signatures still not completely the same as the observed signatures, they already look more similar to the observed ones. The result of matching is shown in Figure 2.18 (field oil production rate). The history data is shown by red dots, the base case model is shown by a light blue line and the updated model is in dark blue. The improvements are quite obvious, from this figure. However, to try to improve the results even further, I decided to include SimOpt into the process. SimOpt is software with a gradient-based method for history matching, made by Schlumberger.

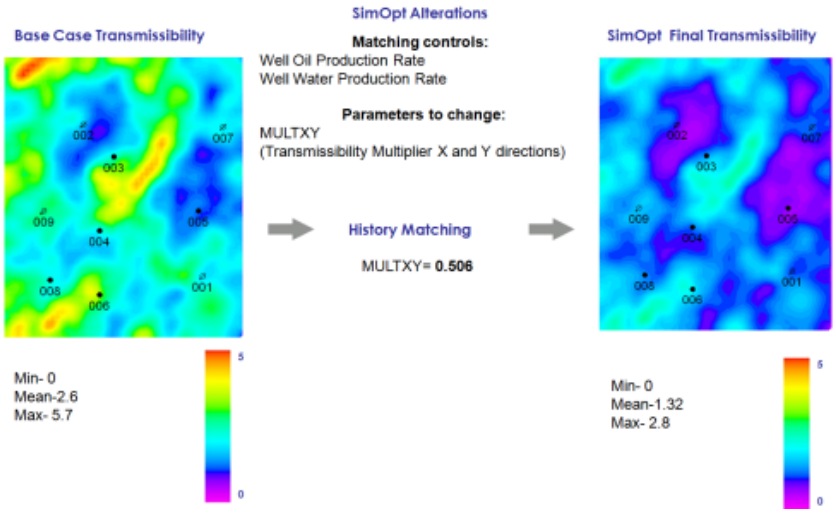

Figure 2.17. Including SimOpt (with integrated gradient-based method) into the process of history matching.

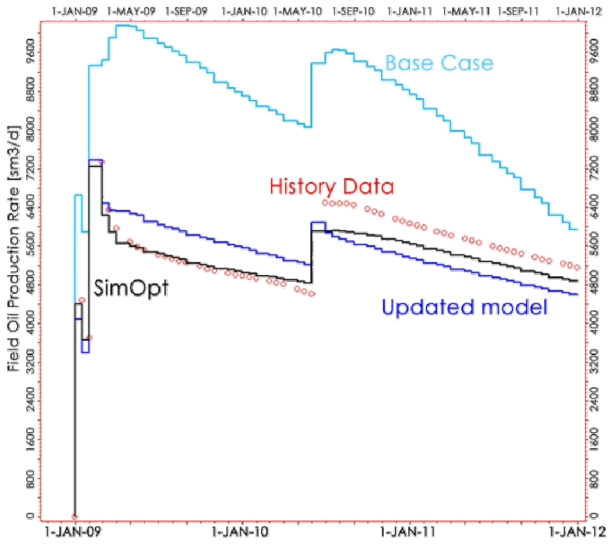

Figure 2.18. History Matching Results for field oil production rate. Red dots: history data; light blue curve: base case model: dark blue curve: results after history matching using the transmissibility multipliers map and black: SimOpt results.

2.3.3 Results

The history matching results were quite promising, but due to non-uniqueness of history matching results, it is necessary to check the geological settings of the resulting model against the "true" geological settings, in this case the transmissibility map.

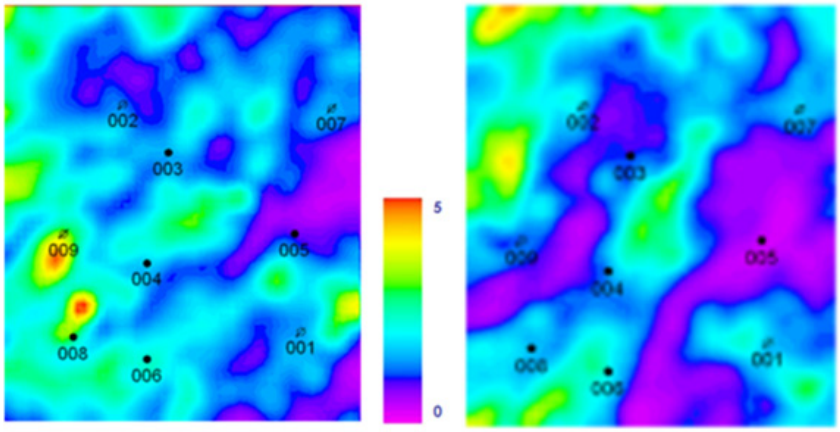

Figure 2.19 Comparison of "true" transmissibility (left hand side) with resulting transmissibility (right hand side).

Analysing Figure 2.19, it can be concluded that the resulting transmissibility does not reflect the "true" geological settings, even though the production history matching shows good results. Actually, the method cannot change the flow pattern sufficiently, due to its limitations and assumptions.

The main problem with this method is the absence of a link with the geology. Even though the matching results have shown sufficient improvements, it is not possible to find a solid explanation for them based on geological reasons. A second reason which makes the technique not completely valid is the lack of consistency: the results are very scattered and all have significant uncertainty. The explanation is the same: there is no solid geological reason for such a procedure.

2.4 Conclusions

All methods and studies presented can be classified in terms of the source of connectivity determination:

1. Geological (Static) Connectivity: Geological data. Sources: 3D seismic, sedimentology, core data, wireline logs.
2. Engineering (Dynamic Connectivity): Sources:
    1. History data: well production and injection volumes and rates
    2. Tracer analysis
    3. Production logging tools (PLTs) that can measure flow, fluid density, water cut and other data.
    4. RFT or MDT
    5. Well testing (pressure: interference test etc.)
    6. Material balance (included as a way to validate some of the above mentioned methods)

What value can 4D seismic add? The observed 4D amplitude difference can result from several processes (Johnston 2013):

- Water replacing hydrocarbons through aquifer movement of injection;
- Oil replacing gas;
- A decline in reservoir pressure (if pressure remains above the bubble point);
- Porosity loss as a result of compaction;
- Gas replacing water;
- Gas replacing oil through gas-cap expansion, secondary gas-cap formation or injection.

According to Johnston, for qualitative 4D interpretation, we know which processes cause changes in impedance, because we rely on our knowledge of the depletion mechanism,

production history and predictions based on reservoir simulation. To sum up, 4D discloses fluid movement, and thus connectivity (both well-to-well and over the field), fluid paths in 3D (water displacing oil or water (due to a difference in salinity). It is better to integrate all the available data from all the possible sources: time-lapse, production/injection history, core and wireline logs. Integration of 3D and 4D is a key to understanding reservoir connectivity. A combination of these surveys can be interpreted as hydraulically active reservoir areas: 3D surveys mostly response for NTG determination (sand channels etc.), while 4D- mostly depicts reservoir connectivity in the areas already involved in production.

Hence, connectivity from 4D seismic analysis can be related to both static (geological) and dynamic (engineering) connectivity. I use the term dynamic connectivity while talking about time-lapse in this project. Dynamic connectivity, in the context of this work, is global connectivity.

Chapter Three

Cluster Based History Matching

This chapter explains the nature of the clustering method, its existing industry applications and describes how this concept can be transformed for time-lapse data interpretation. The necessary criteria are discussed and method of correlation for data of a different domain is explained. The chapter presents the method which will be used in the next Chapters.

Despite the fact that the previous method was not applicable with an appropriate level of confidence, I decide to keep the chosen technique, which will allow the incorporation of time-lapse seismic data directly into the simulation model and reduce the time taken for history matching, and will also be in alignment with geological data.

For any history matching procedure some objective functions should be used as well as convergence criteria. If we add a new matching domain, clusters in this case, it is necessary to form new convergence criteria or state the parameters of the previous one.

It was decided to propose the following scheme (Figure 3.1), based on the previously analysed history matching methods and taking into account the workflow for this thesis (as shown in Figure 1.18.

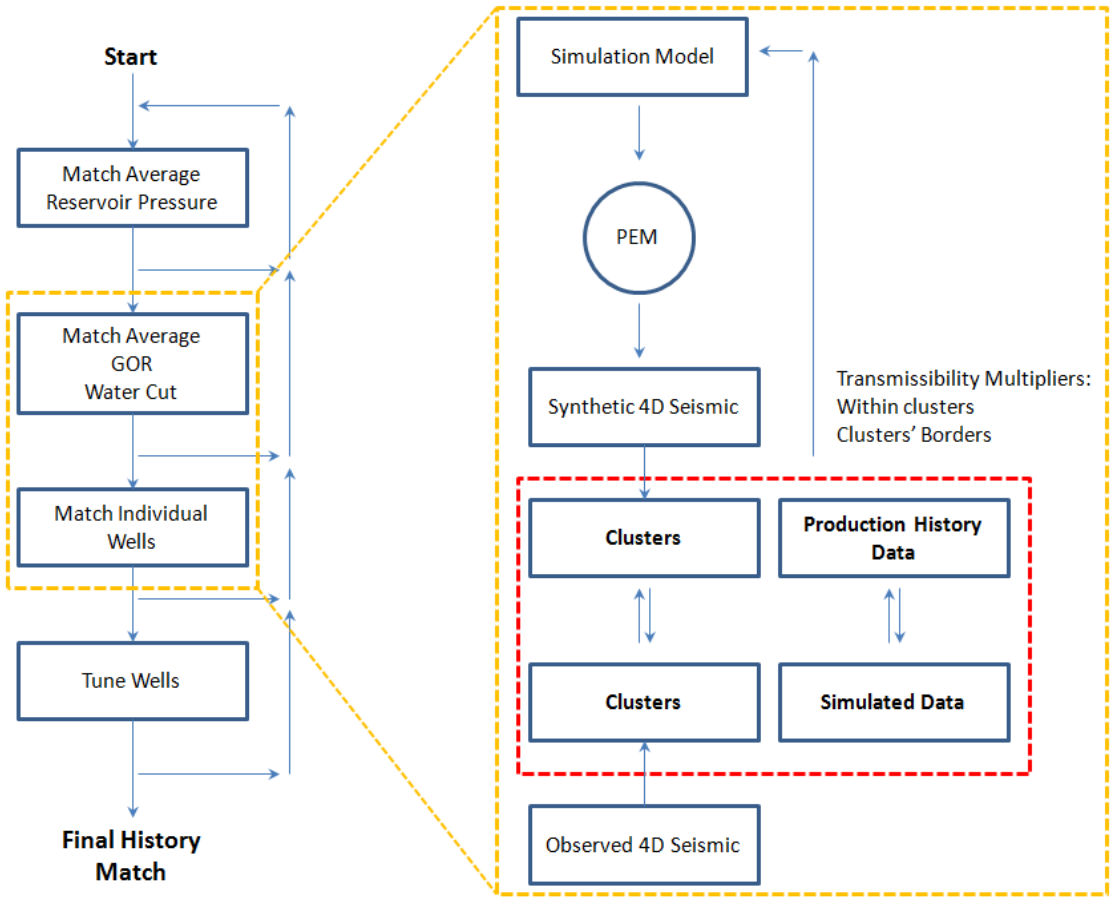

Figure 3.1 Workflow for history matching and the place of clusters in it. (After Carlson, 2008)

Clusters derived from the observed time-lapse are compared with clusters from the synthetic seismic, which is the product from the simulation model; this comparison is mostly visual, due to the limitations (and uncertainties) associated with PEM. Nevertheless, the main criterion of history matching is still the difference between the history and simulated data. Initially, this scheme covered just simulation part, not the geology, but generally it is possible to use cluster analysis (or any other results of matching) to update the geology model update. This aspect has been covered in Chapter 3. The technique presented uses seismic interpretation and processing results, verified by field history data. The seismic data is then used for matching of the field history and local tuning of the model. The each field is unique and so application of the method is case-specific.

3.1 Clustering Sense (statistics and maths)

3.1.1 Introduction

Cluster analysis is a well-known and widely used statistical tool. One of the most well established analyses was presented in Duran and Odell's 'Cluster Analysis' (1977). Cluster analysis itself is not one specific algorithm, but the general task to be solved. It can be achieved by various algorithms that differ significantly in their notion of what establishes a cluster and how to efficiently find them among available data.

In this work, following definition of clustering is more applicable: this is 'conceptual clustering', in which some (two or more) objects belong to the same cluster, if it defines a concept 'common' to all those objects. In other words, objects are grouped according to their fit to descriptive concepts (which are determined in advance and have significant and measurable criteria of dissimilarity), rather than according to simple similarity measures.

The analysis should satisfy some optimality criterion. Usually this is a function representing desirable levels of division and grouping. This function is referred to as an objective function (efficiency function). Here the sum of squared deviations (SSD) is used. Let us see an example:

n=8 objects have the only characteristic (p=1); the results of observations are in the $X = \{3,4,7,4,3,3,4,4\}$ set. SSD is calculated using formulae:

$$SSD_1 = \sum_{i=1}^{n}(x_i - \bar{x})^2 = \sum_{i=1}^{n} x_i^2 - \frac{1}{n}(\sum_{i=1}^{n} x_i)^2, \quad (3.1)$$

where x_i is an observation of object i. For this example:

$$SSD = \sum_{i=1}^{8} x_i^2 - \frac{1}{8}\left(\sum_{i=1}^{8} x_i\right)^2 = 140 - 128 = 12. \quad (3.2)$$

If ensemble X is divided into three groups: $G_1 = \{3,3,3\}$, $G_2 = \{4,4,4,4\}$ and $G_3 = \{7\}$, then all the intragroup SSDs will be equal to zero: $SSD_1 + SSD_2 + SSD_3 = 0 + 0 + 0 = 0$, where SSD_i is sum of squared deviations for the corresponding group G_i.

Obviously, in order to solve cluster task, it is necessary to determine the concepts of similarity and dissimilarity. If two objects I_j and I_k are similar, what does it mean? The task can be solved if the *i-th* and *j-th* objects are in the same cluster every time the distance between corresponding points X_i and X_j is 'sufficiently small' and will be in different clusters if the distance between points X_i and X_j is 'sufficiently large'. In such a way, we need to understand the general idea behind 'distance' between points X_i and X_j in E_p (Euclidian space, for simplicity, is as a set of points satisfying certain relationships, expressible in terms of distance and angle).

The non-negative, real-valued function $d(X_i, X_j)$ is a distance function if:

1. $d(X_i, X_j) \geq 0$ for each X_i and X_j from E_p;
2. $d(X_i, X_j) = 0$ if and only if $X_i = X_j$;
3. $d(X_i, X_j) = d(X_j, X_i)$;
4. $d(X_i, X_j) \leq d(X_i, X_k) + d(X_k, X_j)$, where X_i, X_j and X_k – any three vectors from E_p.

The value of $d(X_i, X_j)$ for specified X_i and X_j is called the distance between X_i and X_j and it is equivalent to the distance between I_i and I_j, correspondingly chosen characteristics $(C_1, C_2, \dots, C_p)^{T*}$.

A synonym for clustering is segmentation.

To sum up, clustering allows:

- Improvement in understanding of data by revealing groups. Analysis of these groups can be carried out through different algorithms and groups representing different physical processes.
- Detection of atypical objects in the examined ensemble, for example- noise in 4D seismic.

3.1.2 K-means method

There are number clustering algorithms; however, among all the existing methods it was decided to utilise the k-means algorithm, as it is relatively easy and fast to apply. The algorithm of K-means is as follows:

First, define a number of clusters (e.g. 5) among all the existing data. Here, before analysis, we need to know the number of clusters; this can be determined by statistics, by simple trial and error methods or by the physical nature of analyzing data.

Then the algorithm randomly guesses *k* cluster centre locations.

Next, each datapoint finds out which centre it is closest to (so that each centre 'owns' a set of datapoints, each in its own colour). However, the distribution may not meet convergence criteria.

Each centre finds the centroid of the points it owns, then the results are checked against the convergence criteria.

This is repeated until the process is terminated (i.e. convergence criteria are met)

Finally after a number of iterations, we will obtain the final distribution of cluster centroids, with their associated datapoints. The significant point is that the area of uncertainty lies inside the transition area between clusters. What is uncertainty in this case? Uncertainty means that the points can be owned by adjacent clusters with compatible probability; the physical meaning of this is that these points have properties that cannot be interpreted in only way. In other words, any of the points lying in the transition area can be part of two or even three clusters, with more or less the same probability. The resultant uncertainty should be assessed and taken into account in further analysis, if possible.

The described above method is one of the easy and fastest to implement with appropriate results, only one problem exist- number of cluster should be known before analysis. To solve this it is possible to use more sophisticated one algorithm.

Self-organizing map (SOM) algorithm with non-supervised learning performs a feature projection nonlinearly from the high-dimensional (input) space into a low-dimensional (output) space (feature space) consisting of 2D array of neurons in an orderly fashion

(Kohonen 1989, Aras et al. 1999). According to Al Moqbel and Wang (2011) SOM consists of two phases, training and mapping. In the training phase, a square grid of neurons is initialized to train the network. Each node is represented by a weight vector of the same dimension as the input vector and the weights are initially set to random values. The network is fed with random input patterns in an iterative process from the high-dimensional input space to the SOM low-dimensional feature space. As the mapping from the input (signal) space to the SOM (surface) space is based only on the internal relations in the structure of input signal, the ordering takes place automatically without external supervision. Therefore, the algorithm creates an internal representation of the incoming signal structure which ensures that similar patterns in the input space are correspondingly located near each other in the SOM space. Appling this technique it is possible automatically solve number of clusters, but it is still necessary to find their physical meaning in terms of reservoir behavior.

3.1.3 Existing industry applications

One of the applications of clustering techniques is seismic facies.

Seismic facies analysis with a mapping of different facies or lithologies based on wave response is not a new technique. The main idea is that a typical geological cross-section is reflected in the typical picture of the seismic cross-section in the time domain as well, and so if this is constant for some distance along the seismic profile, it is possible to conclude constant geological settings on this distance. Changes in wave pattern mean changes in the geological settings, for which the new type can be known or unknown. The geological settings, in this case are facies features or lithology.

Changes in physical parameters of the seismic signal are reflected in changes in the seismic trace form. Allocation of seismic facies based on determination the change in form of the seismic trace and assignment of the traces to a specific class. Usually, it is assumed that changes in trace form are more sufficient, than changes in amplitude. In such a way, during seismic facies analysis, a range of types of traces is determined and each observed trace from the 3D cube is allocated to one of the types.

Seismic facies analysis performed in a constant window interval relative to the datum. The term “seismic facies” originally came from seismic stratigraphy, and has the following

meaning: a volumetric body filled by a typical seismic pattern, which allows the sedimentological environment to be determined based on the structure of the pattern (Razin, Merkulov and Chernov 2010). In any case, it should be rather large objects with more than 2 phases in the vertical direction. In the general case the seismic facies do not necessarily match with the term geological facies.

Usually, the engineer chooses a number of trace types and criteria which are to be used in the assignment. The number of these criteria is based on simple characteristics of wave form.

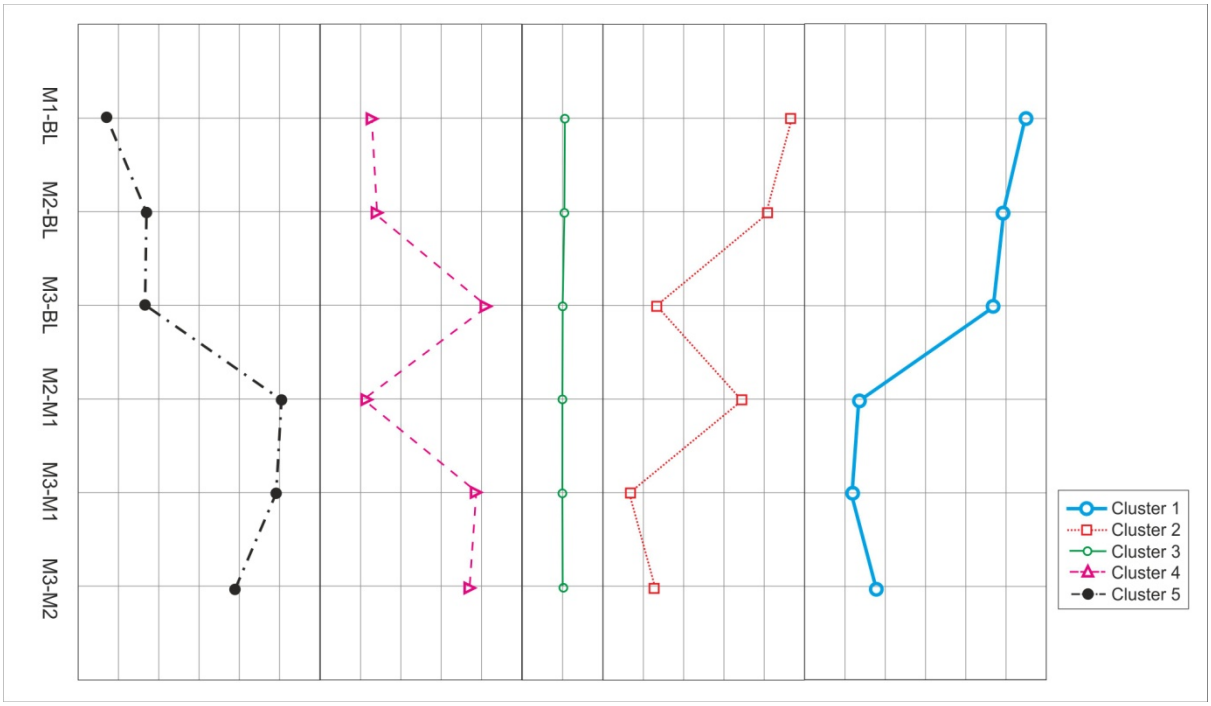

Figure 3.2 Example of seismic cluster curves – five different clusters, each reflecting particular physics, and possible reservoir behavior.

An example of 4D seismic clusters determination in is presented in Figure 3.2. Division was made into five types of wave traces (differences in seismic surveys). It is easy to see that all the modeled traces differ from each other in terms of quantity, location and phase amplitude difference. Detection of types performed automatically. It is expected that these trace features are linked with reservoir behavior features.

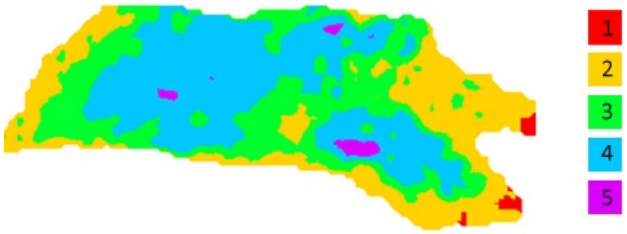

Figure 3.3 Seismic cluster map derived by application of a clustering algorithm

3.2 Method

3.2.1 Data management

Data preparation and management is critical in any analysis. It is important to align the data utilised (input data) with the expected results, in terms of factors such as quality, resolution and availability and also to use the same parameters as for the results. In this case, the main point is resolution: the seismic, geological model and simulation model usually have different resolution in both directions, vertical and horizontal, and spatial density also has a variable range. In the end I used the simulation model with its own resolution, independently of input resolution, for analysis. In the general case, the resolution of the simulation model is a simplification of the detailed geological model, due to upscaling. The reason for upscaling is to improve the performance of the simulation model, without degradation of the geological representation of the reservoir- all the critical features which affect the fluid flow should be preserved. The level of simplification is controlled by the reservoir engineer, according to the aims of the simulation model.

Even if the seismic bin size is 12.5m by 12.5m and simulation cell size is 100m by 100m, the final resolution will be 100 in 100m. Thus, seismic resolution is not adequate if it is better than the simulation model resolution (seismic bin size less or equal simulation model cell size). To perform an analysis, we need to have seismic values and simulation model properties in the same grid/domain. In order to ensure this, seismic cubes were transferred into the simulation grids using Sim2Seis software (Amini, 2009). The next section will cover this process in detail.

3.2.2 'Upscaling' the seismic

When changing domains from seismic grid (12.5 x 12.5m) into simulation grid (where cell size is usually much bigger, 50x50m or 100x100m or even bigger), uncertainties are raised, but these are not very significant in the current case although some useful pieces of information are lost, which were contained in the original seismic data. The same happens during the processing of the seismic, and the reason is that we need good picture to be able to interpret it. Here, as far my ultimate goal is concerned, updating the simulation information, it is more correct to stay in this domain rather than going back to the geological model (which can be very time-consuming) and not to move into the seismic domain, which is for this case 12.5x12.5 m (bin size), throughout the downscaling procedure, which is not straightforward.

The other issue is the vertical resolution of both the simulation model and seismic. Usually, as in this specific case, the simulation model cell thickness is smaller than the layer that can be resolved by the seismic. As for all work was performed in Petrel Software, any seismic cube is a grid with its own i, j, k coordinates. The simulation model grid is 75mx75x1 m, which is about 6 times larger than the seismic cells. So I upscale the seismic cube into the simulation grid, using simple arithmetical averaging.

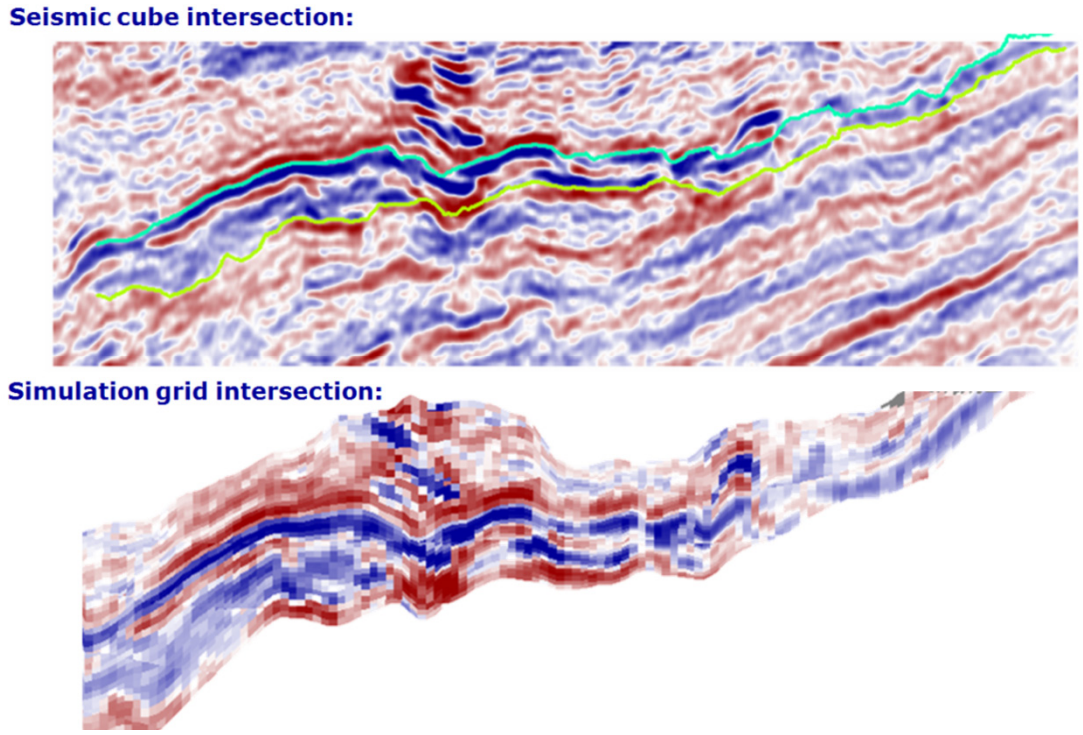

Figure 3.4 Seismic fit to simulation grid. Main horizons are well-traced on the 'upscaled' grid, and the seismic geobodies can be interpreted as well as on the observed seismic (after (Amini, MacBeth and Shams 2011)). Upper panel: seismic cube is 12.5m x12.5m, lower panel: simulation grid 50x50m.

3.2.3 Method workflow

The ultimate aim of this project is to find the method which will allow direct use of time-lapse data in the simulation model, to provide better and less time consuming history matching. The main criterion for doing this is the geological consistency of the data derived from the time-lapse seismic. In order to reach the stated aim, I built following workflow (see Figure 3.5). It is partly similar to the established seismic history matching workflow and with the traditional way of handling 4D seismic. As in any 4D study, it is necessary to build a synthetic seismic; this process depends on a petro-elastic model (PEM), and only then it is possible to perform simultaneous analysis of the modeled seismic and the observed seismic. Actually, I add an additional objective function (convergence criteria). The new domain for comparison is clusters (shown within the red dotted line).

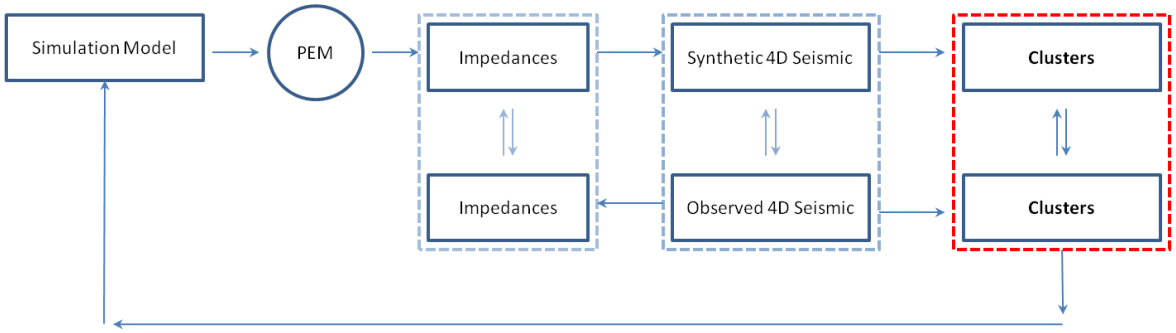

Figure 3.5 Workflow used for model update: three different domains are used, in addition to production data. The key domain in this word is production data and clusters data.

Practically, using this workflow results can be compared in three different domains: impedances, synthetic seismic vs. observed, and clusters (dynamic geobodies). Comparison of impedances is not covered in this research; however, seismic similarities will be discussed briefly. I will focus mainly on the cluster domain, and the process of cluster extraction will be covered in detail in the following sections.

3.2.4 Synthetic Seismic

Process of synthetic seismic response creation from a simulation model referred here as sim2seis (simulator to seismic modeling). Modelling tool is created by Hamed Amini (H. Amini 2013). According to his work the basic steps of sim2seis workflow are as follows:

1. Run the simulation model and extract the static (porosity, shale volume, etc.) and dynamic properties (pore pressure and saturation for different fluid phases, solution gas-oil ratio, oil formation volume factor, etc.) from the simulation model at the selected times steps.
2. Converts the static and dynamic properties into elastic properties (V_p, V_s and density) using a PEM.
3. To be able to calculate the synthetic seismic response, elastic properties should also be assigned to the overburden and underburden.
4. Choose a seismic modeling approach and an appropriate wavelet to generate the pre/post stack synthetic seismic.
5. Assessment of the 4D signal in the presence of non-repeatable noise might also be required in some applications.
6. Interpret the 4D signals be generation attributes that can be tied to the production data.

To sum up, Amini mentioned, sim2seis is a multi-disciplinary tool, which requires data integration from petrophysics, engineering, and geophysics disciplines.

3.2.5 Cluster connectivity

This part will show the link between dynamic connectivity and the results of the cluster method.

The cluster sequence starts from the well and shows the fluid pathway (say, water, for the injection well case) from region to region. It should be mentioned that the presence of active wells is, of course, detectable by clusters, as where there are no working wells, there are no changes in saturation or pressure, -i.e., no changes in the 4D. In the initial stage of production, clusters refer to the reservoir volume connected to the production wells (-dV), or to the reservoir volume connected to the injection wells and to an aquifer (+dV), if it is

present in the field. Different physical effects will be represented by clusters. Around injectors, clusters are volumes corresponding to injected water displacing oil. Later, these volumes can be used for volumetric calculations, which will also be the validation of the clusters. It is possible to divide injection among different intervals, if the well completed in more than one interval. Around producers the clusters represent oil sweep. Hence, the cluster illuminates the reservoir areas in which the flow sweep has occurred, with respect to time and well type.

Different clusters reflect different adjacent time steps (TS) in the reservoir and time step clusters have dynamic connectivity, as water goes through cluster TS_i into cluster TS_{i+1}, and so on. Figure 3.6 shows two different clusters in pink and light blue, which reflect water movement in the reservoir from two injection wells, I1 and I2. Initially water was injected into the pink cluster (TS_i), then it went into the light blue cluster (TS_{i+1}). Thus, clusters are connected dynamically (hydraulically).

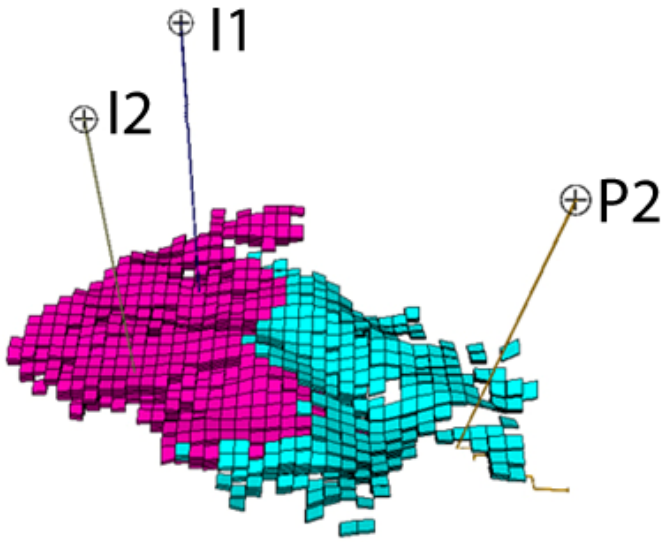

Figure 3.6 Dynamic/static cluster connectivity. TS_i cluster is in pink and TS_{i+1} is in light blue. I2 and I1 are injection wells, P2 is the producer. Synthetic Model

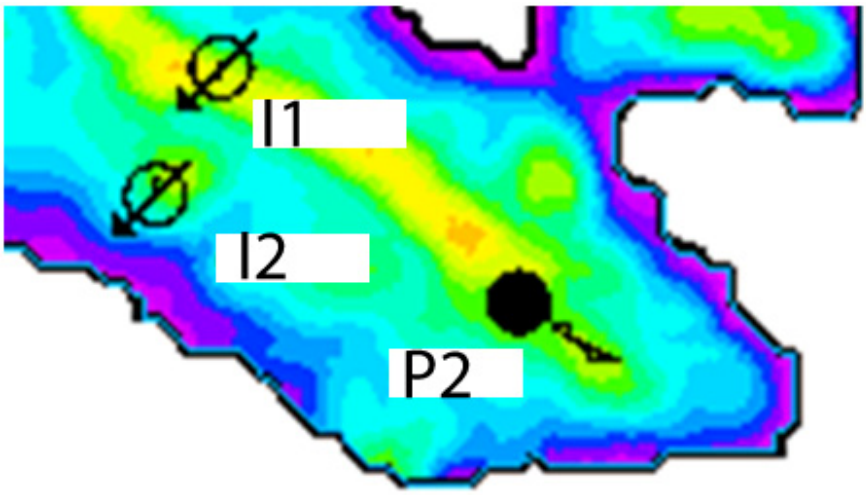

Figure 3.7 Map of static connectivity based on 3D seismic and averaged to get map view.

The traditional way of estimating static connectivity is presented in Figure 3.7. Static connectivity can be analysed using cluster techniques, as well. Unity of all the clusters related to a corresponding well reflects static connectivity, or a geobody, in other words. Taking two clusters in Figure 3.6 and combining them results in one geobody. This is known as static connectivity.

3.2.6 Necessary Criteria

There are certain necessary criteria for applying the new workflow presented here. All of these come from the physical nature of the process and a general understanding of the interaction between production and the seismic survey data.

1. Number of surveys – this must be not less than 4 (including baseline), otherwise the algorithm will not be able differentiate type curves, or otherwise excessively complicate results. Complexity, in this case, means a sufficient number of curves, more than the engineer can interpret according to well behaviour.

2. Time between surveys - this question has been addressed in many papers, but there are a still many disputes. The only obvious fact from the physics point of view is that the volumes of production and injection should be sufficient to be detected by seismic surveys. These criteria should be determined in every particular case, depending on

the geological settings of the field. In addition, for better understanding of reservoir performance, monitor surveys should be timed to different stages of field development (see Figure 3.8). Thus, it is possible to combine these two criteria for determination of optimal survey time.

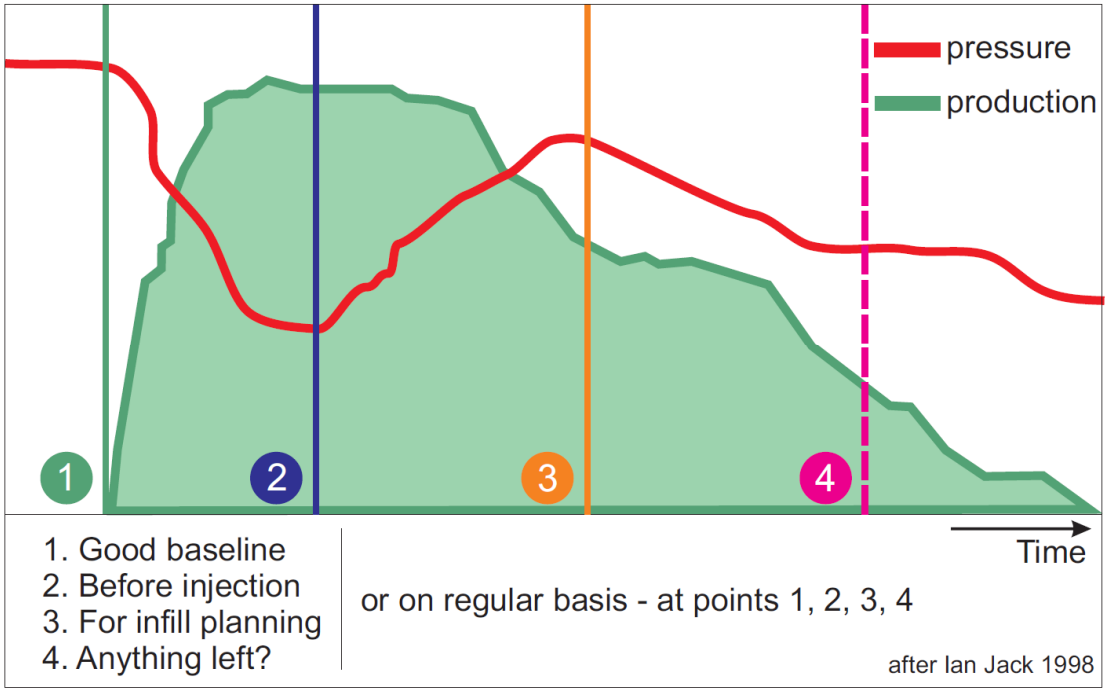

Figure 3.8 The appropriate time for seismic surveys for better reservoir management decisions (after (Jack 1998)). First monitor survey is just before injection, second before infill planning, others are monitors, for anything else, if necessary.

This criterion mostly does not affect the applicability of the method, but rather the general advantages of 4D surveying. Selecting the right timing allows volumetric calculation to be performed, in addition to cluster analysis.

3. Predominantly determined number of clusters. This rule is partly overlapped with the first one. We need avoid over-complexity in the data, because the clustering technique allows a sufficient number of clusters to be generated, even without a physical explanation for them. The following guidelines can be given: the quantity of clusters should be determined on the basis of the number of seismic surveys and the number of well types– usually producers and injectors. Basically, the presence of two well types and 4 surveys gives at least 5 clusters. It is not recommended to generate

more than 10-15 clusters; this gives very detailed picture, but it is too complex to interpret.

The data analysed (input seismic data) has a normal distribution, so the data in each cluster also has a normal distribution. Based on clustering theory, we need to find centres of clusters- points in the case of one seismic survey and curves in the case of more than one; if it is a curve I will refer to it as a type curve. Hence, all the points/curves situated in three SDs-standard deviations (98% of all the curves) from centres are definitely owned by this particular cluster, and the remaining 2% are seismic noise or the uncertainty area. Areas of uncertainty appear due to mutual interference of injectors and producers on this area (i.e., two different sources of signal with opposite signs).

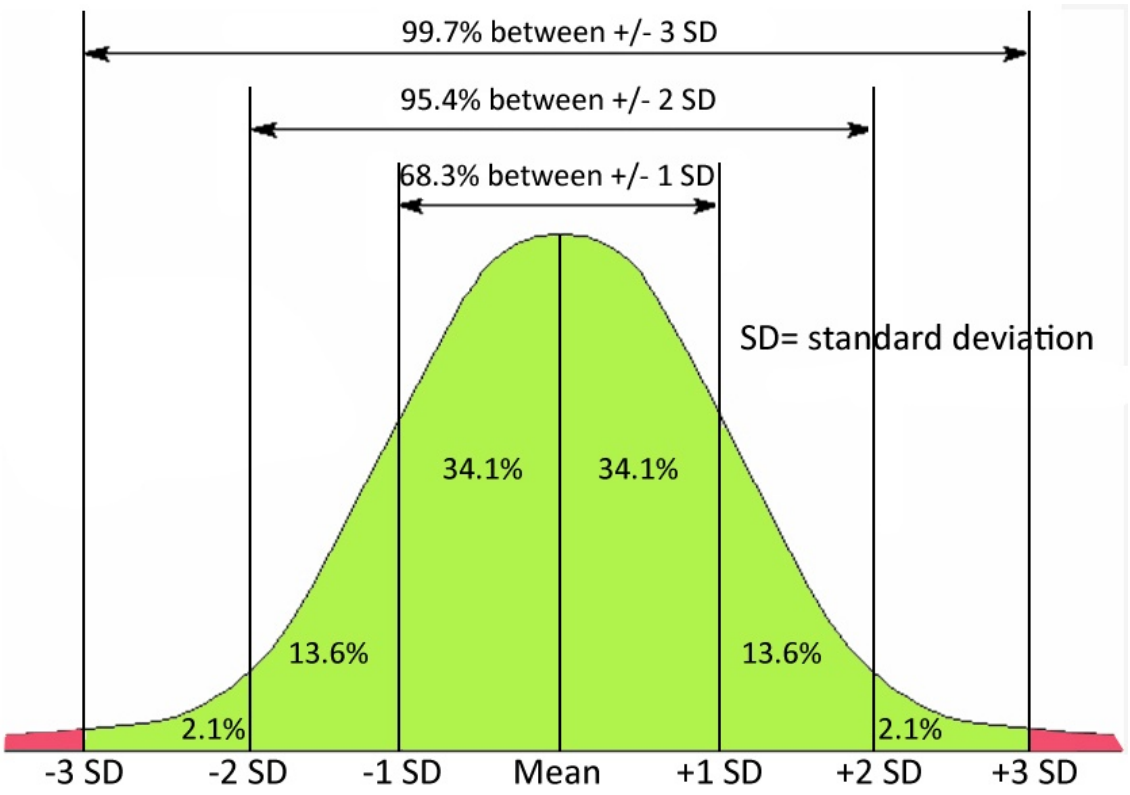

Figure 3.9 Normal Distribution of the data used for. Confidence level is in green (almost 99%); uncertainty areas (about 1-2%) are in red.

The basis of seismic facies determination is static, that is the geology, whereas the basis for 4D seismic clusters is the dynamic behaviour of the reservoir, which is, a strong relation with the static and cannot be in controversy with it, due to the nature of each of these. Actually

each individual facies can affect fluid flow in a different manner. A detailed description of the cluster generation technique will be presented later in this chapter.

3.3 Direct correlation of well activity to time-lapse response

Interpretation of 4D is dependent on understanding well activity and how to link it with the seismic. All data , both 4D and production data are presented in two domains (seismic and engineering) and were aligned to one reference, using a special type of data representation in which all the data is divided into differences between particular time points (which are moments of 4D surveys). In this way I obtained a package of identical time-step formats. This it gives an opportunity to quantify and analyse both well and seismic data in one domain, which reveals the way to develop the proposed method: this is to interpret 4D in a dynamic geobody manner (clusters), the results of which can be directly included in the simulation model for faster history matching.

3.3.1 Correlation of well activity with time-lapse signatures.

To compare the seismic and well activity in one domain, certain assumptions need to be stated:

Produced and injected volumes between surveys should be comparable and sufficient to be detectable by the seismic. 4D seismic signatures, as they are the result of well activity, only detect changes in the reservoir state which were initiated by wells. Definitely, threshold exists, below which the seismic cannot capture any reservoir changes. These changes are defined by volumes produced from and/or injected into the reservoir. This assumption allows us to link produced/injected volumes with the seismic signal and so use seismic in a quantitative way (see Chapter 7). A validation of this approach can be achieved using well data along with seismic. As we know, wells are sources of seismic amplitude changes and at the same time they are sources of saturation (pressure) changes. Here I will focus more on saturation (in other words, wells cause more changes in saturation, than in pressure), but in the more general case, pressure and saturation act simultaneously. The next question asks how it is possible to tie the well's signal with seismic changes?

First of all, we need to understand the differences between typical data organisation and representation in the 'wells' domain and in the '4D seismic' domain. Historical well data usually looks like the graph in Figure 3.10. Only a few parameters are presented, the oil (gas) flow rate, cumulative production and water production (or watercut) for the production well, and the injection flow rate for the injection well. Any other curves, such as BHP and GOR are optional. Discretisation in presenting the data depends on the engineer, it can be daily, weekly or monthly. Each of these curves reflects a crucial parameter for reservoir performance. Exactly these curves (and some others) are used for history matching.

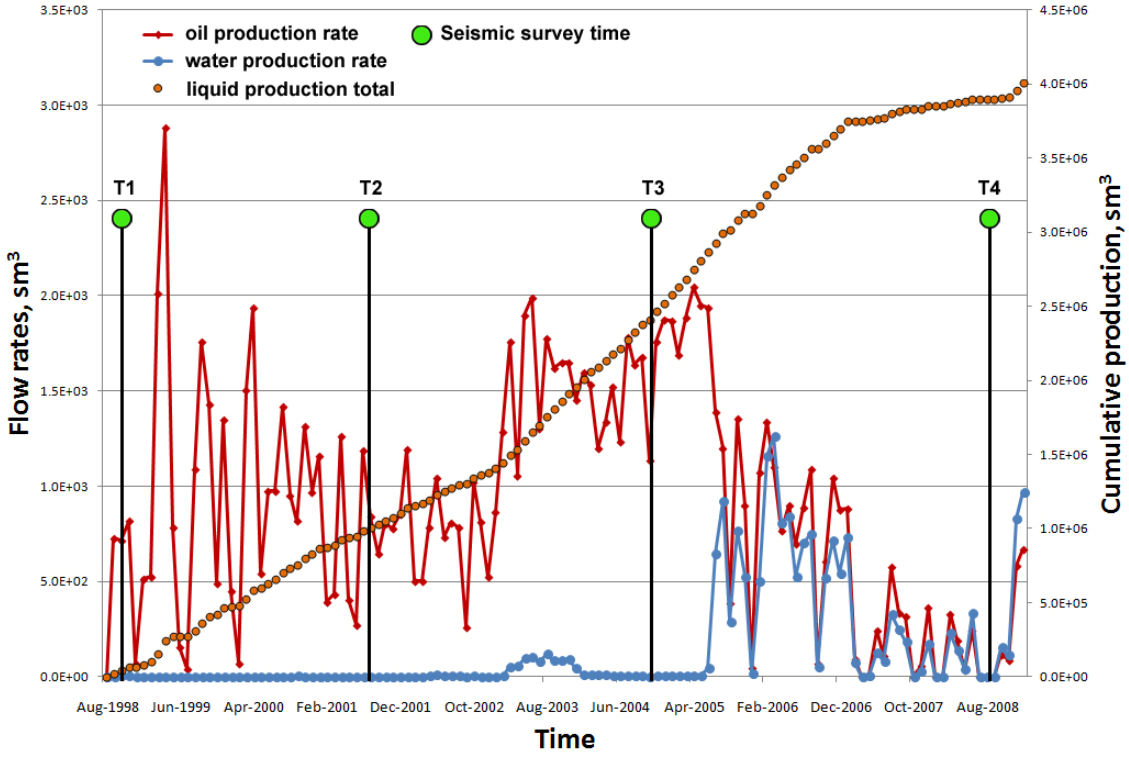

Figure 3.10 Typical well production history, with oil and water production rate indicated by red and blue lines. Cumulative liquid production is shown by orange dots. The time of the time-lapse surveys is shown by the green dots.

All the plotted data are in surface conditions and need to be converted into reservoir conditions using corresponding formation factors for oil, gas and water, according to the following equation:

$$Q_{res}=B*q_{sur} \tag{3.3}$$

Time- lapse seismic surveys are discrete in time, usually carried out not more than once a year. So between two surveys (T1, T2, T3 and T4 in the figure), the reservoir is influenced

by a number of wells active during that time segment. 4D difference is related to changes in saturation and pressure and S and P, in turn, are related to the cumulative produced/injected volumes, rather than just to flow rates. In simple form it can be shown as:

$$d4D = dS + dP = dV_{inj} + dV_{prod} \tag{3.4}$$

This equation is valid for any cell of the model (point of the reservoir) for the fixed time period dT (see Figure 3.11). For a given patch in a reservoir (x_i, y_i), some depositional features such as a channel, high permeability conduit, fractures, etc. determine that fluid will preferentially flow through certain paths,. Reservoir parts can be affected by well activity (i.e. can be detected by seismic surveying) only if they have connectivity with these wells, so time-lapse can be interpreted for understanding connectivity between wells and different reservoir parts. In addition, when the well activity changes, it will subsequently cause changes at parts of the reservoir being considered (x_i, y_i). It is reasonable to assume that, apart from the well's activity, there are some other factors that affect the seismic, and the ones most related to this work are the petro-elastic properties of the reservoir which are in charge of the response to pressure and saturation changes in this particular point. So, the seismic change at a given location should be the function of the nearby wells.

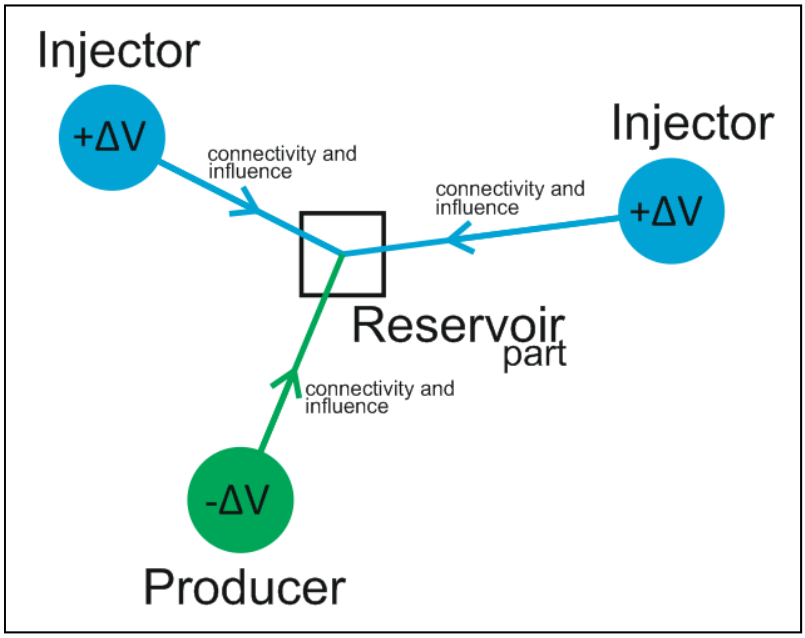

Figure 3.11 Reservoir part affected by three wells. Influence is extended through the connectivity in the reservoir (depicted by lines with arrows). This reservoir part produces a 4D signature which will be determined by differently weighted sums of cumulative produced/injected volumes (-ΔV and +ΔV). If some reservoir parts are not connected to the wells, then seismic will not detect any changes in such reservoir parts.

This function will represents the influence that the neighbouring wells will impose on a given location in the reservoir. We need to ask: what should it look like? Let us assume changes in the affected reservoir part on the upper figure are described by ΔA, so, for the depicted example:

$$\Delta A(x_i, y_j) = \sum \left(a f_P(\Delta V_{ij}\right)\ldots. \tag{3.5}$$

$$\Delta A(x_i, y_i) = \sum_{j=1,N} [\psi_p(x_i, y_i) f_p(\Delta V_j, G_{ij}) + \psi_s(x_i, y_i) f_s(\Delta V_j, G_{ij})] \ . \tag{3.6}$$

According to MacBeth and Huang, the coefficients $\psi_p(x_i, y_i)$ and $\psi_s(x_i, y_i)$ determine the strength of the response to local pressure and saturation change, respectively, and are related to local geological conditions (the petroelastic model). These two coefficients are considered to be unchanged throughout the time of production. The functions $f_p(\Delta V_j, G_{ij})$ and $f_s(\Delta V_j, G_{ij})$ convert the cumulative fluid volumes injected or produced into vertically-averaged changes in pressure and saturation at location (x_i , y_i). These two functions are controlled by G_{ij} which is related to connectivity between the well and location (x_i , y_i), the boundary conditions and initial state of the reservoir. Given the complexities for fluid flow in a heterogeneous reservoir, it is usually not possible to determine the explicit forms for $f_p(\Delta V_j, G_{ij})$ and $f_s(\Delta V_j, G_{ij})$. According to equation *3.6*, it may not be straightforward to relate the 4D response ΔA at location (x_i , y_i) and well activity ΔV injected or produced at a particular well over a survey period ΔT. For instance, consider that the 4D signature is driven by pressure change: the amount of pressure change caused by a given well (e.g. water injection well) may be balanced by the pressure effect of the neighbouring wells (negative ΔV for producer and positive ΔV for injector), resulting in no significant pressure change in the region. This may explain why there could be no 4D changes observed around a well that has been actively producing or injecting. However, most 4D study is based on understanding the 4D signal, which is solely controlled by a production effect related to a single well. Under this condition, equation 3.6 can be simplified. For instance, consider an area influenced by a single well and the seismic change driven by pressure change: the equation can be written in the following format:

$$\Delta A(x_i, y_i) = \psi_p(x_i, y_i) f_p(\Delta V_j, G_{ij}) \ , \tag{3.7}$$

where, $f_p(\Delta V_j, G_{ij})$ represents the function linking the pressure changes to the fluid volume injected or produced at the well over the survey period. Thus, it should reflect two different pressure regimes - the transient and the stable state - established after a well is activated. The function $f_p(\Delta V_j, G_{ij})$ can be as simple as a linear relationship in a closed compartment, once the stable state is established, where equation *3.6* can be further simplified as:

$$f_p(\Delta V_j) = \frac{\Delta V_k}{c_t V} \quad . \tag{3.8}$$

This gives

$$\Delta A_k(x, y, \Delta T_k) = \frac{\psi_p(x_i, y_i)}{c_t V} \Delta V_k \cdot, \tag{3.9}$$

where c_t is the total compressibility of the reservoir rock and V is the total volume of the compartment studied. This relationship is shown to be valid for pressure changes of up to ±8MPa (Floricich 2006). Interpretation of the 4D signals in this work is based on this linear relationship.

3.3.2 Step 1: Generating sequences of seismic differences from multiple seismic cubes

Using time-lapse seismic data, which is actually a sequence of multiple 3D seismic surveys, a time sequence of difference maps for all available pairs of surveys is presented in Figure 3.12. In the general case, independently of the number of seismic surveys, the number of pairs can be expressed by following expression:

$$N = \frac{n(n-1)}{2} \tag{3.10}$$

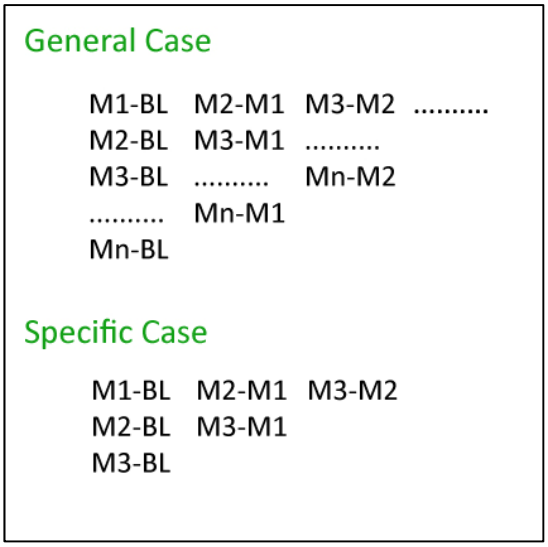

Figure 3.12 All possible time-lapse sequences in general case (upper part) and specific case (lower part) for four available seismic surveys (Baseline and three Monitors). For four surveys, the maximum number of differences is six.

So, by having 4 surveys (Baseline and 3 monitors) N equals six. The time for baseline is equal to T1, the time for the first monitor is T2, for the second monitor, T3, and for the last monitor T4. So, the time between base line and the first monitor is D21=T2-T1 or D21=ABS(T1-T2); in the same manner, D23 is time between second and first monitor and so on. Six maps of differences can be generated, in other words, six values for each point of the reservoir. Moreover, the sequence of these values will uniquely characterise a particular reservoir location, no matter how we transpose them within the sequence (a maximum of 720 variants exists). This is explained by the following equation:

$$A_n^k = \frac{n!}{(n-k)!} = \frac{6!}{1} = 720 \tag{3.11}$$

Unlike a usual seismic trace in a 3D seismic cube, a seismic sequence generated in this way contains information about the dynamic behavior of seismic changes at any given location.

It was decided to arrange the sequence in the following order:

$$A_i = \{(M1 - BL)_i, (M2 - BL)_i, (M3 - BL)_i, (M2 - M1)_i, (M3 - M1)_i, (M3 - M2)_i\} \tag{3.12}$$

Examples of such sequences are displayed in Figure 3.13. The order of differences in the sequence will not affect the analysis.

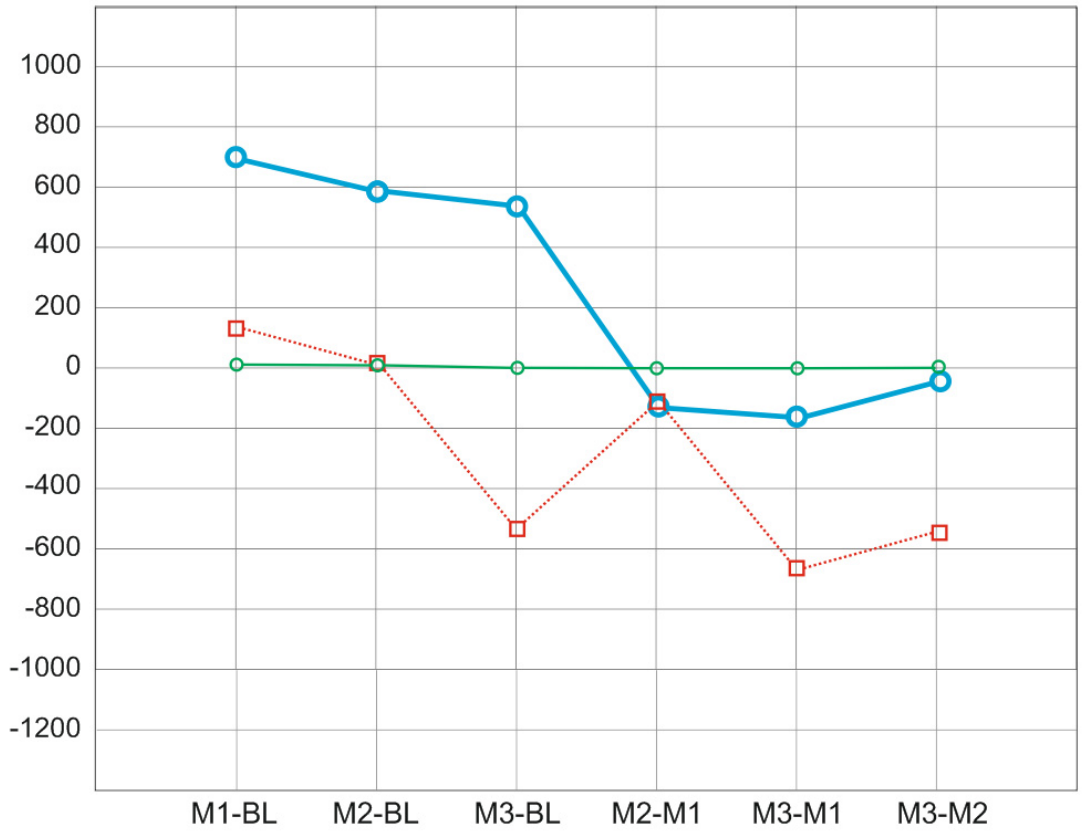

Figure 3.13 Examples of seismic difference sequences from multiple seismic attribute cubes for reservoir points. Curves are not limited to those presented. The number of curves will be equal to the simulation model cell number; curves will not be unique.

So, the number of points characterised by such a sequence will be equal to the simulation model cells, because we are working in the simulation domain. If the number of cells, N>0, then it is possible to perform cluster analysis on this data and derive a few typical clusters.

3.3.3 Step 2: Deriving sequences of cumulative volumes from production data

Production data should be processed and presented in the same way as the seismic data.

Consider a pair of two wells: injector INJ and producer PROD. From the material balance point of view, they have opposite signs: injector "+" (inject/add volume into reservoir) and producer "-" (produce/withdraw from reservoir).

The reservoir volume of original fluids in place= reservoir volume of fluid produced + volume of remaining reserves. Generally, the material balance equation can be presented in the following way (a list of symbols is in the Appendix):

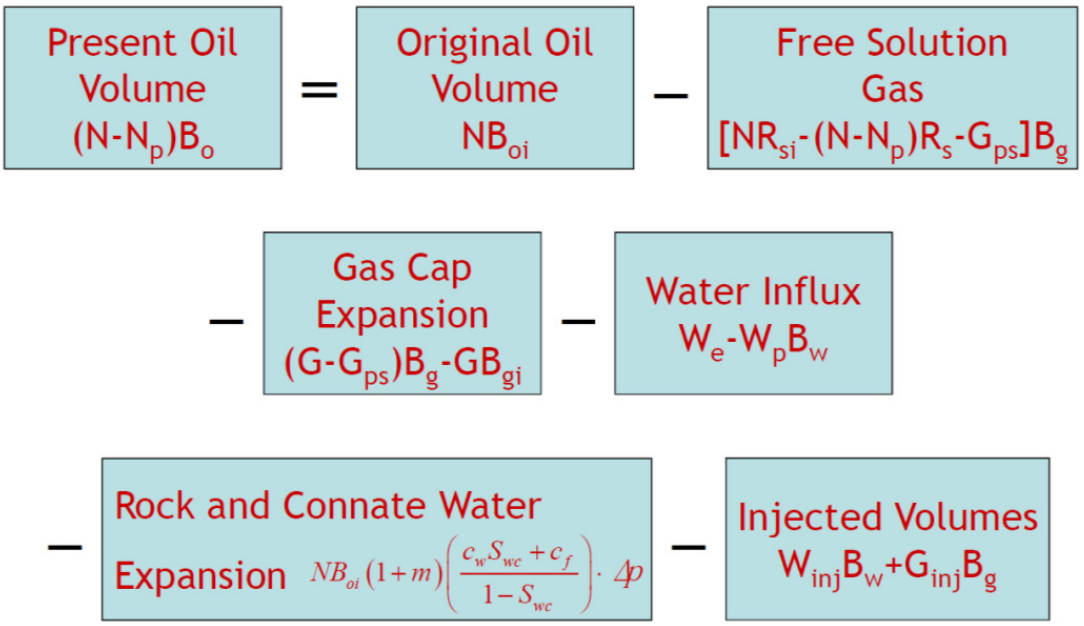

Figure 3.14 Material balance equation (Archer and Wall 1986)

In this case, I assume there is no free solution gas, gas cap expansion or rock and connate water expansion. The main affecting parameters are: present oil volume, original oil volume, injected volume and water influx from aquifer.

As discussed before, to link production data with 4D seismic we need to use cumulative volumes (production and injection); this data can be derived from daily/monthly production rates (see Figure 3.10). The principle of difference calculation is identical. For the same four surveys, we will have six differences in volume between corresponding times of seismic acquisition.

$$\Delta V_I = (\Delta V_1, \Delta V_2, \Delta V_3, \Delta V_4, \Delta V_5, \Delta V_6) \tag{3.13}$$

As an example, Figure 3.10 gives the plot for field production rates (oil and water) and cumulative production. The jagged curve can be explained by the production history- different wells were put into production at different times, and thus, production or injected volumes for each well are unique

Most importantly, I will plot the production data in the 'time-lapse seismic' domain; the difference in produced/injected volumes between seismic surveys can then be integrated with the seismic sequences. To produce the production plot, it is necessary to calculate volumes produced or injected for corresponding time intervals and then plot the results against time segments (see Figure 3.15).

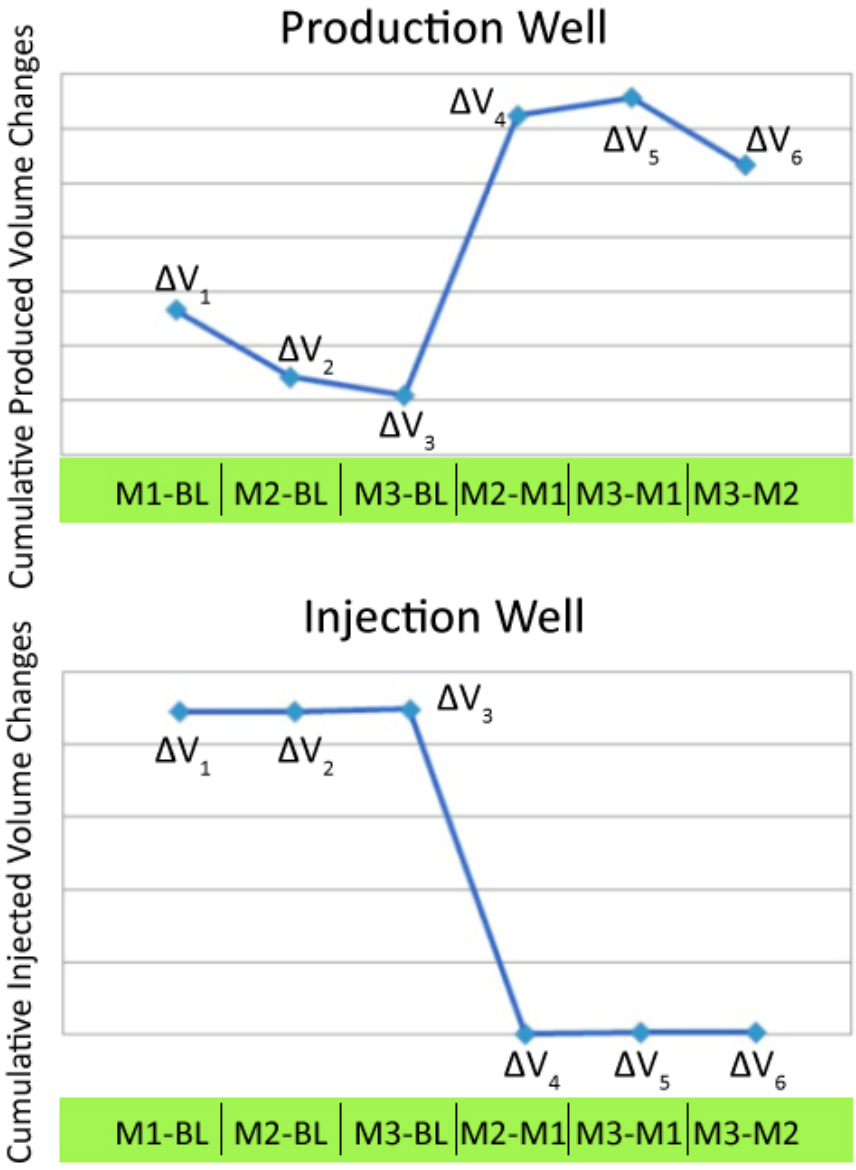

Figure 3.15 Well type curves. Production well is in the upper part, injection below. Real oilfield example. X-axis represents the different seismic survey times. Production volumes have a negative sign, while injection is positive.

This means that the plot reflects changes in cumulative volumes (injected or produced), and those for the injector will be symmetrical with respect to the producer, if these wells have a hydrodynamic connection. The connection in this case can be verified by well testing and historical well data. Detailed consideration of this will be in the following section. The slightly different shape of the type curves can be explained by the fact that INJ was closed after only a few years of injection. Indeed, these curves will be dependent on the time for which the well was on well on stream. All the possible curves for case of the 4 surveys are presented in the Appendix.

Thus, the reservoir usually has two types of wells (producers and injectors) and they have a symmetrical curve of volumes changes and their effect on the seismic signal is different. This fact gives a clue about the different types of reservoir behaviour.

3.3.4 Clustering of time-lapse data.

The seismic discloses reservoir behaviour in the interwell space. Based on the idea of seismic facies analysis, I decided to find reservoir parts with different dynamic behaviour. Each cluster has it is unique characteristic curve, as shown above. The type of curve depends on the well behaviour. The number of types of curves is limited by the number of seismic surveys and the number of well types (injector/producer), as well as the k-number of clusters.

First of all I apply cluster analysis on the seismic difference sequences:

$$A_i = \{(M1 - BL)_i, (M2 - BL)_i, (M3 - BL)_i, (M2 - M1)_i, (M3 - M1)_i, (M3 - M2)_i\} \tag{3.14}$$

Let us consider the steps carried out to obtain the clusters. Each point in the grid has this sequence (3.14), as represented in Table 1:

A_1	M1-BL	M2-BL	M3-BL	M2-M1	M3-M1	M3-M2
A_2	M1-BL	M2-BL	M3-BL	M2-M1	M3-M1	M3-M2
….	….	….	….	….	….	….
A_{n-1}	M1-BL	M2-BL	M3-BL	M2-M1	M3-M1	M3-M2
A_n	M1-BL	M2-BL	M3-BL	M2-M1	M3-M1	M3-M2

Table 3.1 Sequence of seismic differences

At the same time, each point is characterised by its own curve (see Figure 3.13), so each point can be part of some cluster. Thus, each line in the table will be owned by a particular cluster. Working only with seismic, it is almost impossible to understand the physical meaning of each derived cluster: it is possible to generate, say 15 clusters, but what is reason behind each of them? Thus we need wells as a link with the observed production data as a source of seismic changes. The first point which should be mentioned is that the presence of active wells is detectable by clusters. This statement is, indeed, obvious, as pointed out above: if there are no working wells there will be no changes in saturation/pressure and no changes in 4D. We can also consider which physical effects will be presented by clusters. Around injectors, the volumes (clusters) correspond to injected water displacing oil. Later, these volumes can be used for volumetric calculations; and to validate clusters. It is possible to divide injection among different intervals, if the well is completed in more than one interval. Around producers, the physical effect is oil sweep.

Each cluster type is an actual reservoir volume change in a particular time segment (step) and, for full cluster characterisation of the field, we need $2(n-1)+1$ (where n is a number of surveys) clusters. The factor of 2 is because there are two well types- injectors and producer, and the addition of 1 is for the 'non-active' cluster, which reflects shales or areas not involved in the sweep process, so they can be infill drilling targets. Next, we know that clusters can be connected to the well, in most of the cases only one (or two) clusters have a connection with the wellbore: for the first time segment (BL-M1), the next cluster (M1-M2) is adjacent and connected to the first one, and so on. Thus we can see fluid pathways and

understand the exact track of the well connections. The curves depicted on Figure 3.15 reflect two clusters for the first time segment (BL-M1), clusters 1 and 5 (see Figure 3.16). That means that the largest changes of volume in the reservoir described by these curves occurred between baseline and the first monitor survey. This is verified by the history data. The injection well was closed just few months before the first monitor. The producer was opened during the whole reservoir life, but if we compare produced volumes in the corresponding periods, it is clear that about 73% of production occurred in time step 1 (BL-M1). Hence, there are observed similarities between the well and the seismic responses in Figure 3.15 and Figure 3.16 (Cluster 1 is similar to the injection well and Cluster 5 to production well), which implies well connectivity with a particular cluster. This is a tie for the well and the seismic domain.

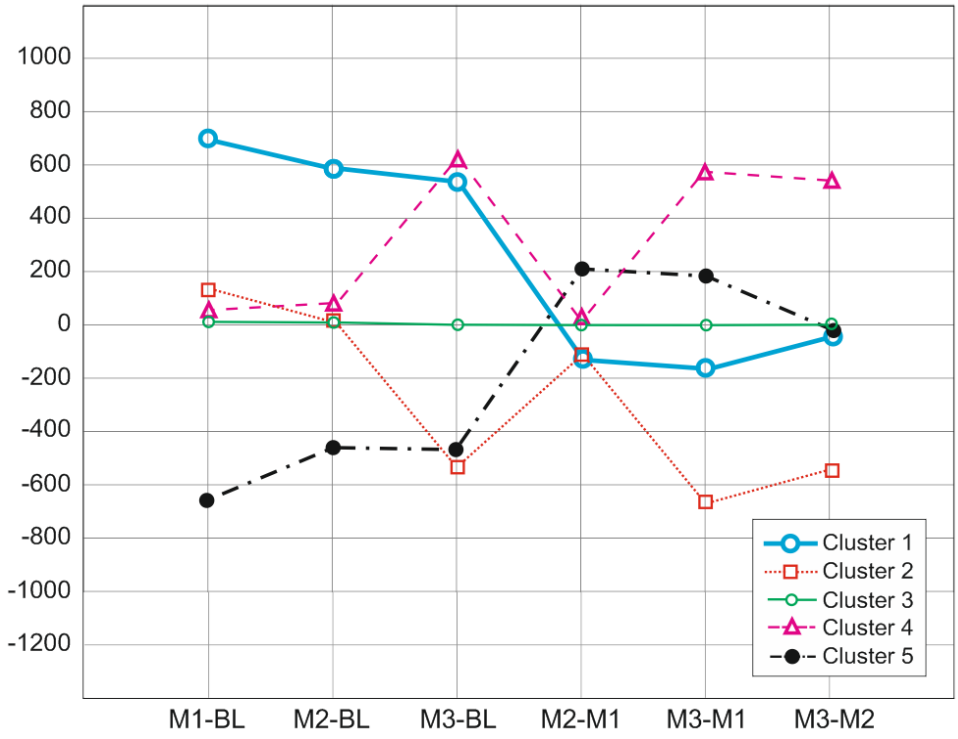

Figure 3.16 Cluster type curves. Y-axis: amplitude difference, X-axis: corresponding time step (D21= time between Monitor 1 and Baseline, D31= time between Monitor 2 and Baseline, D43= time between Monitor 3 and Baseline and etc.). The reason why we get only five clusters instead 7 (according to equation) is that there are not sufficient changes in the reservoir between one of the survey pairs.

Thus I generate 5 clusters, one of which is 'non-active' (in green in Figure 3.16). Actually, there are some reservoir points not related to any of these clusters; this was interpreted as noise. These points are lying beyond 3 SD from each cluster centre.

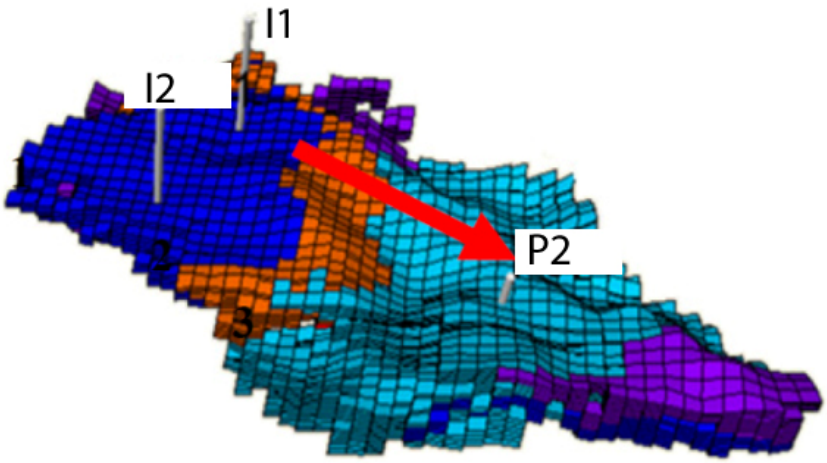

Figure 3.17 3D representation of fluid pathways, synthetic example. Fluids move from cluster 1 (dark blue) through 2 (red) towards 3 (light blue) and 4 (purple). Red arrow indicates flow direction.

This method is strongly linked with both well data and at the same time with seismic data, due to the nature of their relationship (Figure 3.18).

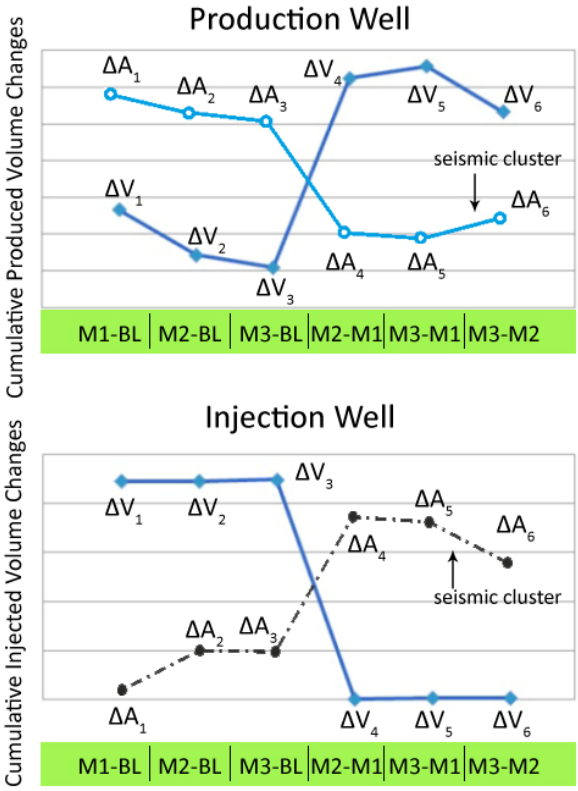

Figure 3.18 Comparison of type curves of production and injection wells (dark blue curve on the upper graph, and blue curve on the lower graph, respectively) and seismic clusters (light blue curve on the upper graph and black on the lower) . The character of the corresponding curves is quite similar.

3.3.5 Pressure and Saturation Discrimination

In addition to the previous figure, case sensitivity was performed. Saturation and pressure changes from the simulation model were compared with the observed seismic response. All the curves are in time-lapse time sequence format (see Figure 3.19). Each curve on the plot-means one particular cell from a cluster response (in the vicinity of the mentioned wells). with mean values.

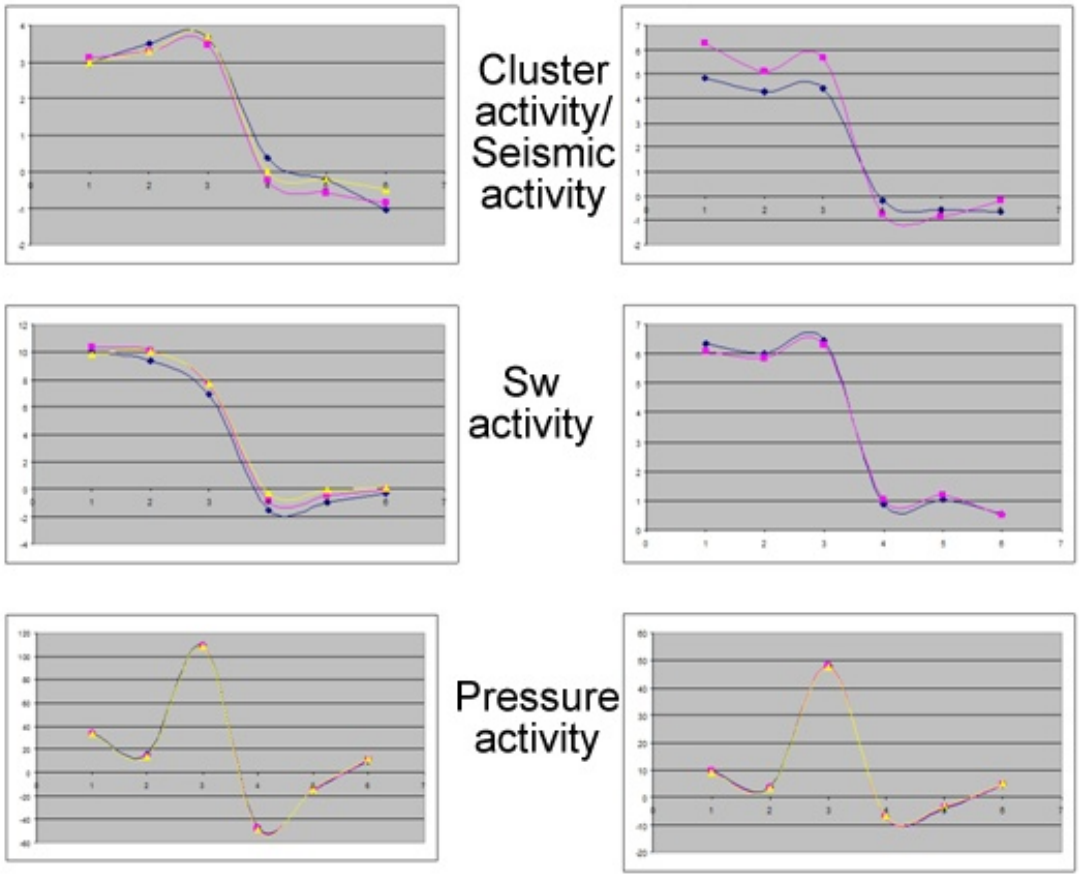

Figure 3.19 Comparison of time-lapse clustering data for case determination. Saturation dominance case-: there is obvious correlation of cluster (seismic activity) with saturation response. Left side- well I2, right side- well I1

It is easy to determine that the case is saturation dominance, because well activity correlates with saturation activity from the seismic. Pressure changes add some noise into the seismic response, but generally it can be concluded that we are working with a saturation dominated case. We now move on to the application for several field datasets in Chapters 4 and 5, before comparing with the well2seis in Chapter 6.

Chapter Four

UKCS field example

This chapter shows the application of the proposed method to a turbidite reservoir in the UKCS field in the North Sea. A high level of reservoir heterogeneity is reflected in poor connectivity within the reservoir, with impacts on production and field management. Here 4D and the cluster method are applied to locate dynamic geobodies within the reservoir and derive connectivity among these geobodies. These methods are also compared with existing techniques (Seis-to-Seis and Well-to-Seis) which can be utilised for connectivity estimation. This chapter provides the description of the simulation model and field reservoir conditions.

4.1 Introduction

The UKCS field is located in the Faeroe-Shetland Basin, west of Shetland, UK, in water depths of 400-450 m (Figure 4.1). It was discovered in 1993 and began production in 1998. The field consists a series of submarine slope turbidite complexes. Generally, there are three main sandstone units, with originally one field-wide OWC. Permeabilities are about 800-1600mD, which is rather high. The pre-production picture of the reservoir (model) proved optimistic, but later development of wells indicated a heterogeneous reservoir with numerous permeability barriers and baffles. The basis for discovery was the presence of 3D seismic anomalies with direct hydrocarbon indicators, i.e. amplitude brightening in oil-bearing sands. Geological barriers to flow are still a major uncertainty after 10 years of production in the UKCS field (Gainsky, et al. 2010). This problem is an explanation for the existing set of time-lapse seismic cubes and a reason for growing surveillance data.

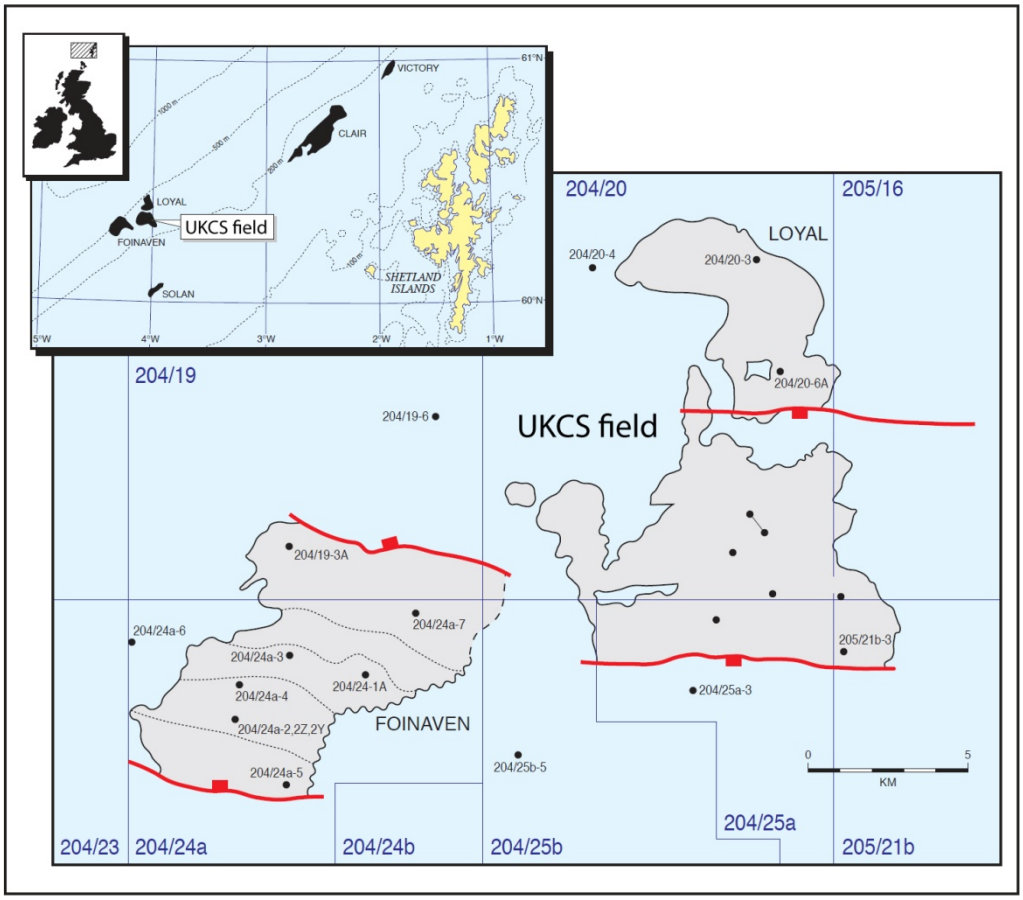

Figure 4.1 Location of the UKCS field, west of the Shetland Islands. Map showing exploration and appraisal well locations (Fyfe and Osbirne, 1996)

4.2 Field geology

The Faeroe-Shetland Basin is one of the several, NE-trending Mesozoic-Tertiary basins lying between the West Shetland platform in the SE and the Faeroe-Shetland Trough in the NW. It extends from the Erland Complex in the NE to the Judd Fault Complex in the SW (Figure 4.2)

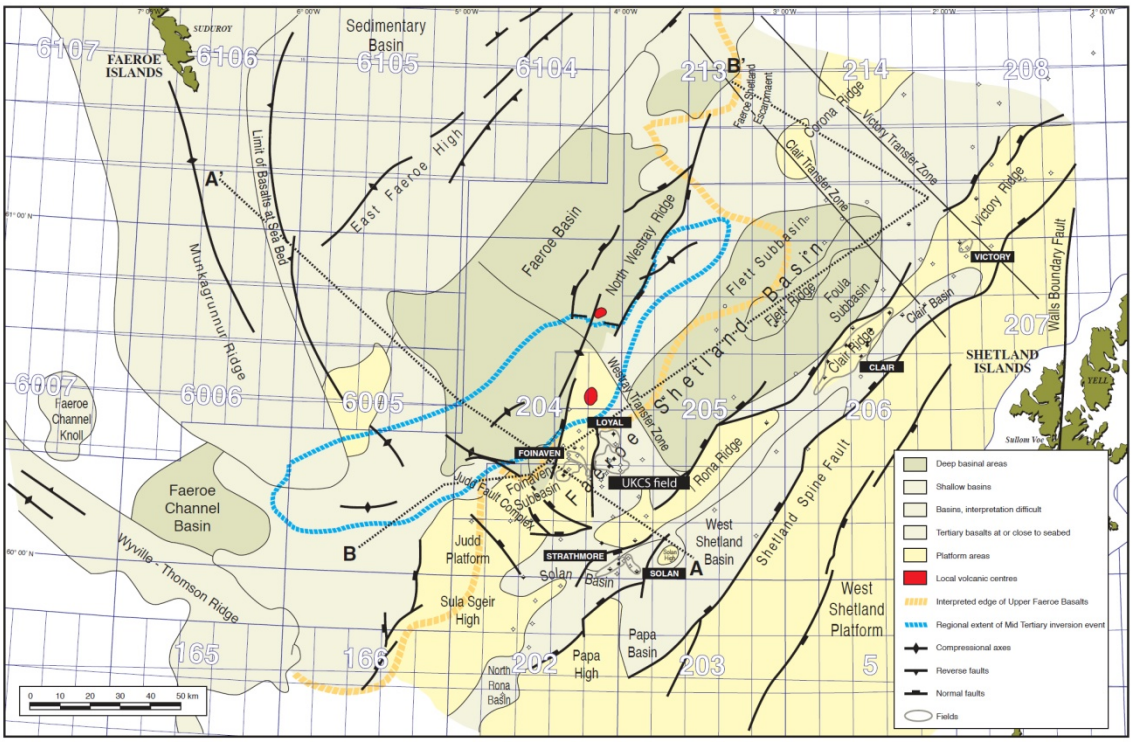

Figure 4.2 Faeroe-Shetland Basin. Structural framework of the area west of the Shetlands. The UKCS field is located in the Foinaven Subbasin of the Faeroe-Shetland Basin. (Iliffe et al., 1999)

The basin is a complex, characterised by a series of rifting episodes, beginning in the Late Paleozoic. The main events caused in the examined reservoirs occurred in the Middle Jurassic – rifting enhanced the Faeroe- Shetland basin to the west of the fault bounded by Rona Ridge and led mainly to the deposition of deltaic and shallow marine clastics, followed by deep-marine facies in the Late Jurassic. The reserves of this field were generated mainly from shales of the Upper Jurassic Kimmeridge Clay Formation. The UKCS field is contained in a combined structural-stratigraphic trap formed during the Late Paleocene reservoir deposition and rifting. The reservoir interval consists of several sandbodies interlayered with shales. The reservoir covers 35 km^2 and is divided into four main fault blocks or "segments."

The gross and net pay sand have been estimated from the seismic data, and seismic facies can be integrated with core and log data to form a geologic facies map of the reservoirs, as presented by Leach and others (Barbican Conference, 1997).

4.2.1 Reservoir connectivity

I have already discussed the concepts and methodology of reservoir connectivity in Chapter 3. The UKCS field is very good example of a compartmentalised field with numerous baffles and barriers.

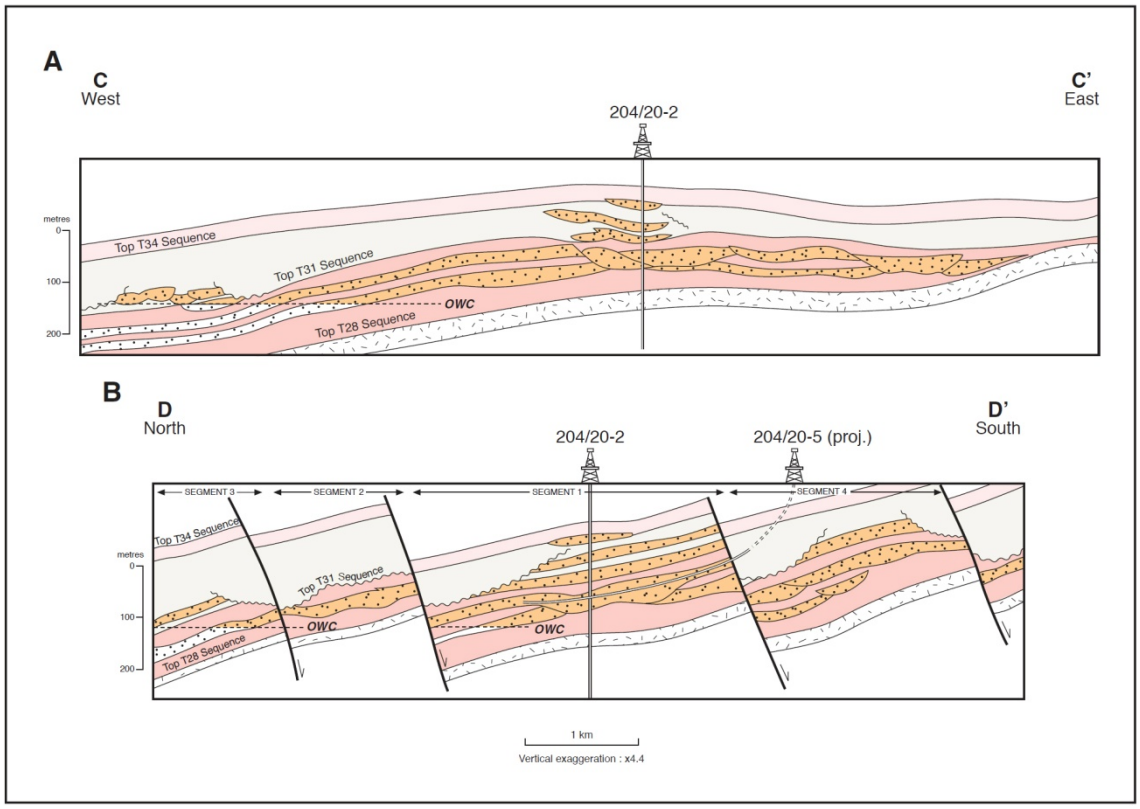

Figure 4.3 (A) W-E cross-section and (B) N-S cross section of the UKCS field (Leach et al., 1999)

The field is divided into four segments, caused by faulting (see Figure 4.3 and Figure 4.4), but presence of faults, which act as barriers, is only the first level of the field compartmentalisation. The main cause of the large number of compartments within the individual segments is the presence of lithological (facies) changes, which can be baffles or barriers to flow. Flow barriers can be geologically subtle, and difficult to image and interpret within existing 3D seismic data. Connectivity, therefore, cannot often be confirmed from a

static 3D seismic image alone (Gainsky, et al. 2010). Hence, we need dynamic data for interpreting differences related to baffles or facies. Before the operator-company obtained the first 4D seismic, poor connectivity was observed via the well's performance. The necessity for injection wells in appropriate positions is explained by a lack of reservoir energy, which, in turn, is explained by limited aquifer support and rather low initial GOR in the western part of Segment 4 (Govan, et al. 2006).

Most of the baffles and barriers were discovered due to integration of time-lapse seismic data and production data. The geological cross-section (Figure 4.3) shows only partly macro scale fluid flow restrictions and dominant sandbody-type channelized turbidites. Generally this depositional system (submarine slope turbidites) contains 3 types of sandbodies – channelized, sheet (channel/levee deposits) and overbank deposits, all of them present in the reservoir deposits (Figure 4.4).

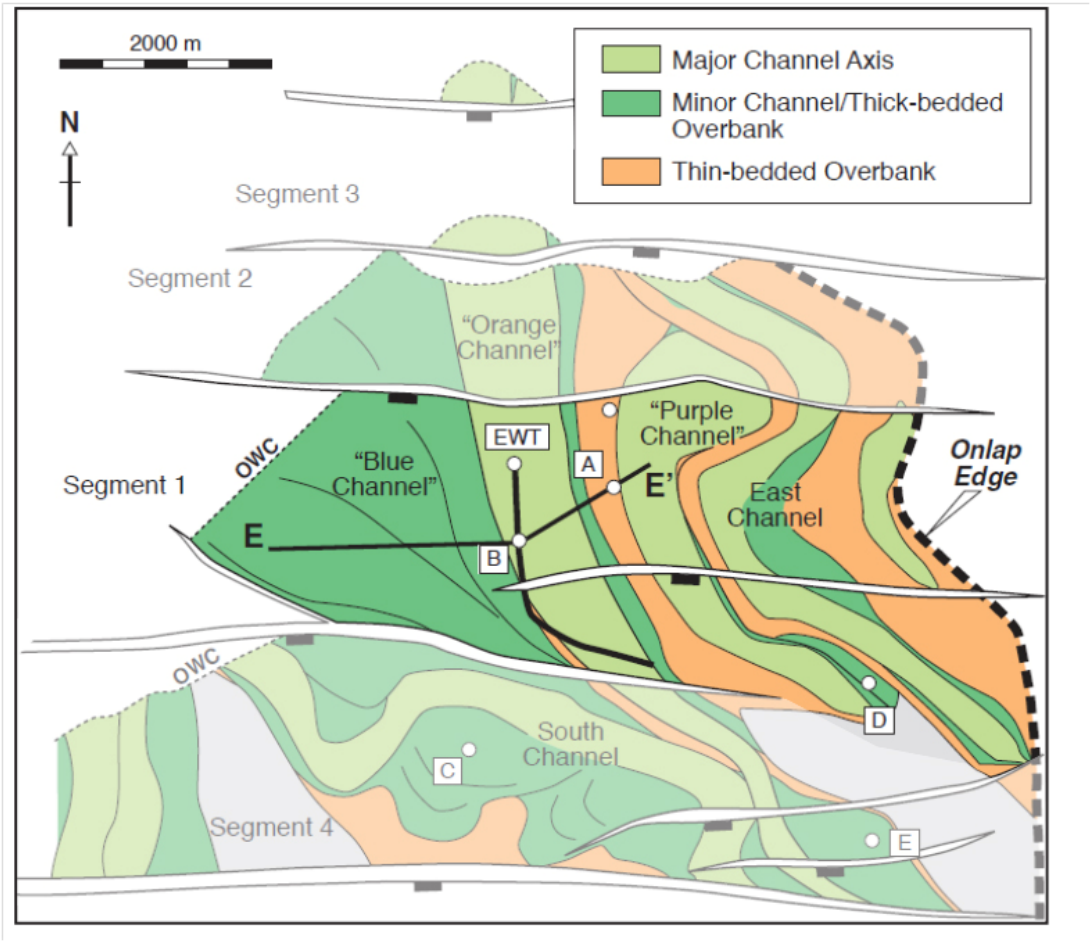

Figure 4.4 Channel distribution map of the T31 reservoir, reflecting degree of connectivity of reservoir (after Chapin et al., 2000)

The reservoir architecture (geometry) can be characterised as a jigsaw puzzle, with a three-scale fluid flow restriction: macro-scale (slope mudstones, faults), meso-scale (slope mudstones) and micro-scale (compaction of ductile grains, blocking pore throats). Only macro- and meso-scale features can be seen in the seismic section- faults can be relatively easily identified from static data, i.e. the 3D seismic. However, their ability to resist the flow can be estimated only by dynamic data.

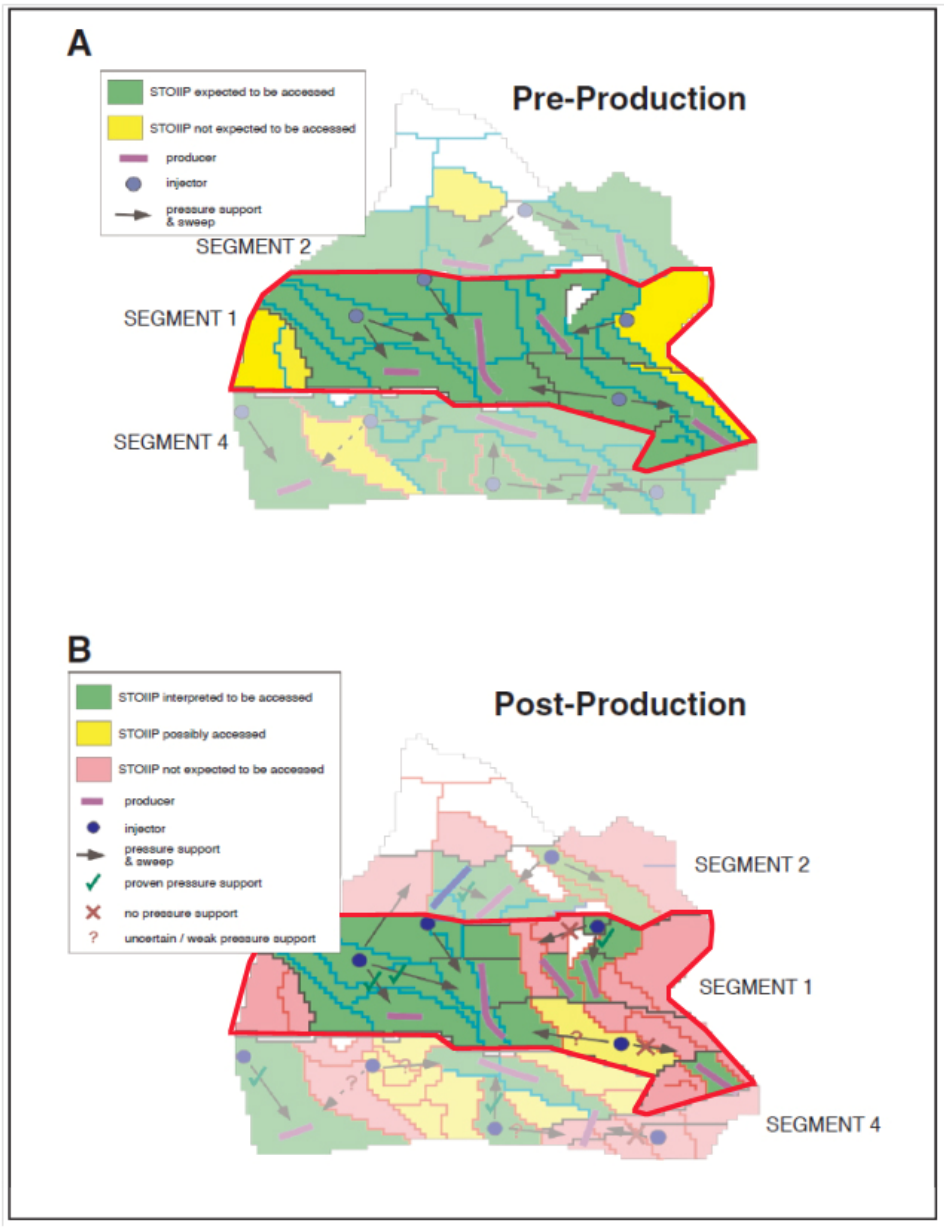

Figure 4.5 The pre-production reservoir model (A) was over-optimistic. Development drilling and field production revealed more complex reservoir architecture (B) (Leonard et al., 2000). Initial assumption: >80% STOIIP contacted. Reality: less than 60% STOIIP contacted, severe barriers at faults and channel boundaries detected. Red boundary: encloses area of investigation.

The Field comprises three main sandstone intervals (T31, T34 and T35). T31 is divided by discontinuous shale layers into two sub layers – T31a and T31b and consist of a series of laterally amalgamated channel complexes (Figure 4.4). The channelised facies have NTG of 0.7 and interchannel areas of 0.3-0.5 (Leonard, 2000). The trend for most of the channels is NW and WNW. T31 is separated from T34 by 10-20 m of mudstone (Leach, 1999). Figure 4.5 shows detailed analysis based on production data (permanent downhole gauges, well tests, well-head pressure and temperature gauge, production logging tools).

The main result of this reservoir study is the understanding that the largest uncertainty is reservoir connectivity. This is a critical factor for reservoir management and opening new wells and sidetracking planning. A special case is management of waterflooding and effective pressure maintenance, so communication between injectors and producers is essential. Thus, integration of all available reservoir data is a key for understanding connectivity and reservoir performance, for which dynamic data are the most valuable. Moreover, there are a number of successful field cases of recovery factor improvements through the use of connectivity estimations based on 4D seismic ((Parr and March 2000), (Webber and Geuns 1990), (Leach 1999), (Saxby 2001) and (Oistein, Kleppe and Nystein 1993)).

The focus of this work will be on the Segment 1 of the field. The table below represents the field description.

Basin	Faeroe-Shetland Basin
HC type	Waxy, medium-gravity oil
Discovery year	1993
First production	July 1998
Number of production wells	16 (1999)
Number of injection wells	12 water injectors + 1 gas-disposal (1999)
Platform	Subsea completions tied back to a FPSO vessel
Elevation of water depth	425m
Trap	
Structural setting	Inverted rift basin
Trap type	Combination structural- stratigraphic trap
Closure mechanisms	Dip and fault closure; depositional pinch-out on eastern flank
Depth to top pay	1700m TVDSS
Original hydrocarbon column height	364m
Original fluid contact	OWC: 2064 TVDSS
Reservoir	
Producing formation	T31, T34, T35
Deposition system	Submarine slope turbidites
Sandbody type (dominant)	Channelized turbidites

Sandbody type (secondary)	Sheet turbidites (channel/levee and overbank facies)
Sandbody type (tertiary)	Overbank turbidites
Reservoir architecture/geometry	Jigsaw puzzle
Fluid flow restrictions, macro-scale	Slope mudstones, faults
Fluid flow restrictions, meso-scale	Slope mudstones
Fluid flow restrictions, micro-scale	Compaction of ductile grains, blocking pore throats
Reservoir flow unit/strat.layers	3
Reservoir structural compartments	4
Reservoir struct./strat/ compartments	12
Net reservoir thickness	about 60m (T31, T34, T35)
NTG	0.5
Net pay	125m max
Lithology	Moderately to well-sorted, fine- to medium grained sublithic to lithic arenites
Porosity types	Primary intergranular; minor secondary porosity
Core porosity	Average 27-29%
Air permeability	Average 800-1600mD
Production-derived permeability	1200mD (from EWT on well 204/20-5)
Source	
Formation and age	Main: Kimmeridge Clay Fm (Up.Jurassic) Minor: Middle Jurassic
Lithology	Shales
Depositional system	Anoxic marine shelf
TOC	4-11%
Kerogen type	II
Time of hydrocarbon explusion	Late Cretaceous and Paleogene
Seal	
Formation and age	T35 sequence (Upper Paleocene)
Lithology	Mudstone
Depositional system	Slope turbidites
Reserves and Production	
OIP	936 MMBO (1997)
Ultimate recoverable	340 MMBO
Max production rate per well	30000 BOPD
Productivity index	74 BOPD/psi (well 204/20-5)
Hydrocarbon Composition	
API gravity	22-28 (average 26)
Viscosity	1.5-2.5 cp (reservoir conditions)
Sulphur content	0.48 wt.%
Initial GOR	342 SCF/STB
Saturation pressure	Bubble point: 2677 psia
Pour point	27 F
Field Characteristics	
Original reservoir pressure	2907 psia @ 1900m TVDSS

Pressure gradient	0.6 psi/ft
Natural drive mechanism	Solution-gas drive, with weak aquifer drive
Secondary recovery method	Water injection
Recovery factor	36%
Completion practice	
Type of completion	Horizontal completion with 7 in. slotted liner
Interval perforated	T30 reservoirs

4.3 Model Overview

4.3.1 Production history overview

The UKCS field was estimated in 1996 to contain a STOIIP of 936 MMBO and ultimate recoverable reserves of 340 MMBO (a recovery factor of 36%). The oil has an API gravity of 22-28^{o} (average 26^{o}), an in-place viscosity of 1.5-2.5 cp and an initial solution GOR of 342 SCF/STB. The oil has a high wax content (7-11%). The reservoir is slightly undersaturated, with a bubble point pressure of 2677 psia and an original reservoir pressure of 2907 psia at 6233 ft TVDSS. Aquifer drive is generally weak, although some aquifer influx has occurred along the field's western flank, which can be detected by 4D. Reservoir pressure has been supported by water injection since the field came onstream. The UKCS field production facilities consist of a floating production, storage and offloading vessel (FPSO), with flow lines and umbilicals tied to five subsea drilling templates (Dick et al., 1999). The facilities were designed with a peak capacity of 220,000 BOPD, 140 MMCFGPD and 225,000 BWPD. Oil from the field is exported by 14 cargo tanks to the Sullom Voe terminal. Gas is exported by pipeline to the Magnus field for re-injection (BP 2009). The planned plateau rate was 140,000 BOPD (Bradbury 1998). The produced gas provides a fuel for the FPSO vessel, with the surplus gas being reinjected into the deep, waterbearing T10 sandstones to the west of Segment 4. Field development was sanctioned in February 1996 and first oil was delivered in July 1998 (Leonard 2000). By 1998, 26 development wells had been drilled from five locations (Bradbury 1998). UKCS Field Central comprised nine producers and four water injectors. UKCS Field West consisted of three producers and three water injectors. The gas-disposal well was drilled from a separate location near UKCS Field West (Schiehallion BP oil field project 1999).

At the present time, the UKCS field subsea development consists of 5 subsea drill centers with 22 oil producers and 24 water injectors tied back to the UKCS field FPSO.

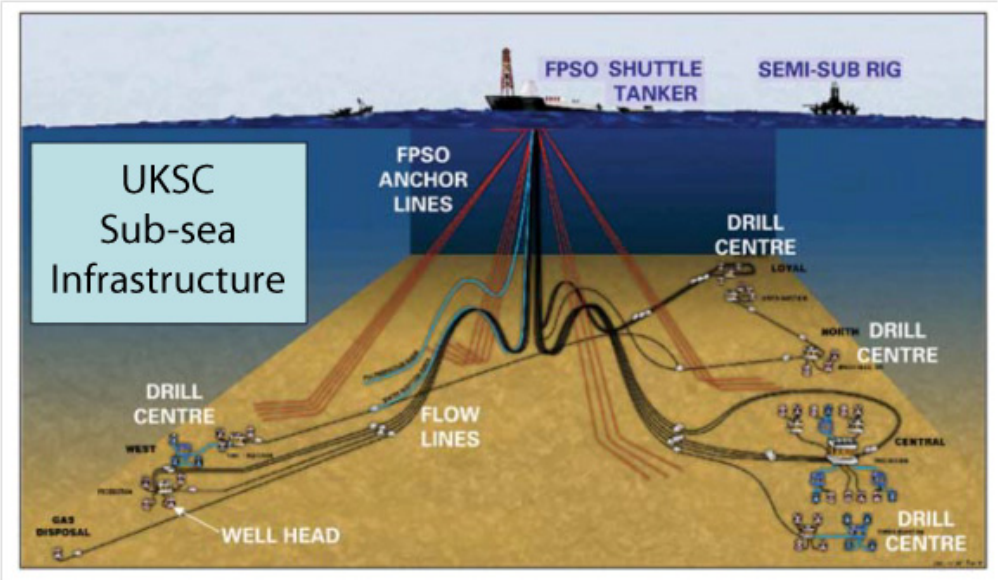

Figure 4.6 Schematic of field infrastructure showing main components: four drill centres, production wells and injection wells are connected through a system of well head and flow lines to UKCS field Floating Production Storage and Offloading (FPSO). A shuttle tanker transports the oil from the FPSO to Sullom Voe (Gainsky, et al. 2010).

As stated previously, reservoir connectivity in the UKCS field is rather complex, due to a high level of compartmentalisation and faulting. Because of concerns around reservoir connectivity in such an apparently channelised and heterogeneous reservoir, a horizontal well was drilled, completed, and flowed as an extended well test (EWT) for 57 days at stable rates of 18 000 b/d. The results of this well test established that sustained, commercial flow rates were achievable, and that a large portion of the reservoir was connected (Chapin, Terwogt and Ketting 2000). The seismic attribute map extracted from 3D seismic data reveals that the reservoir sands are highly channelised, and an important observation from the seismic is that 'bright' signals correspond to sand-rich channels and stacked overbank sandbodies. Considering this high level of geological discontinuity, most of the producers are horizontal wells and the majority of them are placed in the core of the channels imaged by the seismic, in order for each well to gain maximum exposure to net pay. The horizontal section of the horizontal producers can reach as far as 1500 metres. It turned out that this strategy was correct, after some time of production, as the appraisal data from monitoring techniques

indicate that many of these horizontal producers are draining several intersecting compartments.

The initial production strategy was to avoid early water breakthrough by not placing the injector and producers in the same channel. After the first oil, in 1998, it was realised that this strategy was not successful because the connectivity was much poorer than expected. Many injectors and producers were placed in poorly connected compartments, thus the expected pressure support from designed injector-to-producer pairs was not achieved. As a result, pressure in these compartments intersected by producers decreased dramatically in the early period of field life, causing a considerable amount of gas to be liberated from solution. The main aim for the first stage of field management (1998-2003) was to manage the gas by drilling in-fill water injectors. At the same time, all the injectors which penetrated separated compartments were closed. This strategy was right, as reservoir pressure recovered to the level above the bubble point four years after production start-up. However, the downside of this drilling campaign was that water breakthrough was soon observed. Thus, the second stage of field development (starting in 2003) mostly focused on monitoring water flooding. During this stage, new in-fill water injectors continued to be drilled as new flow barriers were identified, to further improve the sweeping efficiency and enhance pressure support, whilst new producers were also drilled to access the unswept zones. Time-lapse became more valuable, especially at this stage, to disclose geological features of the field and estimate connectivity of compartments.

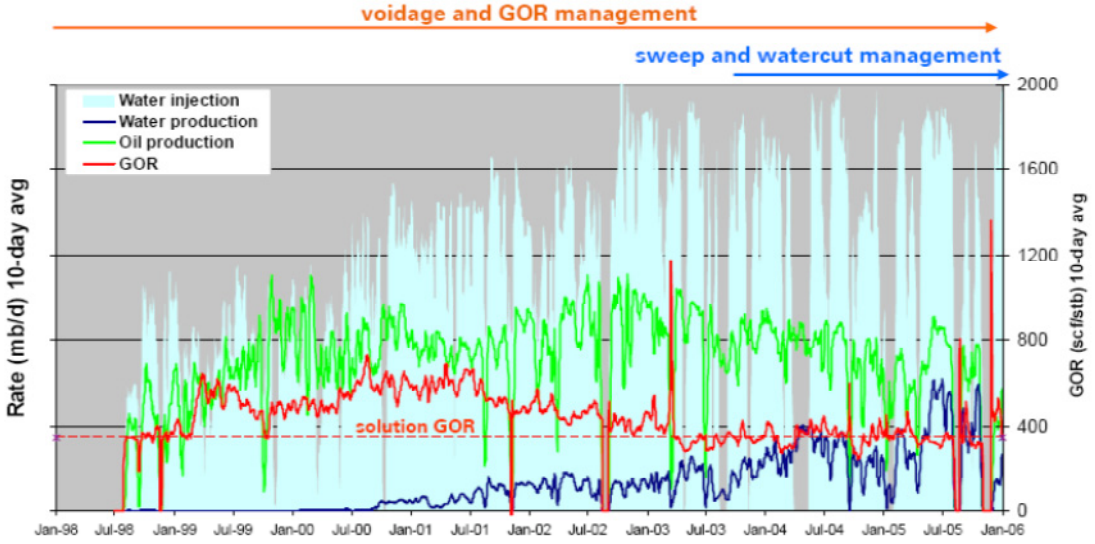

Figure 4.7 The UKCS field voidage history shows GOR (red line), water injection (shaded areas), water production (blue line), and oil production (green line). The variation of these lines reflects changes in reservoir management strategies (after (Govan, et al. 2006).

4.3.2 Simulation model and history matching.

This section will describe the simulation model which was used for the project. This simulation model was provided by the company. The number of cells is 237440 (128x53x35), the average individual cell size is 75x77x8 m. Mean porosity value is 0.27 and permeability is 911 mD; distributions of these parameters are presented in Figure 4.8.

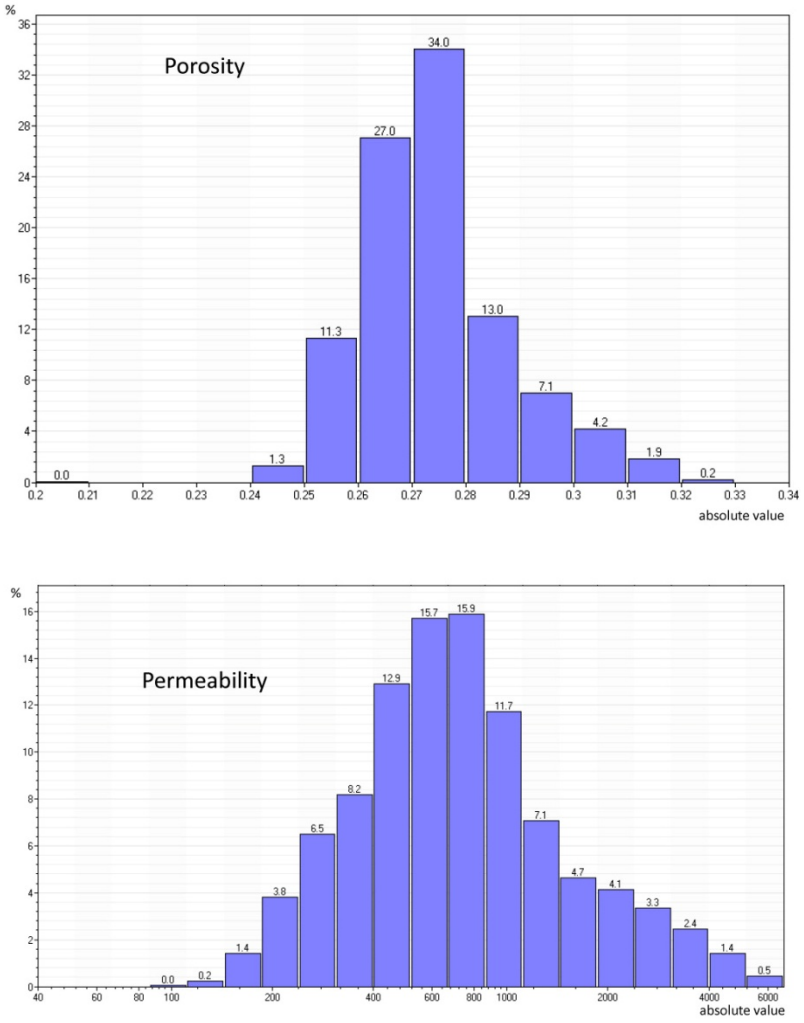

Figure 4.8 Petrophysical properties including into UKCS field simulation model. Upper graph: porosity, lower graph:permeability. Reservoir properties are rather good.

According to Figure 4.8, the reservoir has a rather good properties which are very favorable for fluid flow. Net-to-gross distributions vary from 0.2 up to 1 in the model. Hence, the main controlling property for reservoir connectivity will be NTG; this is a good correlation with modeled depositional environment.

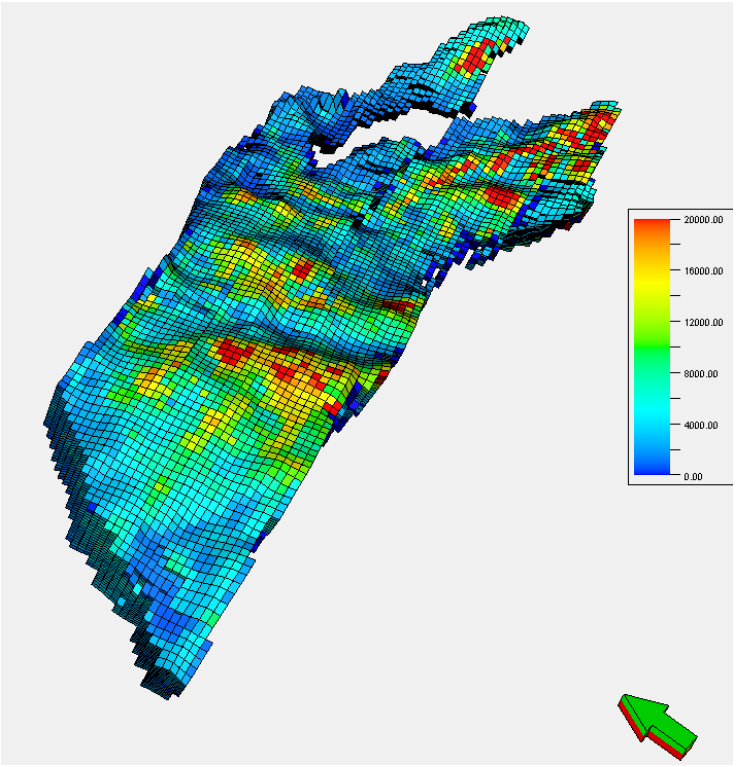

Figure 4.9 UKCS field kh grid in simulation model. Areas of improved properties are perfectly seen and correlated with the NTG grid.

The existing reservoir model for the UKCS field, provided by BP (Base Case model), simulates a black oil system. Pressure maintenance is presented by waterflooding. A rather weak aquifer is present on the western side (see Figure 4.10) of the field, providing the pressure support.

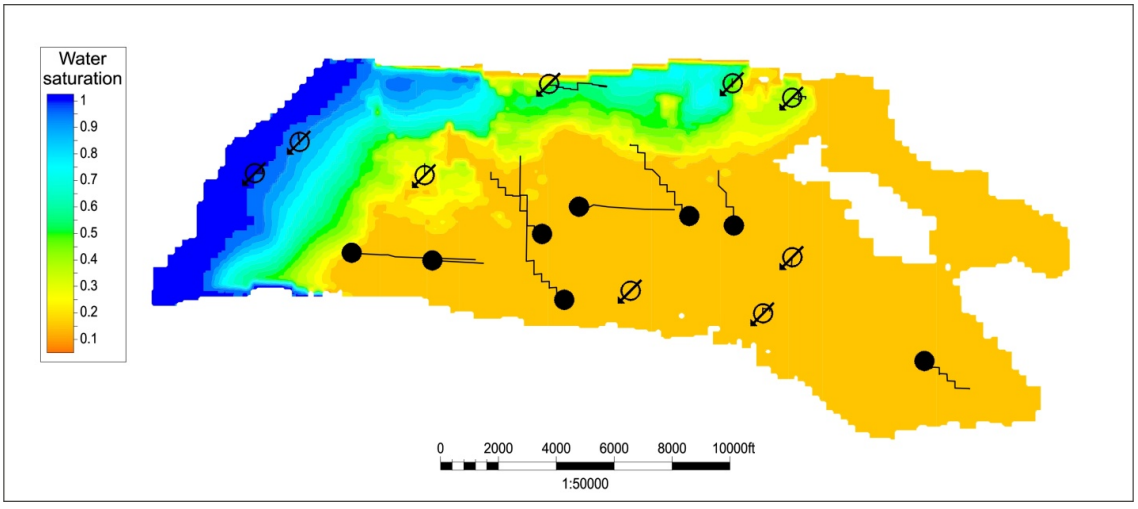

Figure 4.10 Initial water saturation map from simulation model. Aquifer located in the western part of the field.

Matching the model

Initial geological interpretation is based on wireline logs and seismic attributes, but after each monitor survey we gather new data, which needs to be incorporated into the model. Hence, the seismic interpretation have been changed in order to satisfy the newly data after each monitor. The idea behind this is to make a cube of seismic differences, for each time slice pick seismic volumes with more or less the same attribute value, and then use them in geological and simulation modelling. These seismic volumes can be named – 'geobodies'. This concept was presented at DEVEX 2010 (Martin & MacDonald, 2010). A special workflow was developed (see detailed description in Appendix). The final result was about 400 different geobodies (see Figure 4.11). According to this approach, a geobody has a dual-scaled definition:

In geophysics it is a 'small scale', seismically mapped discrete subdivision of the reservoir. In reservoir engineering it is a group of continuous cells in the model, characterised as being in the same transmissibility region (MULTNUM keyword in Eclipse; a description is presented in the Appendix).

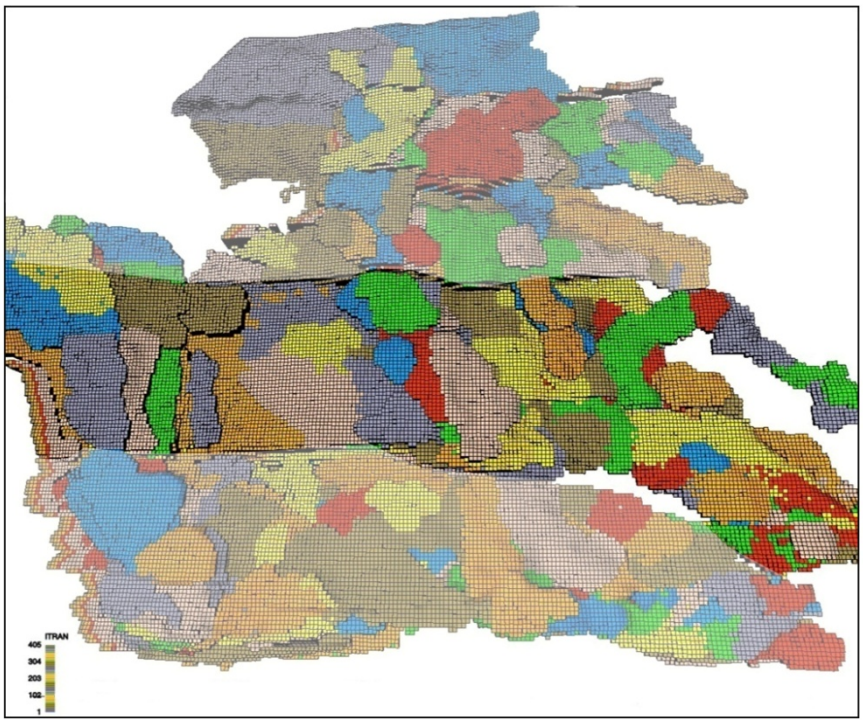

Figure 4.11 Geobody distribution for the initial geological model (2009) (Martin and MacDonald 2010). Engineering domain geobodies.

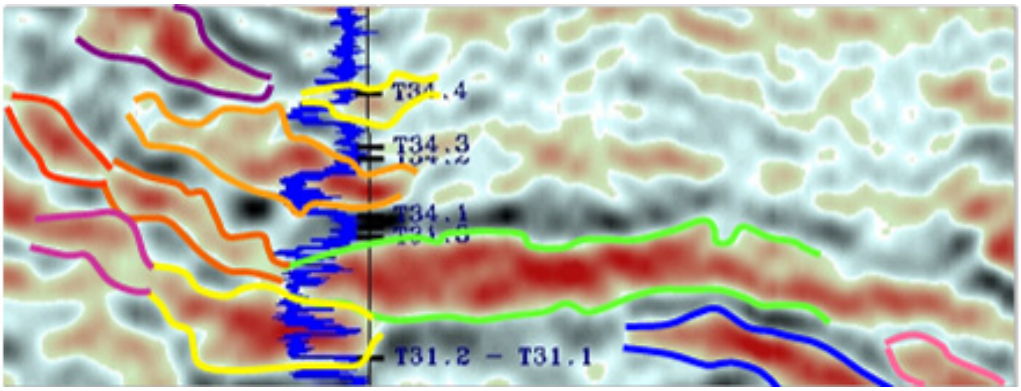

Figure 4.12 Derived geobodies (for example, between green boundaries is one geobody). Geophysical domain geobodies. Lower figure: coloured inversion seismic data, zero phase, negative impedance is red (sand) (Martin and MacDonald 2010).

The reasons for using this method (according to Martin & MacDonald, 2010) are as follows:

1. The previous Full Field model was good but not adequate to capture the evolving understanding of field complexity shown by the sequential 4D seismic surveys and additional production data.
2. The field history predicts geobody connectivity as primary factor in understanding well performance and reservoir sweep.

The derived geobodies were then incorporated into the simulation grid (see Figure 4.13). Using this method is reasonable, as, for a highly compartmentalised reservoir, simulation is not realistic unless major flow units and communication between them have been quantified (Stewart, *et al.,* 1988).

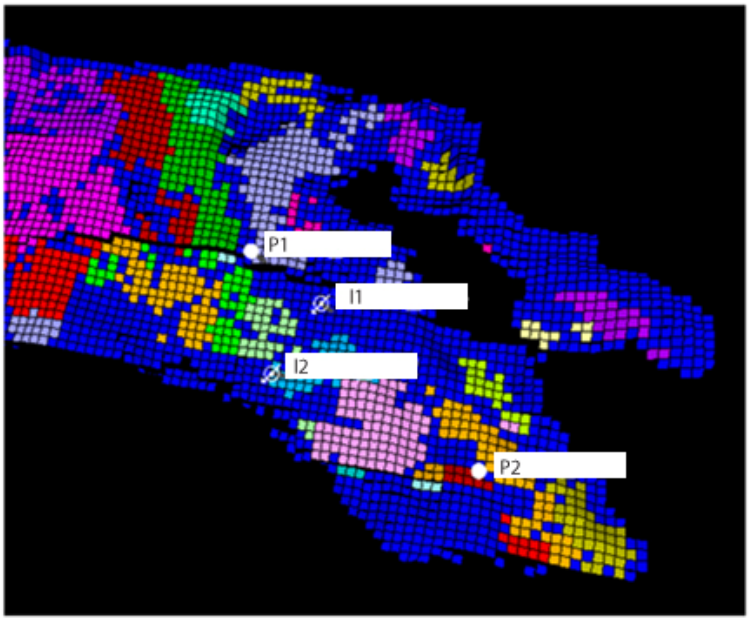

Figure 4.13 Geobodies in simulation model grid. Each colour reflects one separated geobody. Only the South-East simulation model is shown. Dark blue shows separate geobodies without any connections with others.

After incorporating the data, the next question is raised:

How is it possible to use this data in history matching? There are 3 ways to do this:

1. Vary transmissibility between bodies i.e. create an 'artificial' pathway for fluids (usually injected water). Actually, this is the most obvious way, from the geological point of view and results can be rather easily compared with production data: the velocity of the water goes from injector to producer, increasing water cut. Baffles on the boundaries of the geobodies can be explained by mud drapes or channel boundaries in the turbidite system. At the end of the day, this technique was the most applicable in this simulation model.

2. Vary transmissibilities within bodies. Here the same idea is used: it makes the water arrive at the right time to the producer, but for 100% validation of these changes it is necessary to have well test from well penetrating a particular geobody.

3. Vary pore volume within bodies. This procedure can also be implemented, but then there is a need to have additional control over STOIIP in the model, because porosity directly affects STOIIP.

Apart from reservoir geobodies, some non-reservoir geobodies also exist. A typical example

of these is an isolated compartment without wells in it, just non-reservoir facies- shales. These have zero transmissibilities on each border, but pore volume within the body has not been changed. Although this seems reasonable, why is this the case? In the best case, these geobodies could be isolated compartments (parts of the reservoir) and contain hydrocarbons. But we cannot be sure about this until a well is drilled into this compartment.

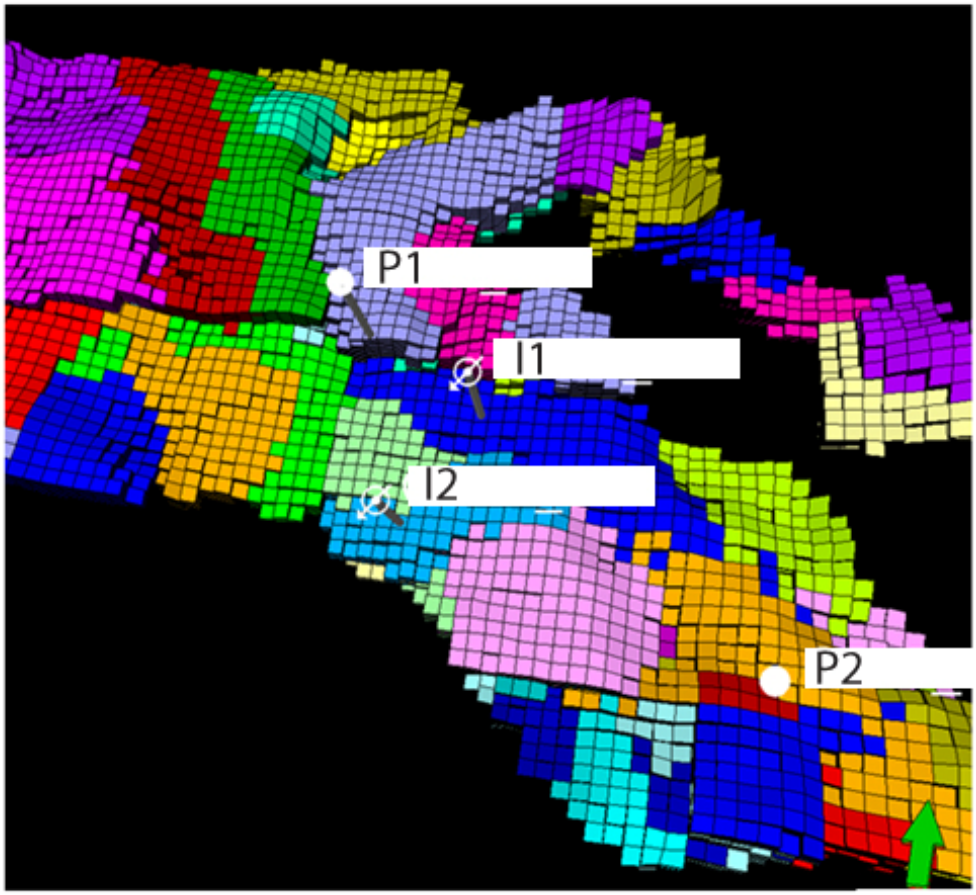

Figure 4.14 Geobodies after excluding the 'dark blue' region. Now it is possible to see the regions which could be a fluid path, having permeability more than zero.

There is a clear example of the latter case. The most abundant body (in dark blue in Figure 4.12 and excluded from Figure 4.14) which is actually a border (conclude) all the pathways- should not be a compartment, although it can be according to the geology, but then, this should be shales, i.e. non-reservoir cells. So we cannot be sure about this and the engineers have decided not to make the pore volume of these cells equal to zero. Unfortunately, this approach has one weak side: using this manual approach, it is impossible to catch up all the small baffles and barriers within the geobody, but in fact, this should not have a significant

effect on fluid flow in the reservoir.

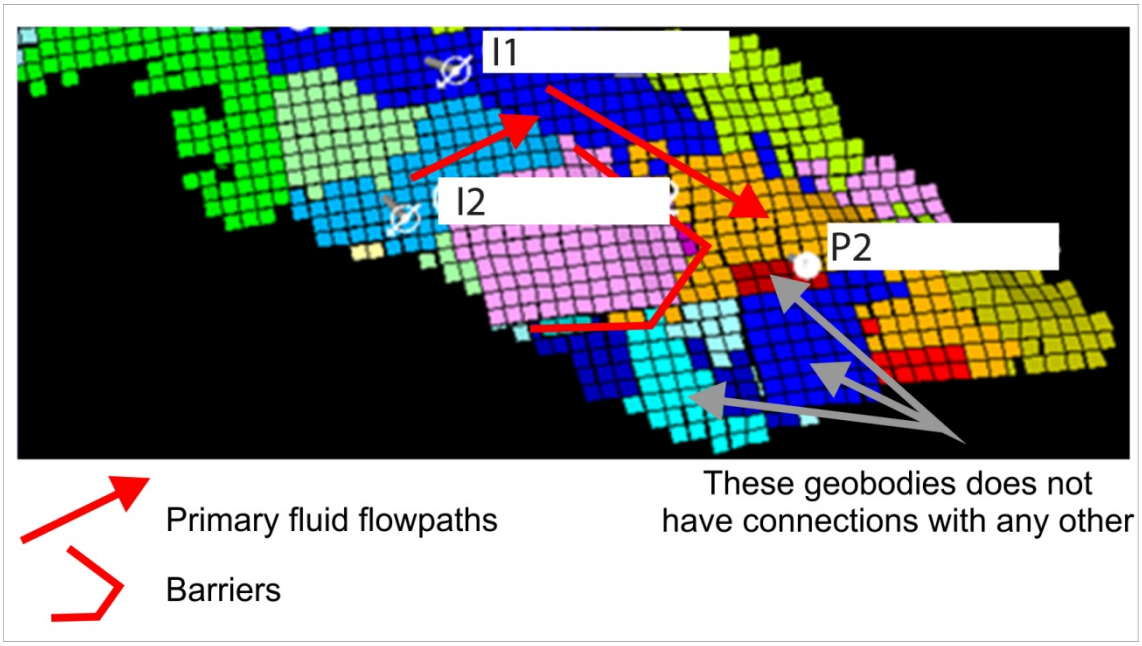

Figure 4.15 How the pathway was created. Red lines: barriers for flow. Red lines: pathway for injected water. Pointed geobodies (white lines) do not have connections to any other geobodies.

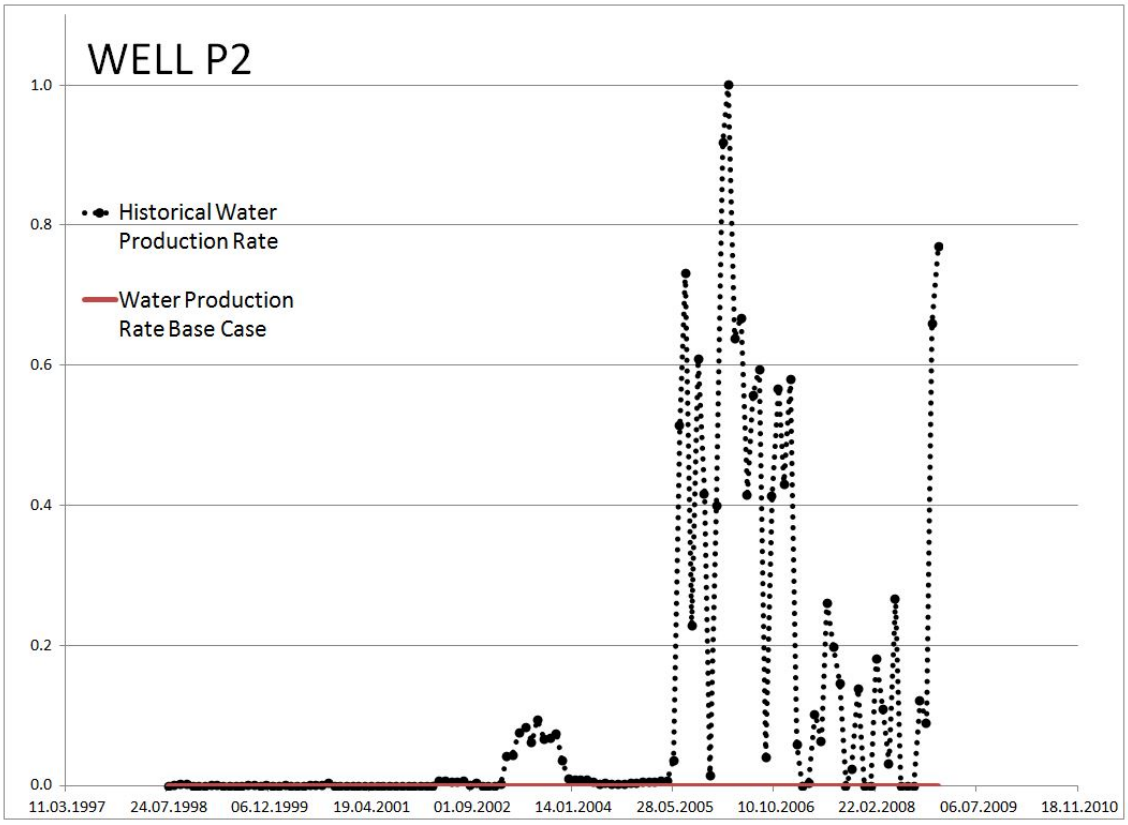

Figure 4.16 Well P2 water production rate history (blue dotted line) and base case simulation model results (red line). It is obvious that there is a lack of water in the well.

Figure 4.15 shows how a fluid pathway was created to solve the lack of water production in P2 (see Figure 4.16).

Let us see this example how one of these pathways shown in Figure 4.15 How the pathway was created. Red lines: barriers for flow. Red lines: pathway for injected water. Pointed geobodies (white lines) do not have connections to any other geobodies. The engineers have decided to make a pathway through the channel (which can be seen on NTG map: see Figure 4.17). There are two reasons for this choice: the NTG map and the 4D differences between M1 and BL highlight changes in this region. However, the interesting fact is that water breakthrough happened in P2, just after the time of M1, and I1 started injection about the same time; thus P2 was affected by water from I2, but this water went through the south part (this fact seen in the time-lapse data, as well). That means even though the matching is right (the simulation model reflects the history data), it cannot be geologically justified. Later, when I1 starts to inject, water was injected into this well, using the same channel to reach P2.

To sum up, the rationale of this method is the creation of an 'artificial' pathway for fluids between wells, with support from the geology.

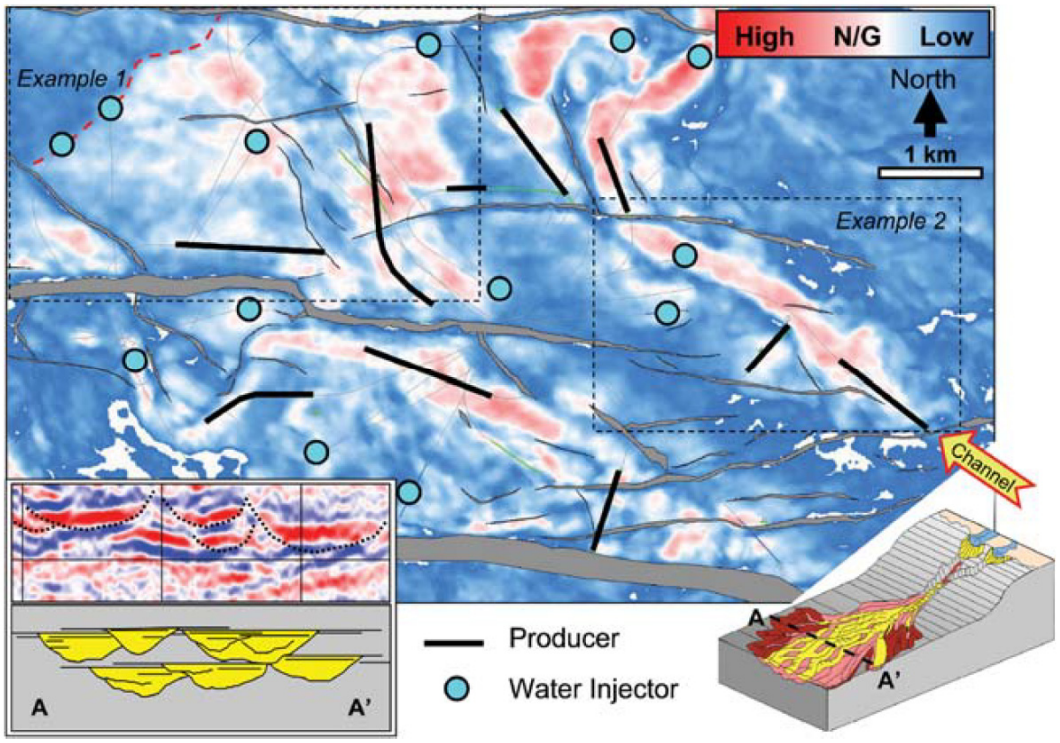

Figure 4.17 Depositional environment and UKCS field main T31 sand reservoir. Higher NTG is highlighted in red. Seismic section A-A' shows typical channel geometry of the NW-trending depositional system. The channels are cut by east-west trending faults (grey lines) (Gainsky, et al. 2010).

In other words, the reason, we should choose the channel as the pathway for injected water is obvious.

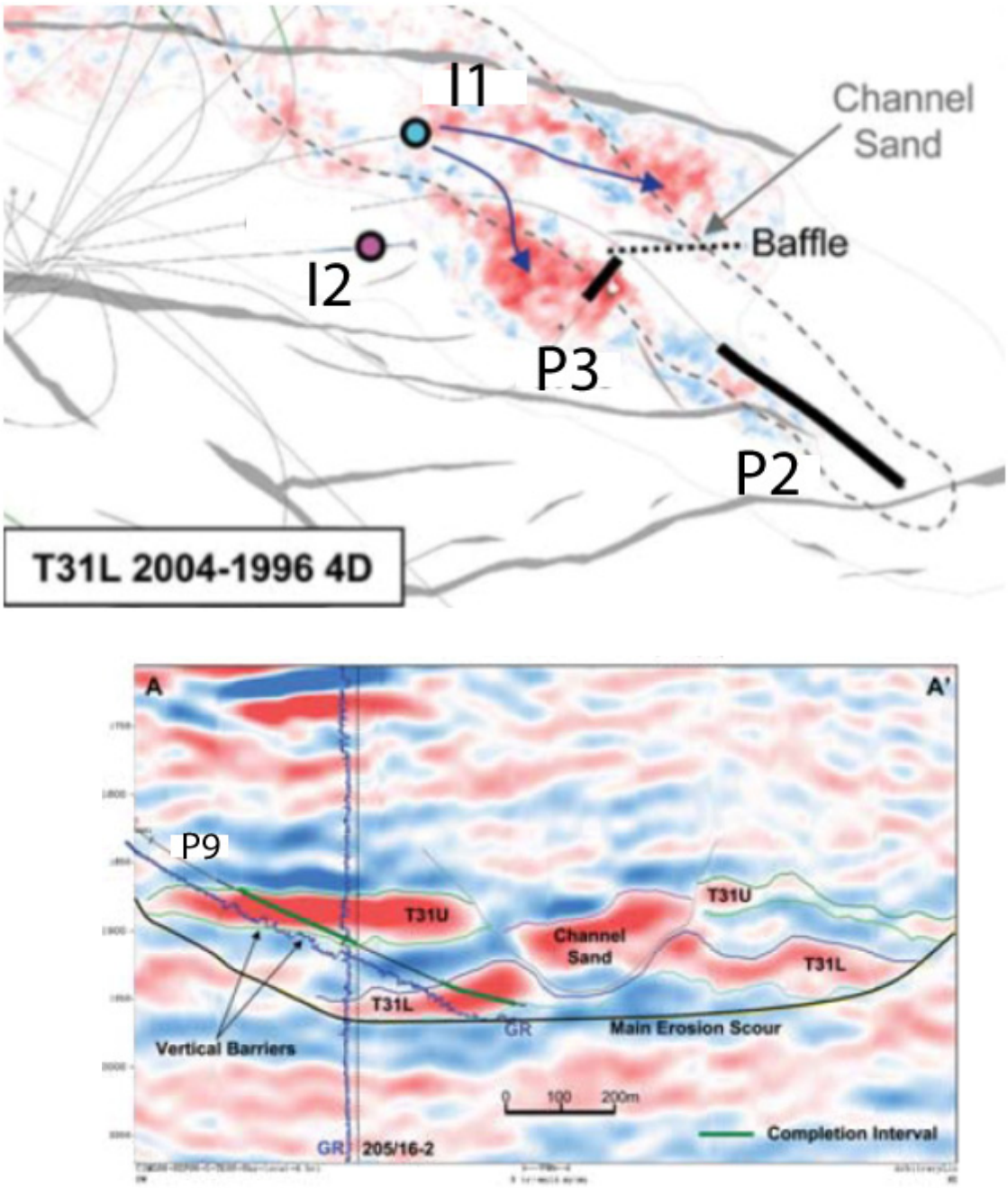

Figure 4.18 3D seismic cross-section along the P9 producer showing infill targets in T31U and T31L sands. The solid green lines are the completion intervals in P9. The blue curve shown along the well trajectory is the gamma ray log with vertical barriers indicated. The T31L sand is partially eroded by a younger channel (Gainsky, et al. 2010).

The 4D difference between M2 and M1 shows directly that changes occurred there. Nevertheless, the assumption, that this channel was the only pathway for water breakthrough to P2 can be argued. Let us examine the difference between BL and M1- along with the channel: a rather large area to the south was affected by production from P2 and injection

from I2 (I1 was closed during that time period). It is possible to conclude that breakthrough occurred not through the channel, but in southern area, but that later, when I1 started injection, water flowed through the channel. So we need to be aware of isolating south region, thus avoiding oil sweeping from this area and water injection in it. At the least, the boundaries of the southern part geobodies need to be baffles, rather than barriers.

The final distribution of barriers and baffles used in matching is presented in Figure 4.19.

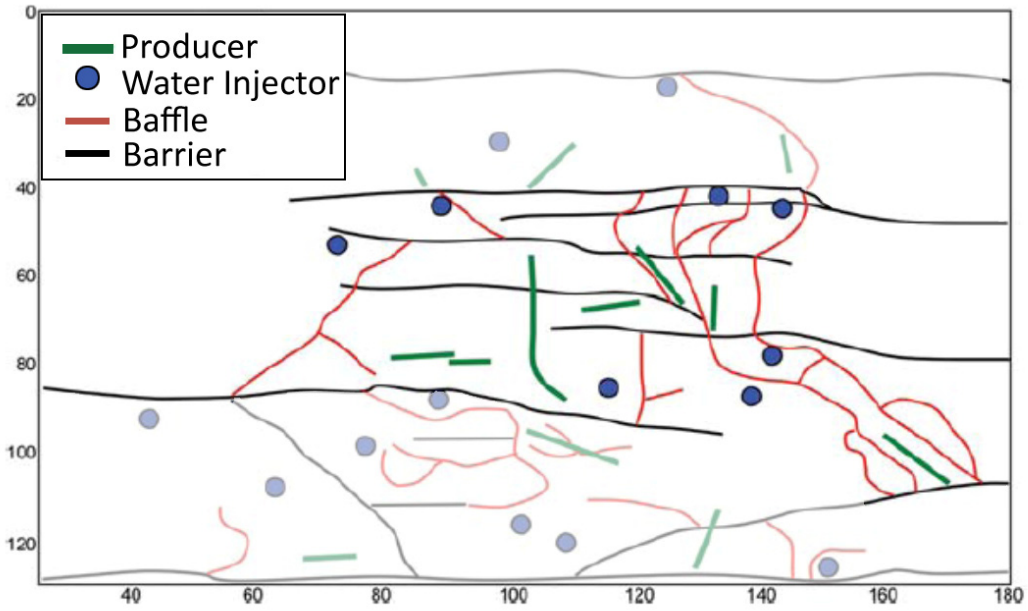

Figure 4.19 Sand barriers (black) and baffles (red) to flow used in matching (Gainsky, et al. 2010). Highlighted area- Segment 4- object of interest.

4.4 Cluster application

In order to test my method, all the transmissibility multipliers and any other changes of the simulation grids used for matching (described in the previous section), were deleted and the simulation model was initialised and simulated. Thus, I started work with initial grids of porosity, permeability and most significantly- transmissibilities. After simulation, water saturation distribution in the end of simulation has the following appearance (see Figure 4.20). Figure 4.21 represents graphs of observed cumulative oil production (red circles) and the simulated curve of cumulative oil production in the Base Case model. It is easy to see a

sufficient difference, starting in 2005, which can be explained by lack of water in the producing fluid. Such a quality of history matching is not appropriate, so the application of cluster technique intended to solve this problem.

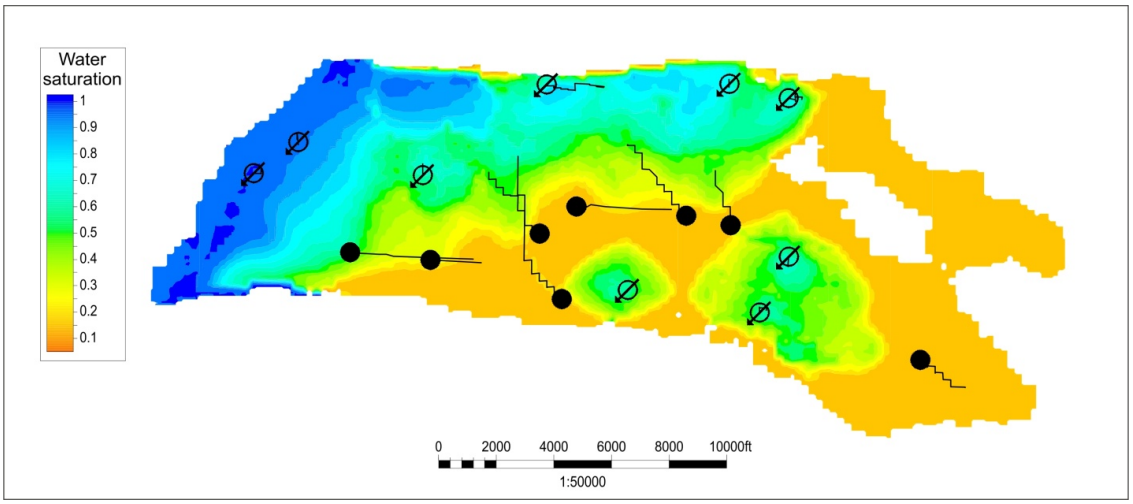

Figure 4.20 Water saturation distribution in August 2008. The last step of simulation: the final distribution of the water, it is quite uniform and does not reflect the geology (channels, baffles etc.)..

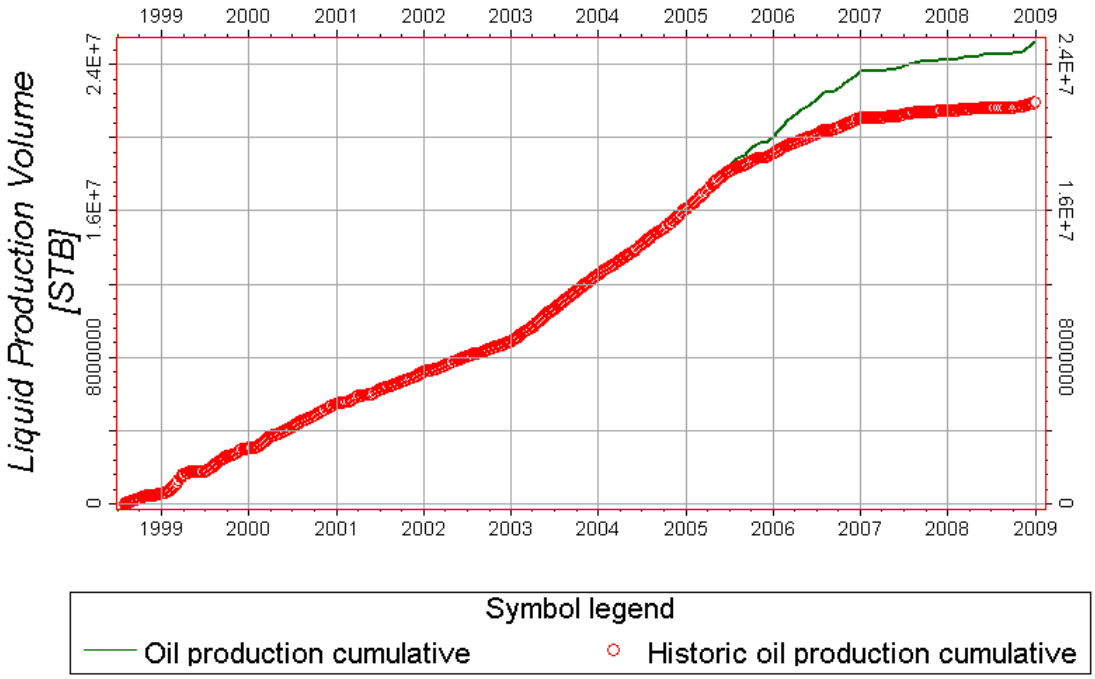

Figure 4.21 History matching quality for Base Case model. Green line: simulated cumulative oil production. Red circles-: observed cumulative oil production

4.4.1 Examples of cluster technique results

This part presents two examples of cluster connectivity update for the UKCS field and an assessment of the results.

The first area examined (Figure 4.22) is a more detailed discussion of the part of the field already presented. The region characterized by the lack of water in P2 producer and poor matching. In the A1, A2 and A3 illustrations, individual clusters are represented by injected water and produced oil, reflecting swept volumes. The small map beside them shows their connectivity: assuming connectivity of the swept volume cell=1, everything else=0. B1 means two time steps have been merged, A1 and A2, so it is possible to get an updated connectivity map, and the final result is B2, a detailed connectivity map. It needs to be understood that the map is in a relative scale; a red colour means better connectivity, than green, and, green in turn, is better than light blue.

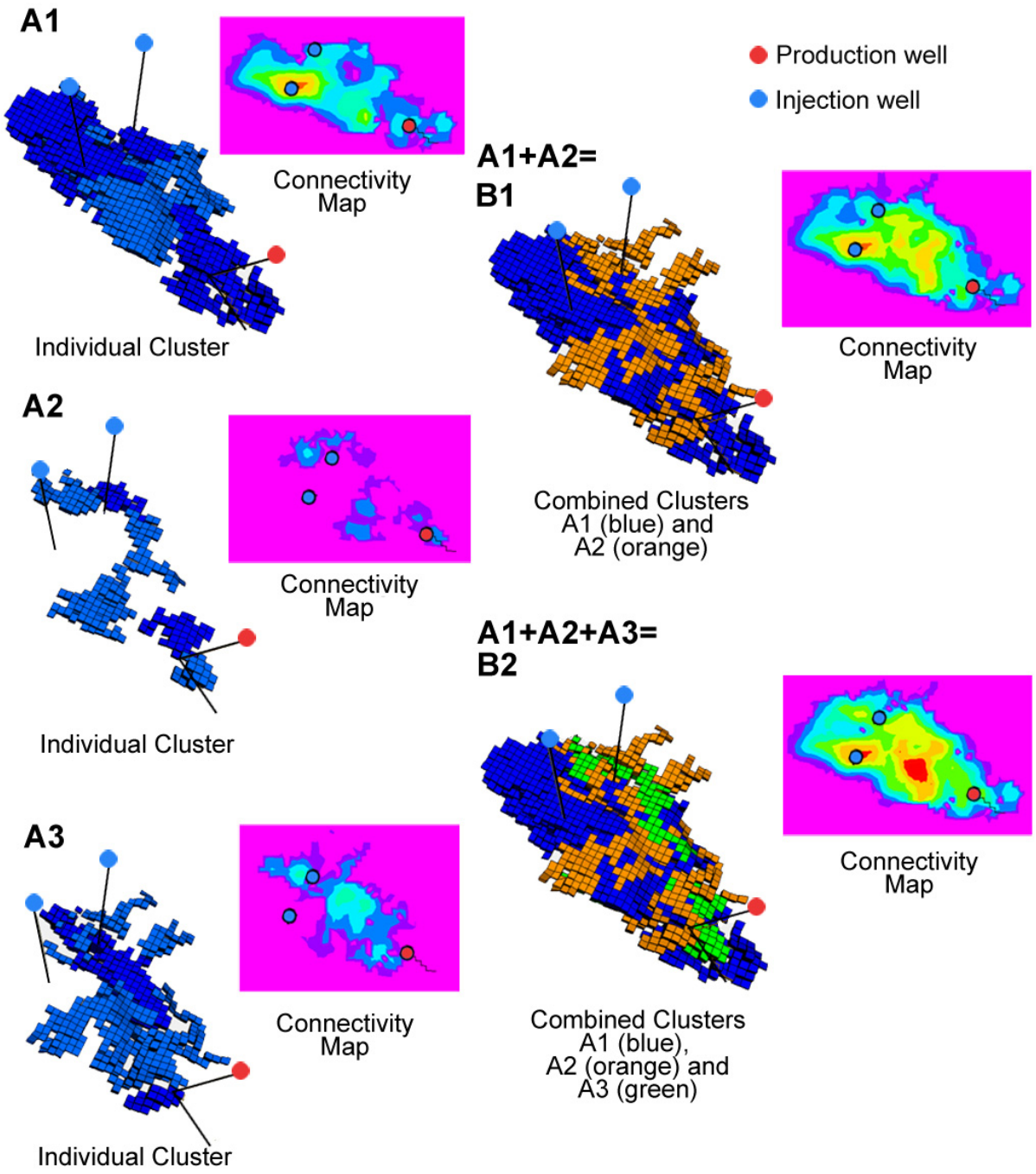

Figure 4.22 A: individual clusters and associated connectivity. B: Combined clusters with resulting connectivity. High connectivity: red; low: pink. Case 1. Production well is P2, injection wells are I1 and I2. For area location details see Figure 4.24.

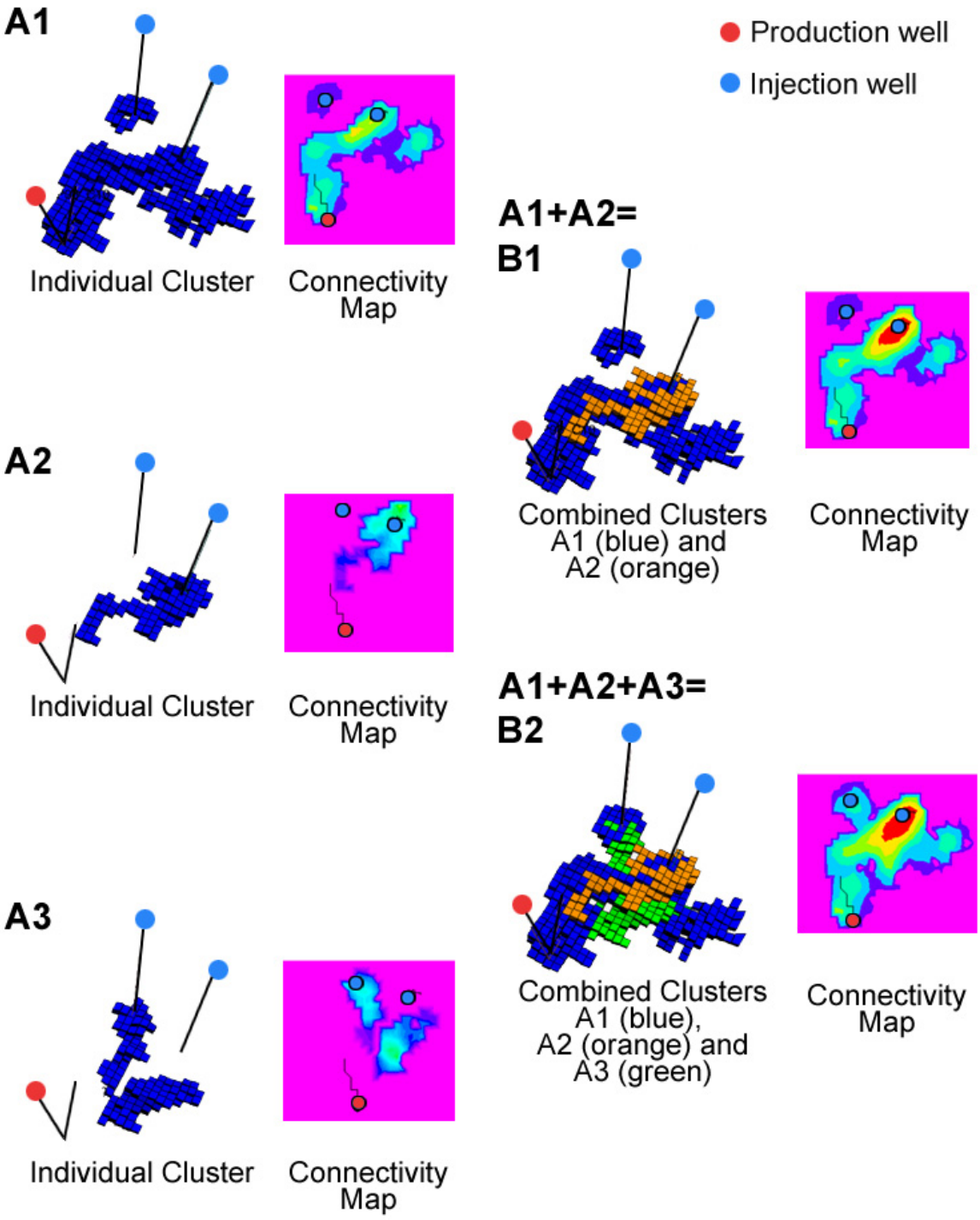

Figure 4.23 A: individual clusters and associated connectivity. B: Combined clusters with resulting connectivity. High connectivity: red; low: pink. Case 2. Production well is P1, injection wells are I3 and I4. For area location details see Figure 4.24.

The interpretation of the B2 maps from Figure 4.22 and Figure 4.23 is presented in Figure 4.24, where the presence of barriers and baffles is shown. The result is compared with

injection analysis of Gainsky et al. (2010) (see upper part of the figure). An interesting conclusion is the presence of hydraulic connectivity between I2 and I1 and P1 (producer), which are on different sides of the main fault (black lines). This fact is confirmed by the extended well test, as well.

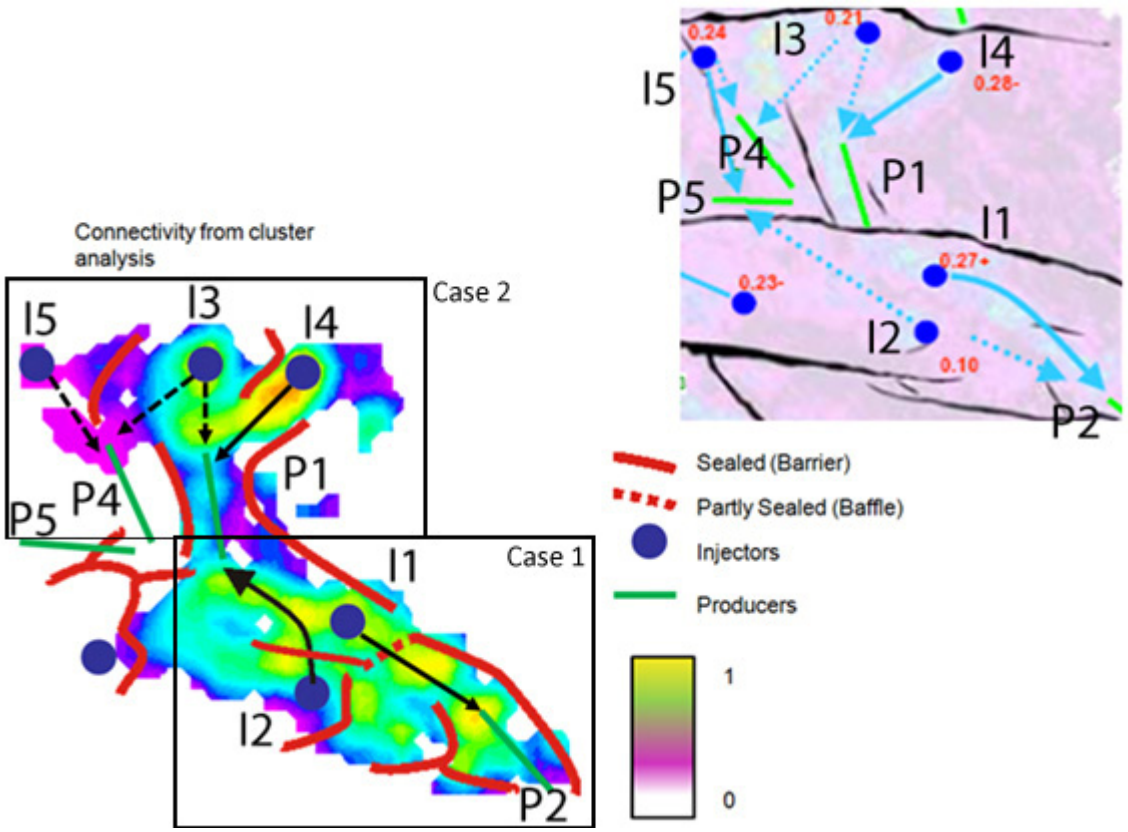

Figure 4.24 Detailed cluster connectivity analysis. Upper figure: injector's fluid flow pathways from (Gainsky, et al. 2010)

The resulting map for the field compartments is shown in Figure 4.25

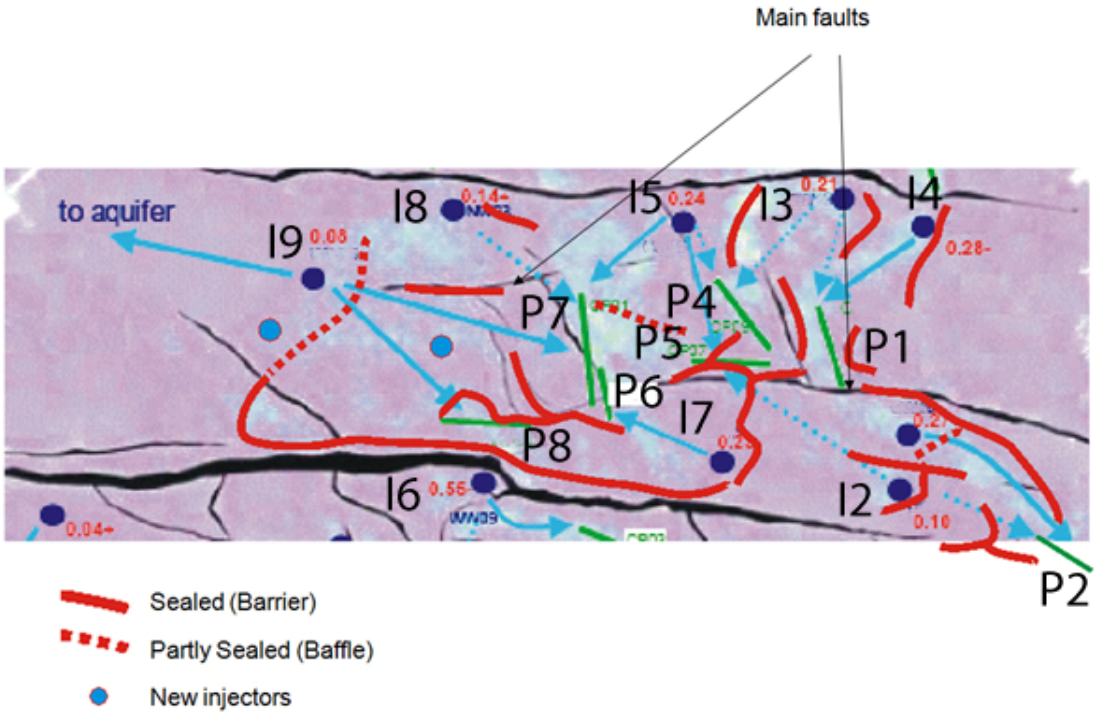

Figure 4.25 Well-to-well connectivity. Barriers and baffles determined by cluster analysis (Gainsky, et al. 2010).

4.5 Cluster and sedimentological consistency

Based on the sedimentological description of the field, it is possible to interpret the cluster technique results. The cross-section in Figure 4.26 shows the results of cluster division into the 'active' (reservoir) part, in orange and the 'non-active' non-reservoir part, in grey. Reservoir parts can be distinctly interpreted, like the "Confined" channel complex in the eastern part of the field, which gradually changes into "Broad Channels" and finally into "Sheet" sand bodies in the west. This interpretation agrees with the sedimentological and geological settings of the field (which were discussed in this chapter previously). The same tendency can be seen in the plane view of the field (see the lower part of Figure 4.26). Different areas of colour represent different types of geobodies: black is for "sheet" sand bodies, green for "broad channels" and dark blue and light blue curves represent a "confined" channel complex. The map also illustrates the reservoir connectivity changing from to zero to one.

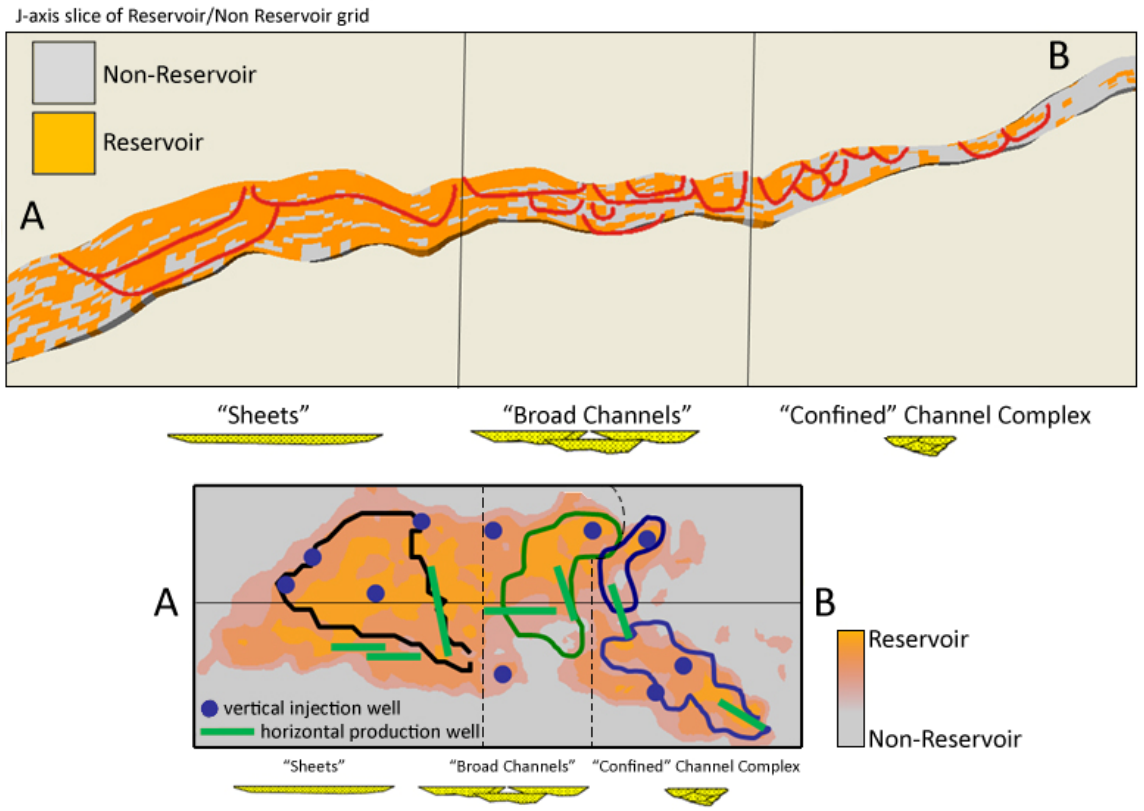

Figure 4.26 Sedimentological consistency of the cluster techniques. Lower map: sum of cell values; where a reservoir cell has a value 1, non-reservoir has a value 0. Injection wells- blue dots, production wells- green lines. A different coloured area means a different type of geobodies- black is for "sheet" sand bodies, green for "broad channels" and dark blue and light blue curves represent a "confined" channel complex.

The geological cross-section shows the ratio of reservoir and non-reservoir cells in the model, after updating of 'non-reservoir' cells using the clustering technique.

4.6 Examining the implications of 4D data integration into the simulation model

The main criterion of history matching results is convergence of simulated production data with observed data. Moreover, proper history matching can be characterised by the physical, meaningful prediction of the production process, which can be reached only by keeping in mind the reservoir geology and its integration into the simulation process. Details of the nature of the history matching process have been discussed in Chapter One. The first type of data, and most easily accessed, which can be used for the judgment of results, is the

production data. Figure 4.27 and Figure 4.28 show matching results for production well P2. The first one demonstrates history matching results of the oil production rate in comparison with the history data: it can be seen that simulated oil production (red line on the graph) sufficiently exceeds observed (black dotted line), due to the lack of produced water. This can happen for geological reasons- the water does not have a pathway to reach the production well, or reservoir properties, such as permeability, are not correct. For the permeability we have core measurements, at least, but not for connectivity. So the main geological reason which can be expected here is connectivity.

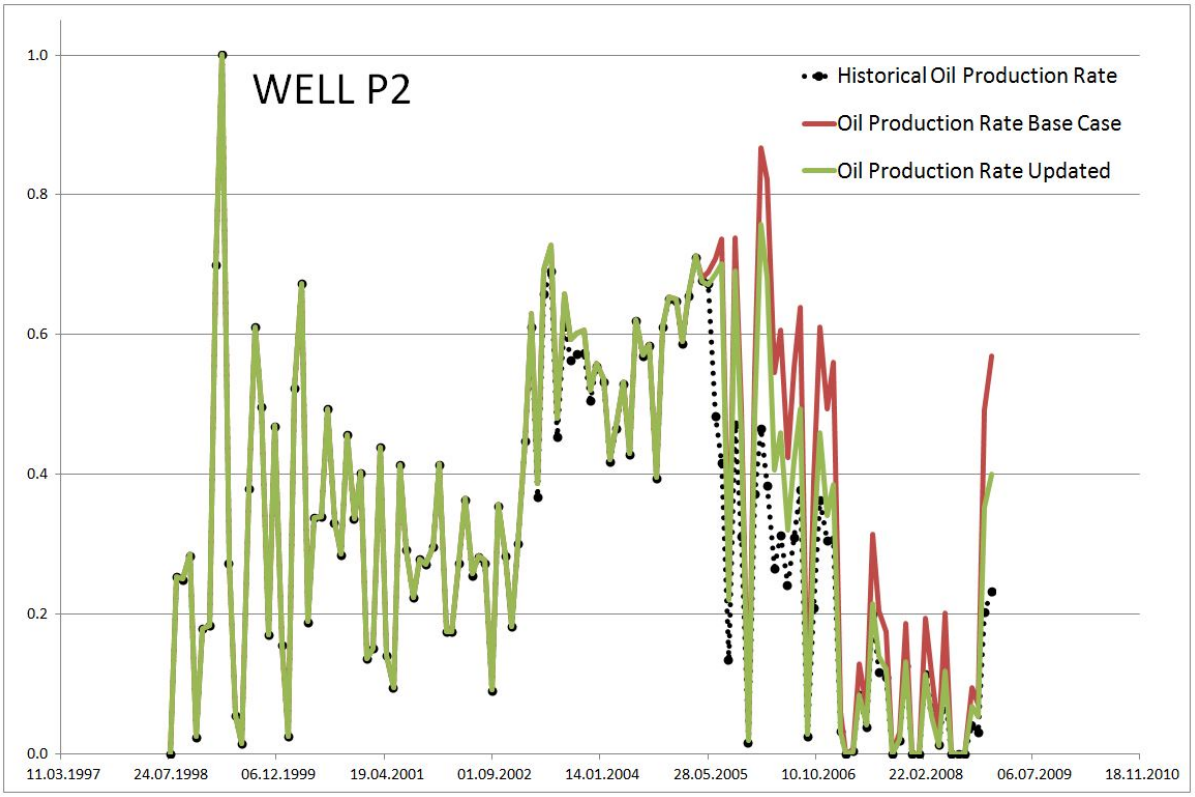

Figure 4.27 Well oil production rate history data and matching results of well P2, after update of 'non-active' cluster.

This geological reason is confirmed by Figure 4.28, which shows the modeled water production (red line on the figure). Over all the time during which the well was on stream, simulated production can be measured as follows: 100% oil, and 0% water. But the observed data (black dotted line) give different results: the water production rate reached up to 100 cubic metres.

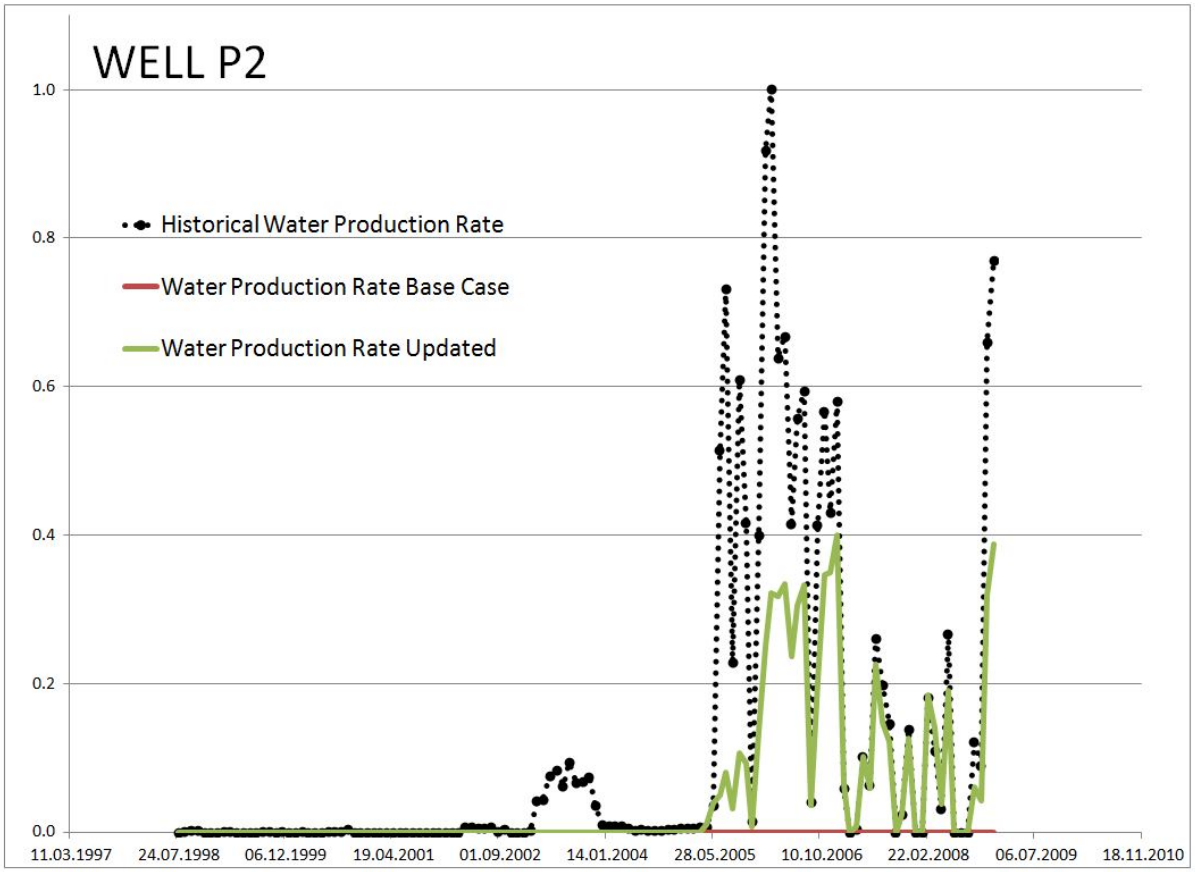

Figure 4.28 Matching results of well P2, after update of 'non-active' cluster. Improvements in water production rate can be seen. It should be noted that there is a good match of water breakthrough time (May 2005). The match is not perfect, but there a lot of possibilities for further matching.

Thus the result was not accurate enough for correct matching, basically because there was not a proper time of water breakthrough. Why did the water not arrive in the well at the right time? As was mentioned before, there could be two reasons: lower permeability in the model, compared to the real-life situation or the wrong fluid pathway (i.e. connectivity). The modelled permeability is based on core data but then corrected for well-test data, so it can be treated as correct. Therefore, the one solid reason for the problems with water breakthrough is connectivity. Unfortunately, in this case, we do not have any connectivity investigations here, for example tracers, for which the procedure is to inject some highlighted water and then trap it in the production well. Moreover, all the connectivity measurements are indirect and related uncertainties are therefore rather high. The related uncertainties were examined in previous chapters.

The method has enabled me to improve our understanding of connectivity, and, as a result, to update the simulation model to represent my understanding of the field geological settings. Hence, introducing 'non-active' clusters (see previous chapter) into the model produces more reliable connectivity in the simulation model.

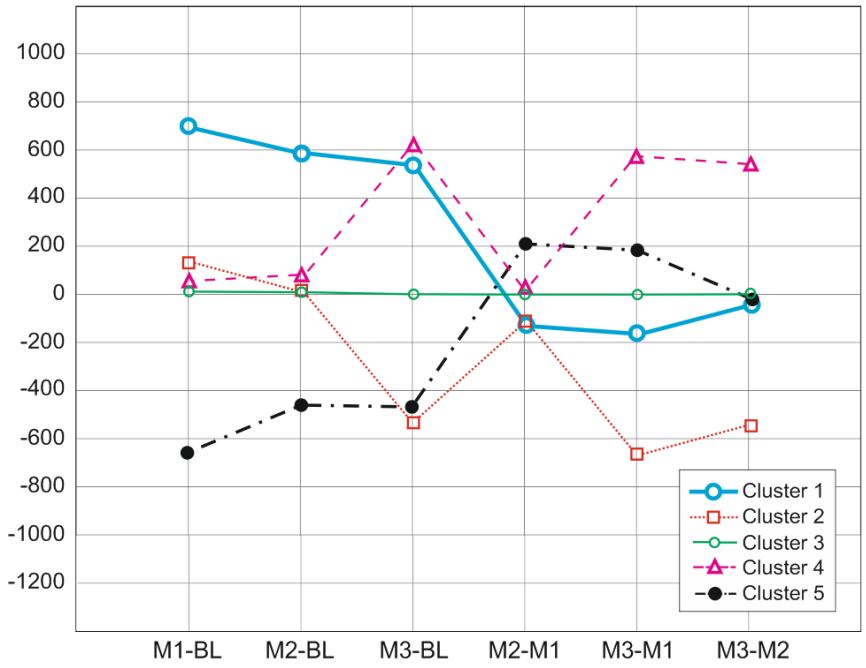

Figure 4.29 Cluster type curves. Y-axis: amplitude difference, X-axis: corresponding time step (D21= time between Monitor 1 and Baseline, D31= time between Monitor 2 and Baseline, D43= time between Monitor 3 and Baseline and etc.) 'Non-active' clusters are presented by the green curve- this is a part of the reservoir without any (significant) changes through time, based on the seismic data

A 'non-active' cluster is a part of the reservoir without any (significant) changes through time, based on the seismic data, cluster number 3 in Figure 4.29. This raises the question of why it appears in the 4D response. According to Johnston (2013), several reasons could account for the lack of observable changes in the seismic response (Johnston 2013):

- Subsurface conditions are unchanged. If that is the result of bypassed or unswept reservoir, there might be infill-well opportunities. However, there is also no change where there is no reservoir. In this work I stick to the latter reason, although generally, to distinguish between infill-well opportunities and no reservoir, the results should be analysed from reservoir engineering, geology and economics positions.
- Production-related rock-property changes might be too small relative to non-repeatable noise.

- The reservoir might be thinner than the seismic detection limit.
- The 4D response might be canceled out as a result of multiple processes.
- Imperfect data acquisition or processing can result in areas of increased noise.

How will the introduction of this cluster influence the simulation model results and history matching?

Even an update of 'non-active' clusters gives very significant improvements in the simulation model. The first example, well P2 (Figure 4.27 and Figure 4.28) shows better convergence of simulated oil production rate with observed data, due to the appropriate time of water breakthrough in the well (May 2005). The update of the 'non-active' cluster means assigning its transmissibility as equal to zero. This occurs because of transmissibility changes within the 'non-active' cluster; in other words, I change fluid paths (the way injected water reaches the production well from the injection well) and, as consequence, change flow velocity. The match is not perfect, but the simulation model already represents observed data and builds an understanding of reservoir connectivity much better compared to the initial model runs. However, there are still a lot of possibilities for further matching. The easiest to implement is to tune P2 well by varying transmissibility between clusters. This is an iterative procedure, but quite quick to implement.

Actually a 'non-active' cluster can be updated in one step throughout the entire model. A 3D view of active and 'non-active' cells in the model is presented in Figure 4.30.

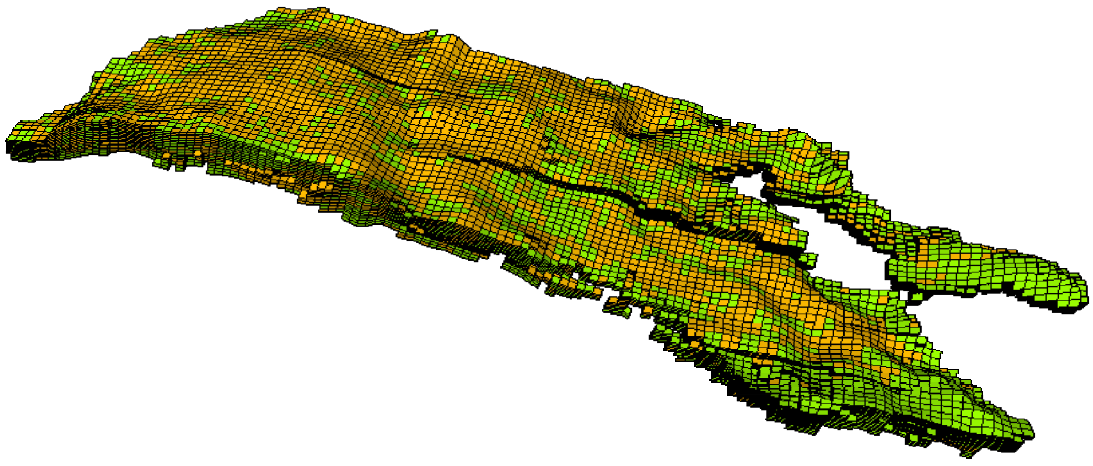

Figure 4.30 3D representation of the reservoir model grid. Active cluster cells (yellow) and 'non-active' cells (green).

So, to update connectivity in the model, it is first of all necessary to assign zero value of transmissibility to all the green cells. The updating procedure for the following wells is similar to the one presented above.

Figure 4.31 and Figure 4.32 show even better results for the well P8. First water in the producing fluid appeared in July 2002, but initially, the model demonstrated almost three years lag for the moment of breakthrough (June 2005). After updating connectivity the timing was not perfectly matched (May 2001 instead of July 2002), but the later dynamic data have been matched almost perfectly.

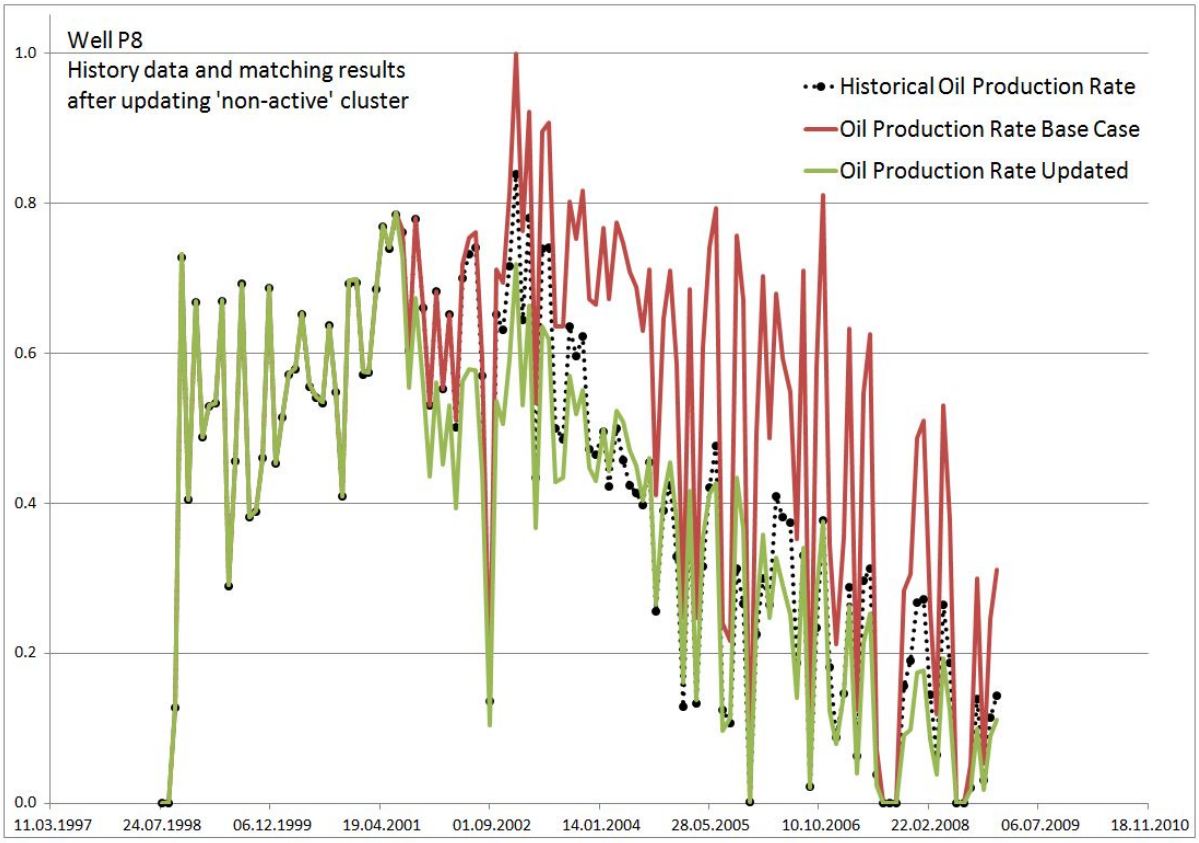

Figure 4.31 Well oil production rate history data and matching results of well P8, after update of 'non-active' cluster. There was a significant decrease in oil production rate due to the increase in water cut (see next figure).

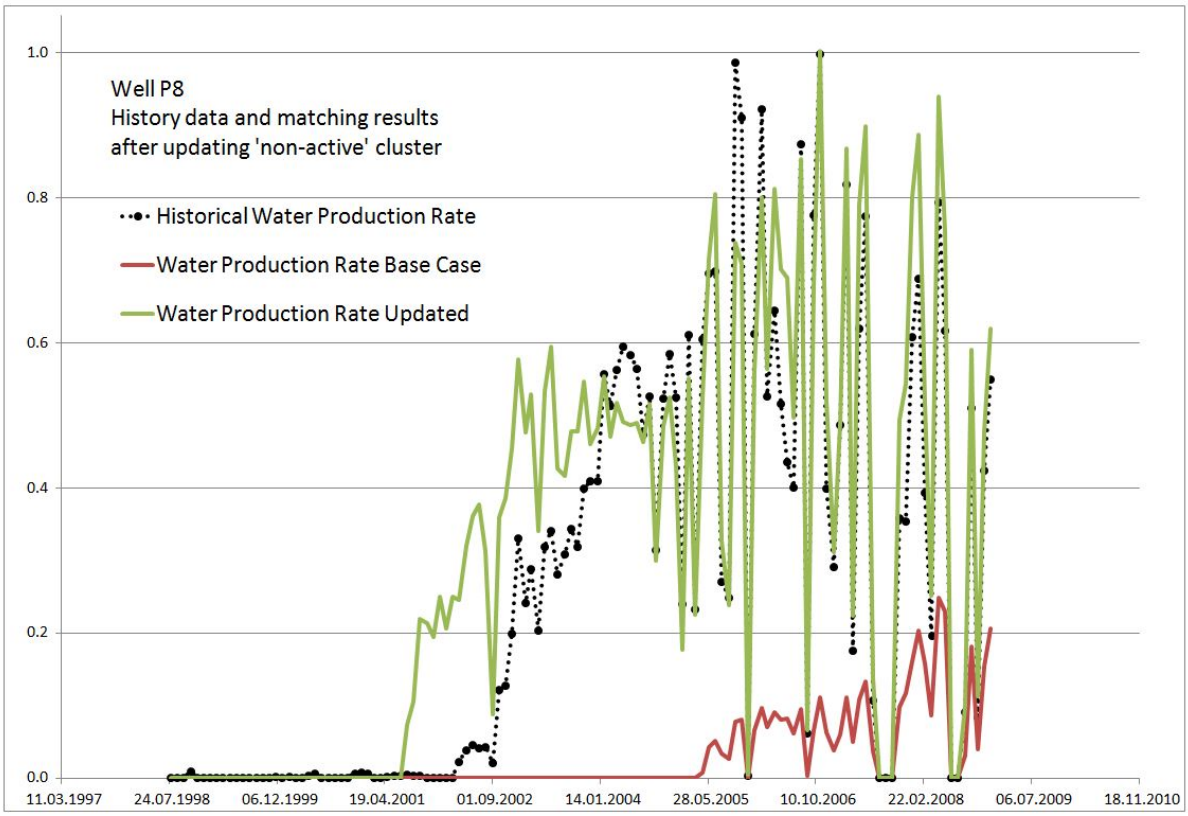

Figure 4.32 Well water production rate history data and matching results of well P8, after update of 'non-active' cluster. There are significant improvements in water cut (green curve) compared with the red curve.

Figure 4.33 and Figure 4.34 represent the well oil production rate history data and matching results of well P1, and matching results after update of the 'non-active' cluster. A significant decrease in oil production rate due to the increase in water cut can be seen, due to representing the appropriate time of water breakthrough in the well (September 2002). This occurred because of transmissibility changes within the 'non-active' cluster, in other words, I changed the fluid paths and flow velocity.

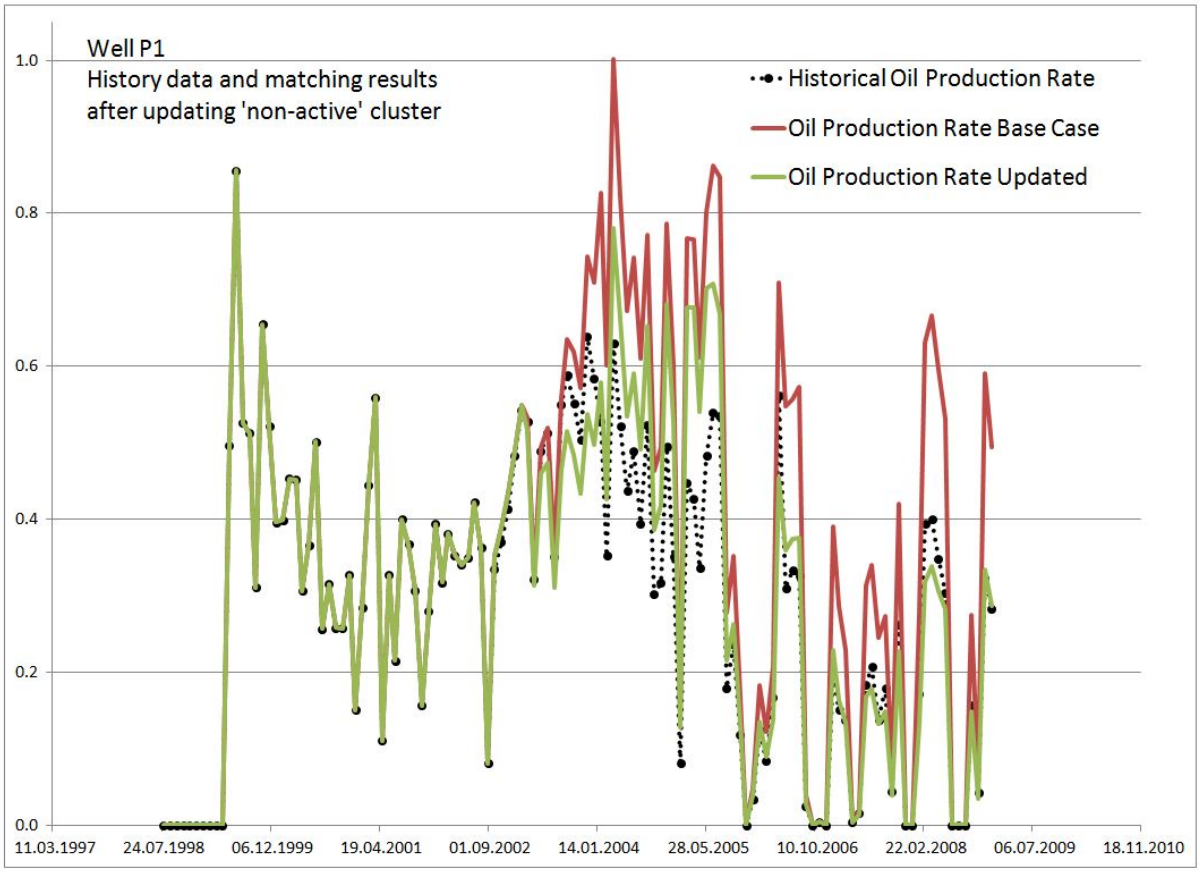

Figure 4.33 Well oil production rate history data and matching results of well P1, after update of 'non-active' cluster. There was a significant decrease in oil production rate due to increase in water cut (see next figure).

Analysing the real oilfield examples presented here, the following conclusions can be drawn: matching is dramatically improved, even after one quick update procedure, but is still not perfect and can be improved with well-known techniques. The method is very fast to implement, due to its nature and nature of the 4D results used in this method. An additional time saver is scale- I work on the full field scale model, and there is no need to go deeper and tune the wells (this can be done later, if necessary). After such an update, this model can be used for prediction calculations with an appropriate level of confidence.

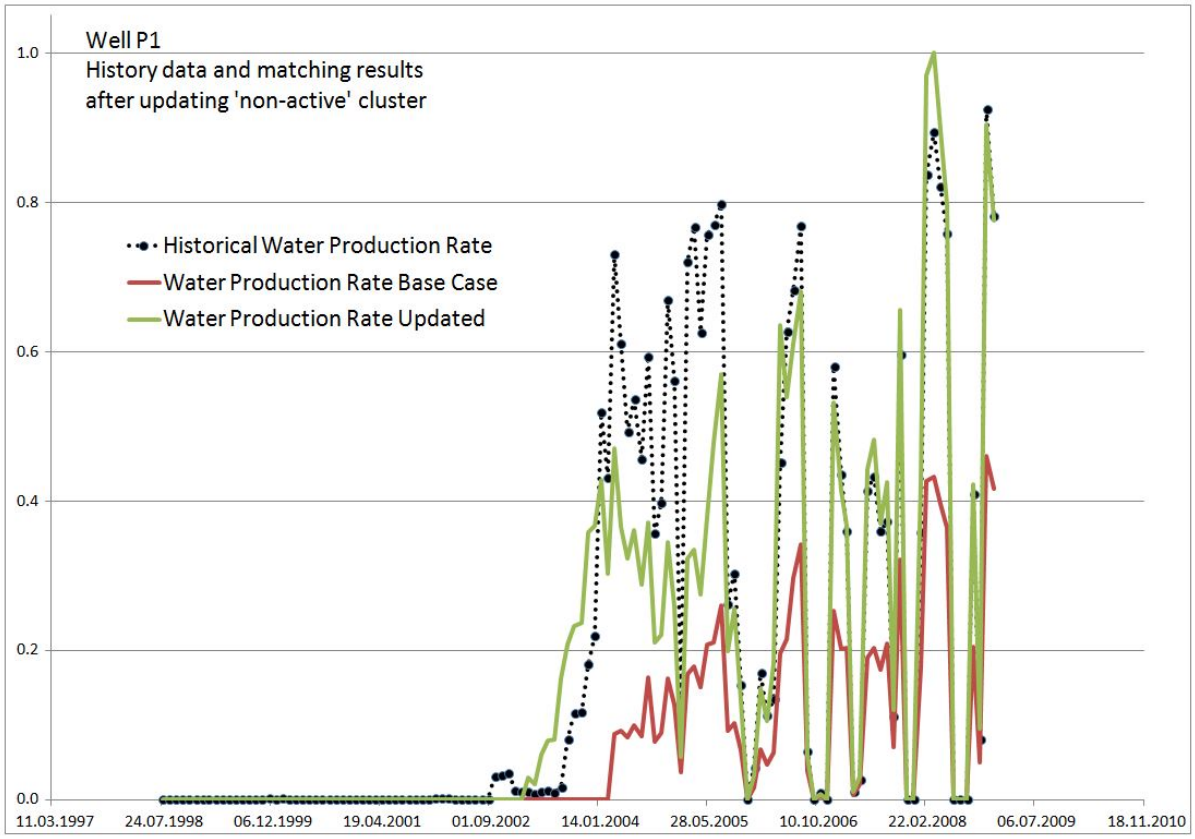

Figure 4.34 Well water production rate history data and matching results of well P1, after update of 'non-active' cluster. There are significant improvements in water cut (green curve compared with the red curve.

4.7 Discrepancy Estimation

To quantify history matching results, it is necessary to estimate the discrepancy function. Discrepancy between observed data and simulated is calculated using the following equation:

$$Misfit = \frac{\sum(Observed - Simulated)^2}{SD^2} \tag{4.1}$$

It was calculated separately in three domains: production data, seismic data and cluster data.

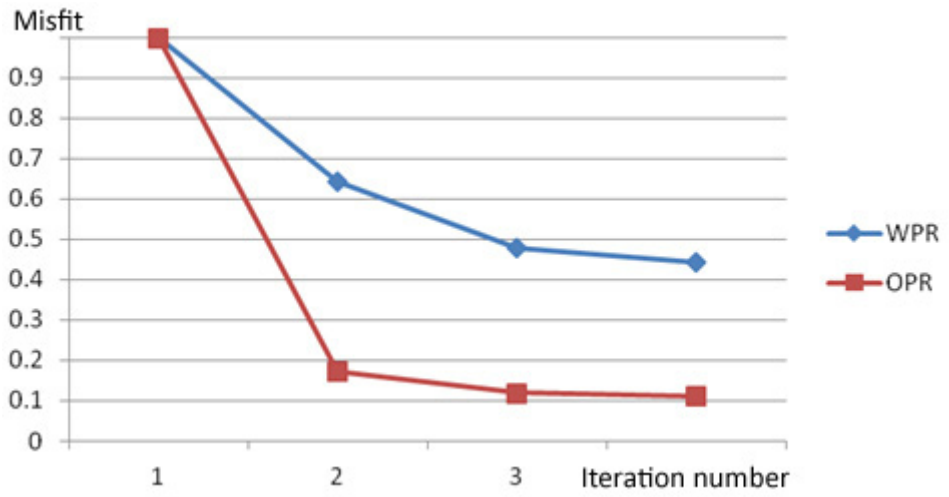

Figure 4.35 Production discrepancy changes for the reservoir part around I1 and P2. Point two: after 'non-active' cluster update; other points: after transmissibility changes between clusters. WRP: field water production rate, OPR: field oil production rate

Production discrepancy, i.e. difference between observed and simulated production data is presented in Figure 4.35. The initial point, #1, means discrepancy in the un-matched model, point 2 is discrepancy after update of the 'non-active' cluster, other points reflect later transmissibility changes between clusters. Most of the improvements (about 80% in oil production rate and 35% in water production rate) occur due to the 'non-active' cluster update in the simulation model. Further steps (3 and 4) are due to well-tuning and application of volumetric calculations to the result of the matching process. The method will be presented later in this chapter.

The seismic discrepancy is also assessed, and the observed improvement is about 22-23%. Visual comparison is presented in Figure 4.36. Obviously, the match is not perfect, but improvements are significant, and they are reached only after the first update step. Areas of special interest are highlighted in the following figure.

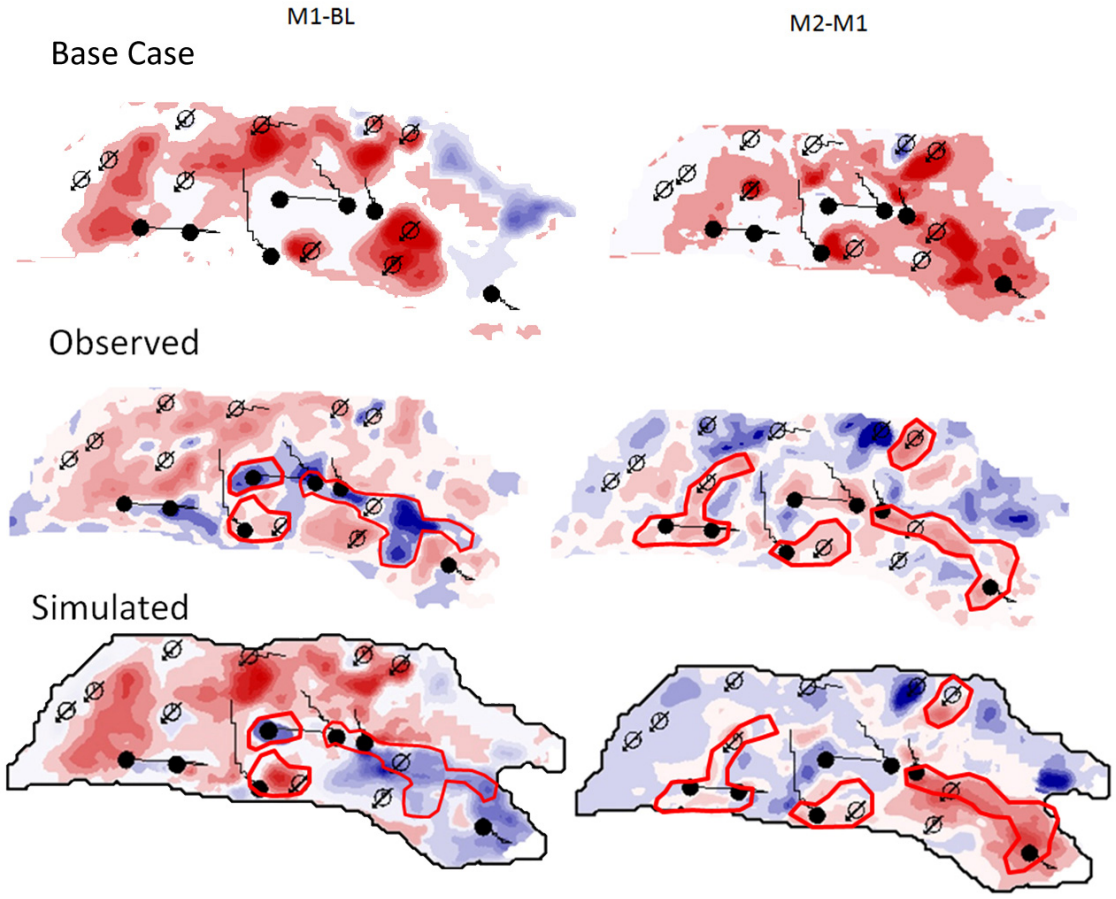

Figure 4.36 Comparison in seismic domain after update of 'non-active' cells.

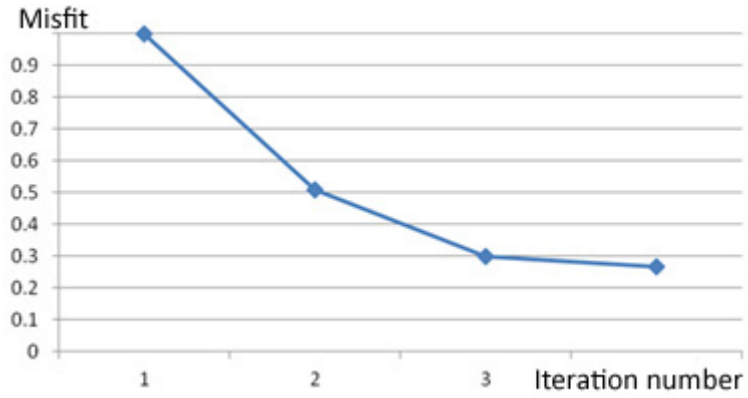

Figure 4.37 Seismic matching improvements

A better understanding of cluster domain matching results can be reached in 3D, but unfortunately, it is impossible to produce a 2D figure out of 3D volumes. It was decided to average the value of cluster number within each column of cells and then compare these (see

Figure 4.38). The cluster representation is much more similar to observed data, than with initial base case model.

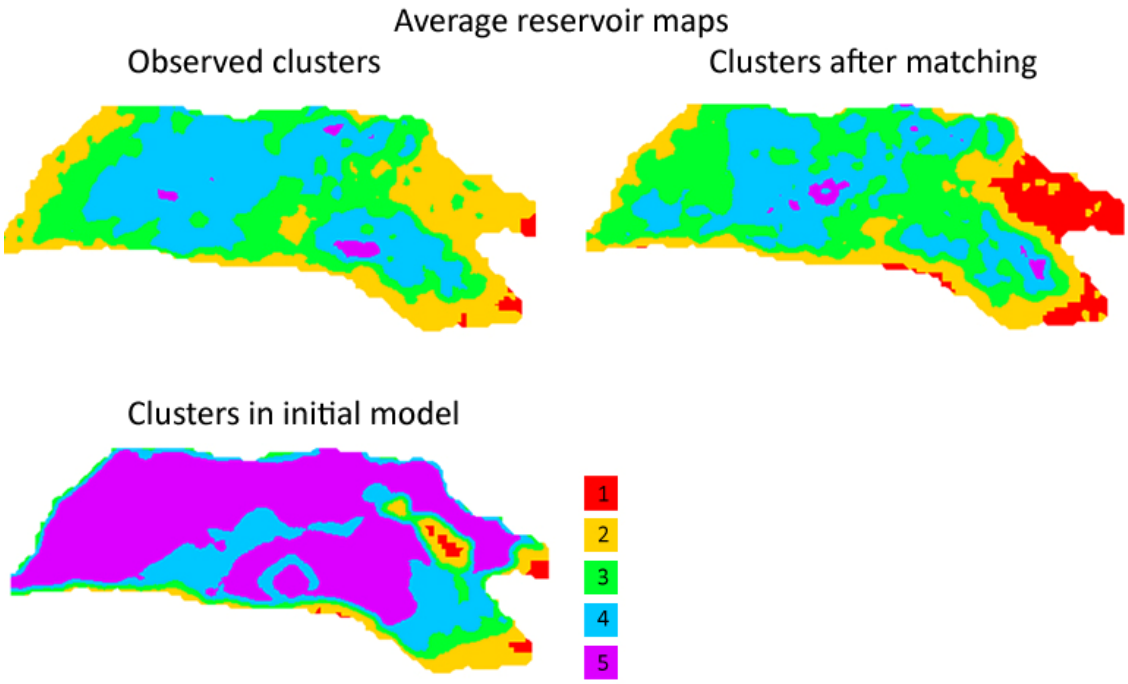

Figure 4.38 Cluster matching. Different clusters have values from 1 to 5. Final maps generated by simple averaging of values of the grid.

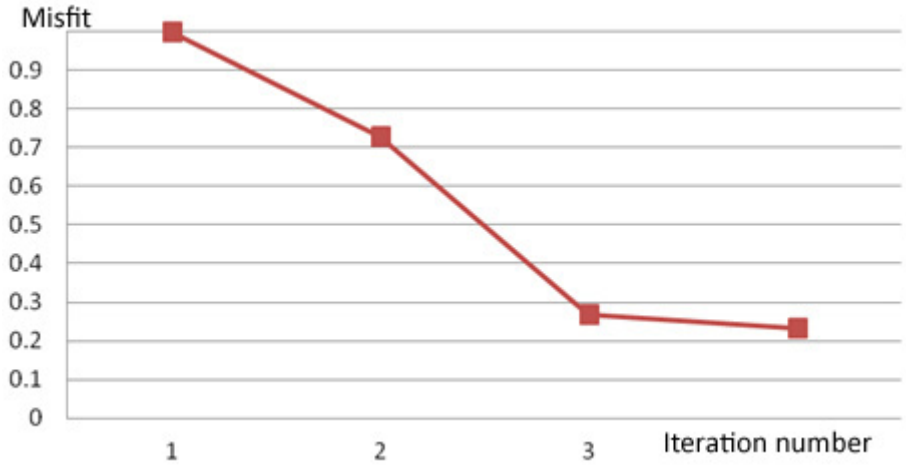

Figure 4.39 Cluster matching improvements

The results of the method appear to be reliable and quite promising. To improve them, integration needs to be carried out with all the available data. In addition, PLT data can validate cluster analysis.

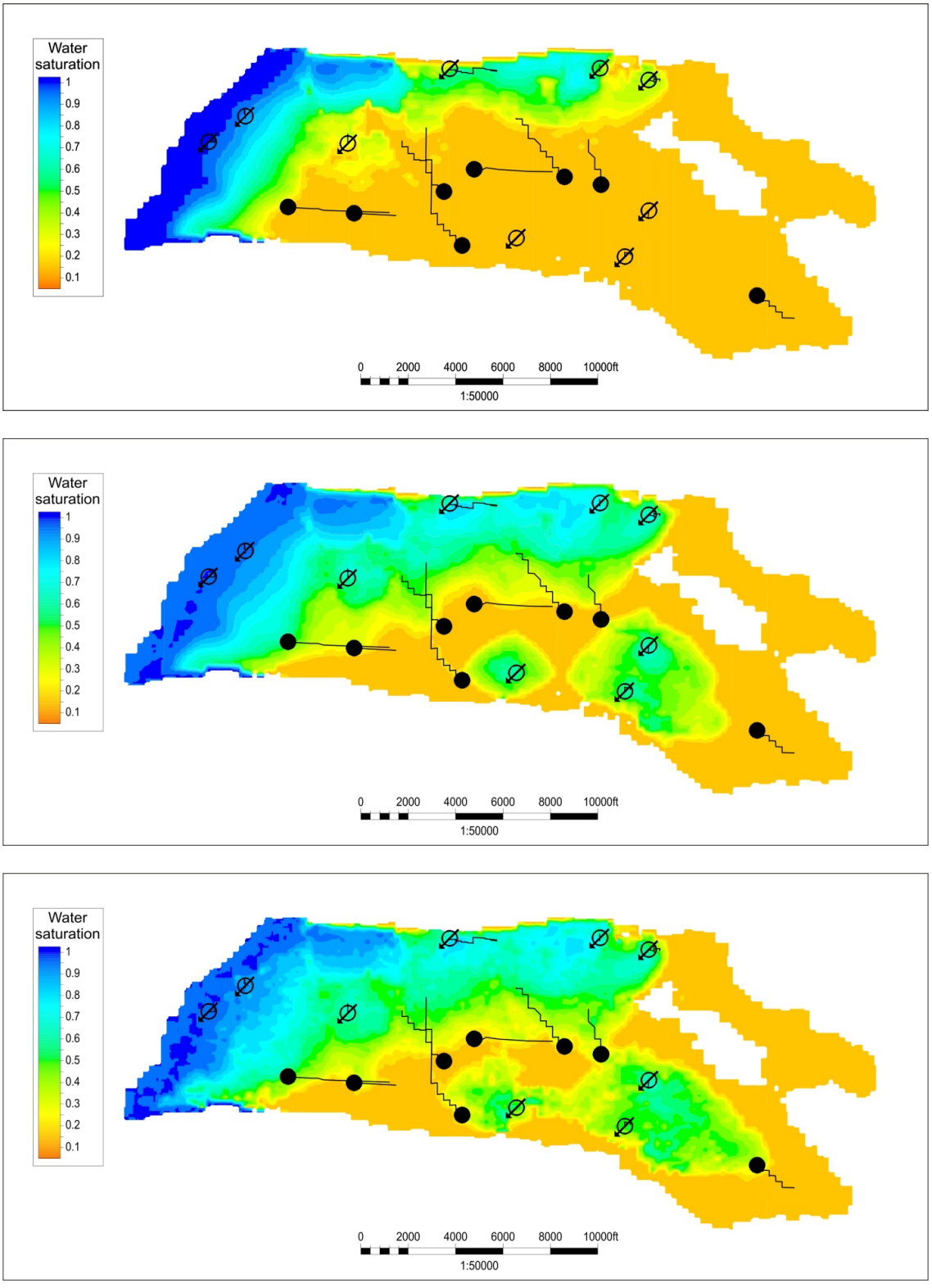

Figure 4.40 Water saturation maps. Upper: initial saturation for model; middle: final saturation for Base Case model; lower: final saturation for updated model. Obvious improvements can be seen in water flooding fronts, due to better reflection of geological features.

The next map that can be used for estimation of method results is the water saturation map or drainage map. I will compare initial saturation with final saturation of the base case model and final saturation of the updated model (see Figure 4.40). Distribution of water flooded areas and water fronts has changed significantly, which actually leads to improvements in the well production match. The water front from I2 and I1 eventually reached P2 producer, causing an increase in water cut in the producer. Aquifer movement into the eastern side became less uniform, due to the change in reservoir connectivity and increase in vertical heterogeneity.

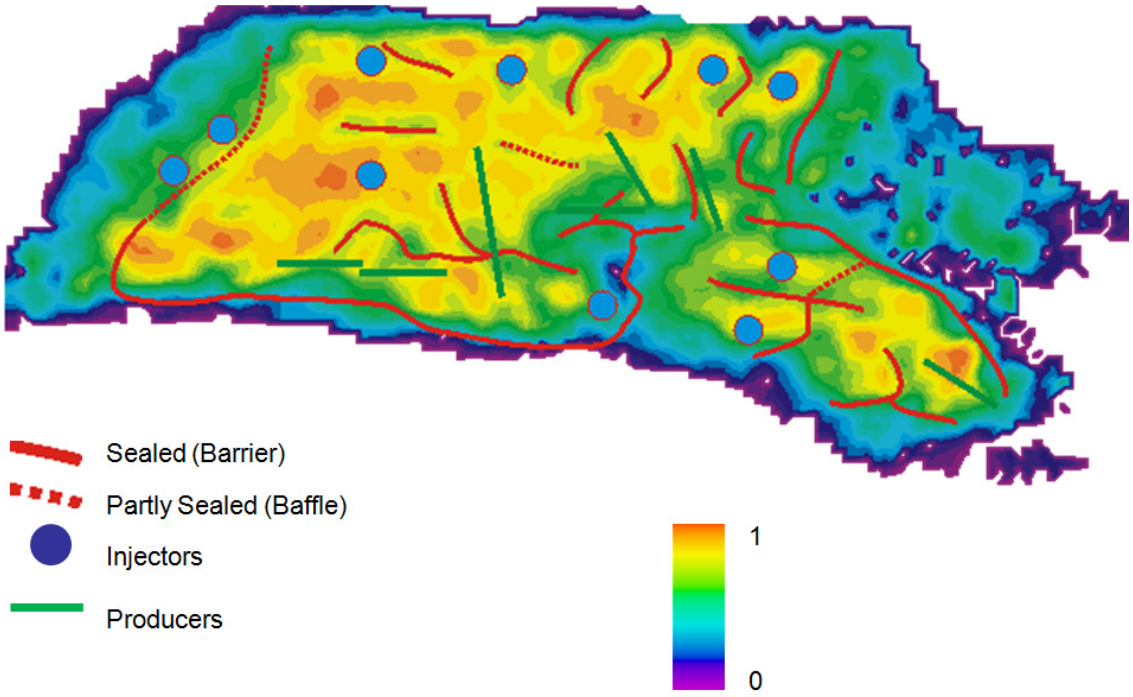

Figure 4.41 Final connectivity map from cluster analysis. Existing NTG values are not taken into account.

Hence, the final map which is used for assessing the result of the implementation of the method is the connectivity map, which changes from 0 (no connectivity) up to 1 (perfect connectivity). It is possible to highlight the sealed barriers (solid red line) and partly sealed baffles (dotted red line), based on the value of connectivity and well history.

4.8 Volumetric

A further development of the method is volumetric calculation. The reason to calculate volumes is based on the idea that the volume of the cluster connected to the well, say injection, should be equal to the volume of injected water at the same time. I will show the applicability and accuracy of this method. The volumetric calculation will be checked against observed data, which in turn, approving the whole concept of clusters.

The following data example will demonstrate how to calculate swept volume, which ideally should be equal to injected volume.

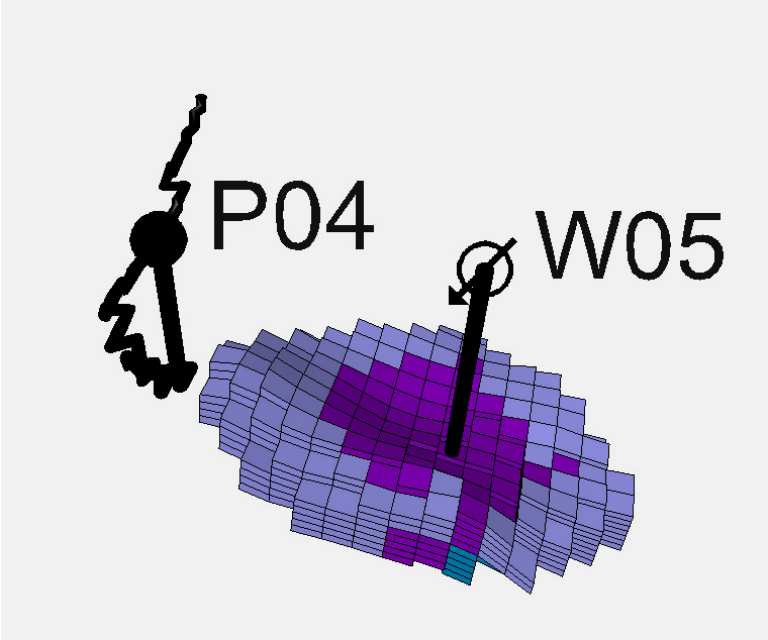

Figure 4.42 Simulated waterfront and injected volumes.

Figure 4.42 shows an injected water front moving from the injection well, W05, towards the production well, based on the simulation model. We know the injected volume is equal to 1253120 m^3, from the history data. Hence, we would expect that the volume of the depicted cluster should be equal to 1253120 (assume volume factor for injected water =1). However, the pore volume (PV_{sim}) of this cluster is 3710728 m^3. The reason why they are different will be explained later. First, let us see what really happened in the reservoir. Analysing the observed cluster data, based on observed time-lapse data, it is obvious that the water front has, indeed, a much more complicated shape (see Figure 4.43). The explanation of this is the

geological heterogeneities, detailed discussion of which has been given in previous parts. Pore volume (PV_{obs}) is 1893488 m^3. This volume has uncertainty related to its calculation; in any case, it comes from simulation model, and thus depends on rock volume (cell size) and porosity. Both of these parameters cannot be constant and determined with 100% accuracy. The first parameter is cell size, which was determined based on geological settings of the field, in such size to reflect any meaningful heterogeneities in reservoir, and then was upscaled in the simulation grid to improve model performance and preserve the desirable level of heterogeneities. Thus, it is assumed that cell size is properly modeled here. Porosity related uncertainties were covered in Chapter 1.

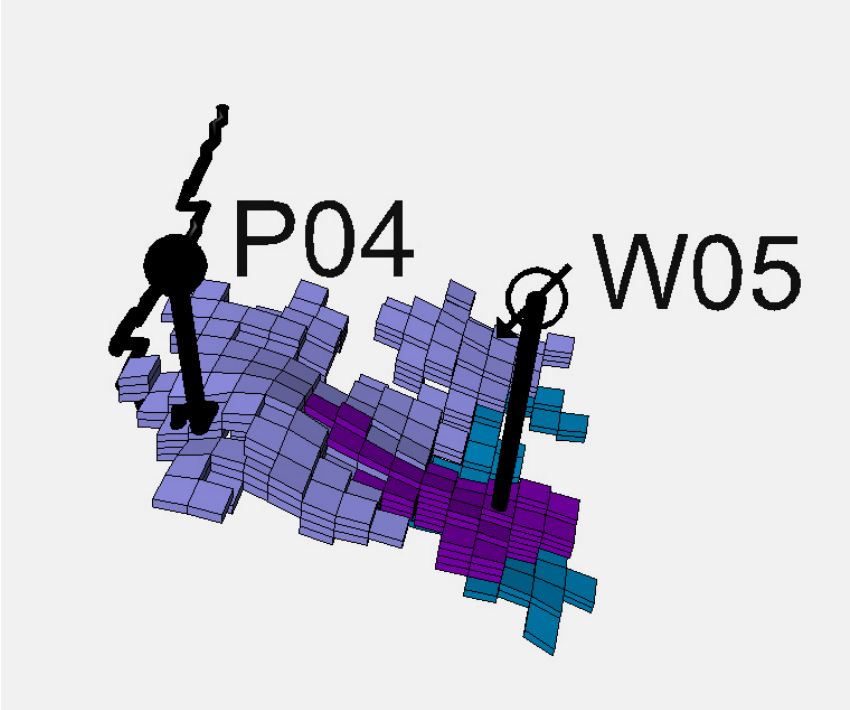

Figure 4.43 Observed waterfronts and injected volumes.

The other question raised here is whether the injected water will occupy all the pore volume. The answer is no, it does not, and this will be explained in the following section.

4.8.1 Displacement, sweep and rock fluid model

Displacement efficiency and sweep efficiency are among fundamentals of reservoir engineering. Their difference is in the process scale: displacement efficiency is at the pore scale and sweep efficiency is at the reservoir scale. So, for 4D studies, reservoir scale is more

applicable. It can be defined as follows: the fraction of the reservoir volume that is depleted by the production process. For a water injection process, it is the percentage of the volume that is contacted by the injected water (Johnston 2013). Actually, sweep efficiency is controlled by different factors, such as flow rates, well locations, reservoir properties, and reservoir heterogeneities, which are functions of the depositional environment and structural conditions. According to Johnston, spatial patterns in 4D seismic data can be a measure of sweep efficiency; they also can be used to characterize the heterogeneities that control HC recovery, i.e. connectivity.

To understand the big picture, we need to go to a lower level, displacement efficiency, which is the fraction of pore space that is depleted by the production process. Details of the process are presented below. To find answer for the question 'Does injected water occupy all the pore volume?' we need to understand the rock fluid model. A generalised rock-fluid model (see Figure 4.44) represents the fundamental petrophysical understanding of pore volume and its saturation. When talking about a producing reservoir, the main point of interest is PHIe, effective porosity, the possible volume that can be filled by fluids. Actually PHIe is exactly the porosity which was modeled in the simulation model. So, which fluids are saturated out of the model? Initially, oil and water are saturated pore volume, in this particular case (for simplicity we assume no gas is coming out of the solution here). There are two critical values to determine the mobile fluid portion: residual oil saturation, S_{or}, and irreducible water saturation, S_{wi}.

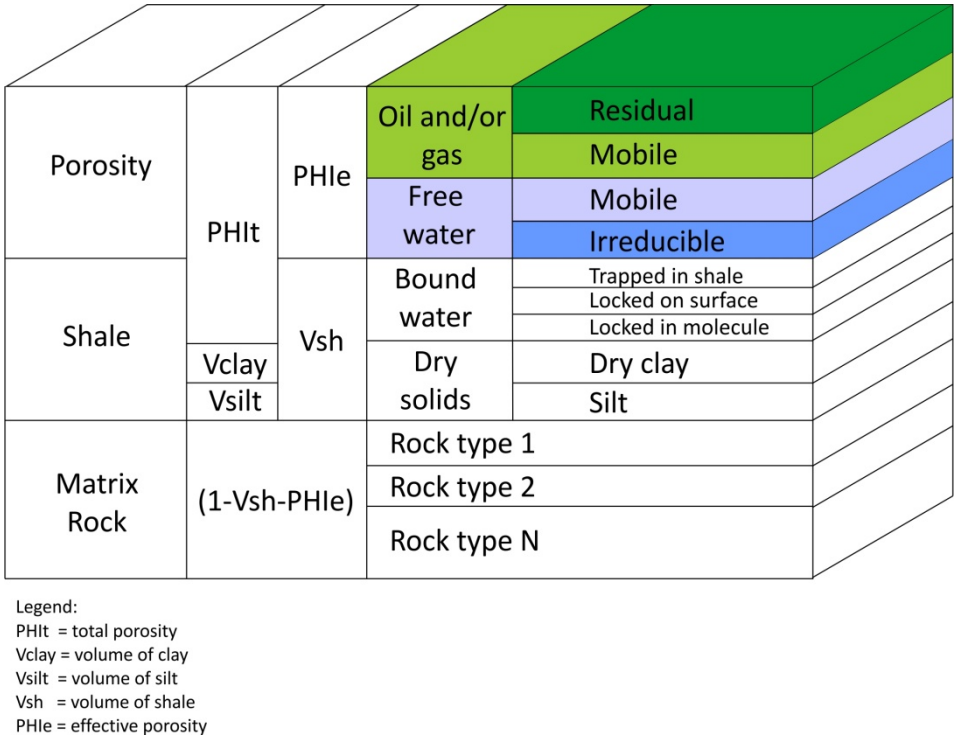

Figure 4.44 Generalised rock-fluid model (after Crain)

Residual oil saturation is oil saturation that cannot be produced from a reservoir; usually it is considered the immobile saturation after conventional displacement. It is S_o at $k_{ro}=0$ (see Figure 4.45). The definition of irreducible water saturation is that it is the fraction of the pore space occupied by water when the hydrocarbon content is at maximum level, so it is S_w at $k_{rw}=0$. These parameters are obtained from laboratory tests. Analysing Figure 4.45, we can find that the area in which fluid will be movable, other words can move in the reservoir and can be produced as a result, is generally located in between Swi and Sor (the green area in the figure)

Hence,

$$S_{mobile} = 1 - S_{wi} - S_{or}.$$

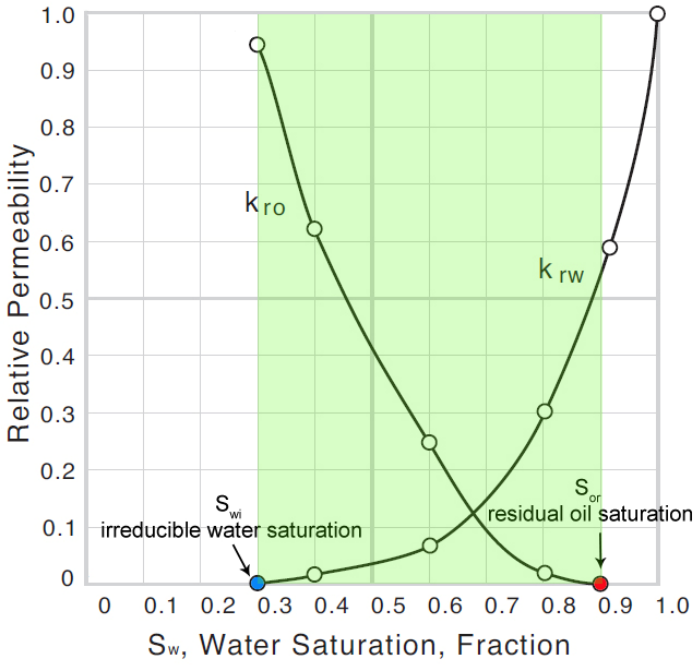

Figure 4.45 Generalised relative permeability curves for water-oil system. Blue dot: irreducible water saturation, red dot: residual oil saturation. Green area: S_{mobile}.

4.8.2 Field case calculations

For the UKCS field, S_{or} is equal to 0.2491 and S_{wi}= 0.1768

So,

$$S_{mobile} = 1 - S_{wi} - S_{or}$$

S_{mobile} represents volume of fluids that can be displaced by injected water, if we consider the injection well case. The volume of the cluster derived from the simulation model is PV_{sim}=3710728. How was this value derived? It is possible to calculate the bulk volume of the model cells, and the porosity grid distribution is already known, as it is in the list of necessary grids for simulation: porosity, permeability, saturation, net-to-gross. Thus, the product of bulk volume and porosity is pore volume. So the available pore volume for injected water can be calculated as follows:

$$PV_{sim}^{inj} = PV_{sim} - PV_{sim} * S_{wi} - PV_{sim} * S_{or},$$

where PV_{sim} is pore volume available for fluids, $PV_{sim}\ S_{wi}$ is pore volume occupied by irreducible water, and $PV_{sim}\ S_{or}$ is pore volume occupied by residual oil. The result is $PV_{sim}^{inj} = 2130329\ m^3$. Hence, this volume can be replaced by injected water in the simulation model. As mentioned above, this value has its own uncertainties related to bulk volume and modeled porosity. We can compare this volume with the observed seismic data. The same for the observed cluster (the cluster was derived from 4D seismic):

$$PV_{obs}^{inj} = PV_{obs} - PV_{obs} * S_{wi} - PV_{obs} * S_{or} = 1087051\ m^3$$

The observed injected volume is $V_{inj} = 1253120\ m^3$; this is the exact volume that was injected into the reservoir by the injecting wells. Comparing the results, the observed PV is just 13% less than the injected volume, whereas the simulated PV exceeds the injected volume by 70%. Hence, we can add a PV multiplier into the simulation model to adequately represent the reservoir. In this case, the pore volume multiplier is 0.6.

To use this technique of volume estimations and its results in history matching, one needs to be aware of following points and assumptions:

1. Injected volume is hard data, with all its related uncertainties, especially if the injected water goes into an aquifer, but for this particular example, it is not applicable, because there is no aquifer in the examined part of the reservoir. In a more general case, it is necessary to divide injected volumes into aquifer and reservoir portions.
2. Injected water displaces 100% of mobile oil; the reservoir volume does not contain mobile water, only irreducible water; these assumptions have been used in the calculations.

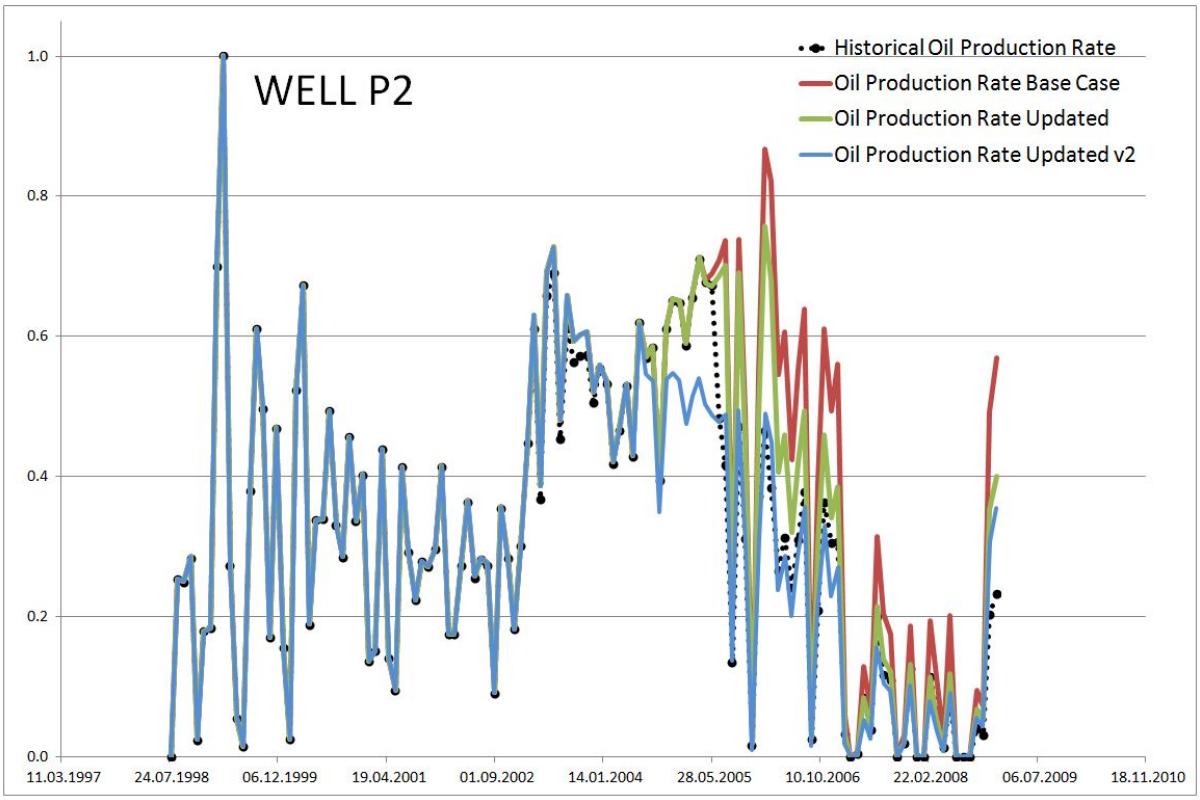

Figure 4.46 History matching results comparison for P2 well. Black dotted line represents the oil production rate from the observed data. The red line represents the oil production rate for the base case simulation model. The green line represents the update only of the shales in the model (only one cluster), while the blue line represents the update of shales and the pore volumes according to the volumetric.

Figure 4.46 represents the history matching results with the application of a different cluster method. The first stage it is the update of 'non-active' cluster- shales, shown by the green curve, which already shows sufficient improvements in well oil production rate; details of this method were discussed previously. The second stage is the update of pore volumes according to presented algorithm, represented by the blue curve which shows the best match with the observed data (black dotted line). Pore volumes were updated using the pore volume multiplier, calculated based on the observed-simulated data difference.

Hence, using the proposed method in history matching allows direct integration of time-lapse seismic data analysis results into the simulation model at the history matching stage. Doing this, I was able to reduce the uncertainties related to connectivity issues (static and especially dynamic) and sufficiently decrease the time of history matching. In the presented example, only 2 model simulations need to be run to get an almost perfect match. A valuable benefit

of this method is its solid geological background, which allows connectivity issues to be solved.

Volumetric calculation is an additional benefit here. This allows us to clarify the amount of oil (STOIIP) and its distribution in the reservoir. Moreover, better volume distribution over the model allows better history matching.

4.9 Conclusions

The main benefit of utilsing time-lapse seismic data interpretation in history matching of a reservoir simulation model is to get an overview of fluid front movement, both vertically in the main reservoirs and laterally across the compartments. This information, when directly used in the simulation model, significantly reduces history matching time and provides additional information regarding reservoir architecture and fluid flow patterns. Moreover, 4D data can be inputted into the geological model in order to clarify geological settings and locations of major and minor heterogeneities affecting flow.

The presented method of 4D data integration into the simulation model is an important tool in communication across disciplines in a multidisciplinary sub-surface team, as it integrates all of the areas, such as geology, production, petrophysics and simulation. Finally, the method can be extremely useful for reservoir management, as it provides understanding of drainage patterns of the field, areas that can be locations for new wells- injector or producer- or even provides insights for geologists as to where to find remaining reserves.

Volumetric calculations give an additional tool to understand and predict reservoir behaviour; and can also provide improved estimation of the uncertainty related to the method.

Chapter Five

Norwegian Sea field

This chapter shows the application of the proposed method to a compartmentalised reservoir in the Norwegian Sea field in the North Sea. Structural compartmentalisation is rather high, as the reservoir is divided into major segments and there are number of relatively small faults within the segments; hence fault transmissibility impacts on production and field management. Here Seis-to-Seis, Well-to-Seis and the cluster method are applied to locate reservoir compartments within the reservoir and derive connectivity among these faults, for some cases. This chapter provides a description of the simulation model, field reservoir conditions and production history together with a review of management decisions.

5.1 Introduction

The Norwegian Sea field is located in Blocks 6507/7 and 6507/8 in the northern part of the Halten Terrace on the Mid-Norway shelf, in a water depth of 345 m (1132 ft) (Figure 4.1). It was discovered in 1985 and began production in 1995. It contains STOIIP of 2907 MMBO, 1.33 TCFG solution gas and 1.65 TCF free gas. The average ultimate oil recovery factor is estimated as 33%. The field consists a series of fault blocks with different levels of OWC. Oil is always saturated and of medium gravity (21-29 API). Hydrocarbons are contained in a very complex, eroded horst-block trap, which is segmented by many non- to partially sealing faults. Permeabilities are about 1450 mD (with a maximum of 20D), which is rather high. The gross reservoir interval is divided into five separately developed reservoirs; the targeted reservoir of this work is Fangst (Upper and Lower) produced by downflank water injection and crestal gas injection. In spite of excellent rates at the beginning of production, the poor oil recovery factor is due to a combination of the strong fault- compartmentalisation, reservoir heterogeneities, and constraints on production required to control waterflood advance and gas-cap expansion. Thus, the connectivity pattern is mainly controlled by the fault pattern of the field. The reservoir is compartmentalised by a complex network of faults associated with several stratigraphic barriers. Forecasting the drainage pattern of the different reservoir compartments is difficult, as communication across segment bounding faults and across the stratigraphy is hard to predict (Roste, et al. 2009).

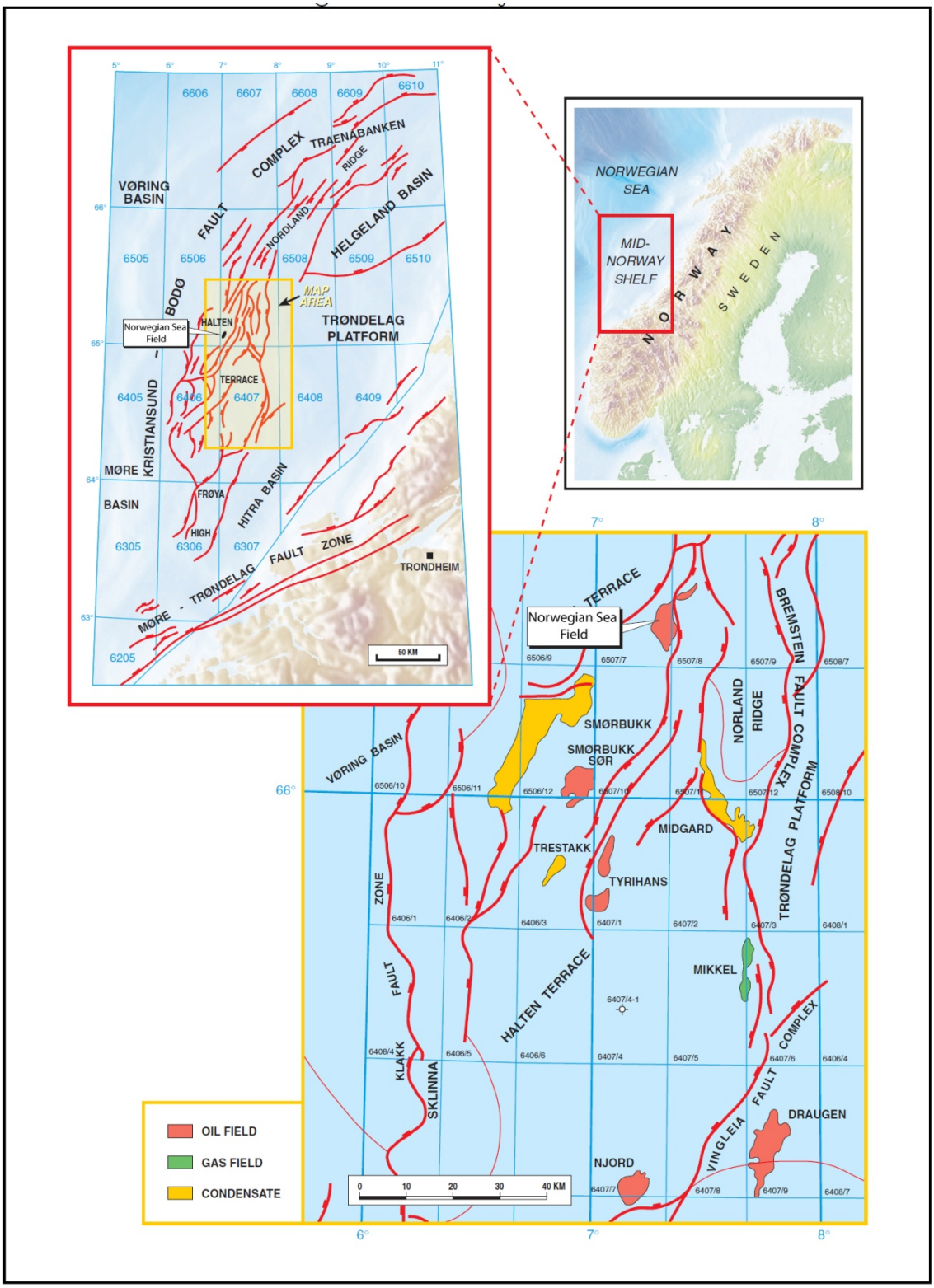

Figure 5.1 Location of the Norwegian Sea field, in the northern part of the Halten Terrace on the Mid-Norway shelf (Karlsen, et al. 1995)

5.2 Field geology

The Norwegian Sea field is situated in the northern part of the Halten Terrace in the Mid-Norway region of the Norwegian Sea (Figure 4.2). The Halten Terrace is a 50-100 km-wide, NNE-SSW trending belt of extensional fault-blocks that downstep from Trondelag Platform in the east to the Voring Basin in the west. The Halten Terrace lies within the passive continental margin formed by oceanic spreading between Greenland and Norway that began in the Paleocene. The Norwegian Sea field occurs close to the junction between the Halten Terrace and the southern termination of the Norland Ridge. The Norwegian Sea field reserves were generated principally from the Upper Jurassic Spekk Formation and secondarily from the Lower Jurassic Are Formation. The Spekk Formation is up to 400m thick in the Mid-Norway region and consists of organic-rich shales, deposited within an anoxic marine shelf environment (Karlsen, et al. 1995, Ho, et al. 1998)

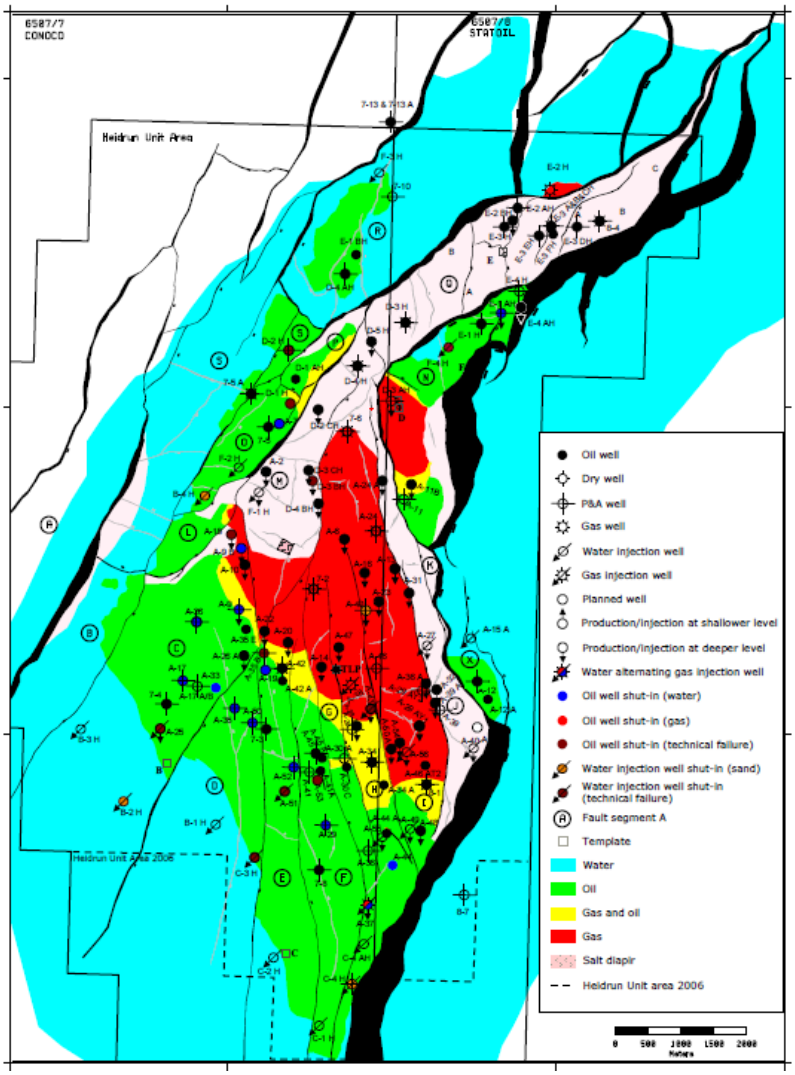

Figure 5.2 Scheme of Norwegian Sea field, Fangst Group (Statoil)

The Norwegian Sea field is contained in a complex, eroded horst-block trap formed by the Late Jurrasic-Early Cretaceous extension. The field contains a saturated oil column beneath a gas cap. The accumulation is trapped to the east against an irregular, east-downthrowing normal fault, but largely dip-closed in the southwest and northwest, with minor fault offsets (Hemmens, et al. 1992).

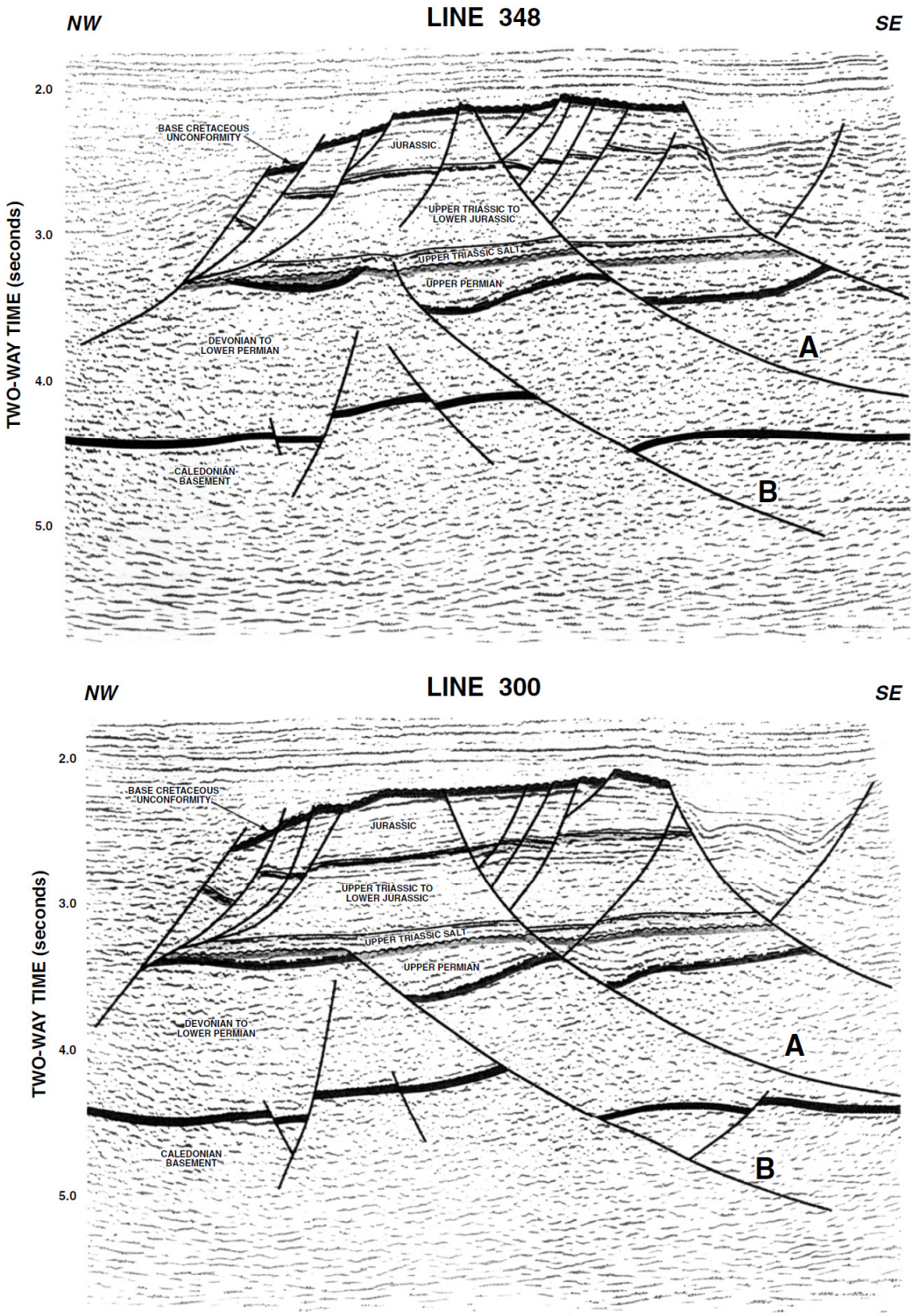

Figure 5.3 NW-SE 3D seismic sections through the Norwegian Sea field, showing basement fault influence on the Late Jurassic-Early Cretaceous structures (Hemmens, et al. 1992).

The accumulation is filled-to-spill and contiguous with the Norwegian Sea field North Field, which is dip-closed to the northwest (Welbon, et al. 1997).

Norwegian Sea field reserves are contained in the Bat and Fangst (object of this study) groups, which are Late Triassic to Middle Jurassic in age and have an average total thickness of 840 m (Olsen, et al. 1999). The Fangst Group is late Toarcian to Bajocian in age, has a total thickness of 79 m and is divided regionally into three formations, named from base to top, Ile, Not and Garn. In the Norwegian Sea field, the Fangst Group is divided into five zones, termed Fangst 1 to 5.

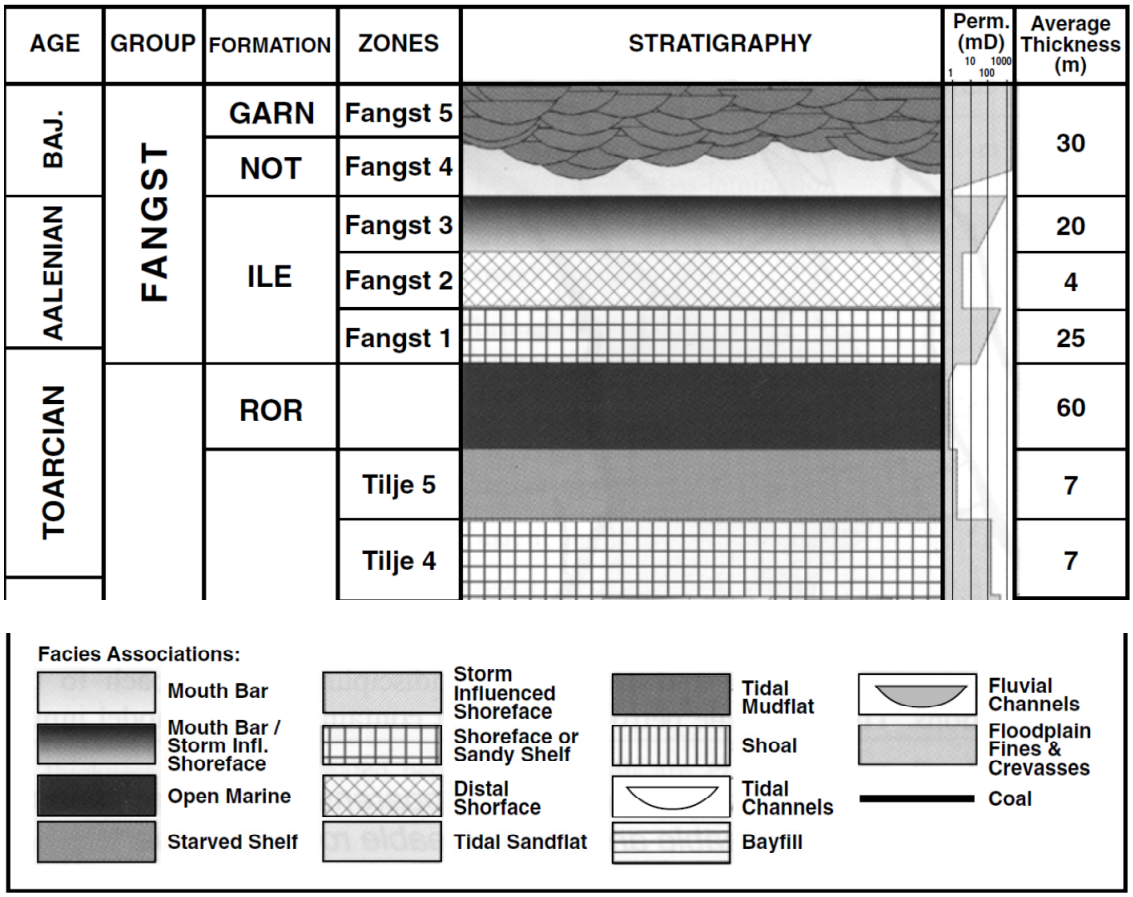

Figure 5.4 Stratigraphy of the Norwegian Sea field (Olsen, et al. 1999)

The Group represents an overall regressive interval with shelf and shoreface facies (Fangst 1 and 2) at base, passing upwards into a tidal flat (Fangst 4) and braided-fluvial facies (Fangst 5) at the top. According to Harris, Fangst 1 unit has an average thickness of 25 m and comprises three facies: (1) variably bioturbated, wave-rippled, fine-grained sandstone with shaly partings; (2) sharp-based, cross-bedded, medium-grained sandstone, with scattered

shale clasts; (3) rarer, thin hummocky cross-stratified (HCS), very fine-grained sandstone. Fangst 1 coarsens upward, reflecting a transition from lower shoreface/shelf to intertidal conditions (Harris 1989). Fangst 2 is a thin unit of HCS, fine- to very fine-grained sandstone. Fangst 3 represents a temporary transgressive phase that interrupted the overall Fangst regressive trend. It is an interval of trough cross-stratified, fine- to coarse-grained sandstone, interpreted as upper shoreface deposits, and subordinate low-angle cross-laminated, well-sorted, fine- to medium-grained sandstone, interpreted as foreshore/beach deposits. Fangst 4 is represented by muddy sandstones, deposited in a shallow marine environment. Fangs 5 with an average thickness of 30 m consists of unbioturbated, cross-stratified fine- to medium-grained sandstone, with coarse-grained sandstone in the top. It was deposited in a non-marine settings, mostly braided-fluvial (Harris 1989, Hemmens, et al. 1992).

5.2.1 Reservoir architecture and connectivity

The connectivity pattern is mainly controlled by the fault pattern on the field. The reservoir is compartmentalised by a complex network of faults, associated with several stratigraphic barriers. Forecasting the drainage pattern of the different reservoir compartments is difficult, as communication across segment bounding faults and across the stratigraphy is hard to predict (Roste, et al. 2009). The intra-field faults are non-sealing or, at worst, partially sealing and the development plan anticipated only limited transmissibility reduction across them (Hemmens, et al. 1992). The reservoir interval has been divided into a total 17 correlatable zones. This layer-cake reservoir architecture at a field scale contrasts with the severe architectural complexity at the scale of individual zones. This fact is reflected in the modeling study, constructed from a total of 16 different facies elements (Figure 4.35), integrating all well log, core and appropriate analogue outcrop models (Olsen, et al. 1999).

The Fangst 2 and 3 units are sand-dominated units with excellent lateral continuity. A thin (1-2 m) shale horizon between Fangst 3 and 4 acts as an important vertical permeability barrier, although cross-flow between the Fangst 3 and 4 units occurs across faults.

Facies	Abbreviation	Unit Thickness Amalgamated (m)	Sedimentary Structures	Grain Size	Bioturbation	Perm.
Fluvial channel sand	FCS	4.0	Trough cross-bedding Current ripple cross-lamination	silt-m	Absent	600 mD
Crevasse splay sand	CSS	1.0	Current ripple cross-lamination Trough cross-bedding	vf-f	Absent	80 mD
Incised valley fill	IVF	10.0	Trough cross-bedding Current ripple cross-lamination	m	Absent	950 mD
Bayfill mud and sand	BMS	4.2	Wave ripple cross-lamination Hummocky cross-stratification Current ripple cross-lamination	vf-f	*Pl, Th, Sk, Di*	70 mD
Splay lobe sand	SLS	8.5	Current ripple cross-lamination	vf-f	Absent	380 mD
Tidal channel sand	TCS	6.0	Trough cross-bedding Current ripple cross-lamination Wave ripple cross-lamination	vf-c	*Pl, Th, large Di*	270 mD
Tidal mud flat	TMF	4.0	Current ripple cross-lamination Wave ripple cross-lamination Trough cross-bedding	mud, silt, vf, f	*Di, Pi*	12 mD
Shoreface sand	SFS	3.3	Hummocky cross-stratification Wave ripple cross-lamination	mud, silt, vf, f	*Te, Sk, Mu, Pl, Th, Pa*	6 mD
Storm dominated delta	HMS	2.6	Hummocky cross-stratification	f	Rare	12 mD
Open marine mud	OMM	1.4	Starved wave ripple cross-lamination	mud	*Te, Di, Ch, Mu*	5 mD
Calcite cementation	CEM	0.7	-	-	-	0 mD
Dipping calcite cementation	CEMX	0.7	-	-	-	0 MD
Floodplain fines	FLF	4.0	Current ripple cross-lamination	mud, silt, vf	Absent	2 mD
Coal	COA	0.4	-	-	-	-
Shoal sand	SHS	7.0	Wave ripple cross-lamination	f-c	*Sk, Pl*	100 mD
Tidal sand flat	TSF	2.0	Current ripple cross-lamination Wave ripple cross-lamination Trough cross-bedding	mud, silt, vf-c	*Pl, Th, Sk, As, Di, Te*	80 mD

Pl – Planolites, Pa – Palaeophycus, Th – Thalassinoides, Sk – Skolithos, Di – Diplocraterion, Cy – Cylindrichnus, As – Asterosoma, Te – Teichichnus, Op - Ophiomorpha, Rh – Rhizocorallium, Ar – Arenicolites, Ta – Taenidium, Ch – Chondrites

Figure 5.5 Table of facies types identified in the reservoir interval in the Norwegian Sea field, showing typical permeabilities, sedimentary structure (Olsen, et al. 1999).

Indeed poro-perm values vary considerably over the reservoir interval, as illustrated in the following table (modified from (Hemmens, et al. 1992, and Reid, et al. 1996).

Property	Fangst Group	
	Range	Average
Gross thickness (m)	0-90	70
Net pay thickness (m)	0-81	63
Porosity (%)	24-32	28
Horizontal permeability (mD)	700-20 000	1450
k_v/k_h	NA	0.9
Water saturation (%)	5-14	NA
Residual oil saturation, water (%)	33-43%	NA
Residual oil saturation, gas (%)	17-28%	NA

Table 5.1 Fangst Group properties.

According to Tybero, reservoir quality is generally good, with porosities rarely falling below 20%: permeabilities in the Fangst Group rarely fall below 1D; the Fangst 4 and 5 units show the best reservoir quality, with permeabilities in the range 2000-6000 mD and averaging about 4000 mD (Tybero, Johannessen and Bouchard 1994). The highest permeabilities (about 950 mD) are shown by trough cross-bedded incised valley-fill facies, fluvial-channel sands (average 600 mD) and splay-lobe sands (380 mD). Lower permeabilities are shown by tidal flat sands (80 mD) and shoreface sands (6 mD). All the reservoirs show water-wettability (Olsen, et al. 1999).

For understanding reservoir compartmentalisation and planning of infill drilling, a 4D time-lapse survey was implemented. According to Roste, the Norwegian Sea field is covered by four 3D seismic surveys (1986, 1991, 2003 and 2006) and four 4D seismic surveys (2001, 2004, 2006 and 2008). A merge between the 1986 and 1991 surveys forms the base survey for the 4D seismic surveys. The acquisition surveys from 2001 and 2004 cover the southern

part of the Norwegian Sea field, whereas the 2006 and 2008 surveys cover the whole field. The main goal of the 4D projects has been to develop and to maintain the Norwegian Sea field flooding maps (Furre, Munkvold and Nordby 2003) which illustrate and describe the drainage of the reservoir, the vital property in such a heterogeneous reservoir.

Figure below shows the expected time-lapse response in the Norwegian Sea field. Brine flooding at Top Fangst is expected to give an amplitude decrease, whereas gas cap expansion will give an amplitude increase. This is shown in the difference section (Figure 5.6, right), where both gas and brine movements are seen (Furre, Munkvold and Nordby 2003).

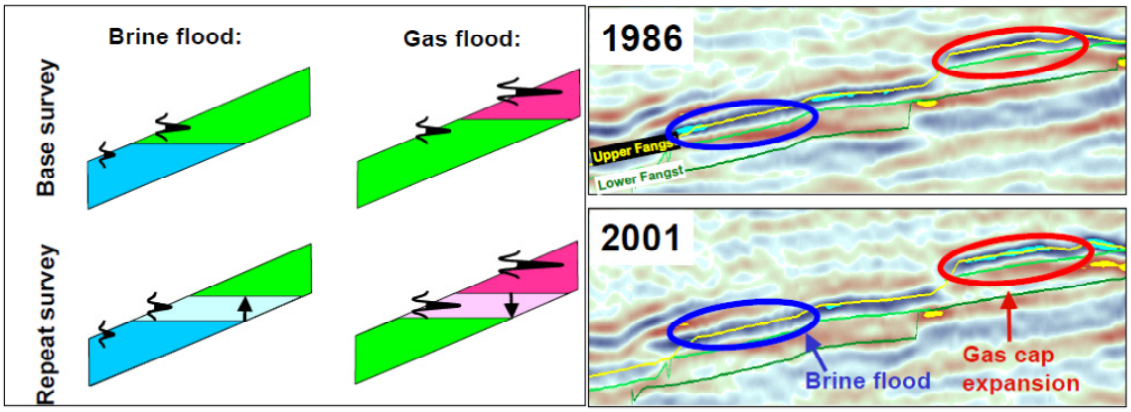

Figure 5.6 Left: Expected time-lapse response at Norwegian Sea field. Right: Arbitrary seismic cross-section showing both brine flooding and gas cap expansion (Furre, Munkvold and Nordby 2003)

To convert this physical level of reservoir understanding into a more analytical and quantitative form, Furre proposed the drainage maps, which have been used in planning infill drilling locations and serve as a tool in improving reservoir understanding , which can be utilised in the history matching procedure. Moreover, these maps can provide a valuable understanding of flow distribution in the reservoir (Furre, Munkvold and Nordby 2003). Thus, using the seismic and simulator maps, together with production data, repeated logging and geological understanding of the field, it is possible to construct a drainage map (Figure 5.7, right). Two wells have been drilled, for which the locations were determined using drainage map.

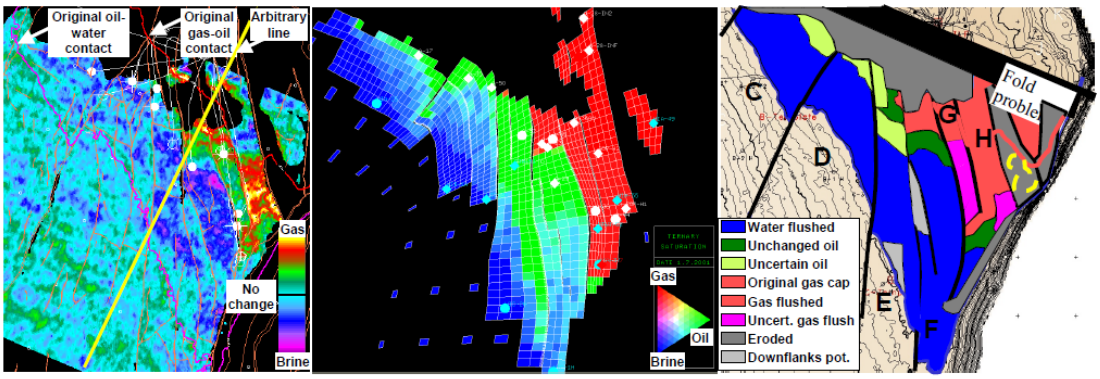

Figure 5.7 Left: Amplitude difference map at Top Fangst. Dark blue and purple colours indicate brine flood, red and yellow colours indicate gas cap expansion. Middle: reservoir simulation map for the uppermost layer in Fangst. Right: drainage map for Upper Fangst. Comparing the amplitude map to reservoir simulation maps for a representative layer in Upper Fangst shows that there are major similarities between the maps. The seismic map confirms massive gas flooding in the H segment, but indicates less flooding in G. It also indicates stronger water-flood in the E and F-segments than predicted from the simulator. (Furre, Munkvold and Nordby 2003)

The drilling of the wells confirmed the overall understanding of the flow pattern, but did provide some surprises, showing that the flow pattern in Fangst is complicated, due to faults, short cuts created by Cretaceous sands, and the two-front gas and water displacement towards the producers. Minor internal shale layers act as flow barriers during production.

Table 5.2 represents the field description.

Basin	Halten Terrace
HC type	Saturated oil and gas
Discovery year	1985
First production	October 1995
Number of production wells	51
Number of injection wells	24 water injectors + 1 gas injectors
Platform	One tension-leg platform
Elevation of water depth	345 m
Trap	
Structural setting	Rift basin
Trap type	Eroded tilted horst-block
Closure mechanisms	Dip and fault closure with supra-unconformity seal at crest
Depth to top pay	2080 m TVDSS
Original hydrocarbon column height	Gas cap: 214 m max; oil zone: 195 m max
Original fluid contact	OWC: 2415-2478 m; GOC: 2283-2322 m TVDSS
Reservoir	
Producing formation	Fangst Gp (Md.Jur.) (75% of reserves); Bat Gp (Up.Triassic-Md.Jurassic)
Deposition system	Fangst Gp: tidally influenced coastal plain to shoreface-shelf
Sandbody type (dominant)	Braided- fluvial channels
Sandbody type (secondary)	Shoreface-shelf
Sandbody type (tertiary)	Mouth bar
Reservoir architecture/geometry	Layer-cake
Fluid flow restrictions, macro-scale	Faults, tidal flat intervals
Fluid flow restrictions, meso-scale	Faults, tidal flat intervals
Fluid flow restrictions, micro-scale	Minor diagenetic cements, detrital clay
Reservoir flow unit/strat.layers	5
Reservoir structural compartments	Multiple
Reservoir struct./strat/ compartments	Multiple
Gross reservoir thickness	about 840 m (entire reservoir)
NTG	0.8
Net pay	253m max
Lithology	Very fine- to coarse-grained sandstone
Porosity types	Primary intergranular; very minor secondary porosity
Core porosity	Average 18-29%
Air permeability	Average 70-20 000mD
Source	
Formation and age	Spekk Formation (Up.Jurassic-Lo.Cretaceous)
Lithology	Organic-rich shales
Depositional system	Anoxic marine shelf
TOC	Max.: 13%; Average: 4%
Kerogen type	II

Time of hydrocarbon explusion	Paleogene, main trap charge in late Neogene
Seal	
Formation and age	Cromer Knoll Group (Lower Cretaceous)
Lithology	Marls, shales
Depositional system	Marine shelf
Reserves and Production	
OIP	2907 MMBO + 1.33 TCF solution gas and 1.65 TCF free gas
Ultimate recoverable	950 MMBO + 1.5 TCFG
Max production rate per well	40 000 BOPD
Productivity index	NA
Hydrocarbon Composition	
API gravity	21-29 (average 26)
Viscosity	0.8-2.9 cp (reservoir conditions)
Sulphur content	NA
Initial GOR	295-620 SCF/STB
Saturation pressure	2900 - 3364 psia
Pour point	NA
Field Characteristics	
Original reservoir pressure	3640 psia @ 2375m TVDSS
Pressure gradient	0.46 psi/ft
Natural drive mechanism	Moderate solution-gas drive, with weak aquifer drive
Secondary recovery method	Water and gas injection
Recovery factor	33%
Completion practice	
Type of completion	7 in. liner
Interval perforated	Mainly Fangst

Table 5.2 Norwegian Sea Field description

5.3 Model Overview

5.3.1 Production history overview

The Norwegian Sea field contains in-place hydrocarbons comprising 2907 MMBO, 1.33 TCF solution gas and 1.649 free gas. The STOIIP is split between the reservoirs as follows: Fangst 34%, Tilje 29% and Åre 37%. The GIIP is split between the reservoirs as follows: Fangst 32%, Tilje 56% and Åre 12%. Most of the Åre hydrocarbons occur in the upper unit, Åre 2, which contains 28% of the field STOIIP; the lower unit, Åre 2, contains only minor gas and 9% of the field STOIIP. Approximately 75% of the resource lies within Block

6707/7 and 25% within Block 6707/8 (Reid, et al. 1996). The most recent estimate of ultimate recoverable reserves is 950 MMBO and 1.5 TCFG (Olsen, et al. 1999), representing an average ultimate recovery factor for oil of 33%. Approximately three-quarters of the oil reserves will be recovered from the Fangst Group (Ramshaw 1991). The proportions of the gas reserves recoverable from the gas cap or as solution gas is unknown. Oil properties vary substantially within the field, as indicated in the following table, which shows key parameters at reservoir conditions (2375 m TVSS; 185 ^{o}F; 3640 psia):

	Fangst Group	Tilje Formation	Åre Formation
API gravity (o)	29	21-28	21-26
Oil viscosity (cp)	0.8	0.8-2.9	1.2-2.6
Initial GOR (SCF/STB)	620	295-654	350-525
Oil FVF (RB/STB)	1.34	1.15-1.32	1.16-1.28
Saturation pressure (psia)	3364	2900-3364	2900

Table 5.3 Norwegian Sea Field fluid properties

Fluid properties are relatively uniform within the Fangst Group, but in the Tilje and Åre formations, the oils become heavier, more viscous and more undersaturated with depth (Fig. 16). In addition there are lateral variations in fluid properties, due to biodegradation related to the shallow depth of burial. The reservoirs are normally pressured. The field is being developed as five separate reservoirs: Upper Fangst, Lower Fangst, Upper Tilje, Lower Tilje and Åre. Aquifer drive in these reservoirs is weak, due mainly to the heavily faulted nature of the field, while solution-gas drive is inadequate, particularly in the deeper reservoirs, where solution GORs are lowest. The Upper and Lower Fangst are being produced by a

combination of water injection and gas injection, while the Upper Tilje is being produced by means of water injection only. Because the Lower Tilje and Åre are more heterogeneous than the overlying units and contain numerous separate sandstones, water injection is not regarded as being an efficient recovery process, and they are instead being produced by pressure depletion, aided by gas-lift.

In the Fangst reservoirs, the seven water injectors are located beneath the OWC, in a line-drive pattern, with two gas injectors completed in the gas cap (Figure 17). The water injectors have capacities of about 330,000 BWPD (Carstensen, Wilk and Van Brocklin 1993). Six producers are dedicated to the Upper Fangst and eight to the Lower Fangst. Separate development of the Upper and Lower Fangst improves the ability to control withdrawal rates and flood front movement. Fangst wells are capable of producing at up to 40,000 BOPD, but are expected to be limited to 20,000 BOPD (Reid, et al. 1996).

The overall poor oil recovery factor is due to a combination of the strong fault-compartmentalisation, reservoir heterogeneities, particularly in the Åre Formation, and constraints on production required to control waterflood advance and gas-cap expansion. Recovery efficiency from the Fangst is expected to be relatively good. The Upper Tilje is being developed with six producers and two water injectors, with a possible two additional producers to be drilled. Recovery efficiency from the Upper Tilje is expected to be high and oil producers are expected to produce at 30,000 BOPD. The Lower Tilje is being developed with six producers, with recovery by natural drive only. Recovery from the Åre reservoir is expected to be relatively poor, due to its higher oil viscosity, lower permeability, and greater heterogeneity and structural complexity. It will be developed using eleven oil producers.

The development strategy was to achieve a rapid build-up in production. To this end, 16 wells were pre-drilled before the platform was installed, as follows: seven Fangst oil producers, two Fangst gas injectors, six Fangst water injectors and one Tilje producer (Deom, et al. 1996). Pre-drilling commenced in 1991 from a 56-slot subsea template. No horizontal wells have yet been drilled, as deviated wells have sufficient permeability-thicknesses to achieve high production rates. Pre-drilled wells were completed using perforated 95/8 in casing, although subsequent wells with 7 in liners have yielded improved recovery. Despite the weak cementation of the reservoirs, most of the production wells are completed without gravel packs (Landrum, et al. 1996). It is hoped that high production rates from the field as a whole will allow moderation of individual well rates to control sand production. Scaling by barium sulphate has been identified as another potential problem and is being countered by

scale squeezes and location of some of the water injectors about 800 m further downdip than originally planned. The latter measure provides a large formation-water buffer between the injectors and producers (Reid, et al. 1996). Production commenced in October 1995 (Figure 18). The daily production rose rapidly, due to the pre-drilled wells, reaching 235,000 BOPD during 1996. Produced gas is re-injected into the gas cap and exported for methanol production to the Norwegian mainland.

According to Furre, Munkvold and Nordby (2003), the primary drainage strategy of the Fangst reservoir at the south flank was a row of producers in the thick part of the oil column in each segment, pressure is supported by down-flank water injectors. Re-injected gas in the gas cap at the top of the structure also provides pressure support. After the first row of producers are watered out, the main challenge is producing the up-flank oil in the thinner part of the reservoir, in addition to tracking any bypassed oil.

5.3.2 Simulation model and history matching.

The reservoir simulation model of the field was provided by the operator, and was used for production predictions and volume calculations, as well as for well planning operations and uncertainty qualifications. The grid dimensions are as follows: 100 m x 100 m x 10 m with a total cell number of about 1.4 mln, which comprises all the producing reservoirs of the field. Structurally, the field is compartmentalised into a few global segments, with minor faults within each segment. According to geological studies, the Fangst Group reflects relatively homogeneous reservoir properties. Manipulations with such a complex model can be rather time consuming and not efficient, so, for optimisation, it was decided to reduce model size and to analyse only the area of interest. The model was simplified, zonations used here are only those included in the Fangst Group, hence we get 20,629 cells (see Figure 5.8 below) in the area of interest.

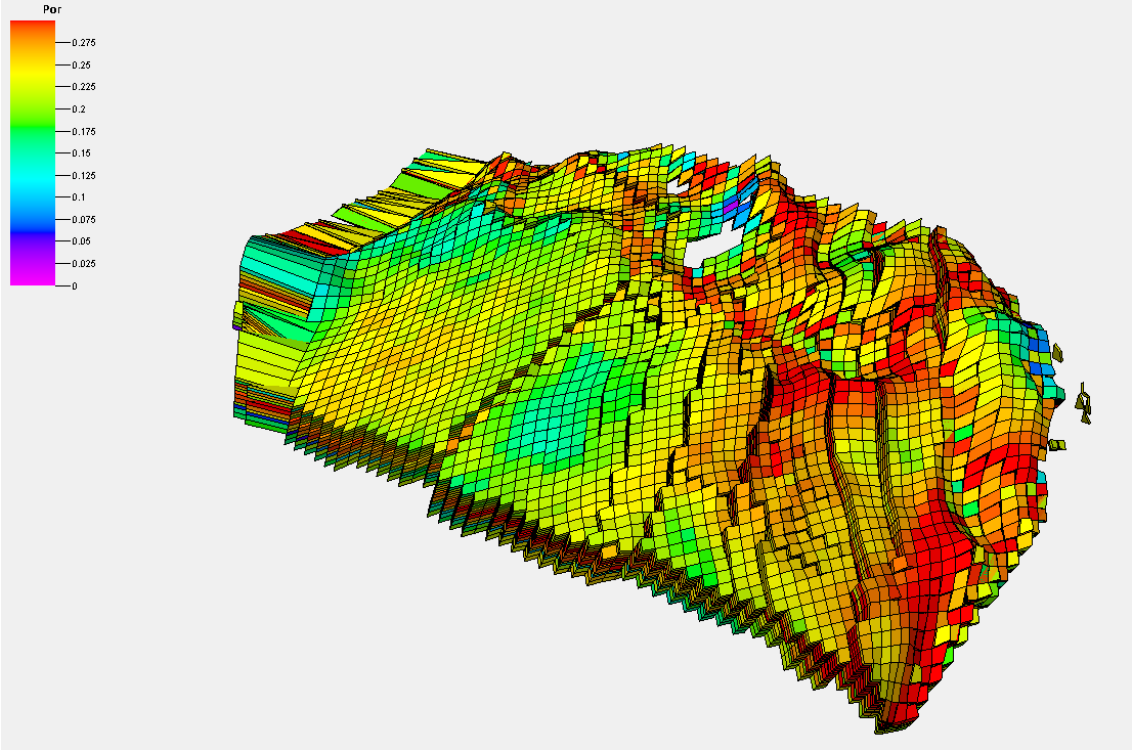

Figure 5.8 Porosity of simulation model grid. 3D view. Average value is about 0.26.

Overall, reservoir properties in the area are rather good: they are laterally continuous, average porosity is 24.5% (Figure 5.9) and permeability average value is 2200 mD (Figure 5.10). The net-to-gross distribution is a constant and has a value equal to one. Hence, reservoir connectivity is strongly dependent on the fault properties, as the faults can act as barriers or baffles for the flow.

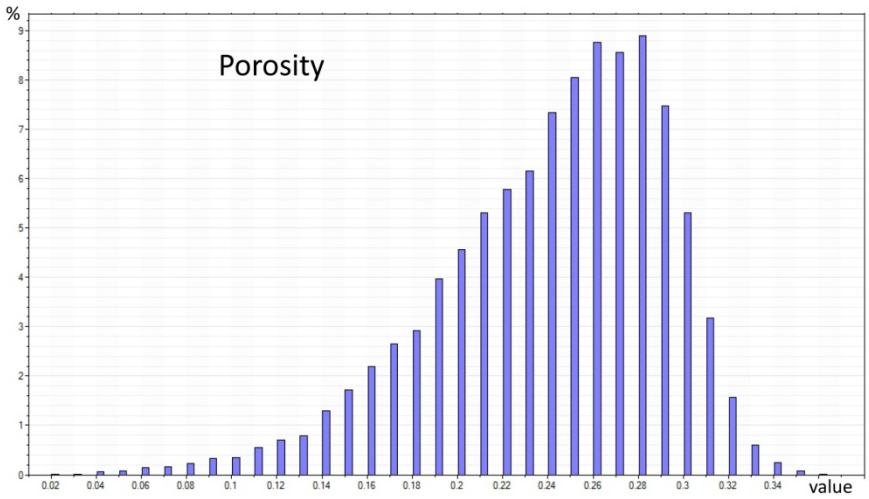

Figure 5.9 Porosity histogram of simulation model.

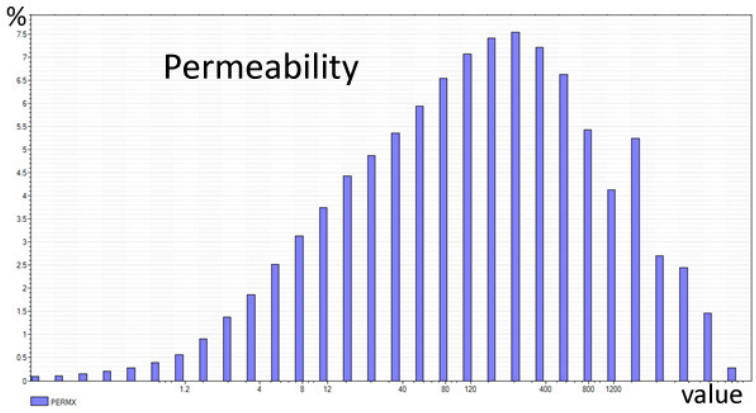

Figure 5.10 Permeability(in mD) histogram of simulation model.

The fluid which saturates the model is black oil. As mentioned, production and pressure support are provided by water injection and aquifer support from the down-flank side of the field, and gas injection in the up-flank edge.

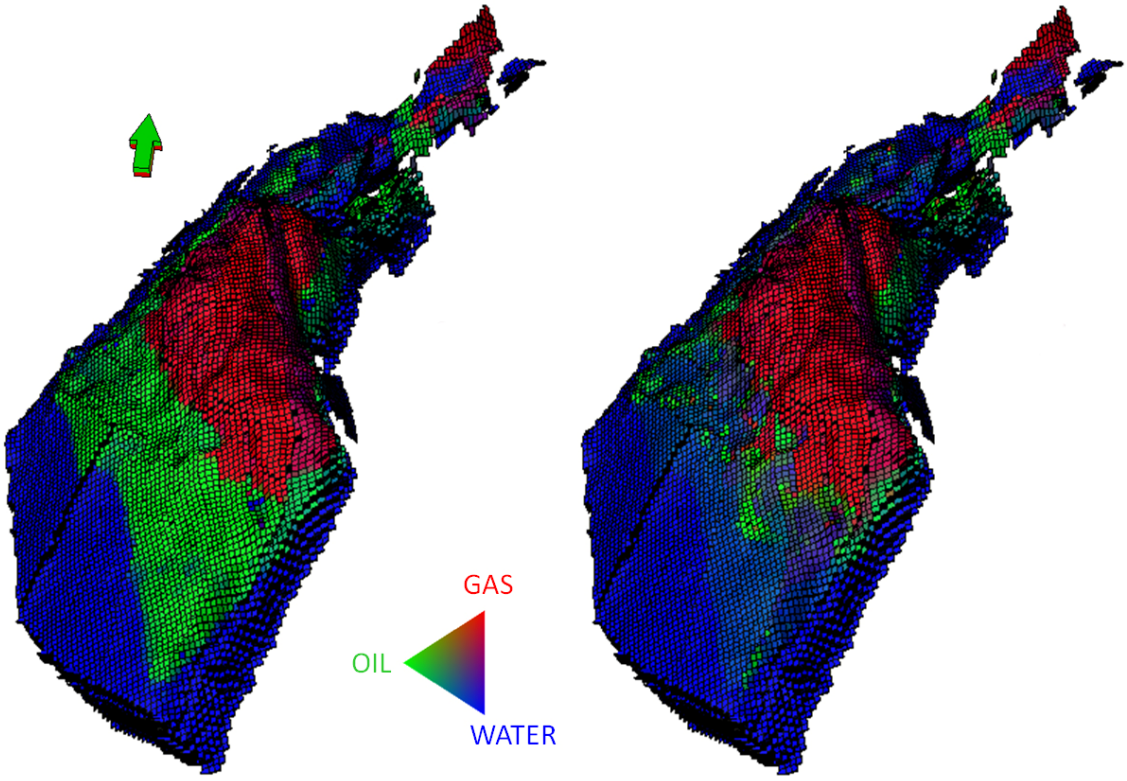

Figure 5.11 Initial fluid distribution along the full field model/ Different fluids: water, oil and gas represented as dark blue, green and red.

According to Figure 5.11, the reservoir has rather good properties which are very favourable for fluid flow. Net-to-gross distribution varies from 0.2 up to 1 in the model. Hence, the main controlling property for reservoir connectivity will be NTG, which is a good correlation with the modeled depositional environment.

5.4 Application of connectivity estimation techniques - S2S, W2S and clusters

Field production started in 1995, and a baseline survey was conducted before this date. Then number of monitors took place in 2001, 2004, 2006, 2008 and 2011. Unfortunately, it is impossible to utilise them all due to different reprocessing procedures; details of which surveys have been used will be discussed later.

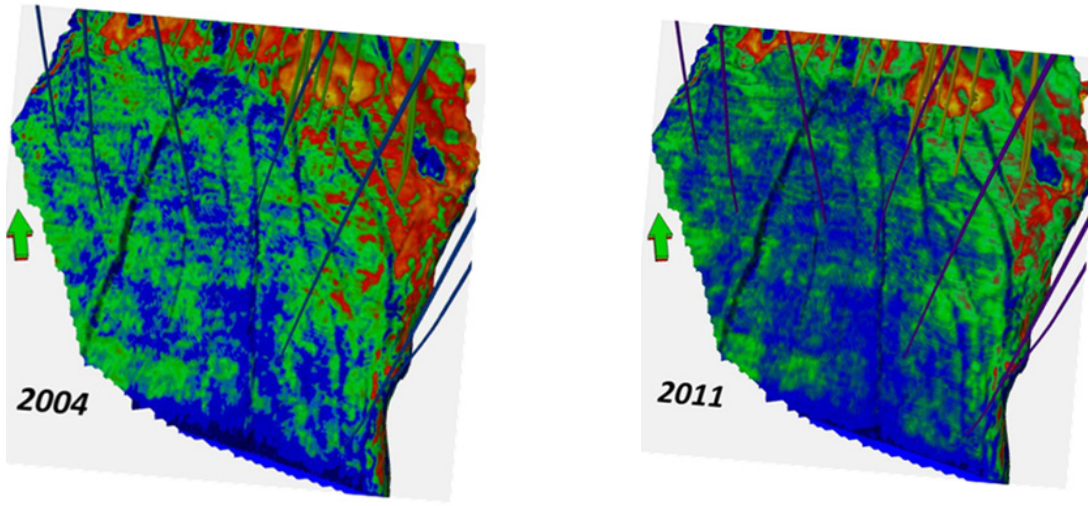

Figure 5.12 Time lapse amplitude map for the Fangst Group (blue: water, green: oil, bright red: gas). Scale 1:50000 meters.

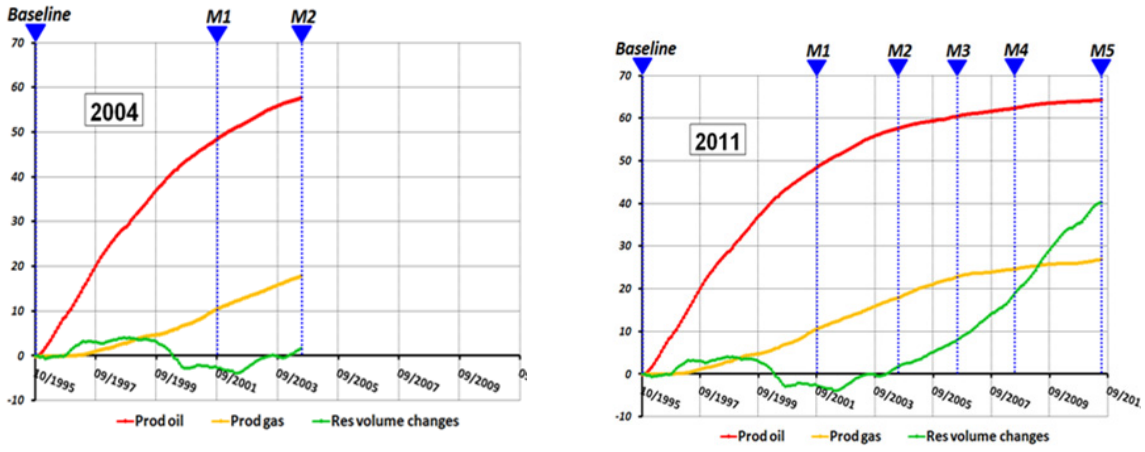

Figure 5.13 Production volume changes in the Fangst Group

It is rather obvious that the 4D signal is quite consistent (see Figure 5.12) due to the water drive regime, where oil is sweep due to the water movement. But here we have a gas signal, so interpretation becomes more complicated. It is easy to see changes in the gas cap from 2004 till 2011; the cap sufficiently expands until it reaches the compartment boundaries. This fact reveals the structural control of the field.

5.4.1 Well-to-Seis (W2S)

Well-2-Seis application to the Norwegian Sea field was conducted by Zhen Yin, who found the following results:

There are certain Well-2-Seis limitations which make it inapplicable to this particular field case:

- It is mainly for pressure dominated reservoirs with 2-phase flow of water and oil
- Correlation results can be contaminated due to the number of 4D surveys and the depletion strategy
- The Norwegian Sea field is a saturation dominated reservoir with three-phase saturation (oil, gas and water).

Hence, it was decided to divide the south flank of the reservoir into three zones (see Figure 5.14): a water injection zone, mostly dominated by pressure, a softening zone, mostly

dominated by gas saturation and a hardening, zone mostly dominated by water saturation. This division was made based on the fluid distribution at the initial state and through almost all production stages and the well pattern scheme.

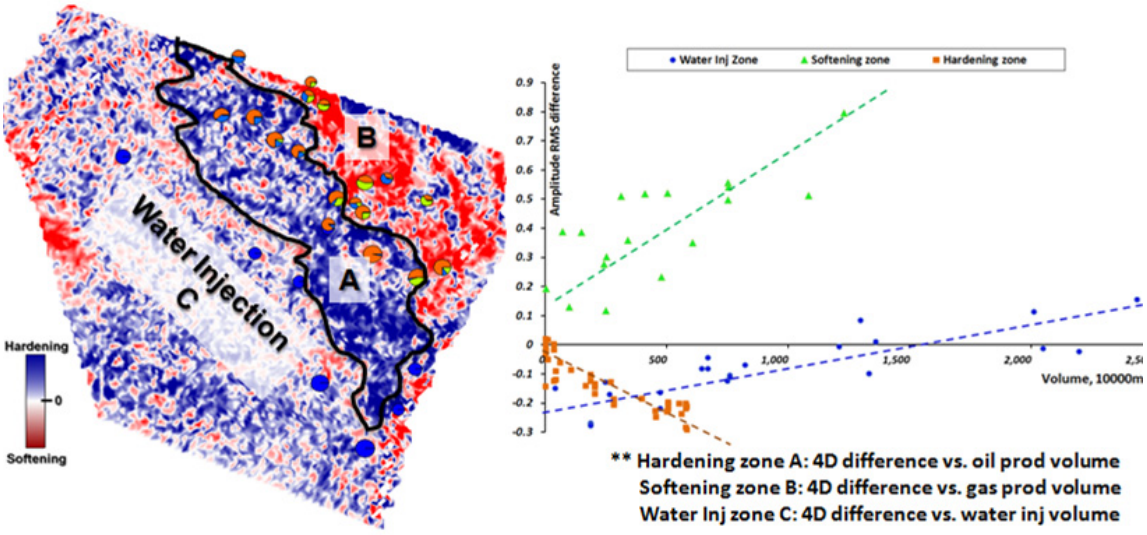

Figure 5.14 Observed amplitude RMS map differences (Base, 2001, 2004 and 2006) vs. cumulative production and injection volumes (Yin and MacBeth 2014).

It was decided that the aquifer would be the water injection part, as it is the only part for water injection and there will be no fluid changes, only the propagation of the water front and changes in pressure. The hardening zone with mainly oil and gas (later) is a saturation dominance region. A linear relationship was observed for all the zones: between oil production volume and 4D response in the hardening zone, between total injected volume and 4D signal in the water injection zone and between gas production and 4D in the softening zone. As shown by Falahat in his thesis, there is a multi-linear relationship between the mapped 4D signature and the pressure and saturation changes, scaled by the corresponding pore volume (or thickness) in clastic reservoirs:

$$\Delta A(\Delta P, \Delta S_g, \Delta S_w) \approx C_p h_p (\varphi NTG)_p \Delta P + C_w h_w (\varphi NTG)_w \Delta S_w + C_g h_g (\varphi NTG)_g \Delta S_g$$

C_P, C_W , C_G represent the contributions of pressure, water and gas.

A new theory of fault transmissibility calculation using 4D was proposed by Yin (Yin ETLP sponsor meeting 2015), together with an optimization algorithm. According to Yin, the algorithm is as follows (for fault transmissibility calculation in the softening zone and the hardening zone):

1. (Optional- only for hardening zone) Divide the major open faults into several segments averagely.
2. Extract all possible 4D differences using multiple surveys.
3. Derive fault transmissibility using new theory.
4. Simple optimisation on the results from 4D.
5. For the faults which are originally closed:
    a. Assign a transmissibility to the fault
    b. Regenerate synthetic seismic using the new simulated results
    c. Apply the fault transmissibility derivation theory to calculate fault transmissibility multipliers to update the model.

The results of the method are presented in the following two figures. This method produces rather good results, which actually improve the history matching results, but a few limitations still exist, including the fact that this is a 2D method and the necessity of few iterations to get the final results.

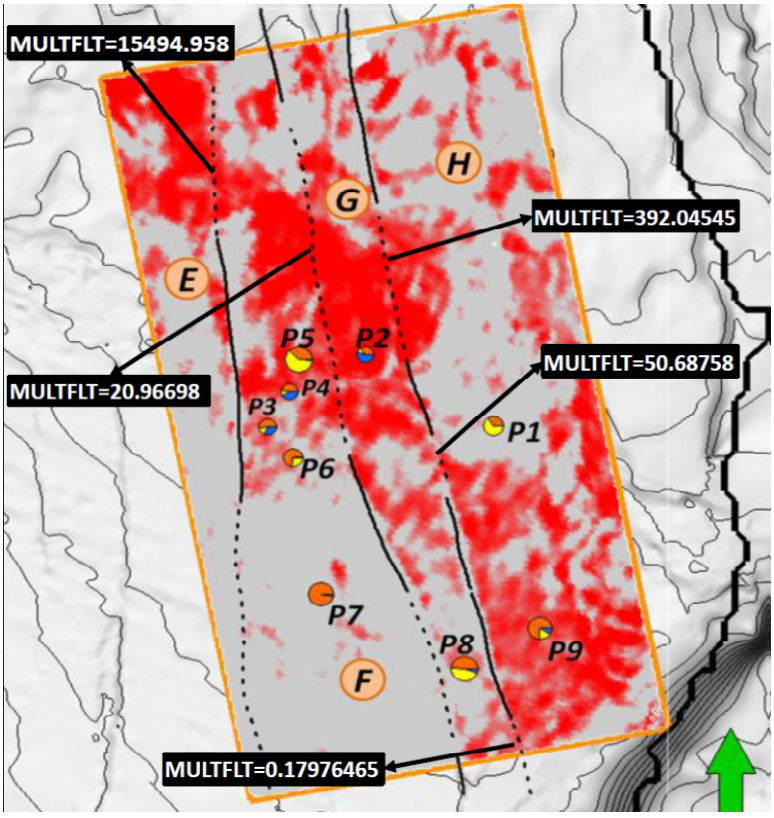

Figure 5.15 Results of fault transmissibility updates in softening zone (Yin and MacBeth 2014). Scale 1:10000 meters.

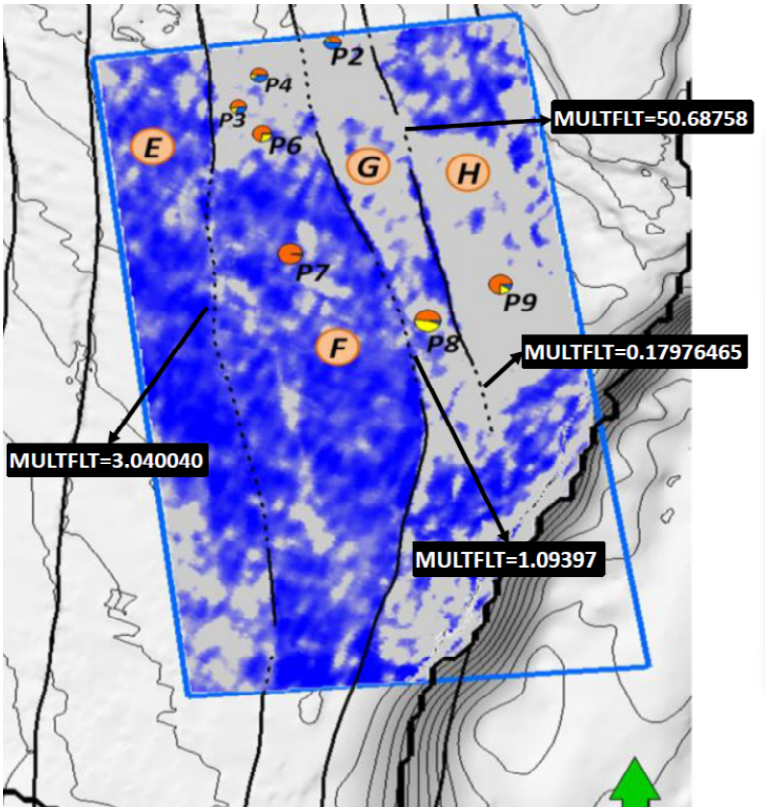

Figure 5.16 Results of fault transmissibility updates in hardening zone (Yin and MacBeth 2014). Scale 1:10000 meters.

5.5 Cluster application

Details and principles of this method are presented in Chapter 3. All the necessary steps were performed, starting from 'upscaling' the seismic into the simulation grid domain. Seismic response changes and production/injection volume changes were calculated and then clusters were are produced, see figure below.

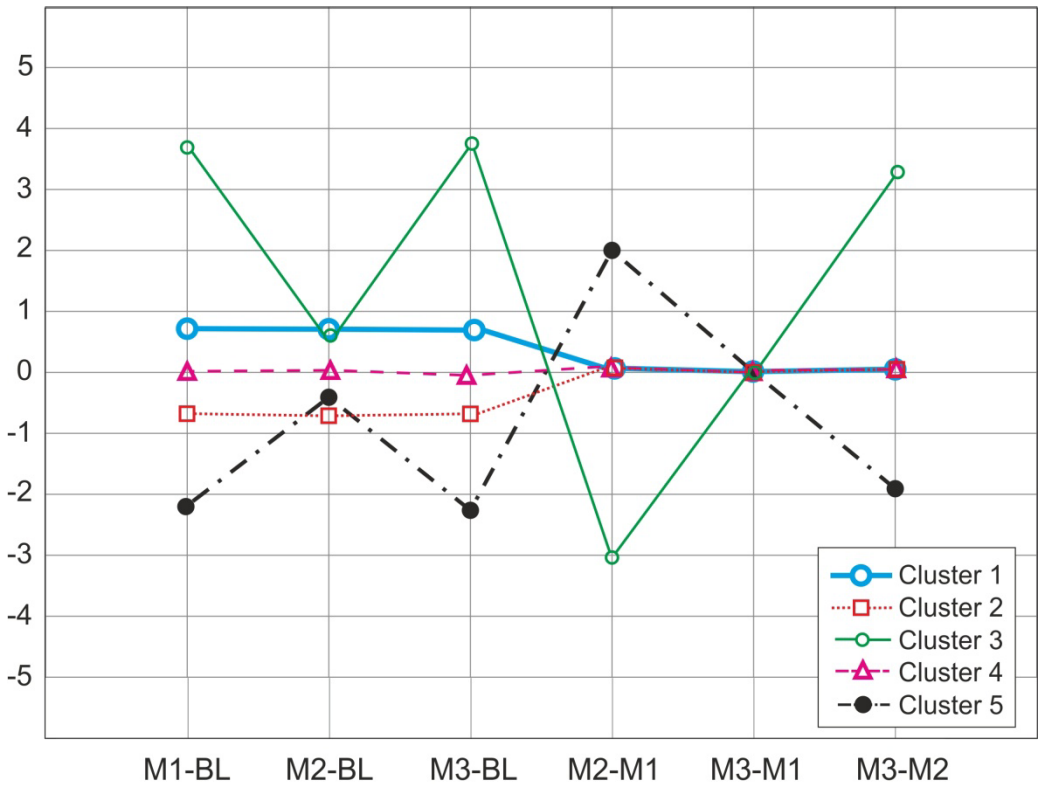

Figure 5.17 Cluster type curves for Norwegian Sea field. Y-axis: amplitude difference, X-axis: corresponding time step (D21= time between Monitor 1 and Baseline, D31= time between Monitor 2 and Baseline, D43= time between Monitor 3 and Baseline etc.) 'Non-active' cluster presented by pink curve- this is a part of the reservoir without any (significant) changes through time, based on seismic data

In order to test my method, all the transmissibility multipliers and any other changes in the simulation grids which were used for matching (as described in the previous section), were deleted and the simulation model was initialised. Thus, the work was started with initial grids of porosity, permeability etc..

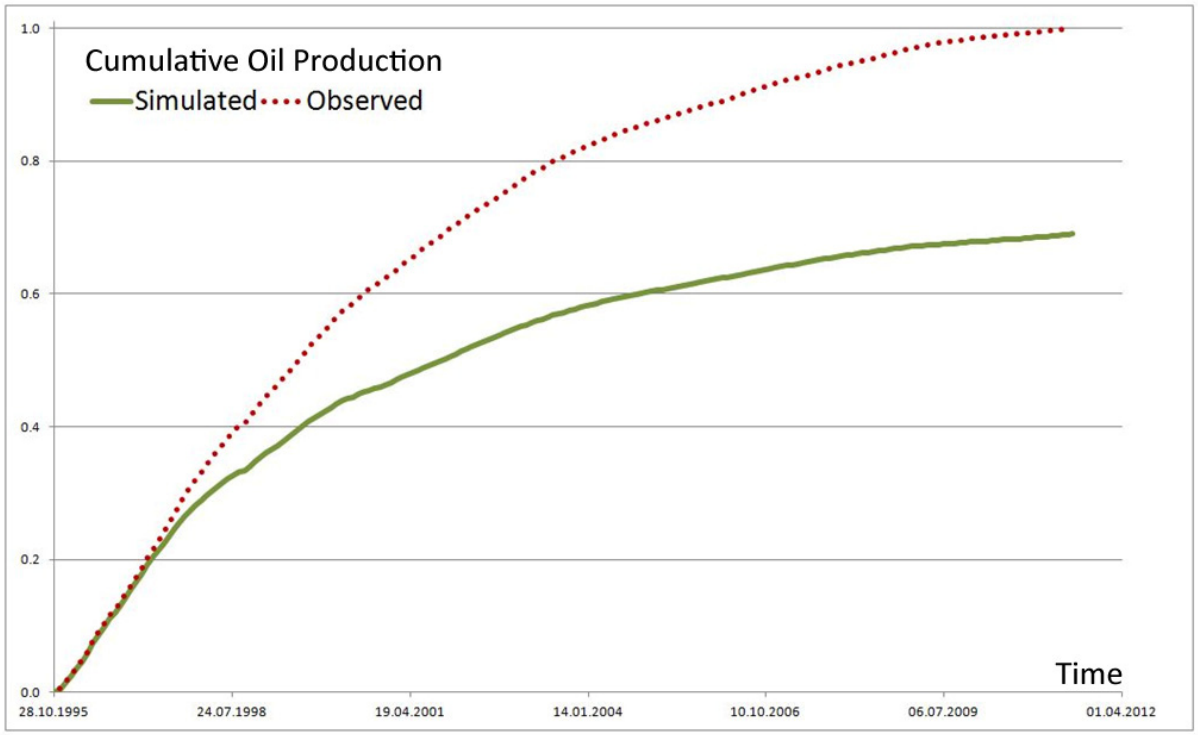

Figure 5.18 History matching quality for Base Case model. Green line: simulated cumulative oil production. Red circles: observed cumulative oil production

The initial reservoir connectivity is presented in Figure 5.19. Overall, the connectivity of the reservoir is rather good and, if we do not mention faults, it is possible to say the reservoir is quite homogeneous, according to the reservoir model. However, the field history indicates the presence of faults and the production challenges conformed to the presence of faults. It can be concluded that faults, or more precisely their sealing abilities, are the paramount parameter for successful reservoir management decisions. Hence, fault transmissibility is a key parameter for history matching in this reservoir.

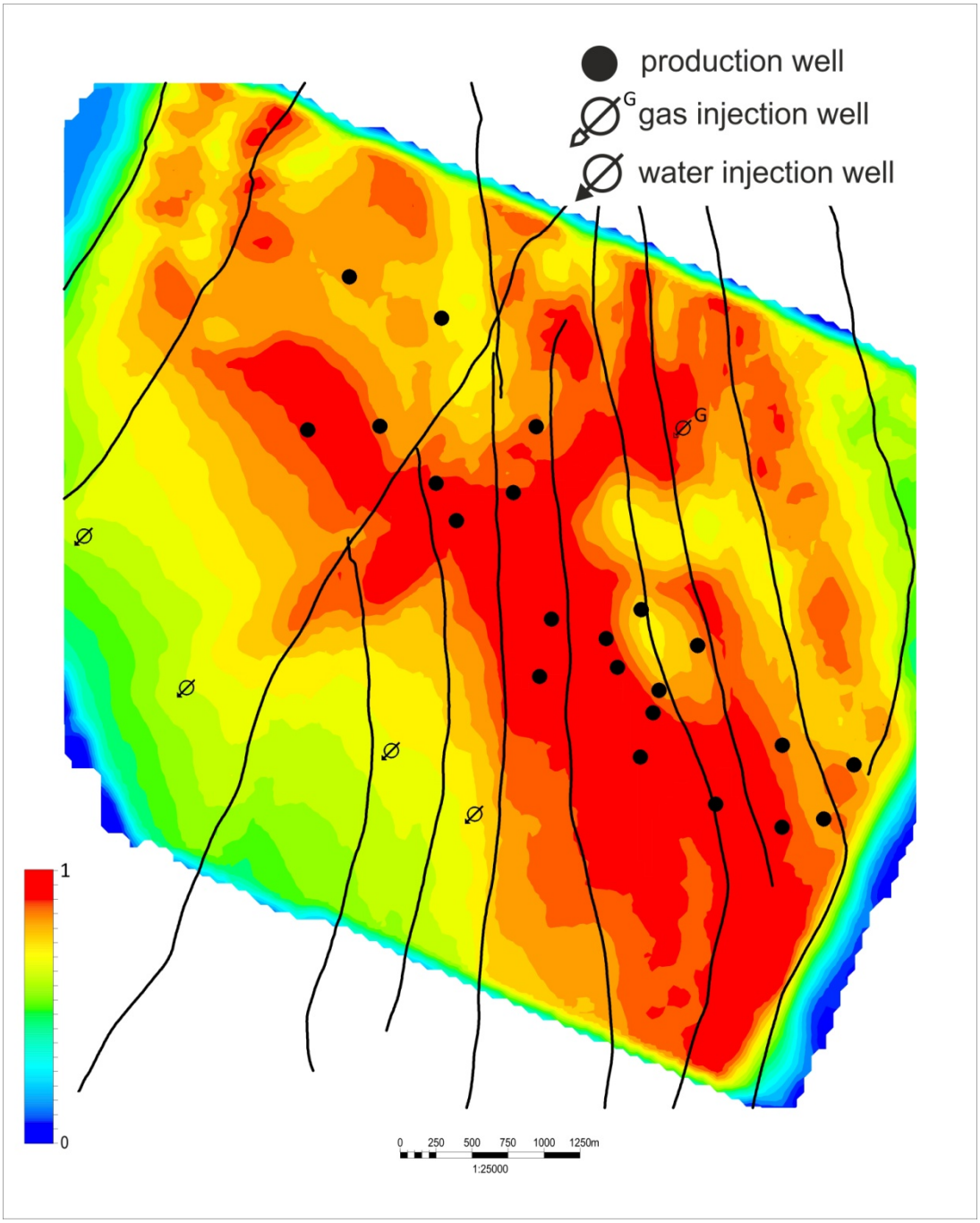

Figure 5.19 Initial connectivity of Norwegian Sea field, with interpreted faults (black curves) from seismic data.

5.5.1 Fault representation in reservoir and simulation model domains

What is a fault in terms of modeling and history matching?

Fault geometry in modeling is usually simplified. Faults are one of the main inputs for model grid creation; they are hard data for building the pillars and then the whole grid geometry. Thus, complicated fault shape can significantly complicate the resulting grid geometry.

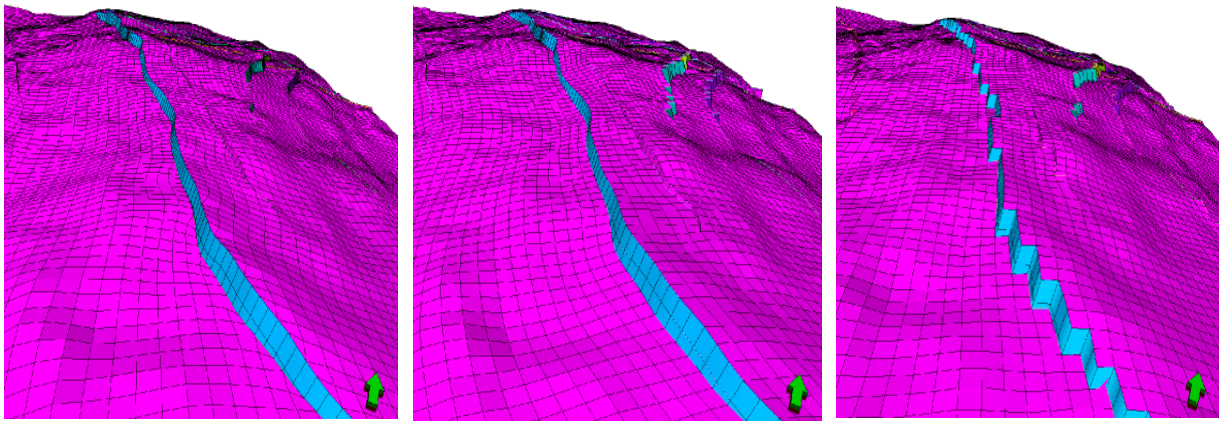

Figure 5.20 Fault modeling types. Left: crossing the cells; centre: along the i- or j- axis and right: zigzag modelling.

In Figure 5.20, the fault modeling types are presented, as used in Petrel Software, and which were actually used for creation of this reservoir model. The variant when fault pillars cross cells can lead to a rather complicated grid with non-uniform cell geometry and size in the vicinity of the faults, which later can produce problems and errors in solutions of differential equations during simulation. The variant of a fault along one of the axes may be not very realistic, due to the changes in the fault position: if we use 100 x 100 m cell size, then this modeling approach can introduce mistakes in 100-300 metres. So to minimise all the possible problems in the simulation model, the zigzag modeling type was used (see Figure 5.21). The next question regarding faults is the vertical shape- are they vertical or inclined or something else. To answer this question, here, we are limited to seismic quality and reservoir model resolution; in this particular case all the modeled faults are vertical.

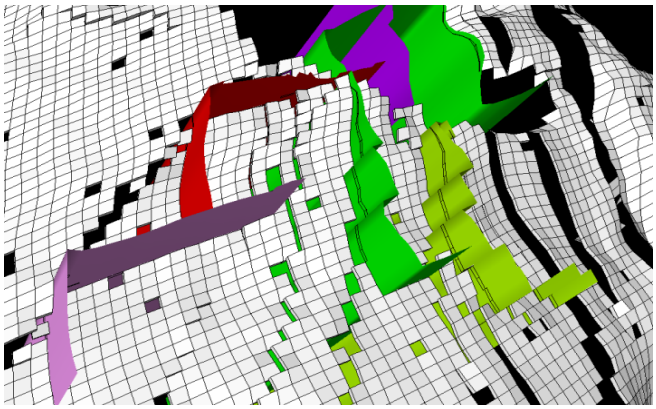

Figure 5.21 Fault modeling in Norwegian Sea field reservoir model. White represents modeled cells, red, green, pink, purple planes represent faults.

If we look at the simulation model, we can ask: do the faults change their geometry or properties or representation? If the geological model needs to be upscaled, then the fault geometry and properties will differ from the original. Here I did not go through the upscaling procedure, and the only point of interest was the fault representation in the simulation model.

Physically, a fault is an artificial plane between two cells or groups of cells in the simulation model (see Figure 5.22). It has an exact transmissibility value and during history matching we are able to vary it, i.e. increase or reduce it. This value can be determined explicitly by declaring a special object a "fault", with a corresponding transmissibility value in the simulation model. The problem here is that the value for the fault plane will be only a single one and cannot be different from point to point on the fault plane. However, this can happen in a real reservoir. So, fault transmissibility can vary along its plane for geological reasons, and it can then be quite complex to integrate this into the simulation model.

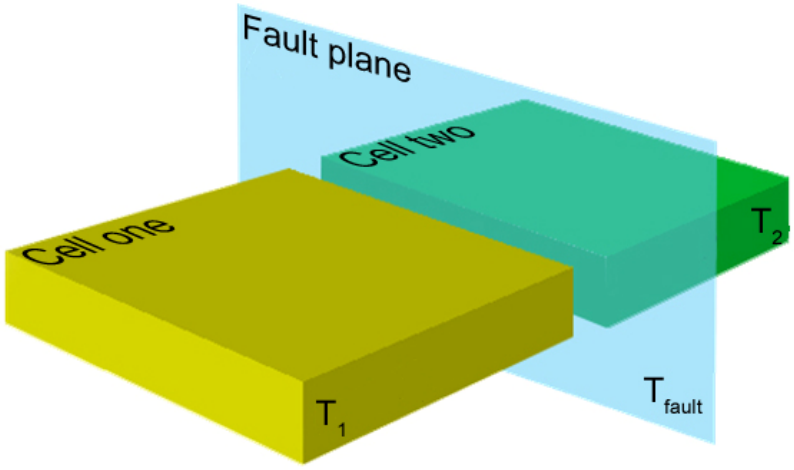

Figure 5.22 Transmissibility of fault- T_{fault} (can be different along the fault plane), as well cell transmissibilities are presented, T_1 and T_2. All these parameters are affecting fluid flow through the fault plane.

To introduce spatial variability of fault transmissibility, it is necessary to change the transmissibility of the adjacent cells in the vicinity of the fault. Thus, it is now clear how reservoir transmissibility can be changed for history matching. As explained in previous chapters, transmissibilities depend on permeability, grid geometry and NTG values in the cells. Figure 5.23 shows the initial transmissibility map calculated by the simulator. Low values along the faults are explained by the predominantly defined values of fault transmissibilities, based on reservoir analysis and production data.

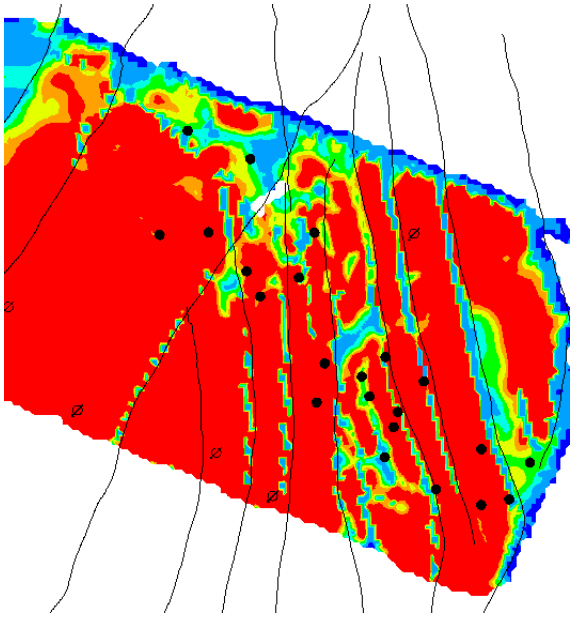

Figure 5.23 Average transmissibility X direction.

As this distribution of transmissibility has not produced good convergence of simulated data and observed, the engineers decided to change transmissibility by using multipliers. After number of simulations resulting multiplier map was produced and this is presented in Figure 5.24. It is easy to see that most of the changes occurred in the vicinity of the faults, with sufficient reduction along fault planes, preventing or resisting fluid flow through the fault plane.

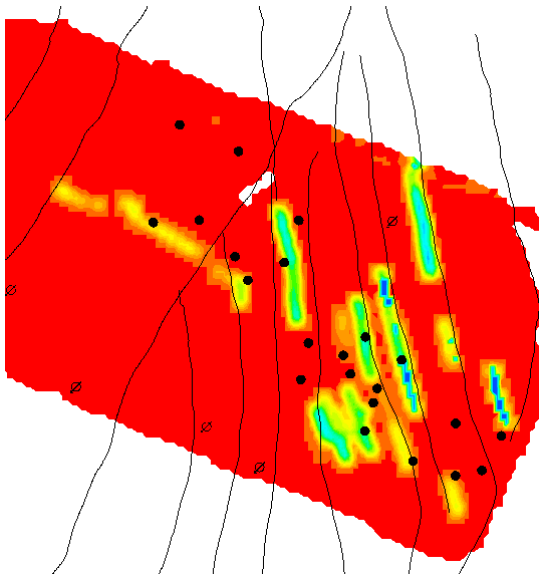

Figure 5.24 MULTX (transmissibility multiplier in X direction) average used in simulation modeling for history matching

5.5.2 Cluster technique results for the Norwegian Sea field

The timing of 4D monitors influences the results of the technique. These effects were not so obvious in the UKCS field case study, but here they are obvious- about 80% of cumulative production occurred between baseline and monitor one, so this actually caused slight problems in clustering, namely, in understanding the cluster and dynamic geobody behaviour in the later time steps (see clusters 1 and 3 on Figure 5.25).

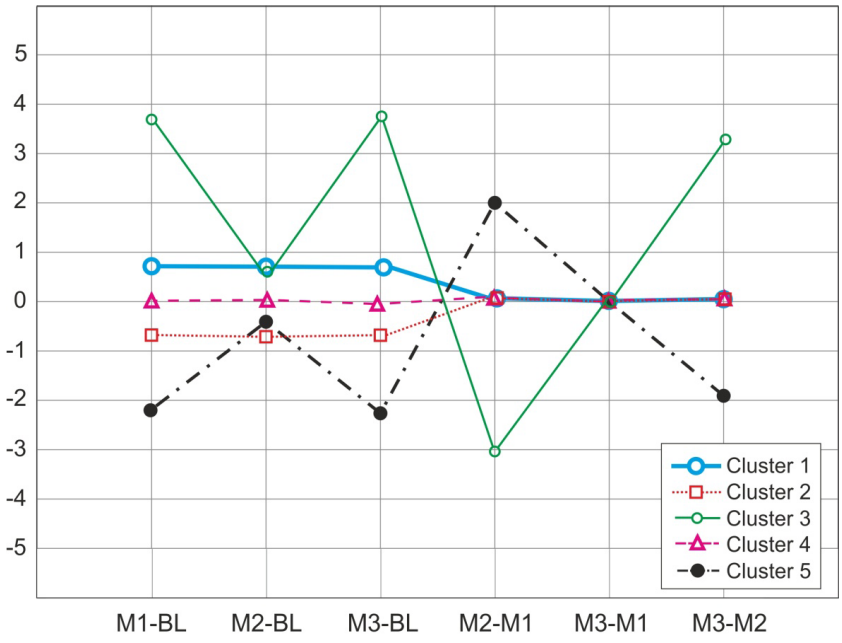

Figure 5.25 Cluster type curves for Norwegian Sea field. Cluster 1 and cluster 3 do not have any activity after monitor 1, so that means no significant changes in the reservoir after this time. Significant means detectable by seismic surveys, in this case.

However, as stated, there is another way to introduce barriers (or baffles) for flow in the simulation model instead of faults. It is possible to change the transmissibility of adjacent cells (yellow and green, in Figure 5.22). The nature of the cluster technique assumes finding non-active cells. The method for updating models with such results was presented in Chapter 4. So, here, non-active cells represent all the barriers in the reservoir- vertical and horizontal, stratigraphic and structural. Other words, this method updates all possible barriers and baffles in the simulation model by one iteration. The resulting connectivity map is presented in the following figure.

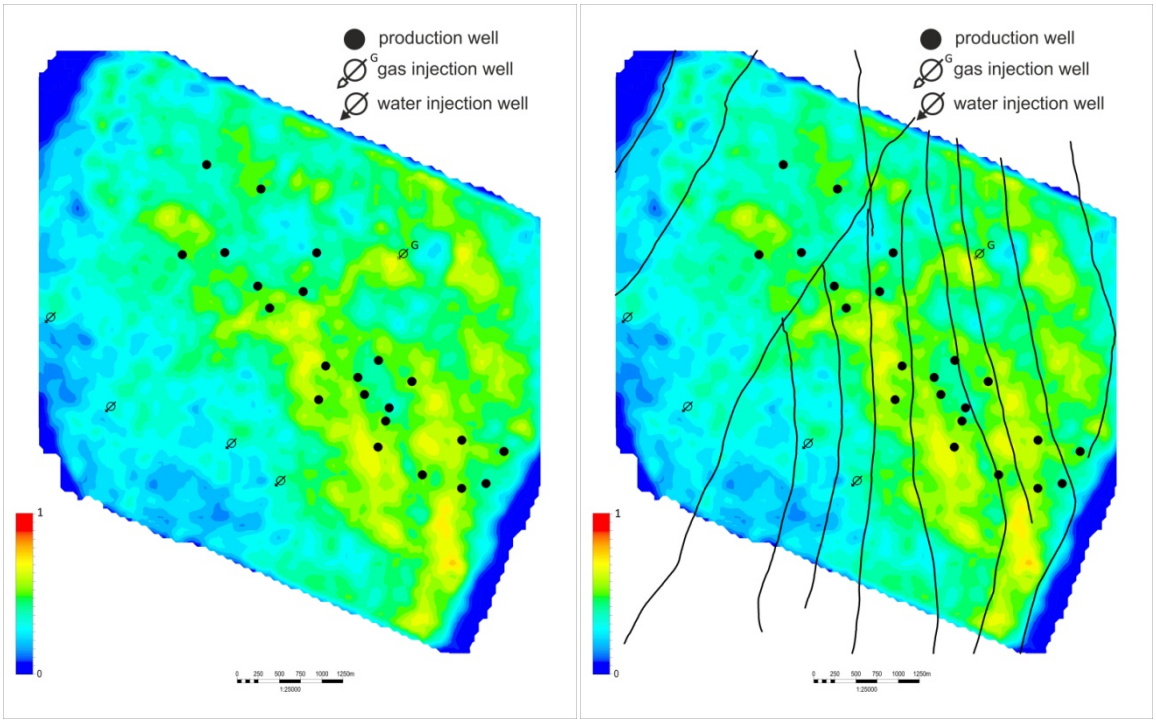

Figure 5.26 Updated connectivity of Norwegian Sea field. Left: without depicted faults, right: with depicted faults. Connectivity varies from 0 to 1.

Analysing this figure, there is no absolute zero connectivity. Connectivity here is of two natures based on two different types of compartmentalisation: stratigraphic (or lithological) and structural. The method does not separate them, and it is, indeed, not necessary. Compared with initial connectivity (Figure 5.27), stratigraphic compartmentalisation trends remain almost the same, but with significantly changed values, and the width of bodies has been significantly reduced. If we put faults on the figure, we will see, some areas associated with low connectivity are actually explained by the presence of faults and their low transmissibility influence. But faults are not completely sealing along their plane from top to the bottom; hence, the method introduces vertical and horizontal fault transmissibilities.

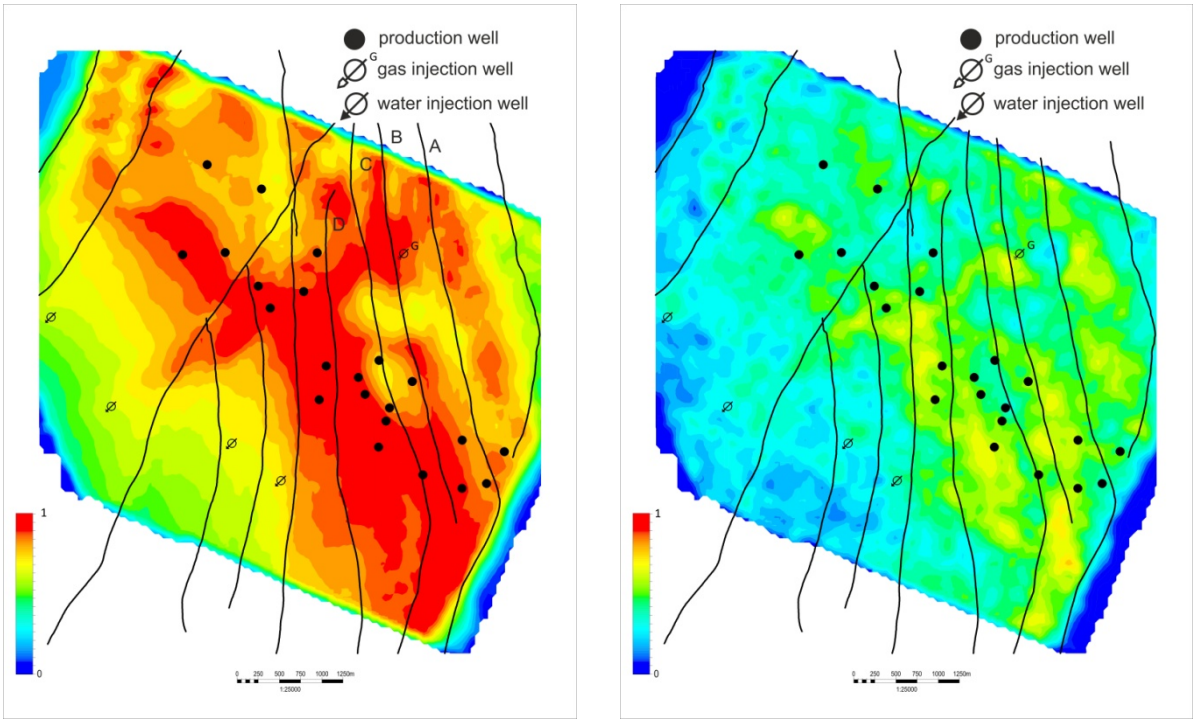

Figure 5.27 Comparison of the initial connectivity of the field (left) and updated connectivity (right). Overall connectivity has been sufficiently reduced, due to the update of the non-active cluster. Faults A, B, C and D are depicted on the left-hand side map. Connectivity varies from 0 to 1.

How has the transmissibility of faults been changed due to the update procedure? Comparison of the initial state of the fault planes and the results is presented in Figure 5.28. On the left-hand side are the fault plane transmissibilities in the initial simulation model: a dark blue colour means zero value, and if the colour is not dark blue, then the transmissibility is more than zero. The left hand side shows the upated fault planes view, with active and non-active cells. Values of transmissibility in non-active cells is equal to zero, for active cells it equals the initial transmissibility value (if this was not zero), or average value (if it was equal to zero initially). Faults A and B were 100% sealed (apart from the south side of fault B); after the update they are no longer barriers, but baffles. Indeed, all the analysed faults became baffles, rather than barriers, in different degrees. Say, fault planes C and D have 50% of non-active cells and 50 active, so these will produce more resistance to flow than fault planes A and B.

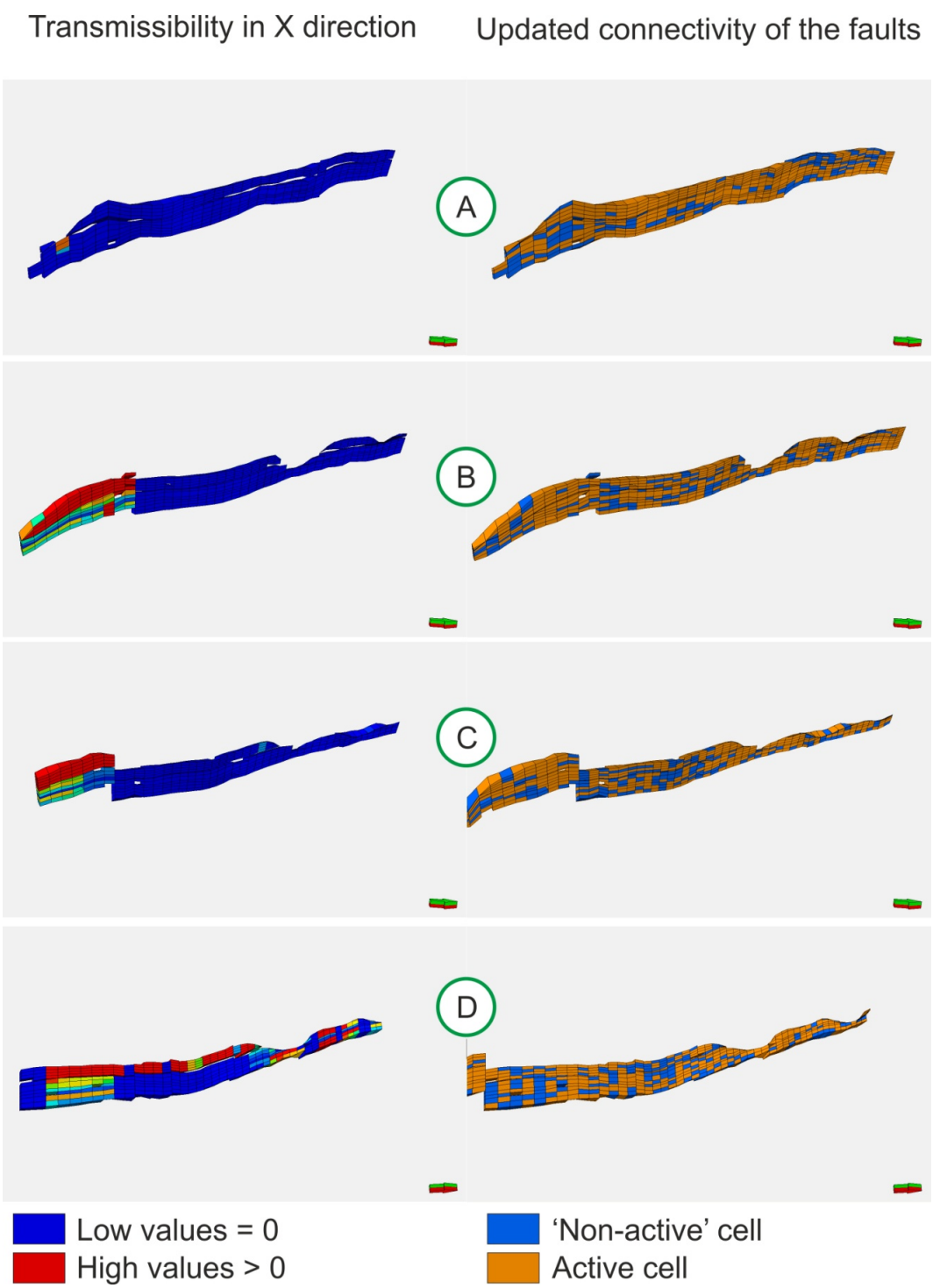

Figure 5.28 Comparison of the fault planes. Left: initial transmissibility values, dark blue indicates zero transmissibility, with no fluid flow through these cells; right: cluster technique result showing active cells (reservoir)in orange, and 'non-active' cells (non-reservoir); here there is no fluid flow, as well.

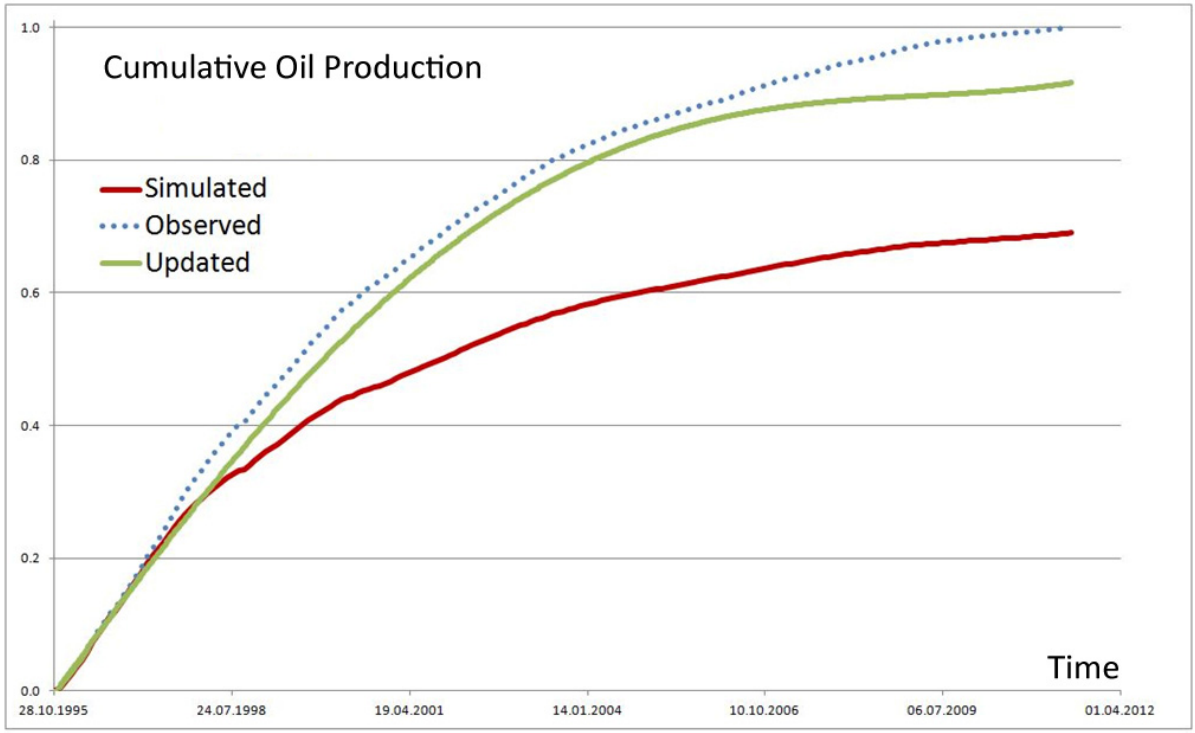

Figure 5.29 History matching results comparison. The blue dotted line indicates the observed data for cumulative oil production; the red line indicates cumulative oil production for the base case simulation model, the green line indicates the update only for the shales (non-active cells) in the model (only one cluster).

Figure 5.29 illustrates changes in matching of cumulative oil production after update of the non-active cells in the model. Significant improvements can be observed.

5.6 Conclusion

The main benefit of utilising time-lapse seismic data in history matching is to get a distribution of the fluid front movement in the reservoir with all related compartments. Stratigraphic or lithological or even structural compartments can be analysed using the proposed method and directly integrated into the simulation model, which significantly reduces history matching time and provides additional information regarding reservoir architecture and fluid flow patterns. This material in this chapter proves the ability of the model to integrate 4D data for fault transmissibility updates in the same manner as this was done for stratigraphic compartments, as presented in Chapter 4. The special benefit is a full specification of fault plane transmissibility in 3D space. The method can be extremely useful

for reservoir management, as it provides an understanding of the drainage patterns of the field and the effect of fault presence on the flood pattern.

Chapter Six

Synergy with Existing ETLP Methods for reducing uncertainties.

This chapter shows all the uncertainty related to the proposed method. In order to reduce the effect of uncertainty on the connectivity assessment, it is better to integrate few methods of estimation. In the framework of the ETLP (Edinburgh Time Lapse Project), two methods for connectivity estimation already exist- Well2Seis and Seis2Seis. In addition, a technique for estimation of fault transmissibilities is presented as a part of ETLP toolbox. Their methodology is briefly described, compared and new modifications of their techniques will be presented.

6.1 Uncertainty in history matching

Uncertainty is "lack of assurance about the truth of a statement or about the exact magnitude of an unknown measurement or number" (Olea 1991). Uncertainty is actually related to all the reservoir properties, to different degrees. Uncertainty (of a particular) parameter comes from the degree of accuracy of measurements of this parameter or from the inability to make direct measurements. Indeed all reservoir parameters affect fluid flow and matching, but not all of them are significant. Let us consider the main uncertainties which are related to history matching and 4D data.

1. In the geophysical domain there are uncertainties linked to acquisition, processing and interpretation (Vincent, Corre and Thore 1998):
    - Uncertainties in picking
    - Uncertainties in depth conversion
    - Uncertainties in migration
    - Uncertainties in well-tie
2. Usually, geological settings of the field is most uncertain parameter and is related to sedimentology concepts and seismic.
    - Uncertainties in gross rock volume (GRV)
    - Uncertainties in distribution, shape, and extension of the reservoir
    - Uncertainties in porosity, permeability and net to gross (NTG)
3. Uncertainties linked to parameters which mostly affect fluid flow such as relative permeability, fault transmissibilities, and the presence of baffles and barriers (transmissibility). (Corre, et al. 2000).
    - Kv/Kh ratio
    - Relative permeability
    - Capillary pressure
    - Fault sealing
    - Aquifer presence and strength
    - Transmissibility and connectivity (in simulation model)

Connectivity-related uncertainties are mostly associated with the geological setting of the field and especially with sedimentology.

Dynamic uncertainties are mostly related to 4D data. One of the most important uncertainties, uncertainty in petro-elastic modelling, will be covered in the following sections.

6.1.1 Uncertainties in petro-elastic modelling

The key process of the synthetic modelling process is the petro-elastic model. A correct PEM allows reservoir properties such as saturations, pore pressure and etc. to be transformed into rock elastic properties, and in such a way as to connect the seismic and engineering domains (see Figure 6.1).

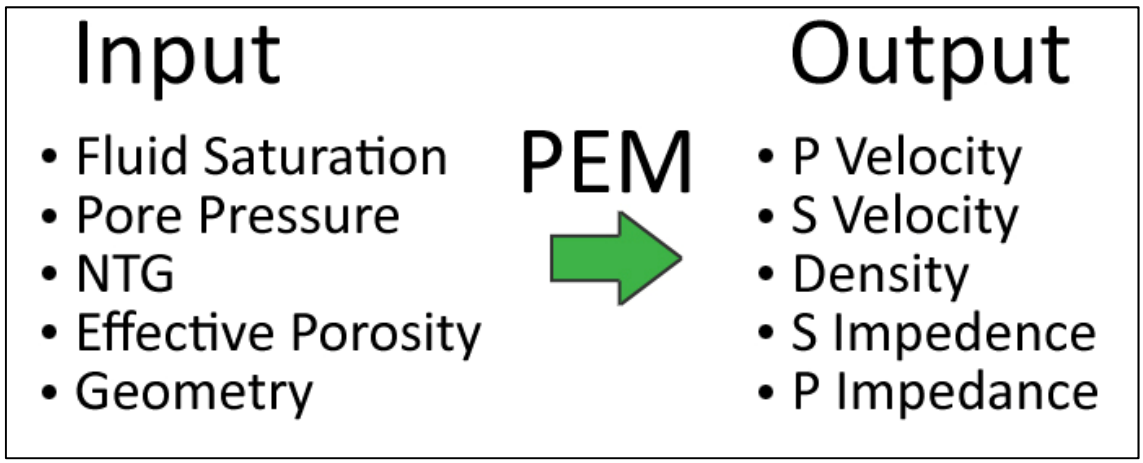

Figure 6.1 Input and output of petro-elastic modelling, which transforms reservoir properties into petro-elastic properties (adapted from (H. Amini, ETLP sponsormeeting 2009)). Input is from simulation model.

Basement for PEM is the Gassmann equation:

$$K_{sat} = K_{dry}(\sigma_{eff}) + \frac{\left(1 - \frac{K_{dry}(\sigma_{eff})}{K_0}\right)^2}{\frac{\varphi(\sigma_{eff})}{K_{fl}(T, P_f, C)} + \frac{(1-\varphi(\sigma_{eff}))}{K_0} + \frac{K_{dry}(\sigma_{eff})}{K_0^2}} \qquad (6.1)$$

where K_{sat} = the saturated bulk modulus, K_0 = the bulk modulus of the mineral matrix, K_{fl} = the bulk modulus of the pore fluid, K_{dry} = the bulk modulus of the porous rock frame, φ = porosity, P_f = average fluid pressure, T = reservoir temperature, σ_{eff} = effective stress and C

is a vector containing the fluid phase-specific parameters: API, salinity, solution gas/oil ratio.The complexity of this equation is obviously due to the number of parameters. Most of these need to be calibrated using additional data: reservoir rock elastic properties (K_{mineral}, mineral bulk modulus, K_{oil}, bulk modulus of oil, μ_{mineral}, rigidity of mineral, μ_{oil}, rigidity of oil). Calibration requires a sufficient number of efforts and this process is quite time consuming.

Most of these values are measured in the laboratory, and hence can be determined with rather good level of confidence, but these are not the exact in-situ values. Unfortunately, the effective stress on the rock, in-situ, cannot be measured or calculated independently. For its calculation, data from simulation is required, which comprises associated uncertainty. Another parameter requiring special awareness is fluid bulk modulus, $K_{fl,}$ due to its averaging method. Moreover, there are geological uncertainties related to PEM. Usually, the depositional environment characterising the field assumes few different facies associated with rock types, each of which has different rock properties. Hence, for Gassmann application, each rock type needs to be described and calibrated. The software used for PEM modeling and synthetic seismic model creation in this work was presented by Amini (2009). It allows to calibrate the set of parameters for each lithofacies using well log data. Fluid moduli at P_{fluid} converts to saturation law, then to the composite fluid modulus, which goes to the Gassmann equation along with the dry rock frame at P_{eff}, and then the saturated rock response is derived at P_{res} and fluids. To sum up, PEM computes the P and S impedances from a set of petrophysical parameters, using the most appropriate rock physics equations, and uncertainties can be estimated through PEM's ability to reconstruct the logs.

At this point the history matching process becomes more sophisticated, as we add the secondary domain of matching criteria, the seismic signature, as well as more time consuming and demanding of computer power. However, it gives a better convergence level and better understanding of reservoir performance, and finally reduces the associated uncertainties.

6.2 The effect of geological uncertainty on subsurface flow estimation

This section will cover the uncertainties related to fluid flow by application of the cluster technique or any of previously described methods, which involves the introduction of transmissibility multipliers into the history matching process.

The two fields examined in this project both have complex geological settings, but the nature of each is different: the compartments in the UKCS field are linked to the stratigraphy, whereas those in the Norwegian Sea field, in turn, are linked with its structural settings. In some extension different types of compartmentalisation can be considered as one phenomenon, some geological uncertainties affecting fluid flow. 'Some' in this case means the presence of barriers or baffles of any type: lithology, stratigraphy, faults etc.. So, all these types are the same for the proposed method of treating them and incorporating them into the simulation model for better history matching. It is better to discuss them stepwise, starting from the UKCS field and then the Norwegian Sea field case.

6.3 Example of a stratigraphy-controlled field: Analogue of the UKCS field.

The following section was presented as a part of the REM MSc project of Artem Kondratyev (HW, ASC at TPU, Tomsk, Russia).

There is a semi-synthetic study to estimate geological uncertainty in subsurface flow estimation and history matching. The sedimentological features of this particular field are rather similar to those in the UKCS field.

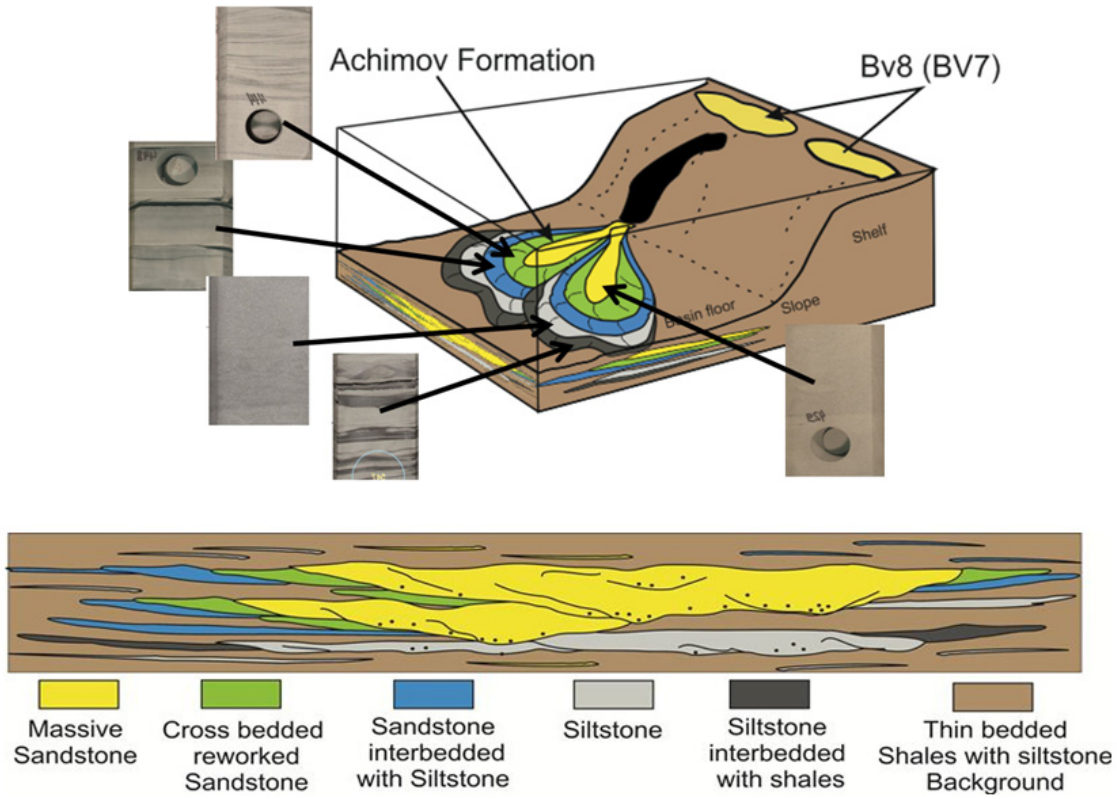

Figure 6.2 Analogue depositional environment: turbidities reservoir. V Field, Western Siberia. After Kondratev 2013.

For the basis of modelling, one of the Western Siberian field data was taken. Analysing typical core succession, 7 rock types were determined, 5 of which are reservoir and 2 are not.

The Achimov Formation of V Field is a complex system of amalgamated channelised lobes, where parts of this system are represented by the certain rock types associated with the structural elements: the axial part represented by massive fine grained sandstone (Rock Type 1), and the off-axis part composed of cross-bedded very fine grained sandstone (Rock Type 2); in the area further from the lobe axis very fine grained sandstone is present, interbedded with shales (Rock Type 3), and also distal deposits of the lobe include massive siltstone in the axial zone and siltstone interbedded with shales in the off-axis zone.

Rock Type 1. Medium grained sandstone with shale cement chlorite and kaolinite of pore-film type.

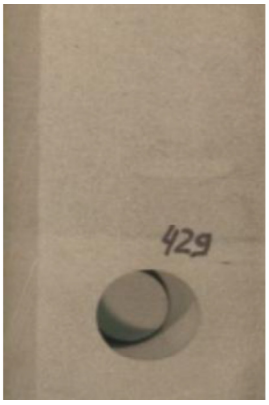

Porosity range, %	k range, mD	Swi	k_v/k_h ratio	Grain size, mm	Sorting	Bedding style
16 - 22 Average 19	4 - 76 Average 15	0.5	0.8	0.13	1.65	Structureless

Rock Type 2. Medium-fine grained sandstone with shale cement chlorite and kaolinite of pore-film type.

Porosity range, %	k range, mD	Swi	k_v/k_h ratio	Grain size, mm	Sorting	Bedding style
3 - 20 Average 17	0.02 – 6.74 Average 2.98	0.58	0.72	0.11	1.49	Planar or cross laminated

Rock Type 3. Very-fine grained sandstone with shale cement chlorite and kaolinite of pore-film type.

Porosity range, %	k range, mD	Swi	k_v/k_h ratio	Grain size, mm	Sorting	Bedding style
6 - 19 Average 16	0.02 – 2.23 Average 0.85	0.75	0.48	0.11	1.46	Cross laminated lenticular bedding

Rock Type 4. Siltstone with shale cement chlorite and kaolinite of pore-film type.

Porosity range, %	k range, mD	Swi	k_v/k_h ratio	Grain size, mm	Sorting	Bedding style
9 - 20 Average 17	0.4 – 8.5 Average 3	0.59	0.51	0.09	1.46	Structureless

Rock Type 5. Siltstone with shale cement chlorite and kaolinite of pore-film type.

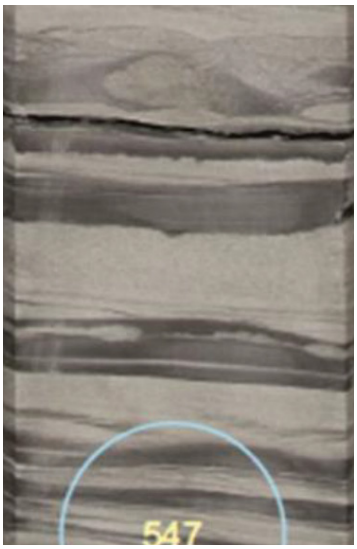

Porosity range, %	k range, mD	Swi	k_v/k_h ratio	Grain size, mm	Sorting	Bedding style
6 - 20 Average 15	0.03 – 8.47 Average 1.42	0.73	0.3	0.08	1.48	Planar or cross laminated

Figure 6.3 Typical rock types in turbidite system.

Usually rock types within the model are distributed using the Sequential Indicator Simulation algorithm of pixel modeling. The first type of model represents a simple case consisting of reservoir and non-reservoir units that is the simplest approach to turbidite depositional system modelling. The model of the second type includes rock types, where the two rock types are non-reservoir and correspond to tight rocks and thin bedded shales and siltstone. In the third type of model, shales and tight rocks were assigned as discrete bodies with the correlation range equal to 100m, representing the case when zones of carbonatisation are

locally developed, whereas shales have a small length. In the fourth type of model; shales and tight rocks have a correlation range equal to 2500m; these bodies are laterally extensive, and that also is a probable scenario. The fifth type is based on a model with extensive non-reservoir rocks: transmissibility between rock types was changed to 0.1, which represents a thin layer of shale material that is a baffle to flow. Conceptual schemes of each model are represented in Figure 6.4.

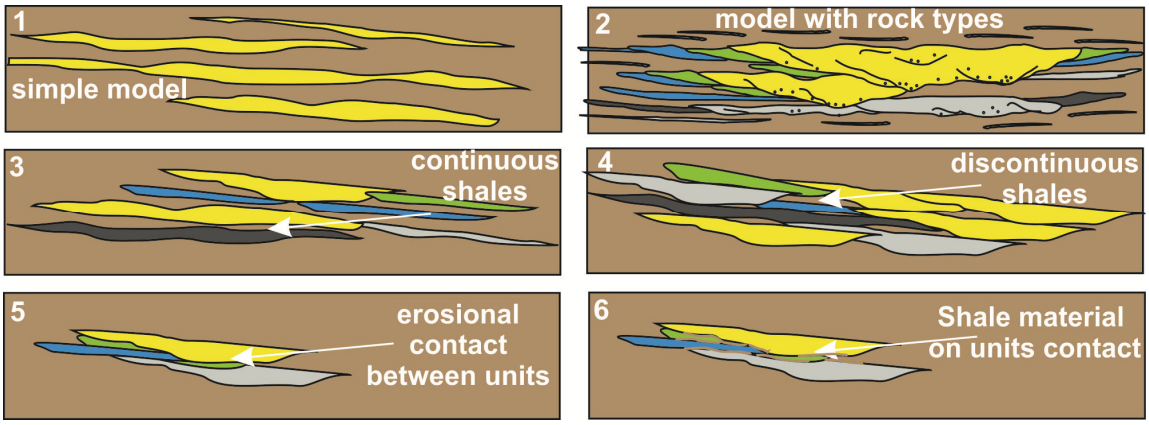

Figure 6.4 – Types of models constructed for simulation

In Figure 6.5 A simulation results of the first and second type of models are compared. Cumulative production in the case of the simple model is higher in 70,000 m^3, which is associated with the absence within the reservoir heterogeneity related to the reservoir architecture, while the prognosis based on the model comprising the full set of submarine fan depositional elements that are represented by the rock types gives more pessimistic results, which are more realistic. In the next Figure 6.5 B, models of the third and fourth types are compared. From the plot of cumulative production, it can be seen that, for the model with continuous shales and tight rocks, production is higher in 40,000m^3. As a result of the presence of the significant amount of small scale heterogeneities prevents subsurface fluid flow that in turn leads to heterogeneity incensement and related with production decreasing.

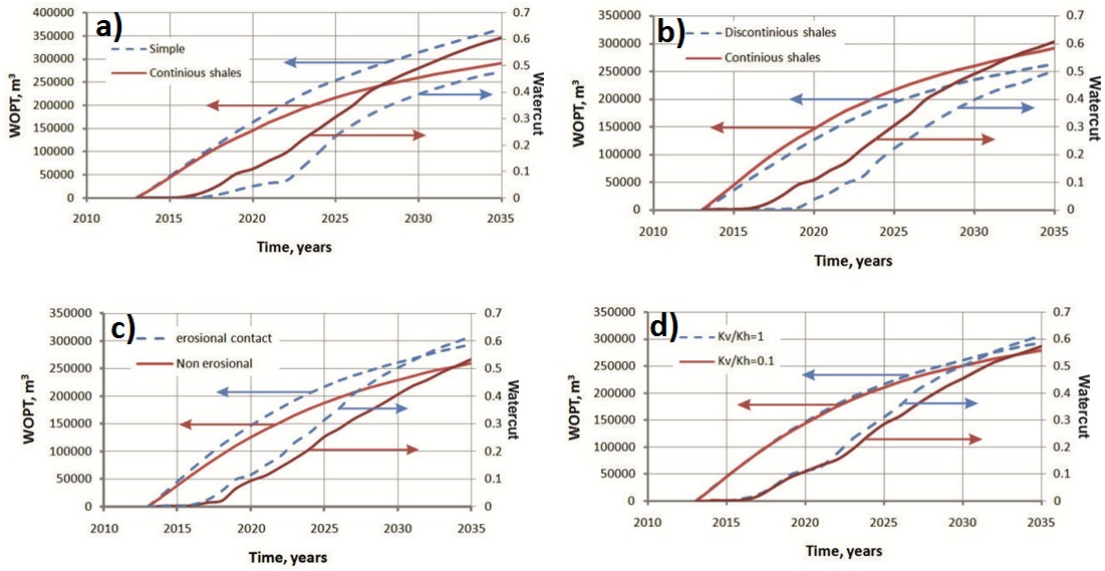

Figure 6.5 Simulation results showing the effect of geology on the simulation results

The presence of laterally extensive units leads to reservoir homogenization, and the result it is seen in the production increment, but due to early breakthrough, the production rates subsequently begin as the same. Figure 6.5 D represents the calculation results of the model where coefficient of permeability anisotropy has been varied from 0.1 to 1, which represents extreme cases. Cumulative production for the case with high Kv/Kh is 20,000m^3 less than that related to vertical permeability restraint. Initially, the difference in rates is not so high, even if water breakthrough occurs simultaneously; the rate of water cut for the case when Kv/Kh=1 is higher, which is related with higher production rates. Figure 6.5 C represents the results of the calculation of the second and fifth type of models. Cumulative production for the case where there are erosional boundaries between the rock types is higher in 45,000m^3. The occurrence of such contacts may be related to the erosion of rock types by the Rock Type 1 that is associated with the channel axis. Thus, as the result of erosion, an increase in transmissibility occurs between the units, which, in turn leads to higher production.

The effect of transmissibility between the rock types on the effectiveness of water flooding was further analysed. Figure 6.6 shows the slice of the geologic model which represents the distribution of rock types and oil saturation for the cases with various units of transmissibility. In the first case, propagation of the displacement front within the unit occurs more easily than between the units. As can be seen in Figure 10, displacement in Rock Type 1, corresponding to the channel axis, is more effective, whereas in rock type 2, it is less effective, as it has poorer reservoir qualities, and the lowest results are for the region of Rock

Type 3. It must be said that, with the reduction in transmissibility between the units, the spatial organisation of the units becomes more significant. In addition, erosion leads to an evenly distributed displacement front and more symmetrical saturation distribution within the element of development.

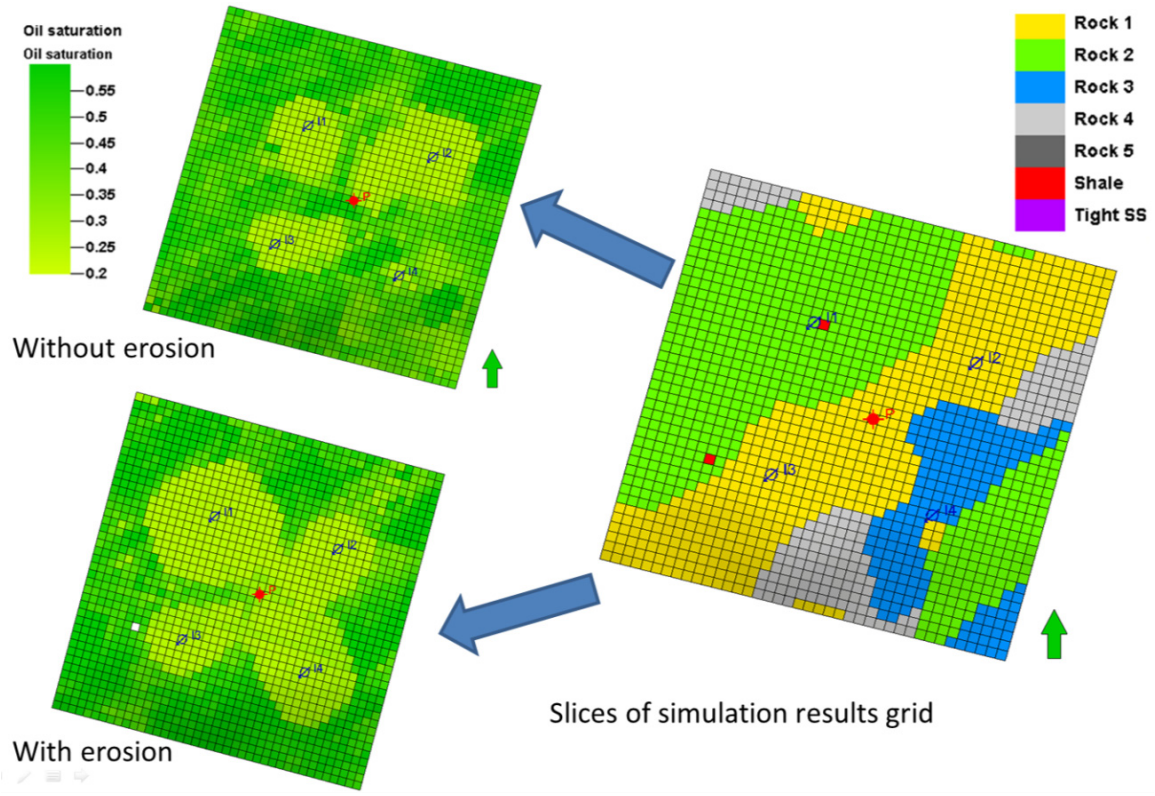

Figure 6.6 Slices of models where the distribution of oil saturation is represented: in the case without erosion (a) and with erosion (b)

6.3.1 Relation between Seis2Seis and Well2Seis

In this section, an analysis of existing methods for connectivity estimation using 4D seismic data will be presented. Then results and relationships of two techniques, Seis2Seis and Well2Seis, will be compared. Both methods were presented by Yi Huang in the framework of ETLP (Edinburgh Time Lapse Project) (Huang and MacBeth, 2009). It is necessary to say that these techniques give very valuable results and are very easy and fast to implement. However, a limitation exists, in that only one well can be analysed per iteration (run), but it is not insufficient.

The following topics will be covered in this section.

1. Well2Seis (2D, based on seismic attribute maps).
2. Well2Seis (3D, based on attributes in the simulation grid, which are 'enhanced'). This is an improved variant of the 2D technique for the 3D space.
3. Seis2Seis (2D, based on seismic maps).
4. Industry approach. This method was utilised in the UKCS field model. It was analysed in the previous section.
5. Cluster method (dynamic connectivity estimation): this will be presented as a consistent evolution (development) of previous Well2Seis techniques.

Actually all these methods can be utilised simultaneously for cross validation of results.

The description and comparison of the techniques will be implemented on a part of the field (see Figure 6.7). This is the most problematic area for localisation of baffles and barriers. The simulation model production data of P2 are presented in Figure 6.8. Well P2 has the same problem: lack of water production (see Figure 4.16). There is no active aquifer in this area and OWC, so the only water that can be produced is injected water.

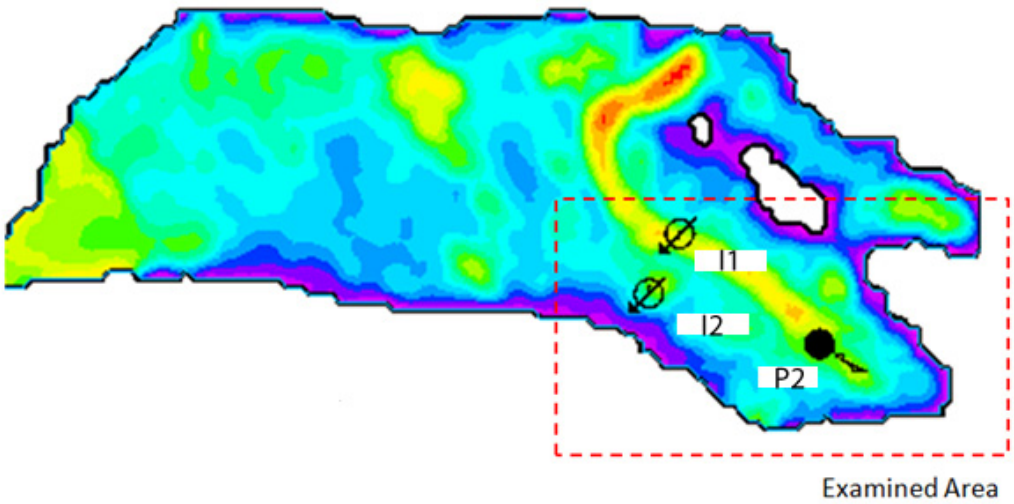

Figure 6.7 NTG map. Examined area with wells.

The NTG map in Figure 6.7 shows higher values in the channel area and it is easy to assume that the produced water in P2 has been previously injected in I1, rather than I2. History matching for this well was not really successful using traditional techniques. Detailed

geological features and the setting, as well as applicability of the techniques mentioned will be covered in the following sections.

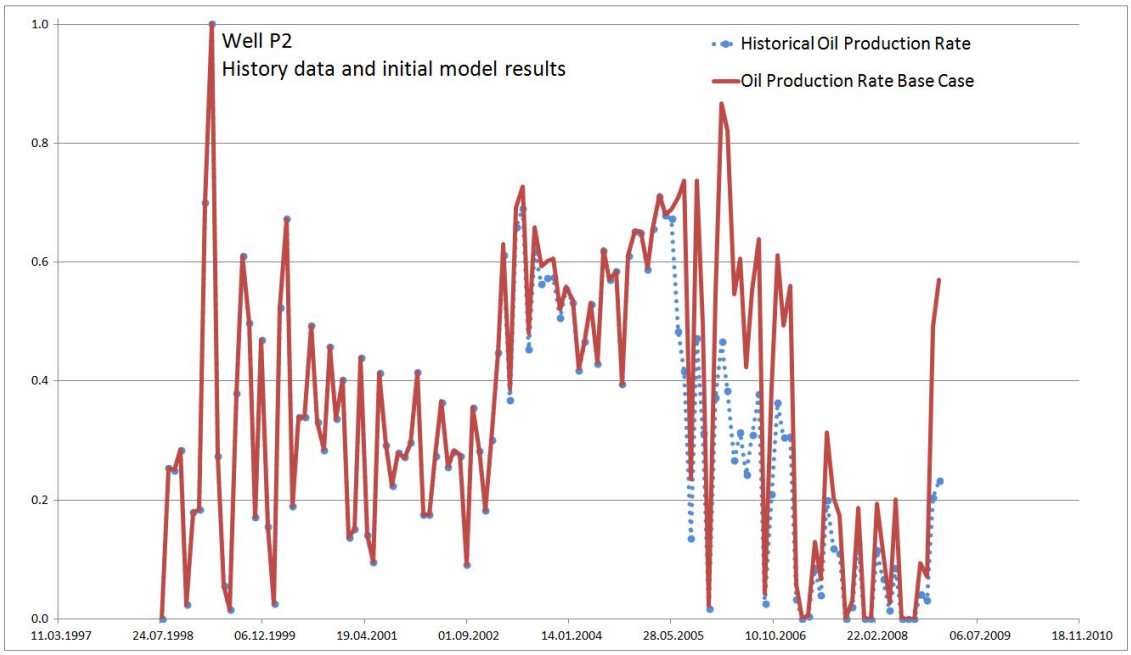

Figure 6.8 Well P2 history data. Well oil production rate in simulation model (red curve) differs sufficiently from observed production data (blue dotted curve).

I now compare all the available methods for connectivity estimation, in order to perform well P2 tuning using time-lapse data.

6.3.2 Well-2-Seis based on 2D attribute maps.

Well2Seis is a technology for well production data correlation with time-lapse seismic surveys.

If there are multiple surveys over the same location of the reservoir, a number of difference maps can be generated for all the combinations between each pair of surveys. These are either the differences between baseline survey and monitors or between different monitor surveys. If we put these difference maps in any order, we will have seismic difference values in a time sequence with a number of steps. The cumulative production or injection volumes over time intervals corresponding to seismic surveys can also be calculated for individual wells or for a group of them. These values can also establish another time sequence. Putting

these two sequences together, the correlation coefficient can be calculated. This value is then allocated to the pixel location where the seismic sequence is extracted. Once the same calculation is done for every location, a map of normalised cross correlation between 4D differences and well production volume can be generated for each well. I have utilised a traditional approach based completely on Yi Huang's work. (Huang and MacBeth, 2009), for which the workflow is presented in Figure 6.9. At the centre of this method is the construction of the time sequences of volume rates and 4D signatures for all possible time intervals (Huang and MacBeth, Direct correlation of 4D seismic and well activity for dynamic reservoir interpretation. 2009). A more or less similar methodology has been discussed in Chapter 3. Firstly, sequences of seismic differences are generated from multiple seismic attribute maps for the all possible pairs of surveys. For *n* surveys there are *(n(n-1))/2* combinations of differences. The second step of the method is calculation of sequences of cumulative volumes from production data. The last but most important step is calculation of Normalised Correlation Coefficients (NCC).

According to Huang, the time sequence vector of 4D signatures $(\Delta A_1, \Delta A_2, \Delta A_3, ..., \Delta A_P)$ for each seismic bin location (x,y) is separately linked to the corresponding sequence of cumulative volumes $(\Delta V_1, \Delta V_2, \Delta V_3, ..., \Delta V_P)$ for a connected well group by calculating the *normalised cross-correlation* (NCC) statistic using following equation (Bevington, 1975).

$$NCC = \frac{\sum_{k=1}^{P} (\Delta A_k - \overline{\Delta A})(\Delta V_k - \overline{\Delta V})}{\sqrt{\sum_{k=1}^{P} (\Delta A_k - \overline{\Delta A})(\Delta A_k - \overline{\Delta A})} \sqrt{\sum_{k=1}^{P} (\Delta V_k - \overline{\Delta V})(\Delta V_k - \overline{\Delta V})}} \tag{6.2}$$

The following part is explained the sense of the method proposed by Yi Huang.

The metric for *NCC* is that '1' indicates a perfect correlation and '-1' a perfectly opposite correlation. The sign assigned to the fluid volumes that constitute a well signature $\{\Delta V_k = \Delta V(x, y, \Delta T_k), k = 1, P\}$ is determined by the polarity of the resulting seismic responses. For instance, a particular water injection well can possibly produce two dynamic changes within its neighbourhood, which result in two opposite effects on rock compressibility – a 'softening' effect caused by pressure increase and a 'hardening' effect due to water saturation increase. Depending on the selected seismic attribute, the softening (or hardening) effect may be represented by either an increase or decrease in values of the

selected attribute. Consider a seismic attribute: a positive change indicates reservoir softening, and negative changes correspond to reservoir hardening. This operation aims to eliminate negative correlation coefficients, so that we can only focus on positive correlation coefficients from 0 to 1. A good well-to-seismic correlation implies that seismic changes occurring at (x, y) over time are very likely to be related to the activity of the well being correlated. The correlation procedure can be performed at each bin location (x,y), producing a map of *NCC* across the region of interest. When mapped, the *NCC* becomes a new seismic attribute with the same resolution as the seismic. More repeat surveys or alterations in well rate lead to an increasingly complicated and finer scale time sequence, hence increasing the statistical robustness of the normalised cross-correlation measure. To ensure stability, a minimum credibility threshold is needed for the *NCC* maps, as, for a particular size of time sequence, the cross-correlation coefficient is only statistically significant above a certain coefficient value. Below this threshold there is a chance that samples drawn at random can yield the same coefficient (Bevington, 1975).

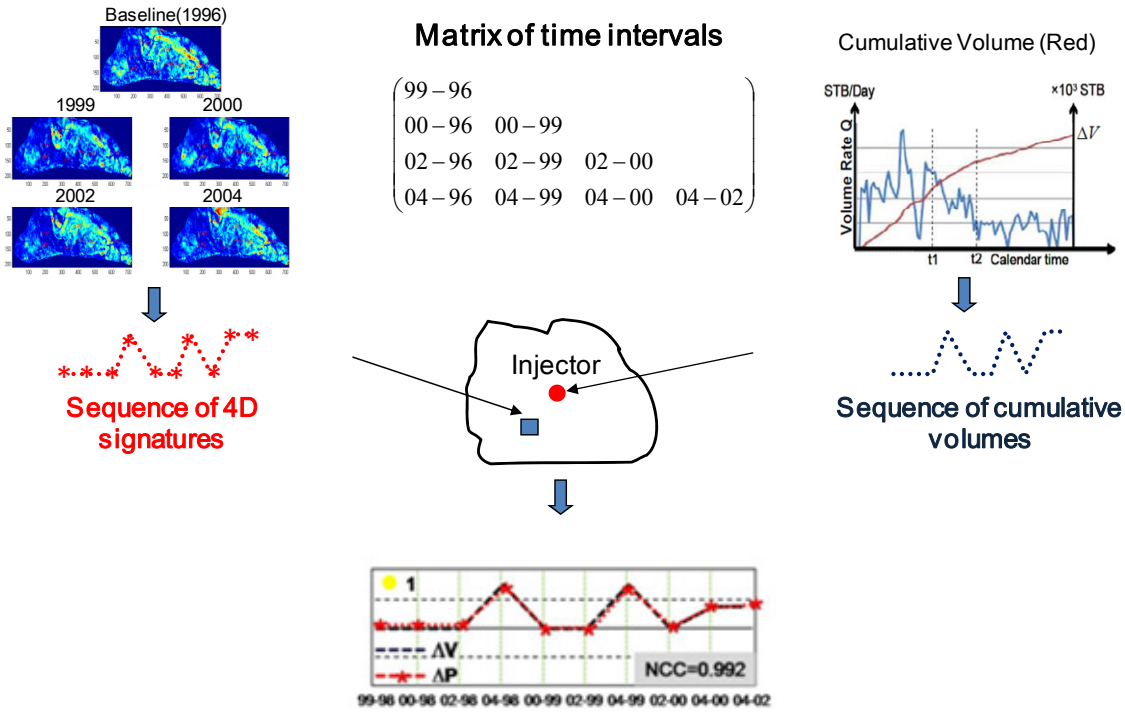

Figure 6.9 Sense of Well2Seis method. Direct Correlation between 4D seismic change and well activities. (Huang, MacBeth and Barkved, et al. 2010)

Well2Seis technique was applied to each of the wells in turn (well I2, I1 and P2), as shown in Figure 6.10, left hand side. Then derived results were united- right hand side. Unfortunately, analysing these results, we cannot draw any conclusions about connectivity among injectors I1, I2 and producer P2, as there are no clear channels between them (just one in the south, but we cannot be sure about this, as there is too low a response), but actually, we know that somewhere in this area a pathway exists, based on production data. The reason for this is the averaging of the reservoir response during attribute calculations. So, although the method cannot produce reliable results, but these uncertainties are clear and understandable and thus can be managed.

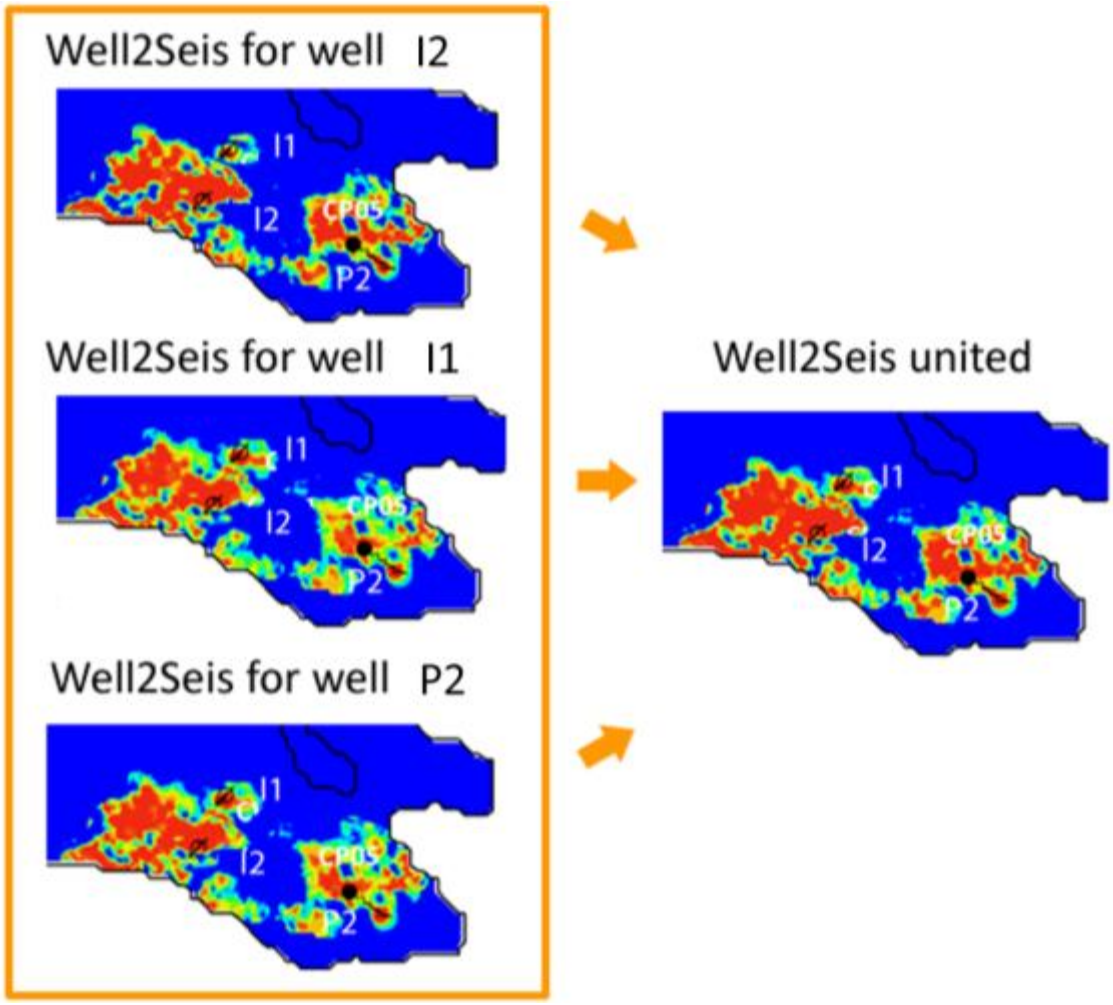

Figure 6.10 Well2Seis 2D results for each well, and overlapped

There is as additional source of uncertainty: well trajectory. Usually, in other fields there will be both vertical and horizontal wells, and horizontal wells sometimes have a complex trajectory. The nature of the method tells us to average the well activity into one point (or

pixel). This works perfectly for vertical or slightly inclined wells (see Figure 6.11). The side view represents simulation model cells with any property (which may even be seismic upscaled into the simulation grid) penetrated by the vertical well. Each of these cells contains a value of the particular property, let it be seismic amplitude, for instance. What will happen if we apply the 2D method? All the values will be averaged into one particular location, well location, in this case (see right hand side of Figure 6.11). We can then compare this value with other map locations.

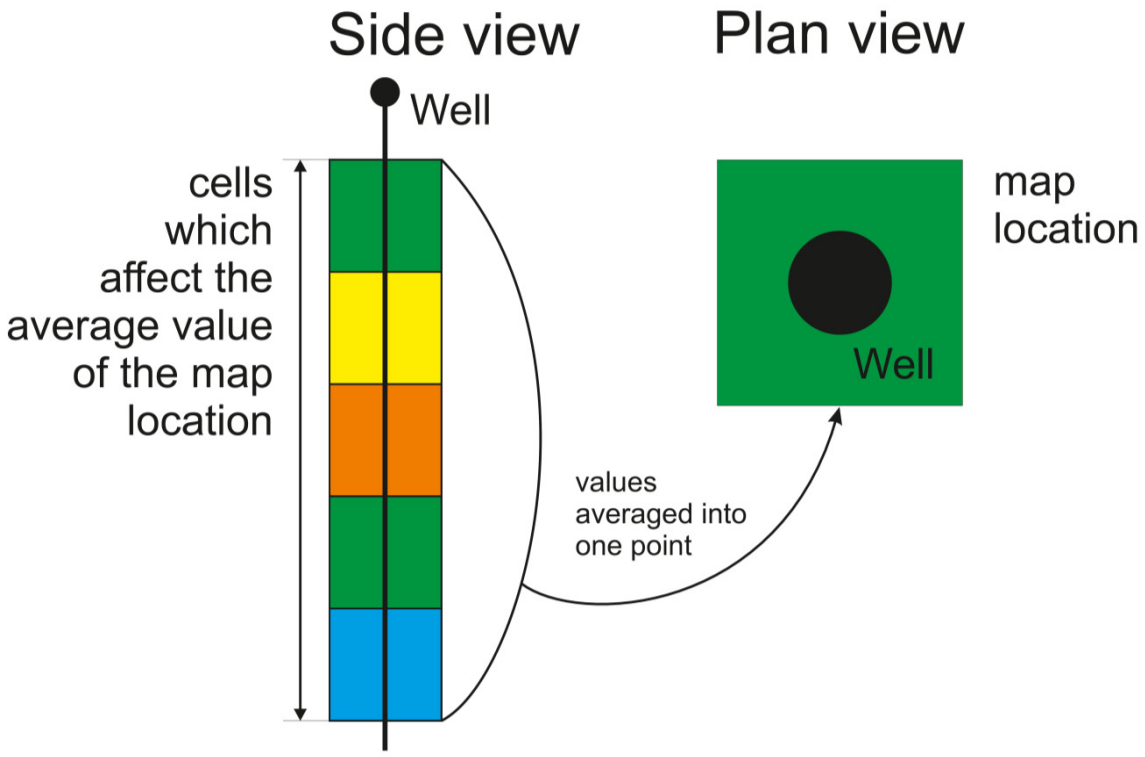

Figure 6.11 Signal averaging along the vertical well. Side view represents simulation model cells with any property (may even be seismic upscaled into simulation grid) penetrated by the vertical well. Each of these cells contains a value of the particular property. Plan view- wellhead with corresponding map location with an averaged property value in it.

However, this is not the best option for horizontal wells. The problem is depicted in Figure 6.12. The well penetrates the second layer of the model. Each cell's values column, numbered from 1 to 5, will be averaged into a particular map location, presented on the right hand side of the figure. So, in this case, it will not be quite right to compare the well signals just from one point, we need at least five.

However, the level of this uncertainty will depend on seismic bin size; for example, if it is 25x25 and horizontal well length is 500m, so we can get an array of 20 points.

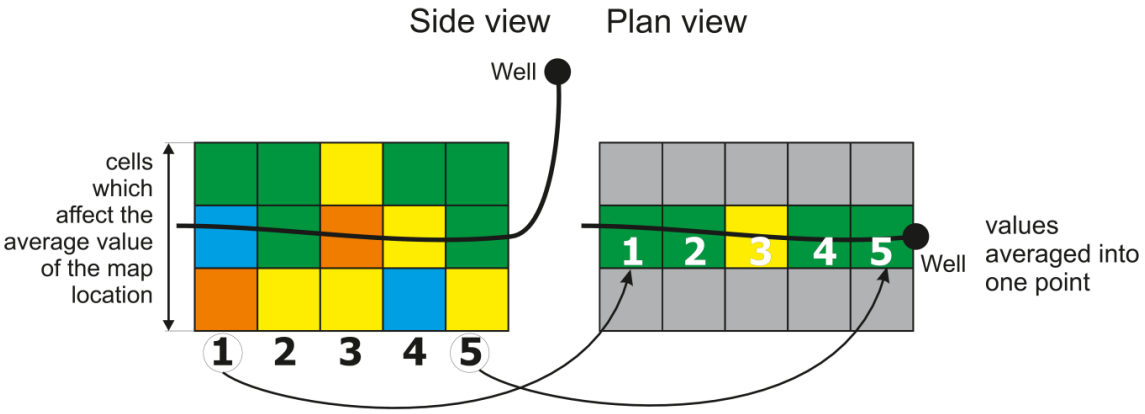

Figure 6.12 Signal averaging along horizontal well. Averaging of such wells' seismic signatures can be incorrect.

Huang's work consisted of several real field examples on which the method was tested and the following conclusions, according to Huang, can be drawn:

Compared to the traditional approaches based on visual correlation or modelling techniques, this approach can achieve the integration of these two data types directly within the data domain. In order for the proposed technique to succeed, several conditions must be met. Firstly, the field must be surveyed by multiple surveys, and, in particular, enough surveys for the well to seismic cross-correlations to be significant. All of these conclusions are valid for other methods described in this chapter.

The following is unique to the Well2Seis method: if connected regions/compartments/geobodies around individual wells are to be highlighted, these wells must also possess distinctly different well rates, such that the correlation coefficient between the well and the 4D signatures is higher than the well-to-well correlation. These conclusions are also confirmed by their tests in this thesis. This method was originally developed only for analysing 2D map sequences. It is actually a balanced decision, it can be explained by the fact- 4D data is usually utilised in map domain. Nevertheless, questions arise- is it possible to apply the method in 3D space? What will the results look like? Will there be a convergence between 2D and 3D results? Could we get additional data from this analysis? Is it time consuming? What will it give us in terms of reservoir understanding?

6.3.3 Well2Seis: 3D approach.

Preparation and discussions on uncertainty

Before answering these questions, it was necessary to make some preparations and modifications for the method. Initially, seismic cubes were transferred into the simulation model domain (details of the process are discussed in 3.2.2:'Upscaling' the seismic). Three reference points were then picked in the vicinity of each well, and the method was applied for these points. Actually, the points were treated as signal sources, but here we are faced with a very specific uncertainty, valid only for the 3D case: wells are not 2D, they have a 3D trajectory and volume where they intersect with the reservoir, and each relatively small part of it has different inflow behaviour, especially for horizontal wells. Hence, we lose some accuracy in the calculation, because we use only a point instead of an array of them, but the sense of the method does not allow the use of an array of points.

Sense and calculation schemes comparison of the 2D and 3D modification is presented in Figure 6.13.

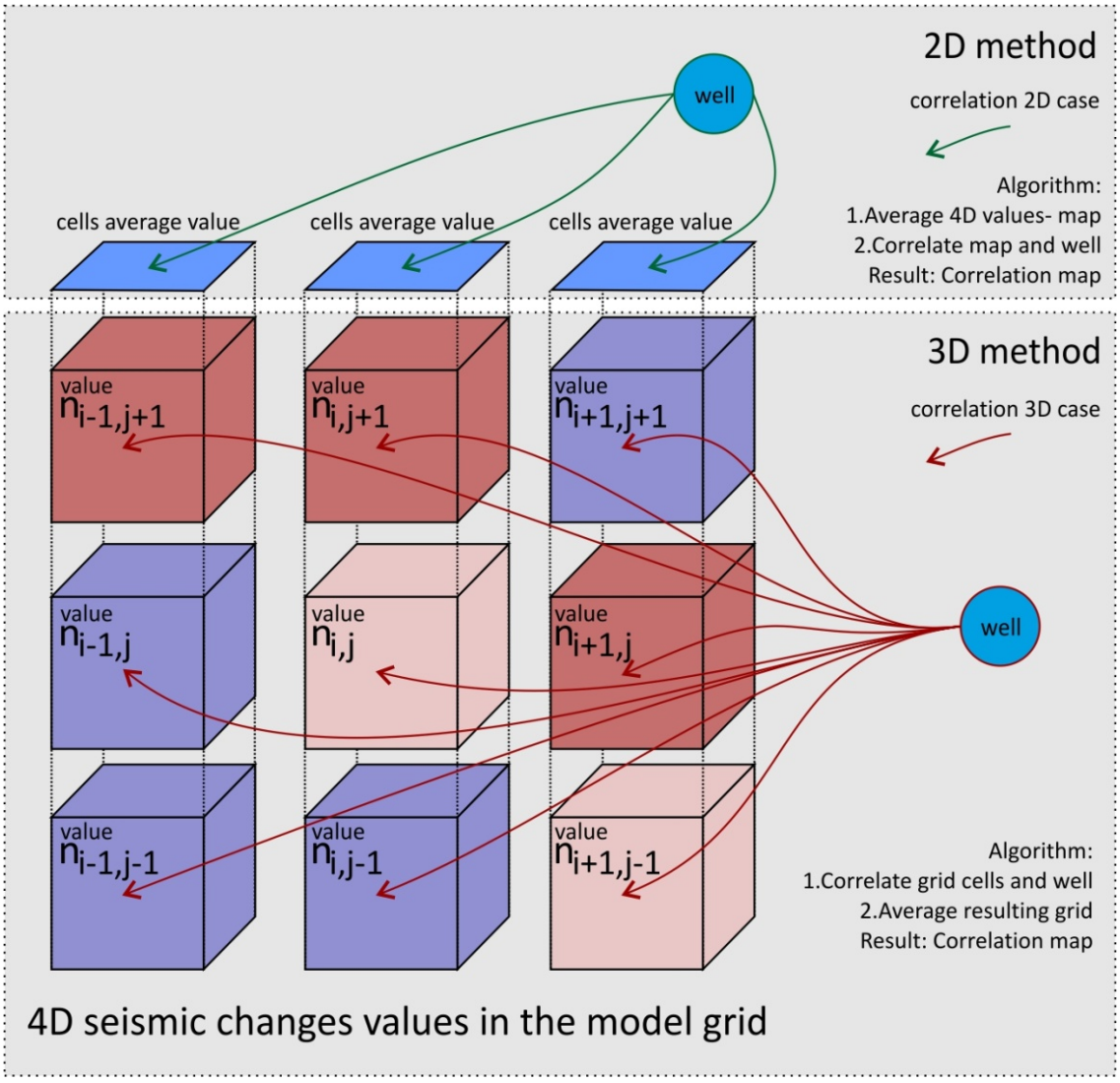

Figure 6.13 Well-to-Seis 2D and 3D modification algorithms. The 2D method correlates well value with average 4D map. This 3D modification instead uses the initial average of the seismic signal, compares well signal with each cell of the grid and only then averages the results into the 2D map.

After the calculations, we obtain three cell arrays in 3D space; each of these arrays reflects the reservoir parts connected to the corresponding well. Next, the average map was constructed (see Figure 6.14, left-hand side; on the right-hand side are the results of 2D modification). Analysing the results, it becomes obvious that these three wells are connected by a channel between I1 and P2 (Figure 4.14), which is also correlated with the sand-rich body in the NTG map. Although vertical resolution of the seismic data is not perfect, it still allows us to see changes in the reservoir. The results are presented in map view, in order to make it more comparable with previous results.

Here we need to note that the results of 3D modification can be represented in a 3D grid, each cell of which will contain the NCC value.

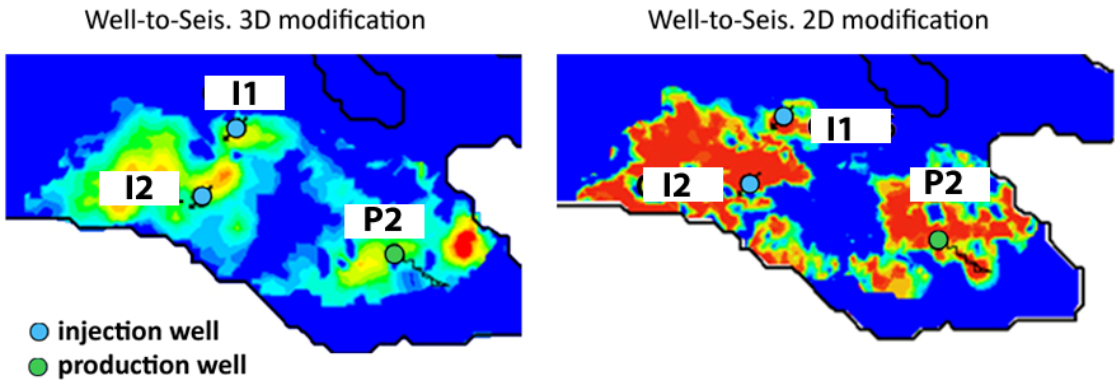

Figure 6.14 Comparison between W2S 2D and W2S 3D. Dark blue: NCC lower than 80%.

To sum up, the developed 3D modification of the Well-to-Seis method is more reliable and provides more precise connectivity estimation. If we see a more or less absolute value in the 2D modification, connected or not, in 3D it is possible to highlight better connectivity and lower values.

6.3.4 Seis2Seis

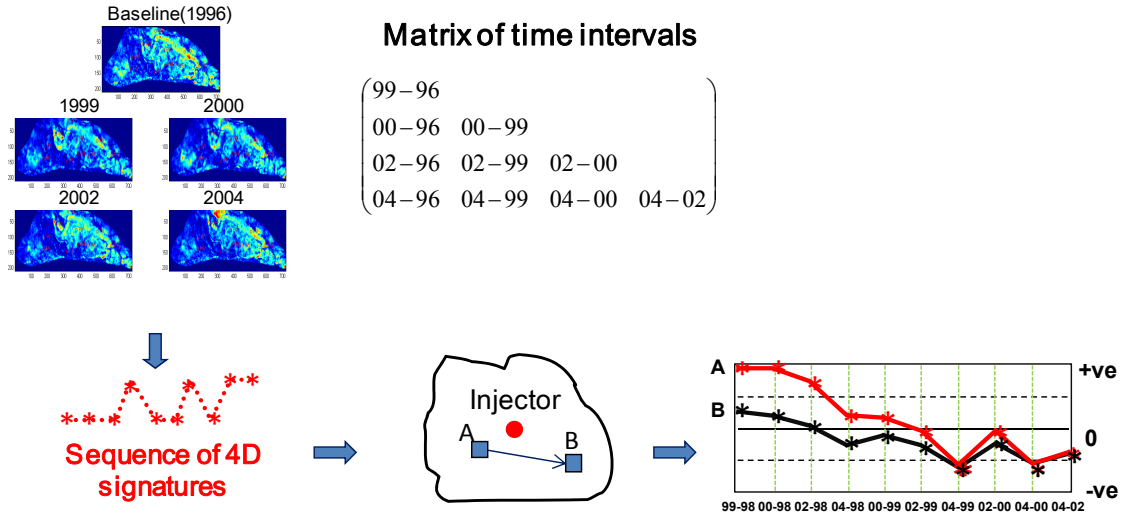

Figure 6.15 Seis2Seis workflow

A method proposed by Floricich (2008) delineated subtle reservoir barriers that were undetected in 3D seismic interpretation by analysing the temporal behaviour of 4D signatures through production time. It is possible to correlate sequences of 4D changes, $A_k = \Delta A(x_i, y_i, \Delta T_{k=1\ldots n})$, to a reference sequence derived from 4D seismic changes at a fixed (reference) location $A_{ref} = \Delta A(x_{ref}, y_{ref}, \Delta T_{k=1\ldots n})$. Preferentially, the reference location is selected close to the well under study, as it is our interest to know the connected reservoir bodies controlled by this particular well (Huang and MacBeth, Direct correlation of 4D seismic and well activity for dynamic reservoir interpretation. 2009).

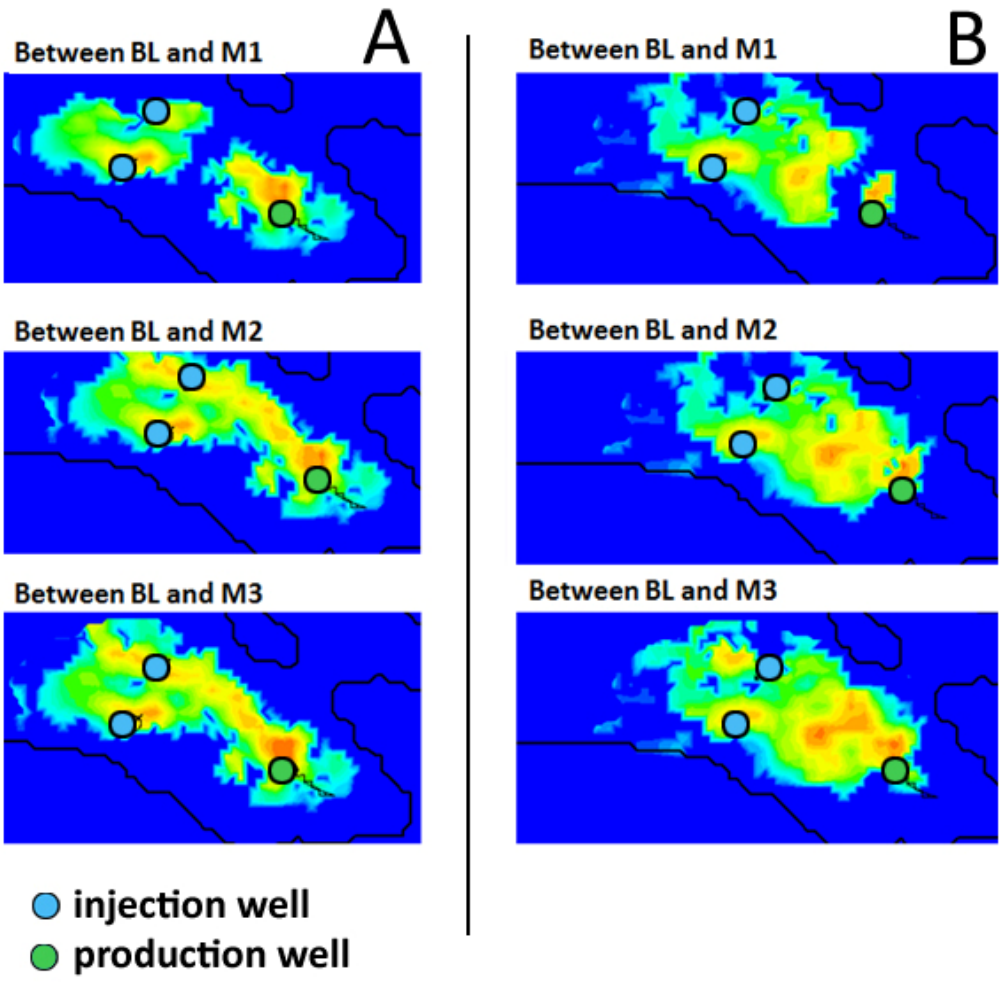

Figure 6.16 Seis2Seis results. Left side (A): 2D case, right side (B): 3D case. Different pairs of surveys are presented. Blue colour indicates absence of connectivity. Production well P2, injection: I1 and I2.

The idea behind implementation of 2D and 3D modifications is exactly the same as in Well2Seis. The results are presented in Figure 6.16, where different pairs of surveys are presented. Connectivity patterns are different, depending on the modification applied. In this

particular case, 3D modification did not produce reliable results; they are not comparable to the 2D and NTG map of the reservoir. The NTG and 2D results have a good correlation between each other.

6.3.5 Cluster Analysis

To estimate the proposed new method, I need to compare all the methods analysed above with the new one. I will start from connectivity evaluation, using the clustering approach. I will consider the same reservoir part as in the previous example for Well2Seis and Seis2Seis. Cluster analysis is a more complex cross-correlation technique. It is 3D-based, and the results can be used directly in the simulation grid. This allows better understanding of fluid paths and patterns and rapid control of the NTG property. To evaluate the results of the different methods, I need to present all of them in 2D map views. Let us have a look sequentially at the reservoir changes: between monitor 1 and baseline, monitor 2 and monitor 1 and finally monitor 3 and monitor 2. Each of these differences bring additional information about connectivity and highlights the areas of injection/production barriers within geobodies. New highlighted areas are located to the south on the channel.

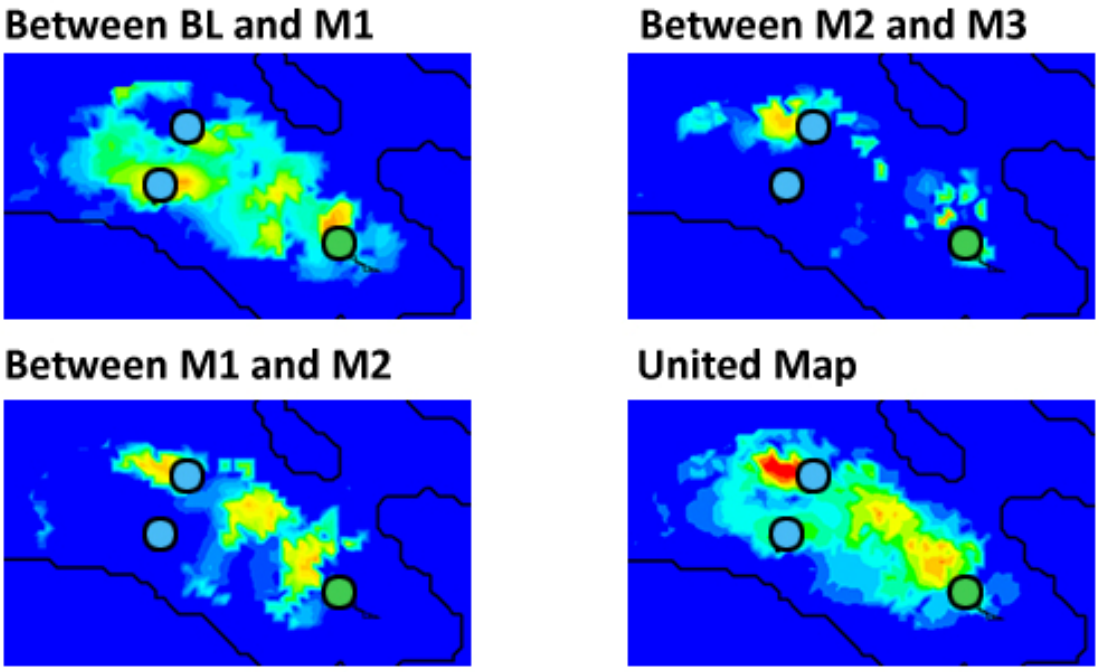

Figure 6.17 Results of cluster connectivity analysis. Production well P2, injection I1 and I2

These results are more aligned with the Well2Seis results, due to the nature of the methods. All of these methods evaluate the same reservoir property, but from slightly different points. Their results are comparable and, on analysis, a sound sequence of improvements in the results can be observed: well2seis 2D, then well2seis 3D, then clusters.

Analysing results of this technique, it is possible to highlight areas with better connectivity and to use these maps in matching in any desirable form, visual or even quantitative, as a trend for connectivity or NTG in geomodelling or as a transmissibility multiplier for simulation modeling. At this point I have a well-established 'workflow' for the understanding of connectivity from technique to technique. In addition, I have presented some ideas on how these data can be utilised in model updating, without any detailed description of this procedure, so far.

6.3.6 Results comparison

In this section I will compare the results of connectivity analysis by the existing and proposed methods. All the results are presented in Figure 6.18. It can be seen that some of the maps

do not correspond with each other. For example, the north channel between well I1 and P2 (easily seen on the NTG map) can be observed on every picture, but with different intensity- Well2Seis 3D captures it only very little. However, the north part of the reservoir is not captured by Seis2Seis 2D, whereas any other methods show this feature quite nicely. The main pathway for fluids (oil or water) is the channel, but some part of the water goes through the south part of the reservoir facies. Unfortunately, due to visualisation issues, it is not trivial to show this situation in 3D space. Indeed, the south part is located lower than the main channel and is hardly connected to the main channel.

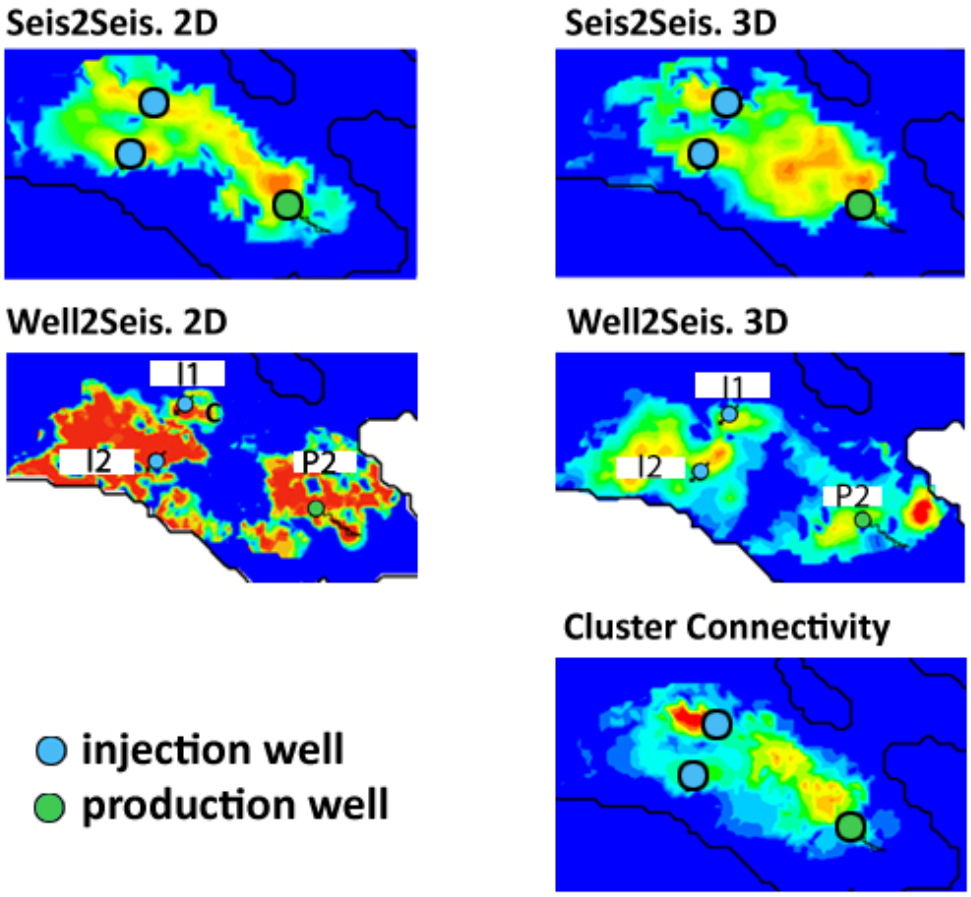

Figure 6.18 Comparison of different methods. Right column: Seis2Seis and Well2Seis 2D modifications; left column: 3D modifications of Seis2Seis. Well2Seis and Cluster analysis results.

6.4 Structurally controlled field example

There is at least one technique for 4D data integration into a structurally controlled field in the ETLP toolbox. A method for fault transmissibility estimation was presented by Benguigui in 2010.

According to Benguigui, the workflow is based on the assumption that, in a deformed and fairly homogeneous reservoir, resistance to flow is mostly controlled by the faults. Benguigui points out, that the challenge lies in the separation of the structural from the stratigraphic constraints in the 4D signature, in order to characterize each component of the compartmentalisation, and then introduce them into the simulation model individually. The other limitation of the method is its inapplicability to the faulted reservoir with vertical fault properties heterogeneity. The results of Benguigui's study are presented in Figure 6.19.

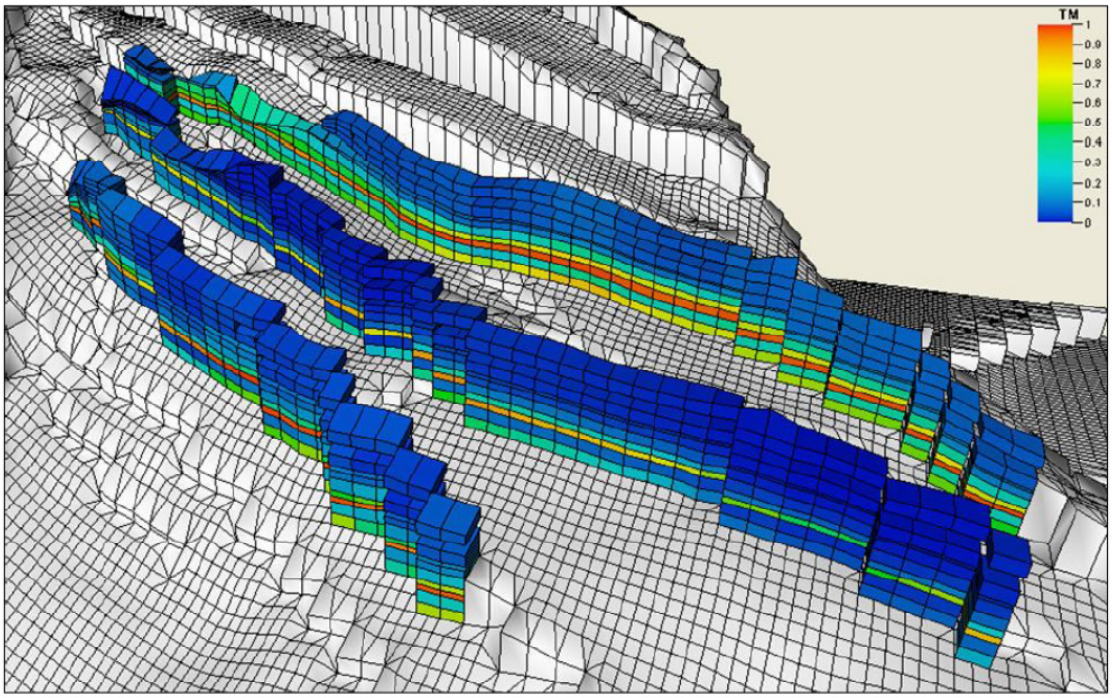

Figure 6.19 4D fault transmissibility multipliers for the three fault segments (Benguigui and MacBeth 2009).

Another ETLP tool was developed recently, by David Yin and represents an extension of the well-2-seis method with an additional optimisation algorithm.

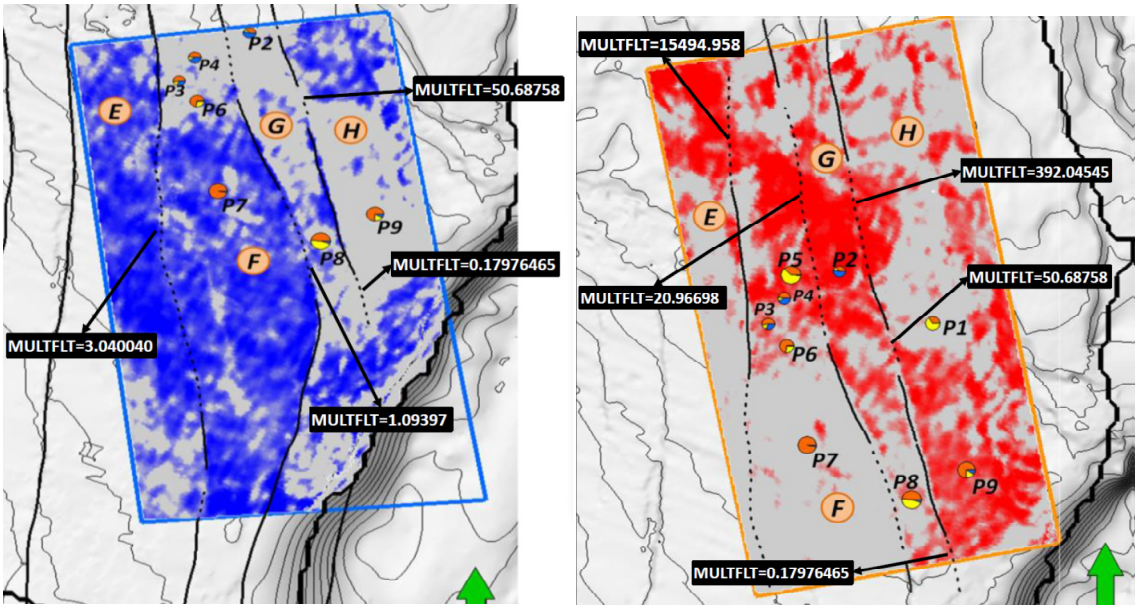

Figure 6.20 Fault transmissibilities based on 4D data.(Yin and MacBeth 2014).

Limitations of the latter method are that this is 2D method and the necessity of few iterations to get the final results

So cluster techniques can solve all the existing problems and assumptions of the methods –

1. A reservoir can include different types of compartmentalisation- stratigraphic and structural (Bentley 2008) and clusters can account for both of these without any special method of application, and without separation of the components of compartmentalisation, but it is not necessary for history matching purposes.
2. Estimation of vertical fault heterogeneity is not a problem for this method. Its result is a 3D grid with property (reservoir and non-reservoir cells) distribution: no matter what the size of the reservoir or its thickness, each cell has its own value, including cells along the fault plane.

For the cluster results see Figure 6.21; faults B, C and D correspond to the faults in Figure 6.19.

These methods are different, but integration of all of them can reduce the uncertainty related to fault transmissibility. The ways in which the faults can be introduced into the simulation model are different as well; details are in the Chapter 5. In both Benguigui's method and the cluster technique, a special fault plane is not needed for assignment of the transmissibility value; the cells adjacent to the fault have values. Yin's method needs a special fault plane

announced in the simulation model data file with a corresponding value of transmissibility multiplier.

Another difference is that the cluster method does not give exact values of fault transmissibilities and transmissibility multipliers, unlike other methods (which produce multiplier values, which will depend on the initial reservoir properties modelled). In cluster techniques, fault transmissibilities also depend on the initial reservoir model; if, after update, some cells have become active (i.e. reservoir) average reservoir properties are assigned to these cells: porosity, permeability, NTG, and hence, transmissibility.

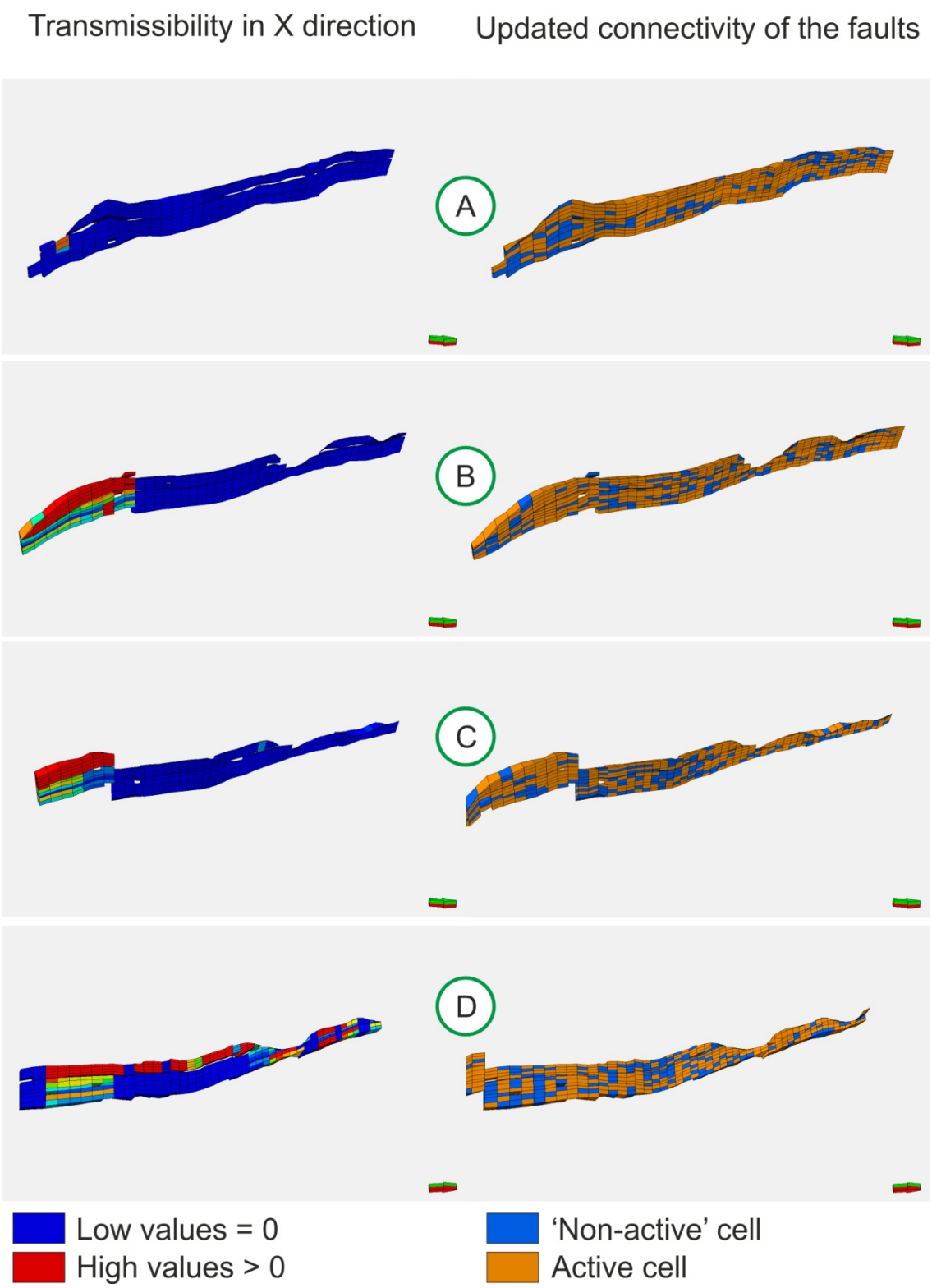

Figure 6.21 Comparison of the fault planes. Left: initial transmissibility values, dark blue- zero transmissibility, no fluid flow through these cells; right: cluster technique result- active cells (reservoir), in orange colour, and 'non-active' cells (non-reservoir), no fluid flow as well

6.5 Summary

This chapter has presented all the uncertainty related to the proposed method. In order to reduce the effect of uncertainty on the connectivity assessment, it is better to integrate some methods of estimation.

Currently, in the framework of the ETLP (Edinburgh Time Lapse Project) two methods for connectivity estimation already exist: Well2Seis, Seis2Seis. These methods have already proved their applicability to real data and their usefulness for reservoir management, including infill drilling planning. The influence of faults on connectivity can be assessed using the method proposed by Benguigui (2010).The proposed cluster method is a next step in connectivity estimation, with results which can be directly used in the simulation model and in history matching in 3D space. The technique sufficiently expands the ability of the ETLP framework methods for history matching. Hence, using the proposed method in history matching allows direct integration of the time-lapse seismic data analysis results into the simulation model at the history matching stage. Doing this I was able to reduce the uncertainties related to connectivity issues (static and especially dynamic) and sufficiently decrease the time for history matching. In the example presented only 2 model simulations needed to be run to get an almost perfect match. A valuable benefit of this method is the solid geological background, which allows connectivity issues to be resolved.

The volumetric calculation presented in Chapter 4 is an additional benefit. This allows the amount of oil (STOIIP) and its distribution in the reservoir to be clarified. We do not need to analyse fault transmissibilities separately from other aspects of reservoir connectivity; the cluster method automatically accounts for any type of compartmentalisation, both stratigraphic (Chapter 4, UKCS field Filed) and structural (Chapter 5, Norwegian Sea field). The presented method of 4D data integration into the simulation model is an important tool in communication across disciplines in a multidisciplinary sub-surface team, as it integrates all of the areas concerned, such as geology, simulation, production and petrophysics.

Finally, integration of the ETLP toolbox can be extremely useful for reservoir management, as it provides an understanding of drainage patterns of the field, areas that can be locations

for new wells, injectors or producers, or may even give insights for geologists, regarding where to find remaining reserves, with low uncertainty.

Chapter Seven

Conclusions and recommendations for future research

7.1 Introduction

There are a number of case-study examples of 4D interpretation approaches and techniques, for which the results can be integrated into the simulation process. Analysing these, one common thread can be highlighted- the key to all the methods is integration of 4D seismic data with dynamic reservoir data, usually observed well data, that is, production and injection volumes. In such a way, accurate and adequate integration can provide confidence in time-lapse interpretation and applicability in dynamic reservoir studies and reservoir management. An understanding of the reservoir production process and of reservoir-engineering fundamentals is absolutely essential for effective application of 4D seismic (Johnston 2013). The reservoir management strategy (and decisions within this strategy) is based on the depletion mechanism, they, in turn, result in different fluid-saturation distribution within the reservoir, and then in 4D data.

It has been underlined that the 4D signature should not be interpreted on its own, but in the integration with well activity. This fundamental link between 4D and well activity is a fundamental base for this thesis. The history matching process has been analysed from the position of directly using 4D interpretation data for matching. Traditional techniques for time-lapse integration into the simulation model were assessed in terms of how well and fast this information can be integrated and produce improvements in history matching. Existing 4D interpretation methods from the ETLP toolbox were also tested for rapid integration into the simulation model and history matching. The parameter which needs to be integrated into the simulation model is reservoir connectivity. As a result, a need has been indicated to develop a new integrated technique which can provide fast, easy to implement integration of time-lapse data into the simulation model and utilise it in history matching. An additional requirement for the new method was that it should be further developed to produce a sound sequence of improvements in the connectivity determination of the existing interpretation methods in the ETLP framework.

To meet this demand, the cluster technique has been proposed in order to address some of the practical problems with 4D interpretation and especially issues with its implication in the history matching process. The cluster technique in this particular case is a method of cross-correlation of well activity with the seismic signature.

Thus, the following workflow has been proposed:

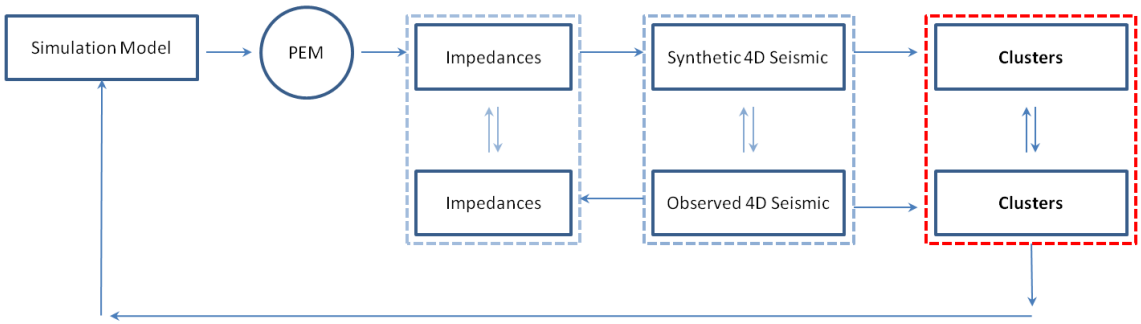

Figure 7.1 Proposed workflow for additional matching domain

Probably, the main difference and key advantage of the proposed method (apart from its mathematics and nature) is its solid geological consistency. This fact was illustrated by two field cases in this thesis. The technique deals with both connectivity and transmissibility of the reservoir. The main benefit of utilising time-lapse seismic data interpretation in history matching of a reservoir simulation model is to get an overview of the fluid front movement both vertically, in the main reservoirs, and laterally, across compartmentalisations of any type. Stratigraphic or lithological or even structural compartments can be analysed using the proposed method and directly integrated into the simulation model, which significantly reduces history matching time and provides additional information regarding reservoir architecture and fluid flow patterns. Based on these results reservoir managements decisions can be made.

7.2 Method Description

The proposed method uses cluster analysis as a foundation. This approach was first used by Tryon (1939), and comprises a number of different classification algorithms. All these algorithms are used for the organisation of observed data into meaningful sets or structures. A K-means clustering algorithm is utilised in this work; the method aims to partition a number of observations (n) into k sets, in such a way, that each observation belongs to the only cluster (set) with the nearest mean:

$$\arg\min_{s} \sum_{i=1}^{k} \sum_{x_j \in S_i} \left(x_j - \mu_i\right)^2 \tag{7.1}$$

where is the mean of points in *mu*. The proposed method is based on cluster analysis of multiply repeated 4D surveys. The consequence of this is that the simulation model grid is divided into clusters of cells with the same behaviour. The idea behind the matching method is as follows: values for transmissibility between (or within) clusters are changed for matching mainly production data and seismic data. Thus, in my case, clusters are representative of reservoir volumes on the basis of the changes in seismic signal similarity through time, where the number of clusters *k* mainly depends on available 4D surveys, but has a limit which can be easily determined. The cluster location, size and volume are constant for a particular number of 4D surveys analysed.

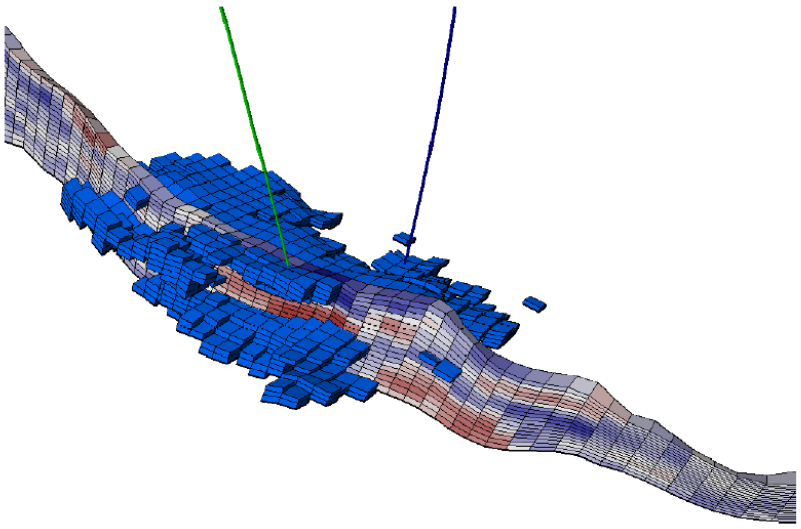

Figure 7.2 3D synthetic cluster representation in simulation model grid overlapped with seismic. Dark blue indicates a cluster; seismic cross section indicates the difference between two 3D seismic surveys; green and dark blue lines indicate wells.

Using multiple seismic surveys forced me to use an alternative time sequence, involving the creation of difference maps, 3D grids or any other kind of data for all possible pairs of seismic surveys and as a consequence, using the same time sequence for production data. Similarity (in the 3D volume) of the clusters derived from the observed seismic and from the simulation model is used as a part of the misfit function, as well as the difference between production history data and the simulated ones. The method has been successfully applied to

a pair of North Sea fields. One oilfield is a compartmentalised turbidite reservoir with a complex geology, the other is a structurally controlled reservoir.

Due to the nature of the method, it takes into account all the presented seismic surveys simultaneously, which dramatically increases the accuracy of the results. As was mentioned, it is very fast to implement. Due to direct use of the seismic data with the simulation model, the method reveals a capability for quantitative seismic understanding in the engineering domain, especially in terms of inter-well connectivity and possible integration of the results with well testing or the PLT. According to the workflow, it is possible to estimate results in at least three different domains: impedances, seismic and clusters as well as in the traditional and compulsory domain of production data. The study of impedances is out of the framework of this project. Thus, matching results need to be estimated in the few domains. First of all: what was changed during matching? Applying the cluster technique allows connectivity in the model to be updated. I conclude, after application of the method, that although initial values of connectivity are rather homogenous and it is possible to say that connectivity does not affect reservoir flow significantly, this is not in fact true (according to the geological settings and production history) for one of the examined field cases.

In the lower part of Figure 7.2, we see significant heterogeneity in the connectivity due to the updating procedures. Unfortunately, it is impossible to numerically measure improvements in this domain, but from the geological stance, the updated connectivity is more reliable and moreover, it can be explained from the sedimentological conditions of the field. The geological aspects and their detailed discussion were covered Chapter 5. Figure 7.3 represents the updated connectivity of the field. Zero implies no connection and unity a very good connection, correspondingly. This result was achieved just after the first iteration step: I determined ‘non-active’ cells in the model and set them to zero transmissibility for the fluids. The connectivity pattern is affected, so this results in a dramatic improvement in production match.

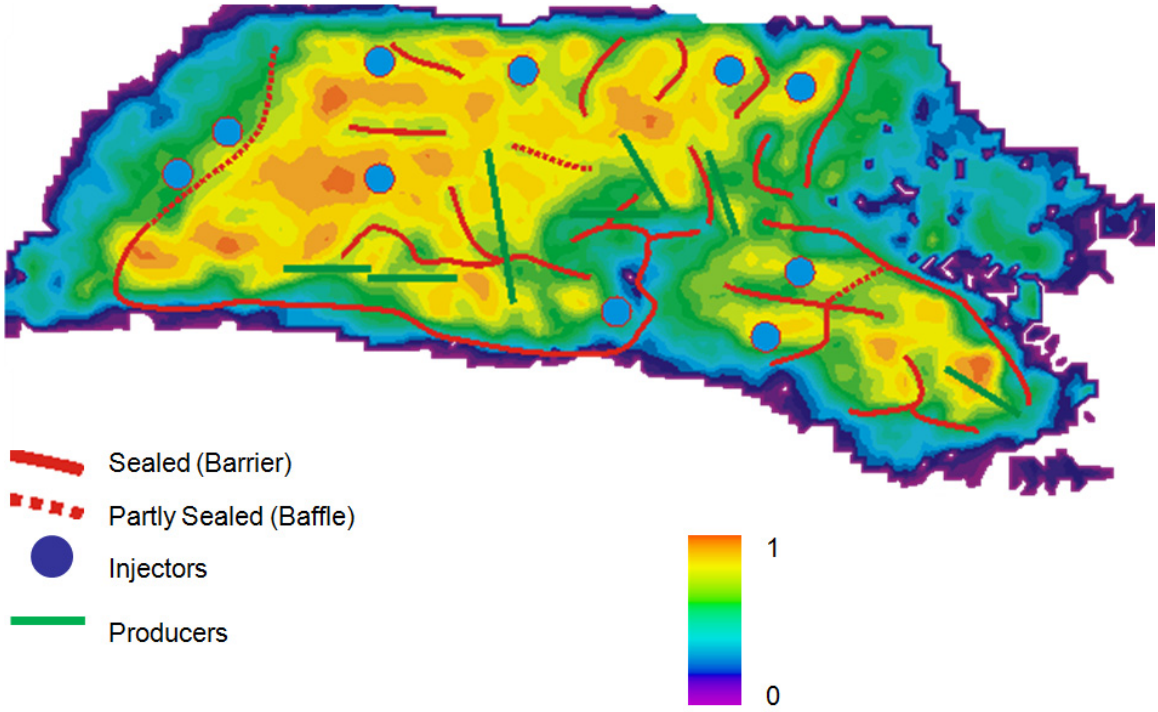

Figure 7.3 Final connectivity map from simulation model, after its update using cluster analysis. Numerous heterogeneities are reflected.

7.3 Main Conclusions

The proposed technique has been applied to pair of datasets from North Sea fields with encouraging results. From an analysis of the results achieved, the following benefits have been recognised as the result of the application of this technique to history matching and general 4D data integration:

1. The proposed technique consolidates the production and the 4D seismic data in a direct manner in such a way as can be easily utilised in a simulation model, with dramatic improvements in history matching. It automatically considers any uncertainties which are in the simulation model and 4D seismic results without any additional uncertainty inputs, because the scale in which method is applied is the same as that in the simulation model. This method suits all the engineering needs and produces reliable results with less effort and less time compare to the traditional history matching process. Moreover, it is consistent with field geology and can be

used even for dynamic clarification in the geological settings of the field, so can be applicable for calibration of static reservoir models. With a high level of reliability, the results from this method can be used in direct reservoir management decisions, especially for infill planning.

2. By performing a correlation between unique sequences of volumes produced or injected by the wells and 4D signatures, the causal relationship between well activity and the 4D response as a consequence of the well activity, can be qualified and can be used directly to match the simulation model. This relationship indicates a strong association of a 4D signal with the well under study, which is an unquestionable fact. For a quantified result of the application of this method, transmissibility and pore volume multipliers can be used, as well as a detailed connectivity grid (or the map). Multipliers of the pore volume of transmissibility can be improved to automate the process, which is actually a well-known technique. The advantage of cluster-derived connectivity is geological consistency.

3. The tools presented for history matching dramatically reduce the time taken for matching. Even though the results of matching using the proposed method are not perfect, they are still impressive and have the potential to be improved.

4. These benefits have been demonstrated in the two field studies discussed in this thesis. These field cases differ from each other in a principal point: the geology conditions controlling fluid flow. The clustering method demonstrates its sustainability and solid results in both.

However, the following weaknesses have also been detected in the proposed method:

1. The fundamental assumption of this method (as well as any other related with well activity) is that the time-lapse seismic signature should respond to the fluid volumes produced/ injected in a linear manner. The fields shown in this thesis do indeed demonstrate linear behavior. However, it should be noted that some other fields, may probably illustrate a complex relationship for produced/injected volumes vs. seismic amplitude, due to complicating factors such as overlapping of pressure and saturation. Discrimination of pressure and saturation in 4D is one of the most important problems of time-lapse interpretation. Indeed, we can qualitatively separate saturation changes from pressure changes based on knowledge of production history, well locations and

their types, production or injection. Taking into account P and S-waves: it is well known that S-waves are responsive to changes in both pressure and saturation, while S-waves are responsive to pressure changes. Understanding this, it can be assumed that 4D P and S wave velocity changes can be useful for distinguishing pressure and saturation. This can probably be done using 4D AVO analysis.

2. Injected/produced volume should be enough to be detected by seismic: this question refers to the proper timing of the 4D survey. Other facts we need to be aware of are comparability of differences of seismic responses (i.e. differences of produced/injected volumes), that is to say, M1-BL should be more or less in the same scale as M2-M1, otherwise there may be some complexity in differentiating clusters.

7.4 Speculative Developments

The progression from a qualitative to quantitative level of 4D interpretation is essential for reservoir understanding and increasing the value of 4D seismic data for the industry. Quantitative interpretation could be very useful in history matching, especially if changes in saturation, pressure and compaction could be inverted directly from the time-lapse seismic. In this thesis, the potential usage and limitations of the technique have been discussed, and its applications to the real reservoir have been presented. The case study presented in the work can be used as a guideline for application of the method on the other fields. Hence, quantitative time-lapse data interpretation has been utilised as an efficient tool for history matching. However, some improvements can be made as well. All of the proposed improvements will produce valuable results for field management along with additional validation of the applied method. From figure 7.2 it can be seen that, after understanding connectivity, there are a number of ways to use it in reservoir studies. There are two global directions-the static reservoir and the dynamic one. Generally speaking, connectivity is a fundamental principle in reservoir studies and reservoir management. Based on the existing ETLP toolbox, connectivity can be derived using 4D seismic data and production data. The cluster technique solves connectivity issues related to the reservoir, including non-reservoir versus reservoir rock/ inactive cells, fault/seal transmissibility, horizontal and vertical barriers and compartmentalisation and even permeability (requiring well test data), as well as mobile

volumes, connectivity of the gas cap and aquifer, and the dynamic response of geological features (boundaries of the reservoir, improvements in geological model).

Connectivity needs to be validated; it is possible to do by applying sedimentological studies. Connectivity can then be integrated into the static reservoir model. Why is this necessary? Initial reservoir models, which are usually based on the baseline 3D survey, have a number of attached uncertainties and a number of realisations. The aim of any reservoir study is to decrease these uncertainties. Hence, dynamic data, such as 4D and production/injection well data, are useful in the disclosure of water pathways and then in reaching a geological understanding of the reservoir. Time-lapse data then can close the big loop for the geological model update, using the cluster method. Increasing activity in unconventional and fractured reservoirs will require developments in rock physics to help geoscientists better understand the relationship between field depletion and the 4D seismic response (Johnston 2013).

There are number of engineering outcomes from 4D which can be active areas of research in the near future- a better understanding of sweep efficiency, fluid pathways, and the understanding of saturation and pressure, which can be a key for reservoir dynamic predictions, and the final area of research concerns stress, strain, fluid density and other rock physics properties.

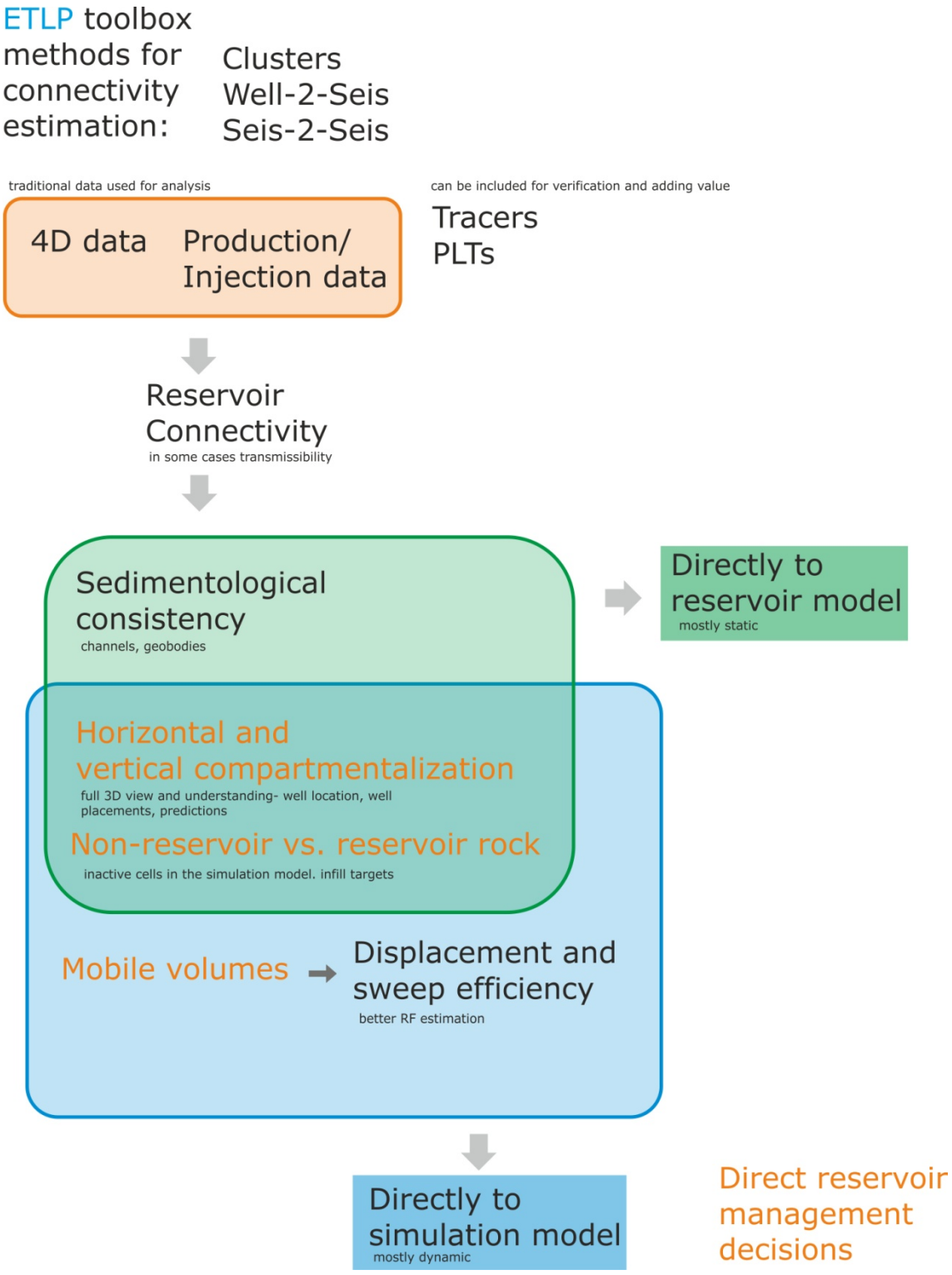

Figure 7.4 Value of the ETLP toolbox for connectivity estimation. Green areas are related to static reservoir models, and blue areas to dynamic reservoir volumes. Orange indicates data which can be used directly for reservoir management decisions.

7.4.1 Integration of additional data sources

According to Johnston (2013), (Johnston 2013) proper time-lapse data interpretation requires the following key points:

- Gain a rigorous understanding of the reservoir-depletion mechanism and the underlying rock physics. These two factors together determine the seismic response to production-initiated changes.
- Evaluate data-quality issues before interpretation.
- Make sure the interpretation makes sense, not only in terms of the depletion mechanism and production data, but geologically as well.

To better fit to these criteria, within the existing framework of the proposed method and the connectivity issue, it is possible to integrate some additional data from various sources.

7.4.1.1 Production logging tool

Integration of additional data sources is a key for management of uncertainties related to time-lapse qualitative analysis. One of the surveys that can be rather easily integrated is PLT (production logging tool), a special well survey which aims to identify reservoir parts with different fluid influx into the wellbore. Generally speaking, production logs are used to allocate production on a zone-by-zone basis. An example from the Andrew Field is presented in the Figure 7.5; this perfectly illustrates the reason for using PLT data in conjunction with 4D data. At initial conditions, there is a clear distinction between the higher acoustic impedance of the water zone (in blue) and the lower acoustic impedance of the HC-bearing zone. A faint lineation marks the GOC. The lower part of the figure- shows the impedance difference section after five years of production, showing water movements towards the well, consistent with the production logging data. (Marsh, 2004). Adding PLT into 4D seismic analysis, especially a cluster study, gives an additional validation of the method and a solid tie with the volumetric calculations. For reservoir management decisions, integration of PLT with 4D will help in identifying potential re-perforation targets.

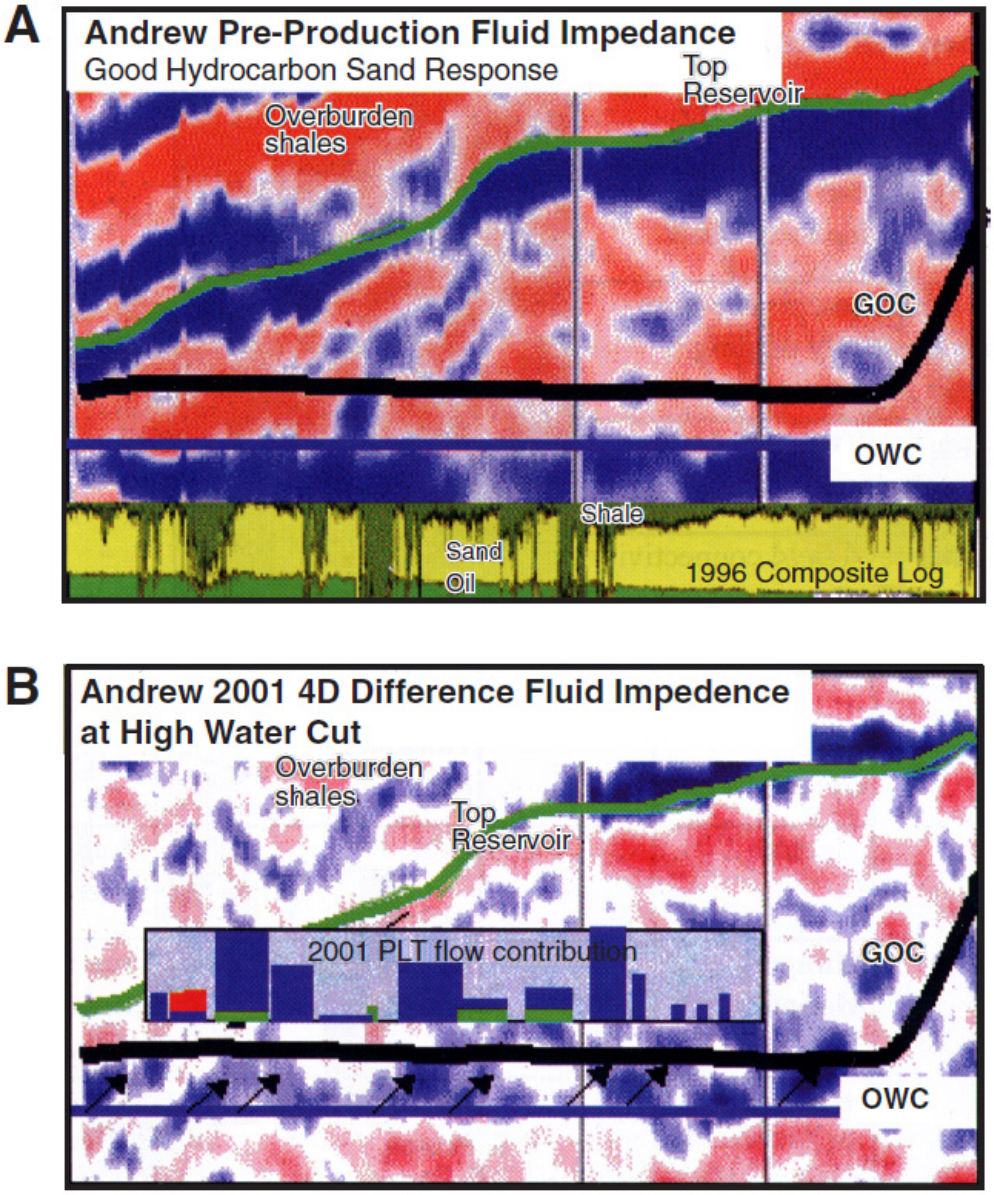

Figure 7.5 Seismic acoustic impedance sections along the path of an Andrew Field producer (Marsh et al., 2003). A. At initial conditions, with a clear distinction between the higher acoustic impedance of the water zone (in blue colour) and the lower acoustic impedance of HC-bearing zone. A faint lineation marks the GOC. B. Impedance difference section after five years of production, showing water movements towards the well, consistent with production logging data.

7.4.1.2 Tracer test

The interwell tracer test is another way to decrease uncertainty in connectivity determination based on the time-lapse data. Here I mean the applicability of tracer tests more for validation

of connectivity results based on 4D, rather than simultaneous application of both methods. The value and importance of tracer tests are broadly recognised. Tracer testing has become a mature technology, and improved knowledge about tracer behaviour in the reservoir, improved tracer analysis, and reduction of pitfalls have made tracer tests reliable. In principle, a passive tracer blindly follows the fluid phase in which it is injected. Generally speaking, tracers reveal reservoir continuity. The information received about which injector influences which producer in terms of rate (breakthrough times) and what percentage of fluid (volume) is going into each well can provide abundant information about reservoir connectivity (Bennion, et al. 1995).

Some details of tracer test applicability for this work are as follows:

1. Volumetric sweep. The volume of injected fluid at an injection well until breakthrough of the traced fluid at an offset producer is a measure of the volumetric sweep efficiency between that pair of wells. This gives us the ability to calculate pore volume as well. So this data can be used in volumetric calculations.
2. Understanding of flow pathways or directions of flow trends. Traces injected at an injection well can reveal flow pathways along part of the field or whole field. This data is able to validate the geological concepts of the field and connectivity analysis from any source, including time-lapse data.

7.4.2 Accurate cluster boundary determination.

Due to the nature of the clustering algorithm, the boundary between the clusters cannot be determined with 100% confidence. As was discussed, clusters have some uncertainty areas, which is actually the level of uncertainty associated with the clustering algorithm. Indeed, in this area, each point x_i can be related to two (or even more) clusters simultaneously, with associated probability of being in particular cluster. So, a reduction in this area will lead to more accurate cluster discrimination, with additional data, and hence, less uncertainty.

So far we have seen only one type of cluster curves, which are actually the mean curve from number of curves belonging to a particular cluster. One of the cluster type's curves is presented in Figure 7.7 with the associated curves (not all of them are presented, for a better view). Each of these curves, representing one reservoir cell property, (seismic amplitude in this case) changes along the timeline.

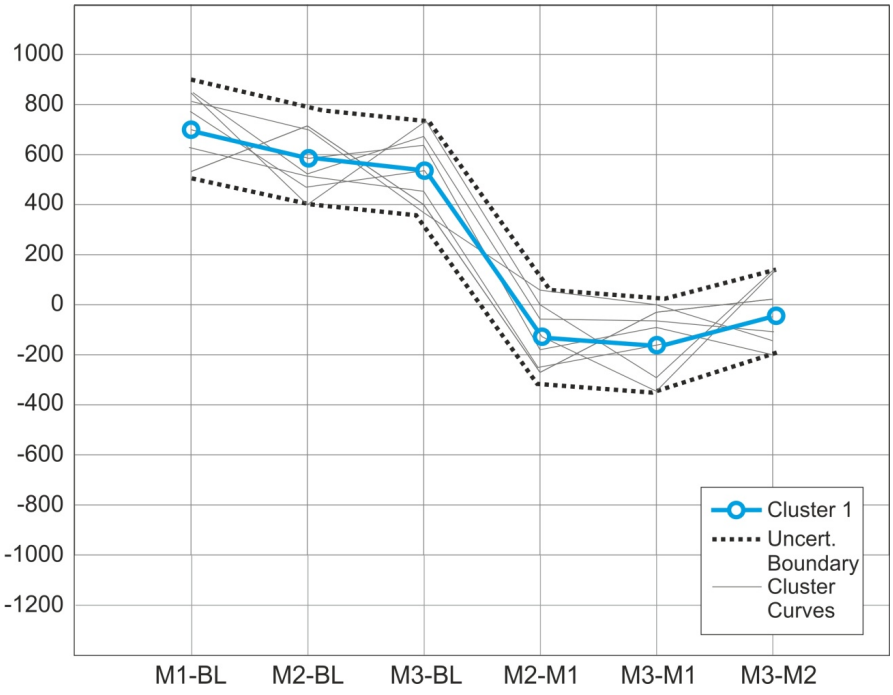

Figure 7.6 One cluster's curves (grey). Mean cluster representation is in blue.

Hence, better delineation of the clusters' boundaries will lead to better localisation of compartments and precise positioning of barriers/baffles in the model, and, as a result, faster history matching with better results. It may also lead to separation of 4D noise from the production-related signal, which, in its turn, should significantly improve understanding of the relationship of time-lapse with well activity.

Another possible area of research here is improvement in the determination of the initial number of clusters. Suppose it is possible to do this with respect to the nature of the time-lapse data and well production/injection data. Probably an engineer can recognise certain well (or even seismic) patterns from the field history and use them as an initial cluster pattern.

7.4.3 Property values in "new" active cells.

It has been demonstrated that cluster analysis can discriminate non-reservoir versus reservoir rock/ inactive cells. Then there are possibly a number variations: an active cell remains active, an active cell becomes inactive, an inactive cell remains inactive, an inactive cell becomes active. The first three cases are simple to treat: actually, if the cell doesn't change

its state then there is no need to do anything; if an active cell is turned into an inactive one (based on cluster analysis), we just make its properties equal to zero (porosity, permeability, volume etc.) and in Eclipse data files we make the ACTNUM property of this cell equal to zero. But what do we need to do if an inactive cell becomes active? The simple and straightforward way is to assign average property values; however, this approach is completely fine and reasonable for a simulation model, but geologically it is not. What if we have different facies in the reservoir? In that case, firstly, we need to determine which facie the cell belongs to. That means going back to the geological model and geological concept and deciding which cells belong to which facies, which can be rather time consuming. Probably, there is also an easier and faster way with respect to geology. Maybe it is possible to find a correlation with the 'new' active cell's location and the existing facies distribution, or if we talk about object modelling – correlation with geobody locations, or even with the distribution of seismic facies. In such a way, we can find out weak points in put facies, geology analysis, and possible underestimation of dynamic characteristics of some field areas.

In some cases areas of fields can be very different in terms of dynamic behaviour. The reason for this can be or geological (i.e. compartments, or different fluid saturation), or technological (different timings of well activity); hence, these will have an effect on the time-lapse signature. Such areas need to be separated for further analysis for proper cluster discrimination. Subsequently, the resulting clusters need to be compared between these areas, and they probably need to be treated as a different fields.

Appendix A

A.1. Transmissibility Calculations

Equations for transmissibility calculations are presented here.

$$A = \frac{DX_j \cdot DY_i \cdot DZ_i \cdot RNTG_i + DX_i \cdot DY_j \cdot DZ_j \cdot RNTG_j}{DX_i + DX_j} \tag{A1.1}$$

$$B = \frac{\left(\frac{DX_i}{PERMX_i} + \frac{DX_j}{PERMX_j}\right)}{2} \tag{A1.2}$$

$$DIPC = \frac{DHS}{DHS + DVS} \tag{A1.3}$$

$$DHS = \left(\frac{DX_i + DX_j}{2}\right)^2 \tag{A1.4}$$

$$DVS = \left[DEPTH_i - DEPTH_j\right]^2 \tag{A1.5}$$

RNTG is the net to gross ratio, which appears in the X and Y transmissibilities but not in the Z.

$$TRANZ_i = \frac{CDARCY \cdot TMLTZ_i \cdot A}{\mathrm{B}} \tag{A1.6}$$

Symbols have their own meaning.

$$A = \frac{DZ_j \cdot DX_i \cdot DY_i + DZ_i \cdot DX_j \cdot DY_j}{DZ_i + DZ_j} \tag{A1.7}$$

$$B = \frac{\left(\frac{DZ_i}{PERMZ_i} + \frac{DZ_j}{PERMZ_j}\right)}{2} \tag{A1.8}$$

There is no dip correction in the Z-transmissibility case.

A.2. Material Balance Calculations

Symbols		Units	SI
B_g	gas formation volume factor	bbl/SCF	M^3/SCM
B_o, B_t, B_w	oil, total and water formation volume factors	bbl/STB	M^3/SCM
c_f, c_w	pore and water compressibility	vol/vol/psi	vol/vol/MPa
G	initial gas-cap volume	SCF	SCM
G_p	cumulative gas produced= $G_{ps}+G_{pc}$	SCF	SCM
G_{ps}	cumulative solution gas produced	SCF	SCM
G_{pc}	cumulative gas cap produced	SCF	SCM
m	ratio initial reservoir free gas volume to initial reservoir oil volume	bbl/bbl	M^3/M^3

Symbols		Units	SI
N	stock tank oil initially in place	STB	STM^3
N_p	cumulative tank oil produced	STB	STM^3
p	average reservoir pressure	psi	MPa
p_i	initial reservoir pressure	psi	MPa
R_p	cumulative gas/oil ratio	SCF/STB	SCM/STM^3
R_s	solution gas/oil ratio	SCF/STB	SCM/STM^3
S_w	average connate water saturation		
W_e	cumulative water influx	bbl or STB	M^3 or STM^3
W_p	cumulative water production	bbl or STB	M^3 or STM^3

A.3. Idealised cluster type curves

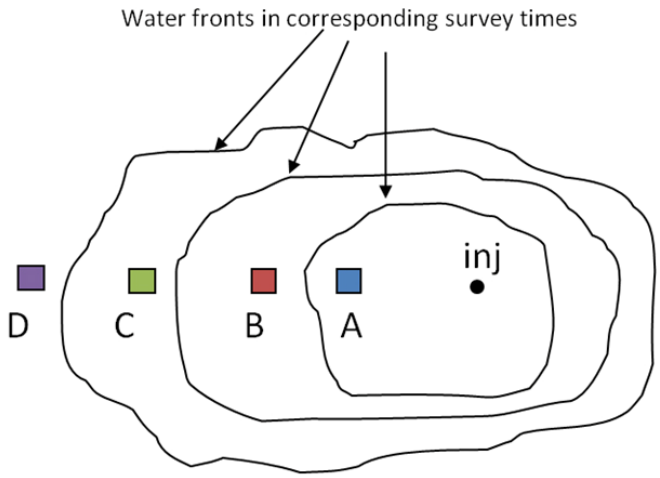

Figure A3.1 Visualisation of water fronts at particular time of seismic surveys with reference points (A-B-C-D)

Based on Figure A.3 the idealised cluster type curve for each reference point can be calculated as follows: the graph is presented as difference in volumes, but according to the presented approach of correlation between seismic and well data, the same graphs will be in the seismic domain. These curves are idealised and represent only simple cases. It needs to be noted that the situation will be much more complicated in real field cases (see Chapters 4 and 5).

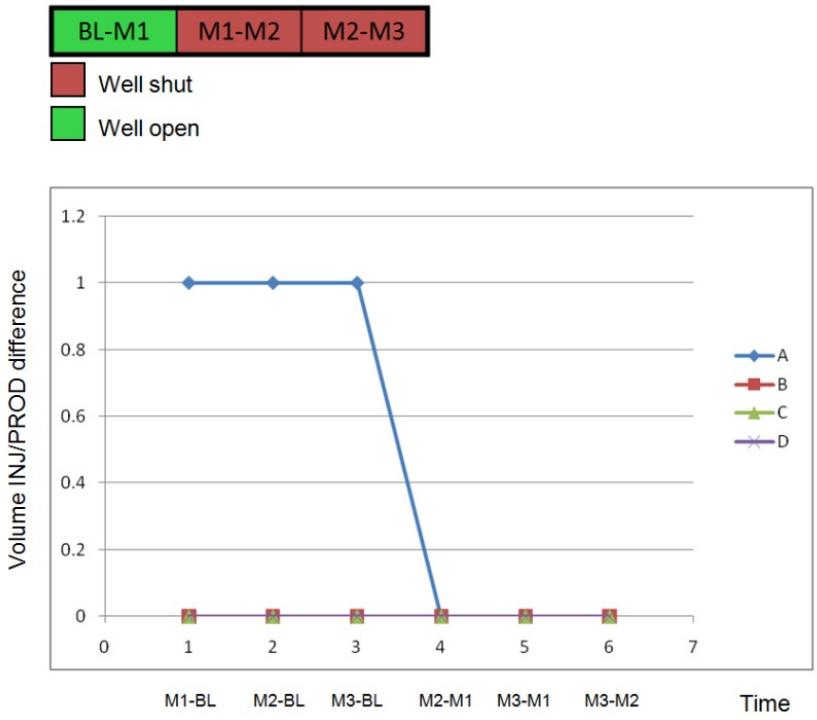

Figure A3.2 Cluster type curves for time step BL-M1: wells open, then closed

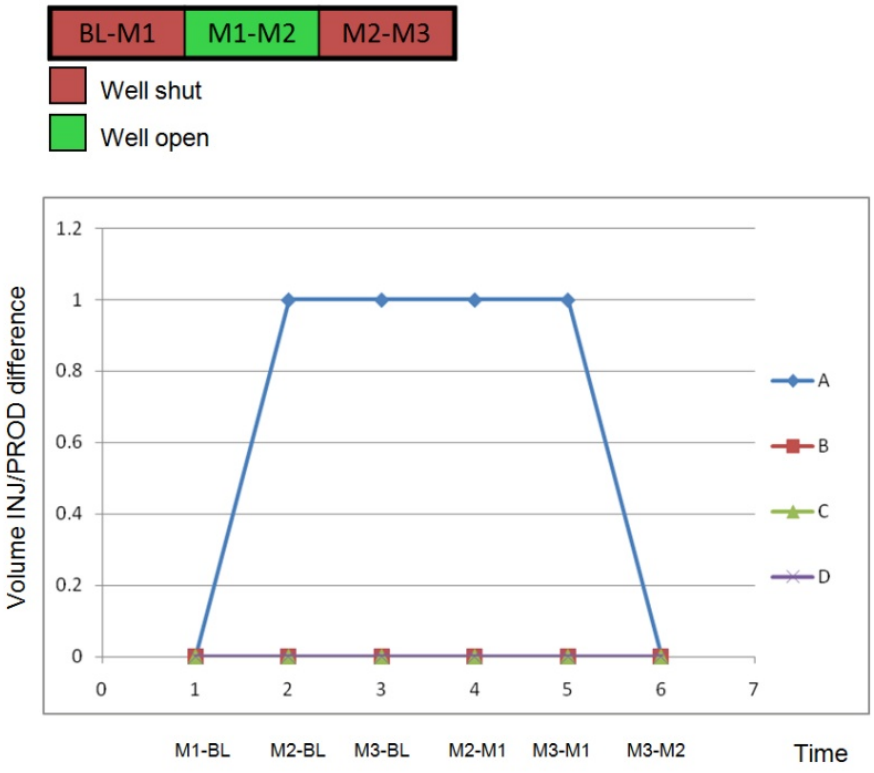

Figure A3.3 Cluster type curves for injection well opened in M1-M2 time step

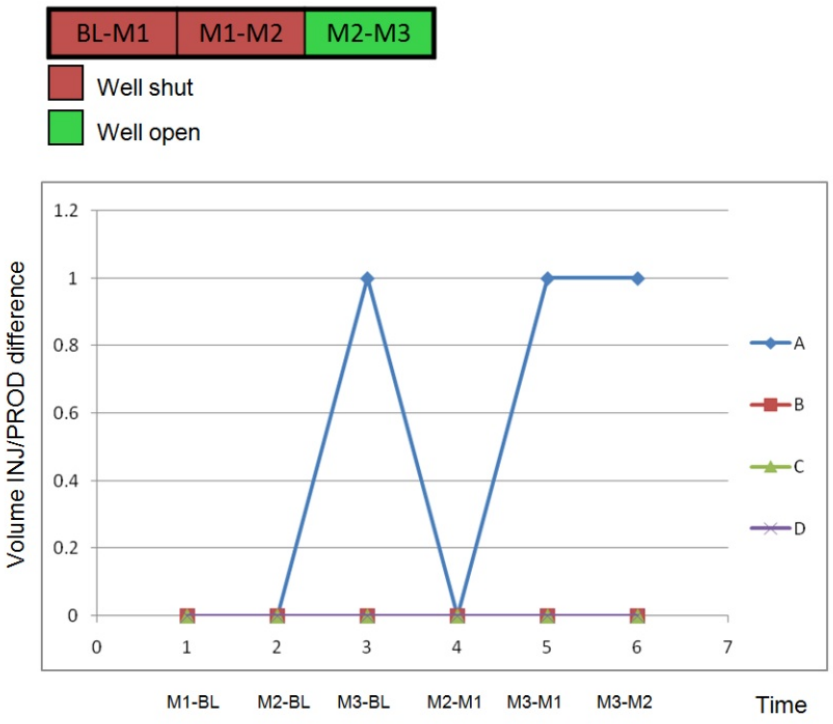

Figure A3.4 Cluster type curves for injection well opened in M2-M3 time step

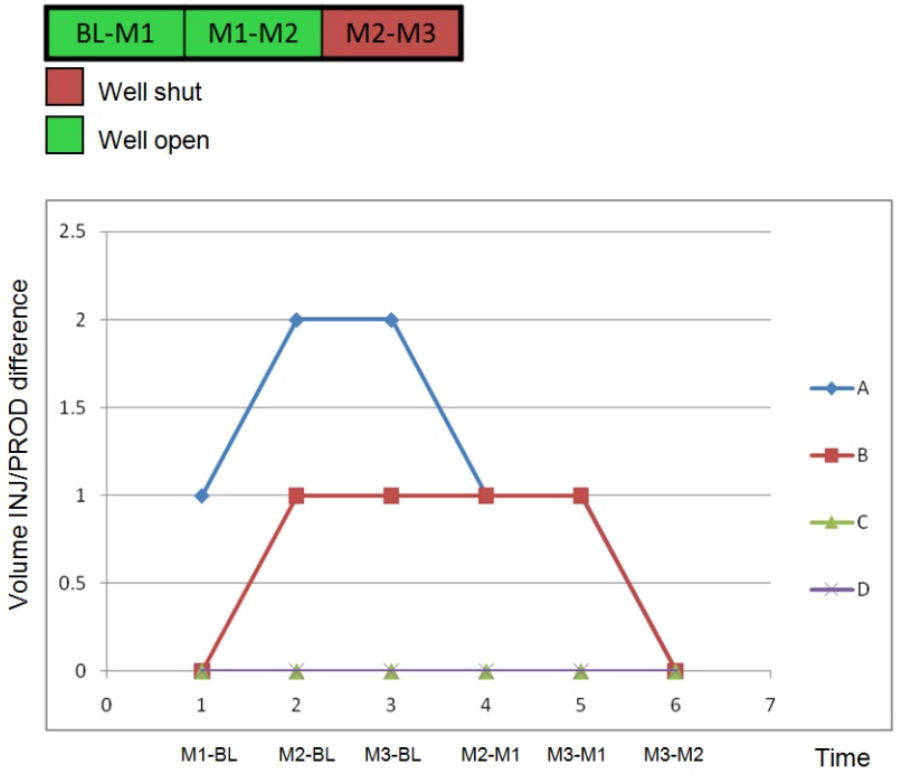

Figure A3.5 Cluster type curve for injection wells opened from BL to M2

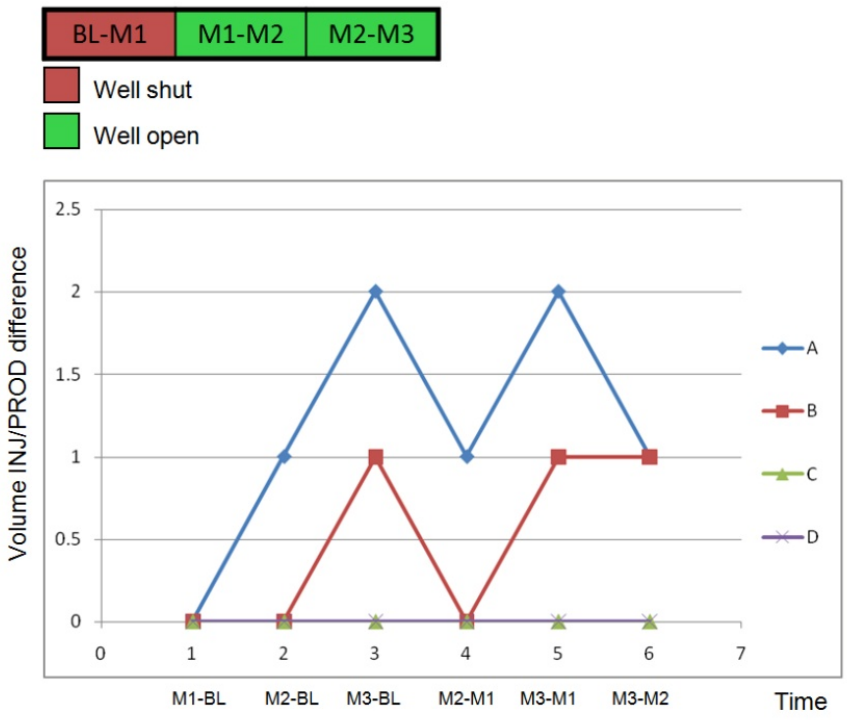

Figure A3.6 Cluster type curve for injection wells opened from M1 to M3

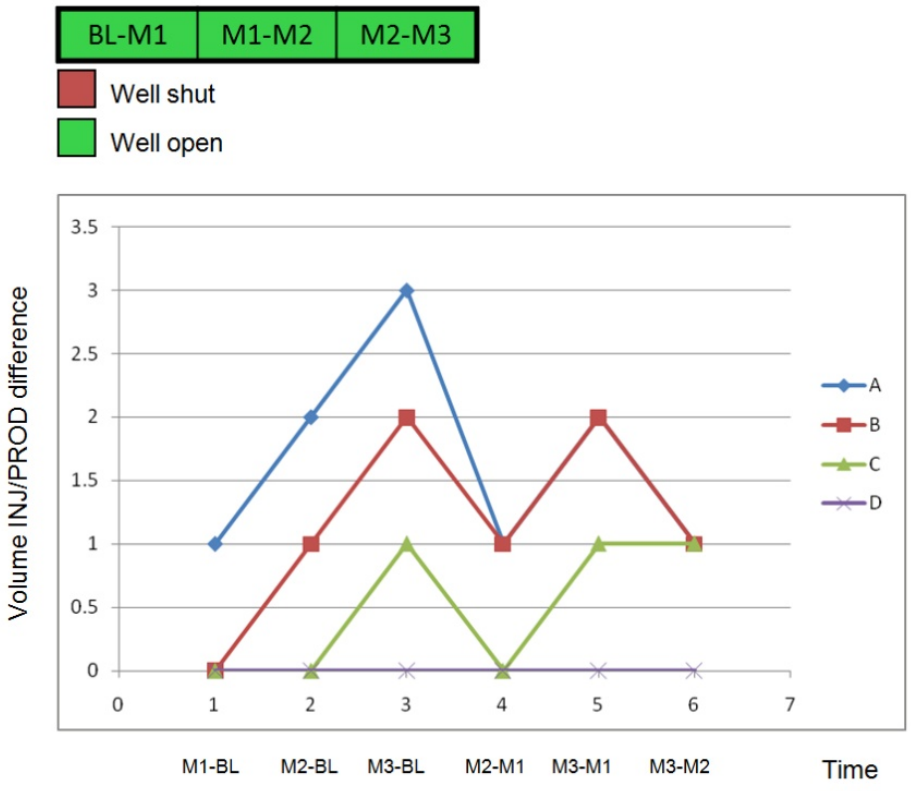

Figure A3.7 Cluster type curve for injection wells opened from BL to M3

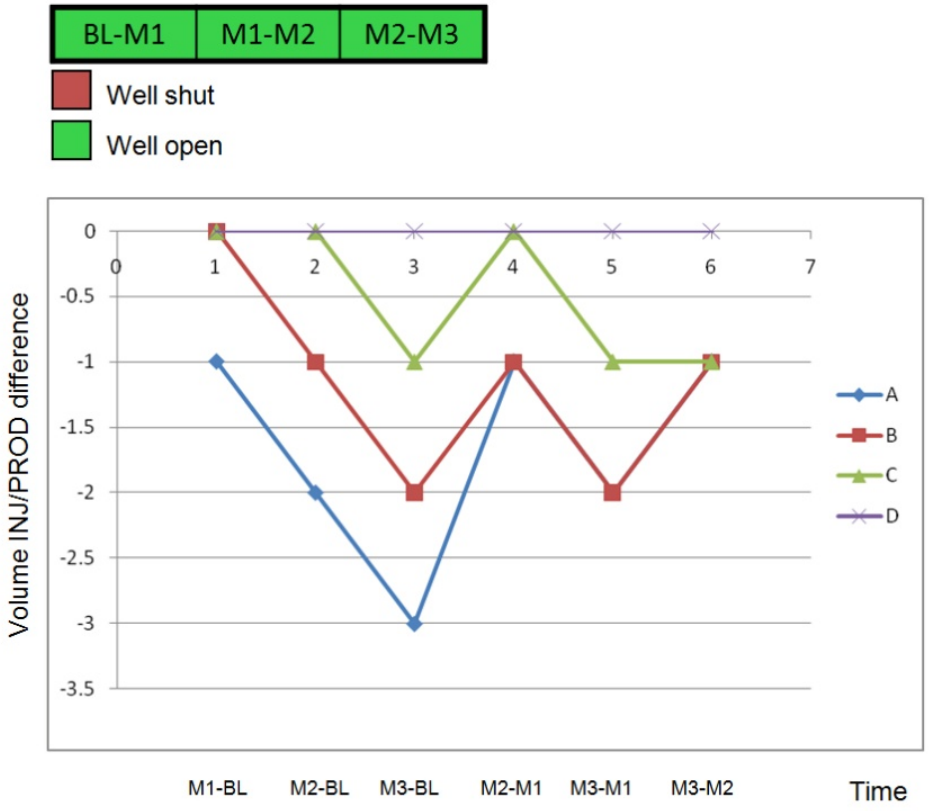

Figure A3.8 Cluster type curve for production wells opened from BL to M3

Appendix B

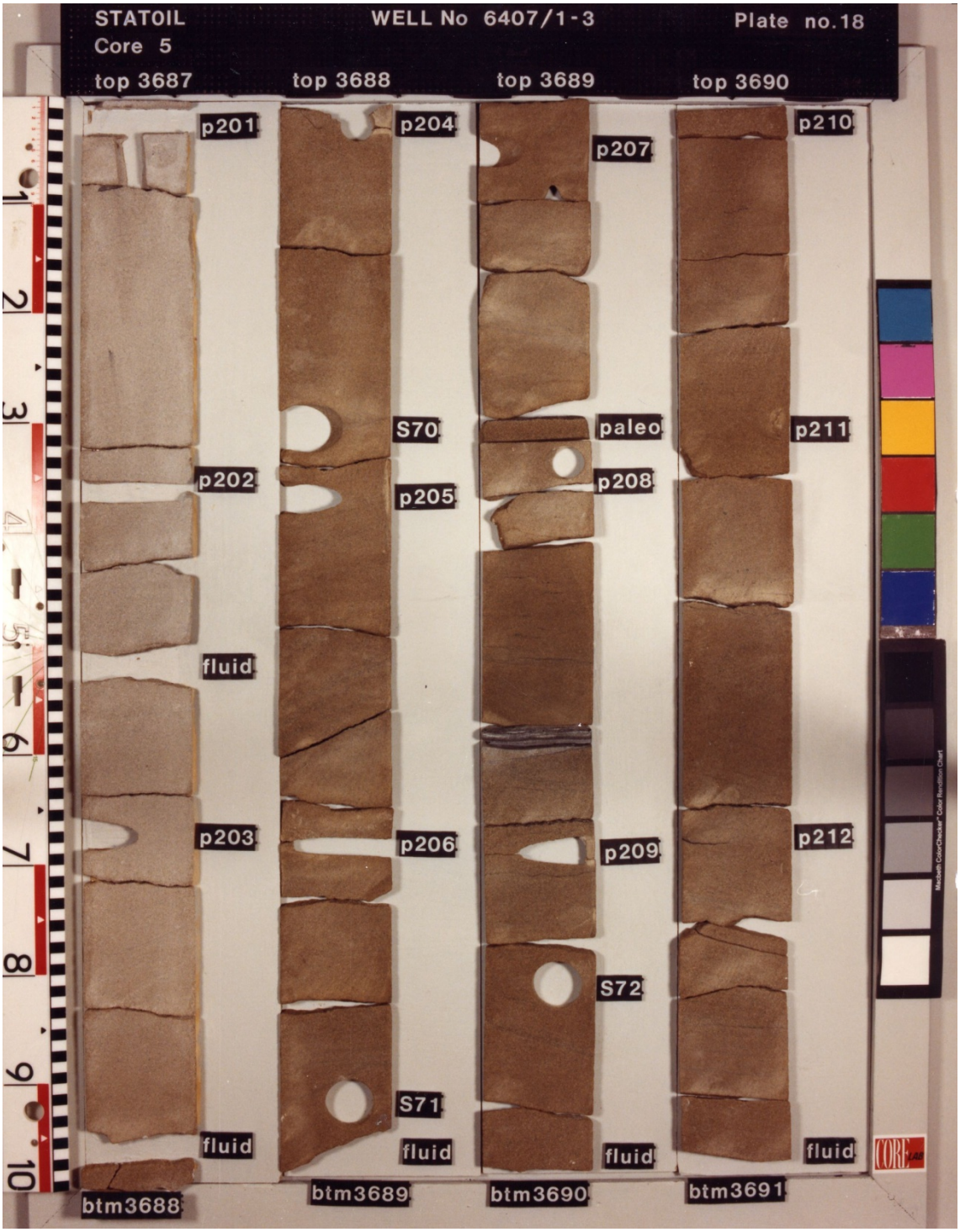

Figure B.1 Reservoir core photographs, Fangst Group.

ECLIPSE 100 Black Oil

The flow rate into cell *i* from a neighbouring cell *n*, F_{ni}, is

$$F_{ni} = T_{ni}\begin{bmatrix} \frac{k_{ro}}{B_o\mu_o} & 0 & \frac{R_v k_{rg}}{B_g\mu_g} \\ 0 & \frac{k_{rw}}{B_w\mu_w} & 0 \\ \frac{R_s k_{ro}}{B_o\mu_o} & 0 & \frac{k_{rg}}{B_g\mu_g} \end{bmatrix}_u \times \begin{bmatrix} dP_{oni} \\ dP_{wni} \\ dP_{gni} \end{bmatrix}$$

where

$$dP_{oni} = P_{on} - P_{oi} - \rho_{oni}G(D_n - D_I)$$

$$dP_{oni} = P_{wn} - P_{wi} - \rho_{wni}G(D_n - D_I)$$

$$= P_{on} - P_{oi} - \rho_{wni}G(D_n - D_I) - P_{cown} + P_{cowi}$$

$$dP_{gni} = P_{gn} - P_{gi} - \rho_{gni}G(D_n - D_I)$$

$$= P_{on} - P_{oi} - \rho_{gni}G(D_n - D_I) + P_{gown} - P_{cogi}$$

T_{ni} is the transmissibility between cells *n* and *i*,

k_r is the relative permeability (k_{ro} is the relative permeability of oil, etc.),

μ- is the viscosity (μ_w - is the viscosity of water etc.),

dP is the potential difference (dP_{gni} is the gas potential difference between cells *n* and *i*),

ρ- is the fluid density (ρ_{oni} is the density of oil at the inrerface between cells *n* and *i*),

G is the acceleration due to gravity

D is the cell centre depth.

The subscript u indicates that the fluid mobilities are to be evaluated in the upstream cell (cell *n* if dP_{ni} is positive, cell *i* if dP_{ni} is negative). The upstream calculation applies separately for each equation (oil, water, gas) so that, for example, oil may flow from cell *i* to cell *n* while water flows from cell *n* to cell *i*.

The net flow rate from cell i into neighbouring cells is obtained by summing over the neighbouring cells:

$$F_{ni} = \sum_{n} F_{ni}$$

Algorithms for model update used in BP

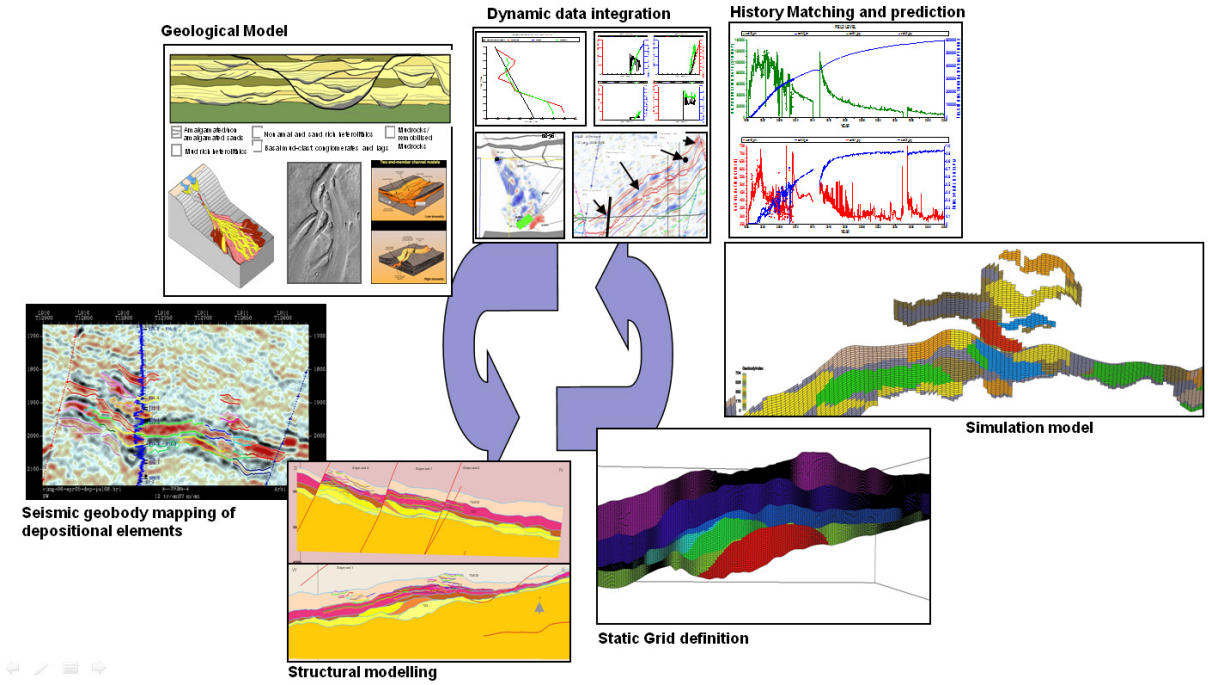

Figure B.2 Integrated workflow for model update (Martin and MacDonald 2010)

- The geobodies are inserted into the model in an erosional depositional order to allow for overlapping mapping of the bodies.
- All this was accomplished using a series of RMS IPL scripts.
- Automated model build and geobody insertion into the grid.
- Provides an audit trail.
- Consistent set of output parameters.
- Large amounts of data can be handled quickly and easily reduces margin for human error.
- The IPL scripts also generate fluid saturations and net to gross parameters for use in seismic inversion.

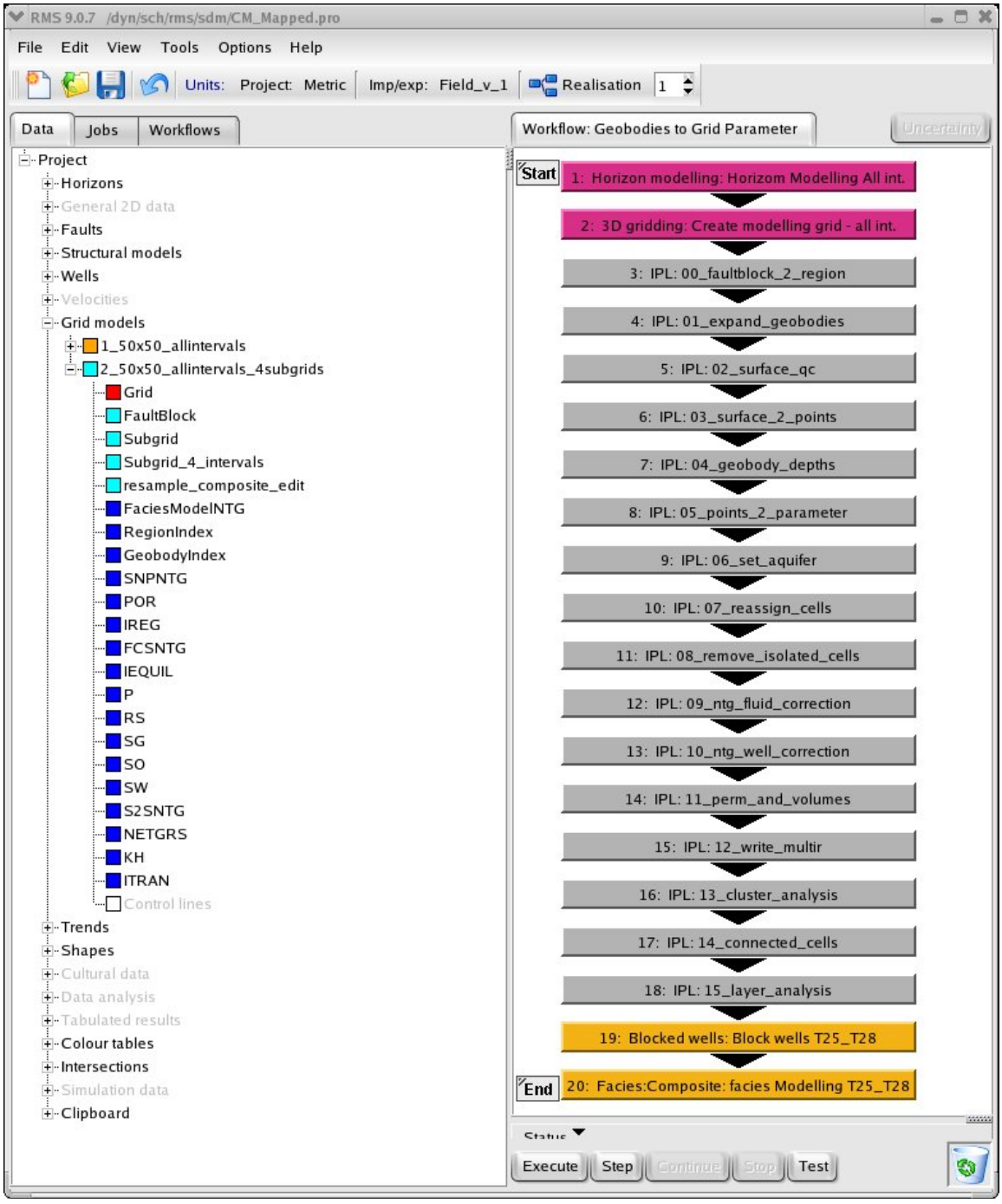

Figure B.3 Workflow for geobody definition and model update. (Martin and MacDonald 2010)

Bibliography

Al Moqbel, Abdulrahman, and Yanghua Wang. "Carbonate Reservoir Characterization with Lithofacies Clustering and Porosity Prediction." *Journal of Geophysics and Engineering*, 2011: 592-598.

Al-Maskeri, Y, and C MacBeth. "Extraction of permeability from time-lapse seismic data." *Geophysical Prospectiong, 54*, 2006: 333-349.

Amini, H. "ETLP sponsormeeting." *Accurate simulator-to-seismic predictions: examples from modelling from full field simulations.* Edinburgh, 2009.

Amini, H, C MacBeth, and A Shams. "SPE EUROPEC/EAGE Annual Conference and Exhibition." *Calibration of Simulator to Seismic Modelling for Quantitative 4D Seismic Interpretation.* Vienna, Austria, 2011.

Amini, Hamed. *A Progmatic Approach to Simulator to Seismic Modelling for 4D Seismic Interpretation, PhD Thesis.* Edinburgh: Institute of Petroleum Egineering, Heriot- Watt University, 2013.

Andersen, T, et al. "SPE Europec/EAGE Annual Conference and Exhibition." *Method for conditioning the reservoir model on 3D and 4D elastic inversion data applied to a fluvial reservoir in the North Sar (SPE 100190).* Vienna, 2011.

Archer, J.S, and C Wall. "Petroleum Engineering Principles and Practices." Craham & Trotman, 1986. 362.

Benguigui, A., MacBeth, C. "EAGE Exhibition and Conference." *Updating the Simulation model using 4D-derived fault transmissibility multipliers: An application to the Heidrun Field.* Amsterdam, 2009. 1706-1710.

Benguigui, Amran, and Colin MacBeth. "Updating the simulation model using 4D- derived fualt transmissiblity multipliers: an application to the Heidrun Field." EAGE Exhibition and Conference, Amsterdam, 2009.

Bennion, B, F.B Thomas, E.C Crowel, and B Freeman. "Annual International Conference on Reservoir Conformance Profile Control Water & Gas Shutoff." *Applications for tracers in reservoir conformance predictions and initial saturation determinations.* Houston, 1995.

Bentley, M.R. "International conference on reservoir compartmentalization." *Reservoir compartments: beyond fault seal (Abstract).* London: The Geological Society, 2008.

Boldreel, L O, and M S Andersen. "Late Paleocene to Miocene compression in the Faeroe-Rockall." In *Petroleum geology of northwest Europe: Proceedings of the 4th Conference:*, 1025-1034. London, 1993.

Booth, J, T Swiecicki, and P Wilcockson. "The tectono-stratigraphy of the Solan Basin, West of." In *Petroleum geology of northwest Europe: Proceedings of the 4th Conference:*, 987-998. London, 1993.

BP. *The UK upstream asset portfolio.* 2009. http://www.bp.com/liveassets/bp_internet/globalbp/STAGING/global_assets/downloads/U/uk_asset_schiehallion.pdf (accessed 6 14, 2011).

Bradbury, J. "Shetland success: BP learns harsh lessons as Schiehallion comes onstream." *Euroil*, 1998: 84-87.

Caers, J. *Petroleum Geostatistics.* SPE, 2005.

Calvert, Rodney. *Insights and Method for 4D Reservoir Monitoring and Characterization.* SEG Distinguished Instructor Series, 2005.

Carlson, Mike. *Practical Reservoir Simulation.* 2003.

Carstensen, C, T Wilk, and K Van Brocklin. "Proceedings 5th I.Mech.E Europe Congress." *The water injection system in the Heidrun platform.* Hague, 1993. 11-18.

Chapin, M, D Terwogt, and J Ketting. "From seismic to simulation using new voxel body and geologic." *The Leading Edge*, April 2000: 408-412.

Corbett, Patrick W.M. "The Role of Geoengineering in Field Development." In *New Technologies in the Oil and Gas Industry*, by J.S Gomes, 181-198. 2012.

Corre, C, P Thore, V deFeraudy, and G Vincent. "SPE European Petroleum Conference." *Integrated Uncertainty Assessment for Project Evaluation and Risk Analysis.* Paris, 2000.

Cowper, D R, P Jackson, R W Storm, F R Halford, and G Stuart. "SPE European Petroleum Conference." *Innovative Data Acquisition-West of Shetlands.* Milan: SPE, 1996. 63-69.

Crichlow, H.B. *Modern Reservoir Engineering- A Simulation Approach.* Prentice Hall, 1977.

Dake, L.P. *Fundamental of Reservoir Engineering.* Amsterdam: ELSEVEIR Science B.V., 2002.

Damuth, J E, and H C Olson. "Preliminary observations of Neogene-Quaternary depositional processes in the Faeroe-Shetland Channel revealed by high-resolution seismic facies analysis." In *Petroleum geology of northwest Europe: Proceedings of the 5th Conference: Geological Society*, by A.J Fleet and S.A.R Boldy, 1035-1045. London, 1993.

Daveridge, S, and S Hiebert. "Offshore Technology Conference." *An Innovative Business Model to Leverage Innovative Well-Placement Technology (OTC 17591).* Houston, USA, 2005.

Deom, D B, J C Eggemeyer, F E Estep, and D M Hejnal. "Proceedings Offshore Technology Conference." *The Heidrun Field - pre-drilling: a case study in designing for and achieving success.* Houston, 1996. 535-548.

Floricich, M. *An engineering-consistent approach for pressure and saturation, PhD Thesis.* Institute of Petroleum Egineering, Heriot- Watt University, 2006.

Freeman, P., S. Kelly, C. Macdonald, J. Millington, and M. Tothill1. "The Schiehallion Field: lessons learned modelling a complex deepwater turbidite." *Geological Society, London, Special Publications* , no. 309 (2008): 205-219.

Furre, A K, F R Munkvold, and L H Nordby. "65th EAGE Conference and Exhibition." *Improving reservoir understanding using time-lapse seismic at the Heidrun Field.* 2003.

Gainsky, M, A.G MacGregor, P.J Freeman, and H.F Nieuwland. "Turbidite reservoir compartmentalization and well targeting with 4D seismic and production data: Schiehallion Field, UK." In *Reservoir Compartmentalization*, by S.J Jolley, Q.J Fisher, R.B Ainsworth and P.J Vrolijk, 89-103. London: Geological Society, 2010.

Govan, A., T. Primmer, C. Douglas, N. Moodie, M. Davies, and F. Nieuwland. "Reservoir Management in a Deepwater Subsea Field--The Schiehallion Experience." *SPE Reservoir Evaluation & Engineering*, 8 2006.

Griffiths, Roger. *Well Placement Fundamentals.* 2009.

Guderian, K, M Kleemeyer, A Kjeldstaad, and S.E Pettersson. "65th EAGE Conference & Exhibition." *Draugen field: Successful reservoir management using 4D seismic.* Stavanger, Norway, 2003.

Harris, N B. "Reservoir geology of Fangst Group (Middle Jurassic), Heidrun Field, offshore Mid-Norway." *AAPG Bulletin v.73*, 1989: 1415-1435.

Hemmens, P D, A Hole, B E Reid, P.R L Leach, and W R Landrum. "3rd North Sea Oil and Gas Reservoirs Conference." *The Heidrun Field.* Springer, 1992.

Hird, K.B, and O Dubrule. "SPE Reservoir Evaluation and Engineering." *Quantification of reservoir connectivity for reservoir description appliacations (SPE 30571).* Dallas, 1995. v.1, p. 12-17.

Ho, T.T Y, R P Jansen, S K Sahai, R H Leadholm, and O Senneseth. "Comparative studies of pre- and post-drilling modelled thermal conductivity and maturity data with post-drilling results: implications for basin modelling and hydrocarbon exploration." In *Basin Modelling: Practice and Progress: Geological Society Special Publications, no.141*, by S J Duppenbecker and J E Iliffe, 187-208. 1998.

Hovadik, J.M, and D.K Larue. "Static characterizations of reservoirs; refaining the concepts of connectivity and continuity." *Petroleum Geoscience*, 2007: 13, 195-21.

Hovadik, J.M, and D.K Larue. "Stratigraphic and structural connectivity." In *Reservoir Compartmentalization*, by S J Jolley, Q J Fisher, R B Ainsworth and P J Vrolijk, 219-243. London: Geological Society, 2010.

Hu, L.Y. "Gradual deformation and iterative calibration of gaussian related stochastic models." *Mathematical Geology*, 2000: 32(1), 87-108.

Huang, X, and Y Ling. "SPE Annual Technical Conference and Exhibition." *Water injection optimization using historical production and seismic data (SPE 102499).* San-Antonio, Texas, USA, 2006.

Huang, Yi, and Colin MacBeth. "Direct correlation of 4D seismic and well activity for dynamic reservoir interpretation." *SEG Technical Program Expanded Abstracts.* Houston, 2009. 3840-3844.

Huang, Yi, Colin MacBeth, Olav Barkved, and J Van Gestel. "SPE Europec/72nd EAGE Conference and Exhibition." *Correlation of well activity to time-lapsed signatures in the Valhall field for enhanced dynamic interpretation. Extended Abstract (M020).* Barcelona, 2010. 1-5.

Jack, Ian. *Time-Lapse Seismic in Reservoir Management.* SEG, 1998.

Jin, L, et al. "73rd EAGE Conference and Exhibition incorporating SPE EUROPEC." *4D Seismic History Matching Using Flood Front Information. Extended Abstract (J040).* Vienna, 2011.

Johann, P, R Sansonowski, R Olivera, and D Bampi. "4D seismic in a heavy oil turbidite reservoir offshore Brazil." *The Leading Edge*, 2009: 718-729.

Johansen, Kent. *Statistical Methods for History Matching.* Technical University of Denmark, 2008.

Johnston, David H. *Practical Applications of Time-Lapse Seismic Data.* Tulsa: SEG, 2013.

Jolley, S.J, D Barr, J.J Walsh, and R.J Knipe. "Treatment of faults in production simulation models." In *Structurally Complex Reservoirs*, by S.J Jolley, D Barr, J.J Walsh and R.J Knipe, 1-24. London: Geological Society, 2007.

Jolley, S.J, Q.J Fisher, and R.B Ainsworth. "Reservoir compartmentalization: an introduction." In *Reservoir Compartmentalization*, by S.J Jolley, Q.J Fisher, R.B Ainsworth and P.J. Vrolijk, 1-9. The Geological Society of London, 2010.

Jourdan, J.M, F Lefeuvre, and D Dubucq. "Integration of 4D seismic into the dynamic model: Girassol, deep offshore Angola." *First Break*, 2006: 51-58.

Karlsen, D A, et al. "Petroleum Geochemistry of the Haltenbanken, Norwegian continental shelf." *The Geochemistry of Reservoirs: Geological Society Special Publication, no.86*, 1995: 203-256.

Lake, L, and J L Jensen. "SPE 20156." *A review of heterogeneity measures used in reservoir characterization.* 1989.

Landrum, W R, R C Burton, W M Mackinlay, A Erlandsen, and A Vigen. "Proceedings Offshore Technology Conference." *Heidrun- results from pre-completed wells using innovative gravelpacking techniques.* Houston, 1996. 549-556, OTC paper 8087.

Larue, D K, and J Hovadik. "Connectivity of channelized reservoirs: a modelling approach." *Petroleum Geoscience*, 2006: 291-308.

Leach, H.M., Herbert, N., Los, A., Smith, R.L. "The Schiehallion development." In *Petroleum geology of northwest Europe: Proceedings of the 5th Conference: Geological Society*, 683-692. London, 1999.

Leghorn, J., Brookes, D.A., Shearman, M.G. "28th Annual Offshore Technology Conference." *The Foinaven and Schiehallion developments.* Houston, 1996. 41-56 (OTC 8033).

Leonard, A., Jolley, E., Carter, A., Mills, C., Jones, N., Bowman, M. "GCSSEPM Foundation 20th Annual Research Conference." *Lessons learned from the management of basin floor submarine fan reservoirs in the UKCS.* 2000. 478-501.

Lumley, David E, Alan G Nunns, Guy Delorme, A.A Adeogba, and Michel F Bee. "Offshore Technology Conference." *Meren Field, Nigeria: a 4D Seismic Case Study.* 2001. 1-4.

Manzocchi, T, J.J Walsh, P Nell, and G Yielding. "Fault transmissibility multipliers for flow simulation models." *Petroleum Geoscience*, 1999: 53-63.

Martin, Karen, and Christopher MacDonald. "DEVEX." *The Schiehallion Field: Applying a Geobody Modelling Approach to Piece Together a Complex Turbidite Field.* Aberdeen, 2010.

Mattax, C. C., and R. L. Dalton. "Reservoir Simulation." In *SPE Monograph, Vol. 13*. 1990.

McInally, A, et al. "Optimizing 4D fluid imaging." *Pertoleum Geoscience, Vol. 9, No. 1*, 2003: 91-101.

McLennan, J, and C Deutsch. "SPE International Thermal Operations and Heavy Oil Symposium." *Ranking geostatistical realizations by measures of connectivity (SPE 98168).* Calgary, Canada: SPE, 2005.

Oistein, H, A Kleppe, and J.P Nystein. "Effects of heterogeneities in a braided stream channel sandbody on the simulation of oil recovery: a case study from the Lower Jurassic Stratfjord Formation, Snorre Field, North Sea." In *Andvences in Reservoir Geology*, 105-134. Geological Society Special Publications, 1993.

Olea, R.A. *Geostatistical Glossary and Multilingual Dictionary.* Oxford University Press, 1991.

Olivera, Rildo M. "The Marlim Field: Incorporating 4D Seismic in Reservoir Management Decisions." *Distingushed Author Series. JPT*, April 2008: 52-53, 107-110.

Olsen, T, et al. "Integrated reservoir characterization and uncertainty analysisi, Heidrun Field, Norway." In *Petroleum Geology of Northwest Europe*, by A J Fleet and S.A. R Boldy, 1209-1220. London: Geological Society, 1999.

Parr, R, and M March. "Development of 4D reservoir management West of Shetland." *World Oil, Vol.221, No. 9*, 2000: 39-47.

Paydayesh, M. *Permeability Estimation From Time-Lapse Seismic Data For Updating the Flow-Simulation Model, PhD Thesis.* Institute of Petroleum Engineering, Heriot- Watt University, 2010.

Ramshaw, R S. "Deep Offshore Technology, 6th International Conference." *Heidrun Field development.* 1991. 13-25.

Razin, A.V, V.P Merkulov, and S.A Chernov. *Application of Geophysics for Reservoir Description.* Tomsk, Russia: TPU, 2010.

Reid, B E, L A Hoyland, S R Olsen, and O Petterson. "Offshore Technology Conference." *The Heidrun Field- challenges in reservoir development and production.* 1996. 521-534.

Richardson, S.M., Herbert, N., Leach, H.M. "Offshore Europe Conference." *How well is the reservoir connected? (SPE 38560).* Aberdeen, 1997. 603-609.

Roggero, F, et al. "History Matching of Production and 4D Seismic Data: Application to the Girassol Field, Offshore Angola." *Oil & Gas Science and Technology*, 2012: 237-262.

Roste, T, et al. "71st EAGE Conference and Exhibition incorporating SPE EUROPEC 2009." *Using 4D Seismic to Monitor Fluid Flow in a Heterogeneous and Compartmentalised Reservoir - Cases from the Heidrun Field (R019).* Amsterdam, 2009.

Saxby, I. "UKCS: 2001 AAPG Annual Meeting." *Impact of 4-D seismic reservoir monitoring in Schiehallion Field.* 2001. 4.

Schiehallion BP oil field project. 1999. http://www.offshore-technology.com/projects/schiehallion/.

Schulze-Reigert R., Ghedan S. "Proceedings of the 9th International Forum On Reservoir Simulation." *Modern Techniques for History Matching.* Abu Dhabi, 2007.

Shams, A, C MacBeth, and L Barens. "Devex Conference." *Local connectivity analysis in a deep water complex turbidite using seismic time lapse and well interference test.* Aberdeen, 2007.

Smith, P, J.I Berg, S Eidsvig, I Magnus, J Helgesen, and F Verhelst. "4-D seismic in a complex fluvial reservoir: the Snorre feasibility study." *The Leading Edge*, 2001: 270-276.

Snedden, J.W, et al. "IPTC: International Petroleum Technology Conference." *Reservoir Connectivity: Definitions, Examples, and Strategies (IPTC 11375).* Dubai: IPTC, 2007.

Soldo, J.C. *Quantitative integration of time-lapse seismic information using multiple model history matching and engineering data, PhD Thesis.* Edinburgh, UK: Institute of Petroleum Engineering, Heriot- Watt University, 2004.

Stephen, K, and C MacBeth. "Seismic History Matching in the Schiehallion UKCS Field." *First Break*, 2006: 43-49.

Sverdrup, E, J Helgesen, and J Vold. "Sealing properties and their influence on water altering-gas injection efficiency in the Snorre Fieldm Northern North Sea." *AAPG Bulletin v.87*, 2003: 1437-1458.

Talukdar, S, and R Instefjord. "Europec/EAGE Conference and Exhibition." *Reservoir Management of the Gullfaks Main Field (SPE 113260).* Rome, 2008.

Tybero, G, L Johannessen, and A J Bouchard. "Heidrun long core study- an alternative approach to relative permeability determination." In *North Sea Oil and Gas Reservoirs - III*, 325-329. 1994.

Valstar, J.R. *Inverse modelling of groundwater flow and transport, PhD Thesis.* Delft University of Technology, 2001.

Vasco, D.W. "Seismic imaging of reservoir flow properties: time-lapse amplitude." *Geophysics, 69*, 2004: 1425-1442.

Villegas, R. "Simulataneous characterization of geological shapes and permeability." Proceeding of SPE Europec/EAGE Annaul Conference. Vienna, 2006.

Villegas, R, C MacBeth, and M Paydayesh. "SPE/EAGE Reservoir Characterization amd Simulation Conference." *Permeability updating of the simualtion model using 4D seismic data (SPE-125632-MS).* Abu Dhabi, UAE, 2009. 7.

Vincent, G, B Corre, and P Thore. "SPE Annual Technical Conference and Exhibition." *Managing Structural Uncertainty in a Mature Field for Optimal Well Placement (SPE-48953-MS).* New Orleans, Louisiana, 1998. 11.

Webber, K.J, and L.C Geuns. "Framework for constructing clastic reservoir simulation models (SPE 19582)." *Journal of Petroleum Technology, Vol. 42, No. 10*, 1990: 1248-1253, 1296-1297.

Welbon, A I, et al. "Fault seal analysis in hydrocarbon exploration and appraisal: examples from offshore Mid-Norway." In *Hydrocarbon Seals: Importance for Exploration and Production*, by P Moller-Pedersen and A G Koestler, 125-138. NPF Special Publications, no.7, 1997.

Yin, Z, and C MacBeth. "76th EAGE Conference and Exhibition 2014 ." *Simulation model updating with multiple 4D seismic in a fault-compartmentalized Norwegian Sea field (We G102 12).* Amsterdam, 2014.

Zhang, F, J.A Skjervheim, A.C Reynolds, and D.S Oliver. "Automatic history matching in a Bayesian framework (SPE 84461)." *SPE Reservoir Evaluation and Engineering, Vol. 8, No. 3,*, 2005: 214-223.